Investigations on Load Frequency Control of Microgrid and Interconnected Power Systems using Artificial Intelligent Techniques

Submitted in partial fulfilment of the requirements
for the award of the degree of

DOCTOR OF PHILOSOPHY
in
Electrical Engineering

By

Annamraju Anil Kumar
(Roll No. 716010)

Supervisor:

Dr. N.V. Srikanth
Associate Professor

DEPARTMENT OF ELECTRICAL ENGINEERING
NATIONAL INSTITUTE OF TECHNOLOGY
WARANGAL – 506004, TELANGANA STATE, INDIA
JUNE-2020

APPROVAL SHEET

This Thesis entitled "**Investigations on Load Frequency Control of Microgrid and Interconnected Power Systems using Artificial Intelligent Techniques**" by **Annamraju Anil Kumar** is approved for the degree of Doctor of Philosophy

Examiners

_____

_____

_____

Supervisor
Dr. N.V. Srikanth
Associate Professor
EED, NIT Warangal

Chairman
Dr. M. Sailaja Kumari
Professor& Head,
EED,NIT Warangal

Date: _____

DEPARTMENT OF ELECTRICAL ENGINEERING
NATIONAL INSTITUTE OF TECHNOLOGY
WARANGAL – 506 004, TELANGANA STATE, INDIA

CERTIFICATE

This is to certify that the thesis entitled **"Investigations on Load Frequency Control of Microgrid and Interconnected Power Systems using Artificial Intelligent Techniques"**, which is being submitted by **Mr. Annamraju Anil Kumar** (Roll No. 716010), is a bonafide work submitted to National Institute of Technology, Warangal in partial fulfilment of the requirement for the award of the degree of **Doctor of Philosophy** in Department of Electrical Engineering. To the best of my knowledge, the work incorporated in this thesis has not been submitted elsewhere for the award of any degree.

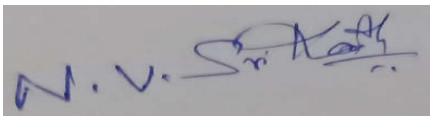

Dr. N.V. Srikanth
(Supervisor)
Associate Professor
Department of Electrical Engineering
National Institute of Technology
Warangal – 506004

Date: 09/01/2021

Place: NIT Warangal

DECLARATION

This is to certify that the work presented in the thesis entitled "**Investigations on Load Frequency Control of Microgrid and Interconnected Power Systems using Artificial Intelligent Techniques"** is a bonafide work done by me under the supervision of **Dr. N. V. Srikanth** , Department of Electrical Engineering, National Institute of Technology, Warangal, India and was not submitted elsewhere for the award of any degree.

I declare that this written submission represents my ideas in my own words and where others ideas or words have been included; I have adequately cited and referenced the original sources. I also declare that I have adhered to all principles of academic honesty and integrity and have not misrepresented or fabricated or falsified any idea/date/fact/source in my submission. I understand that any violation of the above will be a cause for disciplinary action by the institute and can also evoke penal action from the sources which have thus not been properly cited or from whom proper permission has not been taken when needed.

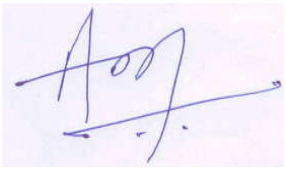

Annamraju Anil Kumar

(Roll No: 716010)

Date: 09/01/2021

Place: Warangal

ACKNOWLEDGEMENTS

It gives me immense pleasure to express my deep sense of gratitude and thanks to my supervisor **Dr. N. V. Srikanth,** Associate Professor, Department of Electrical Engineering, National Institute of Technology Warangal, for his invaluable guidance, support, and suggestions. His knowledge, suggestions, and discussions helped me to become a capable researcher. He has shown me the interesting side of this wonderful and potential research area. His encouragement helped me to overcome the difficulties encountered in my research as well in my life.

I am very much thankful to **Prof. Sailaja Kumari** Head, Department of Electrical Engineering for her constant encouragement, support and cooperation.

I take this privilege to thank all my Doctoral Scrutiny Committee members, **Dr. N. Viswanatham**, Professor, Department of Electrical Engineering, **Dr. CH.Venkaiah,** Associate Professor, Department of Electrical Engineering and **Dr. R.V.B. Subramanyam,** Professor, Department of Computer Science Engineering for their detailed review, constructive suggestions and excellent advice during the progress of this research work.

I also appreciate the encouragement from teaching, non-teaching members, and fraternity of Department of Electrical Engineering of NIT Warangal. They have always been encouraging and supportive.

I wish to express my sincere thanks to **Prof. N.V. Ramana Rao**, Director, NIT Warangal for his official support and encouragement.

I convey my special thanks to contemporary Research Scholars Mr. Rahul Jammy, Mr. Laxman B, Mr. Vikram Raju G, Mr. Sachidananda Prasad, Mr. Sreenivasa Ratnam C, Mr. Pranay Kumar A, Madhukishore CH and also M Tech (Power System) students Dattu D (2018), Rundan M(2018), Arun Kumar (2018) and Aravind Goud (2019). I acknowledge my gratitude to all my teachers and colleagues at various places for supporting me to complete the work.

My special, sincere acknowledge, heartfelt gratitude and indebtedness are due to my parents **Shri. Annamraju Sai Kumar** &**Smt. A. Syamala Rani**, my brother **Mr. A. Manoj Kumar** and other family members for their sincere prayers, blessings, constant encouragement, shouldering the responsibilities and moral support rendered to me throughout my life, without which my research work would not have been possible. I heartily acknowledge all my relatives for their love and affection towards me.

Above all, I express my deepest regards and gratitude to "**ALMIGHTY**" whose divine light and warmth showered upon me the perseverance, inspiration, faith and enough strength to keep the momentum of work high even at tough moments of research work.

Annamraju Anil Kumar

Ж

ABSTRACT

Emerging renewable power generations such as photovoltaic, geothermal, bio, ocean, and wind are gaining much attention in the present power system scenario due to dwindling conventional energy resources and increasing environmental concerns. Among these, photovoltaic (PV) and wind power generation has witnessed an exponential increase during the last decade due to their reduced installation cost and deserved a top two places with an overall global installation of 1312 GW capacity by 2020. Despite the advantages, the increasing penetration of wind power and solar power into power systems poses new technical challenges, mainly on power system reliability and stability. The primary objective of power system operation is to ensure reliability and quality of supply. One of the key actions that assists in the fulfillment of this objective is load frequency control (LFC).

Primarily, LFC is an automatic action that aims to restore system frequency and net tie-line powers between a control area and its neighbors to their nominal values. These variables deviate when there is a mismatch between generation and power demand in an interconnected power system. Diversity in generation, functional complexity, continuous change of structure, and volatile nature of output power are known as some critical characteristics of renewable energy sources. These characteristics introduce new technical challenges concerning the secure operation of the power system, particularly in load frequency control (LFC). A comprehensive review of the LFC literature in terms of the strengths and weakness of various control techniques are presented to identify the key gaps. Literature survey divulgs that the AI techniques, in particular, fuzzy logic based controllers can bring some added advantages under renewable environment, but its key strengths are still underexploited. Concerning it, this thesis aims to investigate various AI techniques for LFC problems in autonomous microgrid and even for the main grid under the renewable environment, which is becoming a challenging task.

In the first half of the thesis, a mathematical model for an autonomous microgrid (MG) with various energy sources has been developed. Later, to control the MG frequency deviations, a recently developed grasshopper optimization algorithm (GOA) is applied to fine-tune the proposed PID controller gains. The performance of the proposed GOA-based method is

demonstrated on an isolated microgrid and are studied under various operating conditions. The scenarios include sun irradiance, variations in wind speed, and load fluctuations employing real site measurements. The results obtained with the proposed GOA-PID controller are compared with that of the conventional PID controller, Social Spider Optimization(SSO) based PID controller, and well known Genetic Algorithm(GA) optimized PID controller for validation.

Furthermore, the limitations encountered by GOA optimized PID controller in MG frequency control are addressed by the developed novel two-stage adaptive fuzzy approach. Due to the intrinsic MG characteristics, conventional control may fail to meet the specified frequency control objective in the MGs. To address the above issues, this work proposes a novel adaptive fuzzy PI controller. The feasibility of the proposed controller is demonstrated on BELLACOOLA MG, Canada. The objective function is to minimize the frequency deviations and ensures the robustness of the proposed controller against various critical operating scenarios. Time-domain simulations of the proposed controller are compared with that of the conventional PI controller, GOA-PI controller, Fuzzy-PI controller and Adaptive Fuzzy-PI controller for validation of the results.

Later, the second half of the thesis, proposes a novel coordinated control strategy between conventional power sources and plug-in hybrid electric vehicles (PHEVs) for load frequency control of a renewable penetrated main grid. Where, the coordinated control strategy is based on the PID controller, which is optimally tuned by the recently developed JAYA Algorithm (JA) to minimize the frequency deviations of the power system. In this work, an optimal trade-off is established between conventional sources and PHEVs. The feasibility of the proposed methodology is demonstrated on the IEE Japan East 107-bus-30-machine power system. The Japanese power system includes conventional power sources with inherent nonlinearities, and RESs (i.e., solar and wind energy). To prove the effectiveness of the proposed coordinated control strategy, the results have been compared with both: the optimal load frequency control (JA-PID controller) with/without the effect of PHEVs.

Furthermore, the limitations encountered by the JAYA algorithm optimized PID controller in the main power system are addressed by a developed novel adaptive fractional order fuzzy PID approach for extensive LFC analysis. Since the performance of the controller depends on its parameters, optimization of these parameters can play a significant role in promoting the output performance of the LFC control; hence, a recently developed TLBO algorithm is utilized for the adaptive tuning of the non-integer fuzzy PID controller coefficients. The effectiveness of the proposed controller is demonstrated on the IEE Japan East 107-bus-30-machine power system. The performance of the proposed controller is evaluated by using real-world wind and solar radiation data. Finally, the extensive studies for different scenarios are presented in order to prove that the proposed controller tracks the frequency with lower frequency deviations and fast settling time. Moreover, the proposed controller is more robust to various uncertainties in the power system, RES and energy storage devices in comparison with the prior-art controllers used in the literature.

From the last three decades, many research works have been reported on the LFC problem on conventional and deregulated power systems. Due to structural changes and complexities in modern power systems, still, there is further scope in extensions and improvements of LFC schemes under a renewable environment. In this thesis, various AI techniques have been presented and improved dynamic response and robust performance obtained for microgrid and the main grid.

Table of Contents

List of Figures

List of Tables

Abbreviations

ACE	Area Control Error
ACE*	Change in Area Control Error
AFLA	Adaptive fuzzy logic Approach
AI	Artificial Intelligence
ANFIS	Adaptive Neuro Fuzzy Inference System
ANN	Artificial Neural Networks
BESS	Battery Energy Storage System
BFO	Bacterial Foraging Optimization
BHO	Black Hole Optimization
CPS	Conventional Power Sources
CSA	Cuckoo Search Algorithm
DE	Differential Evolution
EMs	Evolutionary Methods
ESSs	Energy Storage Systems
FA	Firefly Algorithm
FC	Fuel cell
FF	Fitness Function
FLA	Fuzzy Logic Approach
FLC	Fuzzy Logic Control
FOC	Fractional Order Control
FO-FLC-PID	Fractional Order Fuzzy Logic Control PID
FO-PID	Fractional Order PID
FPA	Flower Pollination Algorithm
Freq	Frequency
GA	Genetic Algorithm
GOA	Grasshopper Optimization Algorithm
GRC	Generation Rate Constraint
GWO	Grey Wolf Optimization
IAE	Integral Absolute Error

IMC	Internal Model Control
IOPID	Integer Order PID
ISE	Integral Square Error
ITAE	Integral-of-Time-Multiplied Absolute Error
JA	JAYA Algorithm
lb	Lower Bound
LFC	Load Frequency Control
MFs	Membership Functions
MAPS	Multi-Area Power System
MG	Microgrid
MIMO	Multi Input Multi Output
MPC	Model Predictive Control
NL	Negative Large
NM	Negative Medium
NS	Negative Small
PFC	Primary Frequency Control
PHEVs	Plug-in Hybrid Electric Vehicles
PID	Proportional-Integral-Derivative
PL	Positive Large
PM	Positive Medium
PS	Positive Small
PSO	Particle Swarm Optimization
PUS	Peak Undershoot
POS	Peak Overshoot
PV	Photo Voltaic
rand()	Random Value Between 0 and 1
RES	Renewable Energy Sources
RFBs	Redox Flow Batteries
sec	Seconds
SFC	Secondary Frequency Control

SG	Synchronous Generator
SISO	Single Input Single Output
SMES	Superconducting Magnetic Energy Storage
SOC	State of Charge
SSO	Social Spider Optimization
TF	Transfer function
TLBO	Teaching Learning Based Optimization
ub	Upper Bound
V2G	Vehicle to Grid
WTG	Wind Turbine Generator
ZE	Zero
Z-N	Ziegler- Nichols

List of symbols

A_i	Wind advection
ACE_1, ACE_2	Area control error in area-1 & area-2
β	Frequency response characteristics of MG
β_1, β_2	Frequency bias factors of area-1, area-2
c	Adaptation factor
c_{min}, c_{max}	Acceleration factor minimum and maximum limits
d	Search dimension
D	Load damping coefficient of autonomous MG
D_1, D_2	Load damping coefficient of the area-1 & area-2
D_{ij}	The distance between the i^{th} and j^{th} grasshopper
$\widehat{e_w}$, $\widehat{e_g}$	The unit vector in the direction of the wind &ground
Δf	Frequency deviation of autonomous MG
Δf^*	Change in frequency deviation of autonomous MG
$\Delta f_1, \Delta f_2$	Frequency deviation in the area-1 & area-2
Δf_l	Lower frequency dead band of PHEV aggregator
Δf_u	Upper frequency dead band of PHEV aggregator
G_i	i^{th} grasshopper Gravity force
G	Gravity constant
K_P, K_I, K_D	Gains of the proportional, integral and derivative controllers
K_{BESS}, K_{FC}	Gains of BESS, FC
K_{PV}, K_{WTG}	Gains of PV model, WTG
K_{RFB}	Droop constant of RFB
K_e	Scaling factor of MFs of input1
K_{ce}	Scaling factor of MFs of input2
K_{u1}	Scaling factor of MFs of output1
K_{u2}	Scaling factor of MFs of output1
K_P	Gain constant of power system
M	Moment of inertia of autonomous MG

M_1, M_2	Moment of inertia of the area-1 & area-2
N_A	Number of PV arrays
N_G	Number of wind generators
N_{EV}	Number of electric vehicles
N_{pop}	Population size
P_{solar}	The panel rated power at standard operating conditions
P_{PV}	Solar output power of PV array
$\Delta P_{DEG1}, \Delta P_{DEG2}$	Change in DEG output power in area-1 & area-2
ΔP_{PHEV}	Change in PHEV output power
ΔP_{RFB}	Change in the RFB output power
ΔP_{WTG}	Change in wind turbine generator output power
ΔP_{Solar}	Steady state change in solar power output
ΔP_W	Wind power changes
ΔP_{MG}	Change in microgrid power
ΔP_{DEG}	Change in DEG power
ΔP_{FC}	Change in fuel cell power
ΔP_L	Change in load
ΔP_{BESS}	Change in BESS power
ΔP_{PV}	Change in solar power
ΔP_{WF}	Change in wind farm output power
ΔP_G	Change in governor position of SG
ΔP_C	Change in speed changer setting of SG
ΔP_{GEN}	Change in SG output power
ΔP_D	Change in load demand
$\Delta P_{tie,12}$	Tie-line power deviations between area-1 & area-2
$\Delta P_{tie,1j}$	Tie-line power deviations between area-1 & area-j
$\Delta P_{L1}, \Delta P_{L2}$	Change in load profile in the area-1 & area-2
R	Speed regulation constant of DEG
R_{SG}	Speed regulation constant of SG
$1/R_1, 1/R_2$	Droop characteristics of area-1 and area-2
r_1, r_2, r_3	Random numbers between 0 - 1
S_i	Social interaction of the i^{th} grasshopper
T_1	Time constant of governor
T_2	Time constant of transport delay
T_3	Time constant of diesel generator

T_{DEG}	Time constant of DEG
T_{BESS},T_{FC}	Time constant of BESS and FC
T_P	Time constant of power system
T_{WTG},T_{PV}	Time constant of WTG and PV
T_{SG}	Governor time constant of SG
T_{ST}	Turbine time constant of SG
T_s	Settling time
U_{c1}, U_{c2}	Command signal to the governor in area-1 & area-2
u	Drift constant
U_f	Updating factor from fuzzy logic controller
U_c	Control signal fed to the governor of DEG
$U(s)$	Controller output
V_{rated}	Rated wind speed
V_{cut-in}	Cut-in voltage
V_{cutout}	Cut-out voltage
V_N	Equivalent voltage at N^{th} area
V_W	Wind velocity
ΔV_W	Change in wind velocity
ΔX	Change in valve position of DEG and Steam Turbine
ΔY	Change in valve position of hydro turbine
λ & μ	Fractional integrator and differentiator operators
φ_{STC}	Reference sun irradiance (1000 $^{w}/_{m^2}$)
φ	Solar irradiance
δ_N	Relative load angle of N^{th} area

Chapter 1

Introduction

In this chapter, a general introduction on Load Frequency Control (LFC), basic loops in LFC and mathematical modelling of a single area and multi-area interconnected power systems (MAPS) are presented. Later, the challenges in LFC of the power system under renewable environment are briefly evaluated and the scope for the present thesis work will be stated. Furthermore, the main contributions of the current thesis are briefly presented with a workflow diagram and finally, the organization of various chapters in the thesis will be outlined.

1.1 Load Frequency Control

In power systems, the LFC problem has a long history and it is one of the key topics in the research to study the dynamics of the power system. LFC plays an essential and important role in maintaining power system stability and reliability at an appropriate level against various power system uncertainties. Recently, LFC gained much importance and attention due to the structural changes in power systems, the variable nature of energy sources, and increased complexity in the operation of interconnected power systems. The smooth operation of power systems requires the matching of total power generation with the load demand. Frequency is the parameter that describes how the generation is close to load. Frequency deviation in the power system is a direct consequence of the mismatch between the load demand and the power generation. As the load diverged from the normal value with a small amount, the operating points of power system change, and hence, the system may experience frequency deviations and net tie-line power flow deviations with neighbouring areas, which may lead to undesirable effects [1]. A long-term system frequency deviation from the rated value (50Hz or 60 Hz) is harmful to the secure operation of the power system and it causes following problems such as:

i. Most of the rotating machines and AC motors run at some speeds that are directly related to system frequency. So, with the change of frequency of the power circuit, the induced Electro Motive Force (EMF) and the speed of the motor may vary.
ii. For some types of steam turbines, certain rotor states undergo excessive vibration when operating frequencies go below 49.5 Hz and above 50.2 Hz.
iii. The change in frequency over a long-time can produce harmonics in power converters and hence more chances for mal-operation of power converters.

iv. For power stations running in parallel, there is a chance to lose synchronization, so, the frequency of the network must remain constant for synchronization of generators.

The primary objectives of the LFC in a power system are:

a. To maintain the system frequency to the specified rated value against various disturbances.
b. To maintain the net tie-line power flow between the control areas at the scheduled values [2].

1.2 Basics of LFC Loops

LFC system consists of a primary frequency loop (PFC) and secondary frequency control (SFC) loops. Small frequency deviations (higher than the speed governor dead band) can be attenuated by the natural governor response called PFC. The SFC mechanism uses an additional controller to restore area frequency to the rated value. In each area, an LFC mechanism is there to monitor the system frequency and tie-line power exchanges with other neighbouring areas [3]. A linear combination of these two variables is called area control error (ACE). To maintain the stability of the power system, both area frequency and exchanging tie-line power should be maintained within the nominal values against various power system disturbances. In the power system, this problem is known as LFC [4].

Besides a PFC, most of the large SGs are equipped with an SFC loop, i.e. LFC loop. Fig. 1.1 depicts the schematic model of SG equipped with PFC and LFC loops [2]. Where the speed governing system senses the change in speed (frequency) via the PFC and LFC loops. Based on the speed governor signal, the hydraulic amplifier provides the required mechanical force to position the main valve against the high hydro or steam pressure and the speed changer provides a steady-state output power signal to the turbine.

In a control area, each SG is associated with a speed governing mechanism and provides primary frequency support. Irrespective of the location of the change in load demand, each SG in an area has to contribute to frequency support depending on their droop characteristics. However, PFC helps to arrest in initial large frequency deviations but it does not restore the frequency to the nominal value. Hence, an SFC loop is required to restore the frequency to the nominal value which is called an LFC loop [3]. This loop consists of a dynamic controller to

restore the frequency by eliminating the steady-state error, which is usually a PI or PID controller.

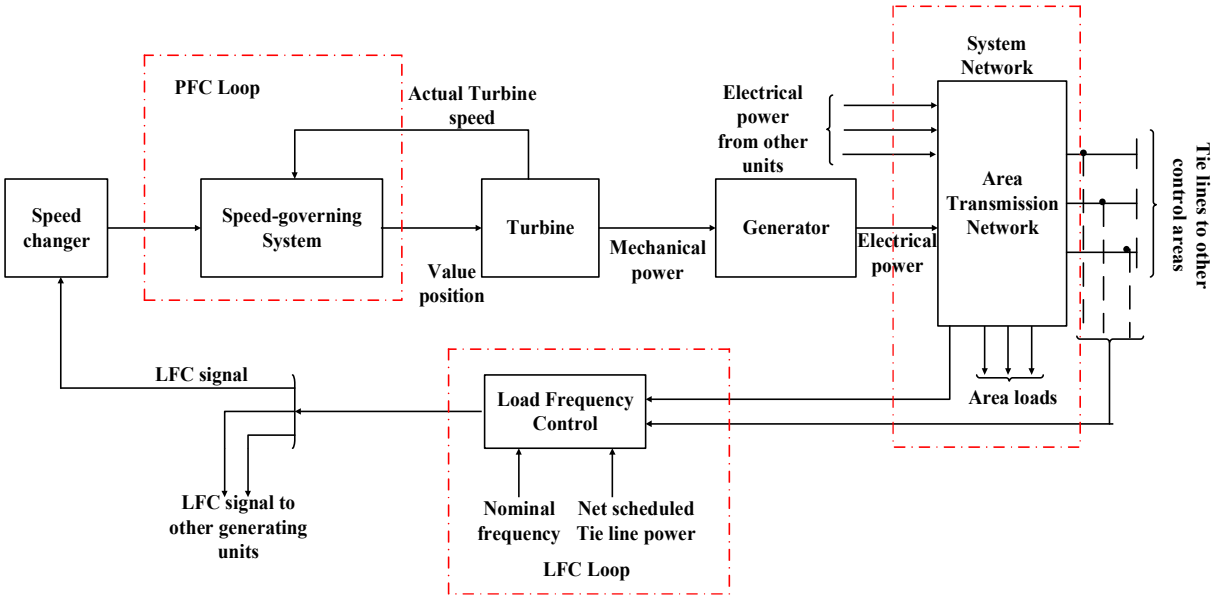

Fig. 1.1 Schematic block diagram of synchronous generators with basic frequency control loops

1.3 Mathematical Modelling of Frequency Control Loops

Power systems constitute highly dynamic, nonlinear, time-varying, and complex nature components. For frequency response analysis and synthesis against load disturbances, a simple first-order linearized model is used. In contrast to rotor angle and voltage dynamics, the frequency dynamic response is relatively slow which varies in the range of several seconds to minutes.

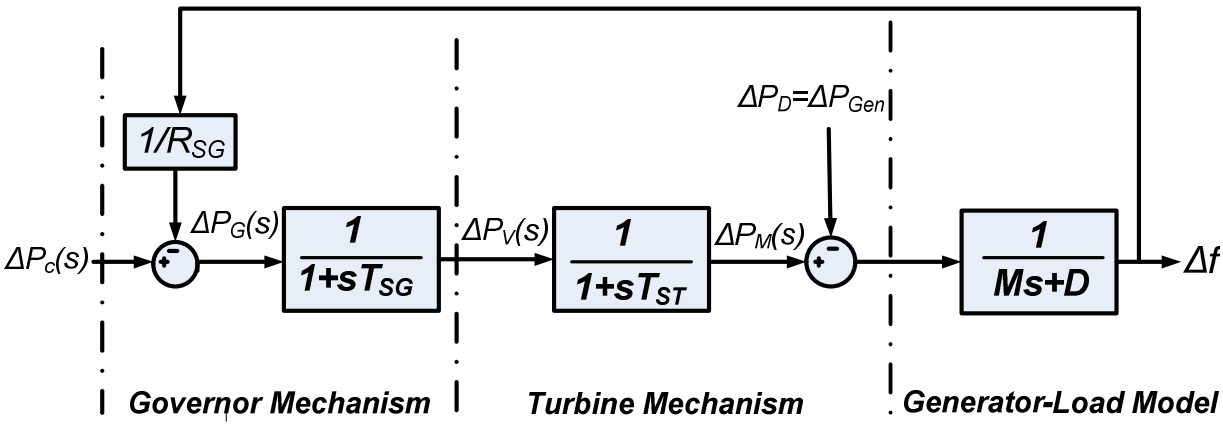

Fig. 1.2 Mathematical Model of SG with PFC loop

In this section, a simplified frequency response model of SG in terms of PFC and LFC loops are described. However, it can be considered as a single area power system. Fig. 1.2 shows the mathematical model of SG with the PFC loop [2].

For a change in frequency deviation (Δf) due to a random change in load disturbance (ΔP_d), the change in governor position (ΔP_G) according to speed changer setting (ΔP_c) can be expressed as:

$$\Delta P_G = \Delta P_C - \frac{1}{R_{SG}} * \Delta f \tag{1.1}$$

where 'R_{SG}' denotes the speed regulation constant of SG. This can be defined as the ratio of frequency deviation with respect to power output.

The Eq. (1.1) can be expressed in the laplacian form as:

$$\Delta P_G(s) = \Delta P_C(s) - \frac{1}{R_{SG}} * \Delta f(s) \tag{1.2}$$

The speed governor transfer function can be expressed as:

$$\frac{\Delta P_V(s)}{\Delta P_G(s)} = \frac{1}{1+sT_{SG}} \tag{1.3}$$

Where 'T_{SG}' denotes the governor time constant of SG and this value varies with the rating of the machine.

The change in turbine output power (ΔP_M) with respect to change in valve position (ΔP_V) can be expressed as:

$$\frac{\Delta P_M(s)}{\Delta P_V(s)} = \frac{1}{1+sT_{ST}} \tag{1.4}$$

Where 'T_{ST}' denotes the turbine time constant of SG and this time constant of the generator varies with the rating of the machine and type of turbine.

The generator power (ΔP_{Gen}) increment depends on the change in a random load disturbance (ΔP_D) being fed from the generator. These adjustments are instantaneous compared to the governor and turbine output power. Therefore, it can be written as:

$$\Delta P_{Gen} = \Delta P_D \tag{1.5}$$

The simplified mathematical model of the power system can be expressed as:

$$\frac{\Delta f(s)}{\Delta P_M(s)-\Delta P_D(s)} = \frac{1}{Ms+D} = \frac{K_P}{1+sT_P} \tag{1.6}$$

where $'K_P'$ (i.e. *1/D*) is the power system gain, '*M* ' is the moment of inertia, $'T_P'(\text{i.e.}\frac{M}{D})$ is the time constant of the power system and $'D'$ is the damping coefficient which represents the frequency-dependent loads under that SG.

Fig. 1.2 depicts the mathematical model of PFC response of a single area power system without any supplementary LFC loop based on the above equations and results. To restore the frequency to the nominal value and move the power system to the new equilibrium point, a supplementary control action is needed with a suitable controller as shown in Fig. 1.3.

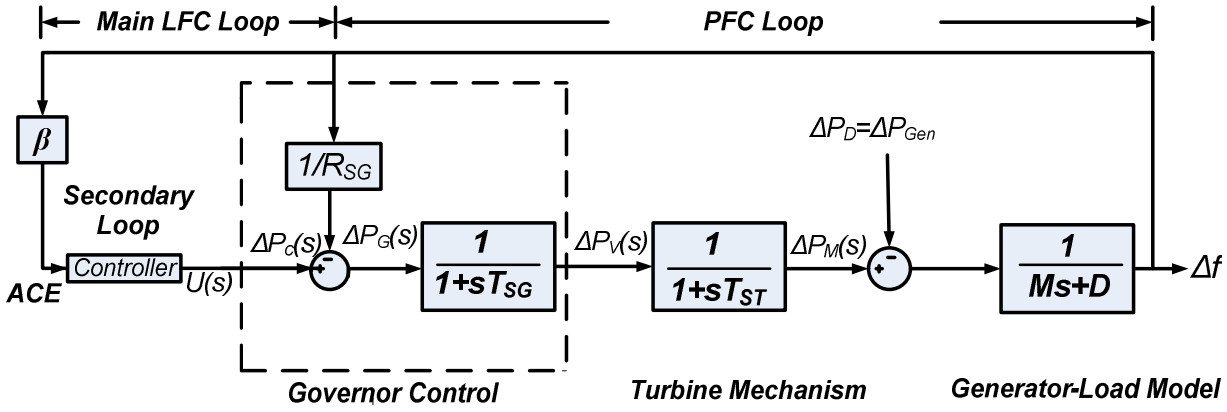

Fig. 1.3 Mathematical Modelling of SG with supplementary LFC loop

Fig. 1.3 shows the mathematical model of SG for the schematic diagram as shown in Fig. 1.1. The error signal fed to the controller is called ACE. For a single area power system, the ACE can be defined as:

$$ACE = \beta * \Delta f \tag{1.7}$$

where the frequency bias factor ('β ') in Eq. (1.7) can be defined as:

$$\beta = D + \frac{1}{R_{SG}} \tag{1.8}$$

Now the controller signal fed to the speed changer adjustments based on disturbances can be expressed as:

$$\Delta P_C = U(s)*ACE \tag{1.9}$$

where *U(s)* is the controller output. Suppose, the controller is PID, the *U(s)* can be expressed as:

$$U(s) = (K_P + \frac{K_I}{s} + sK_D)*ACE \tag{1.10}$$

Based on the controller signal, the speed changer adjusts its position and attains constant value only when the frequency reaches its rated value, i.e., frequency deviation (ACE) reduced to zero.

1.3.1 LFC Model for MAPS

For a single area/islanded power system, there would be no tie-line power control issues. The objective of LFC is to restore the frequency to the rated value. But in real-time, most of the power systems comprise multi-areas and each area is interconnected with its neighbouring areas through tie-lines. These tie-lines are usually a high voltage AC/DC transmission lines. The frequency measured in each area is an indicator of the trend of mismatch power in the interconnection and not in the control area alone. Irrespective of the disturbance in the particular control area, in interconnected power systems, each area should control its local frequency as well as interchange power with neighbouring control areas [1-3]. Therefore, the dynamic LFC model for the single area shown in Fig. 1.2 must be modified by taking into account the tie-line power signals. Fig. 1.4 shows the schematic diagram of MAPS with N control areas.

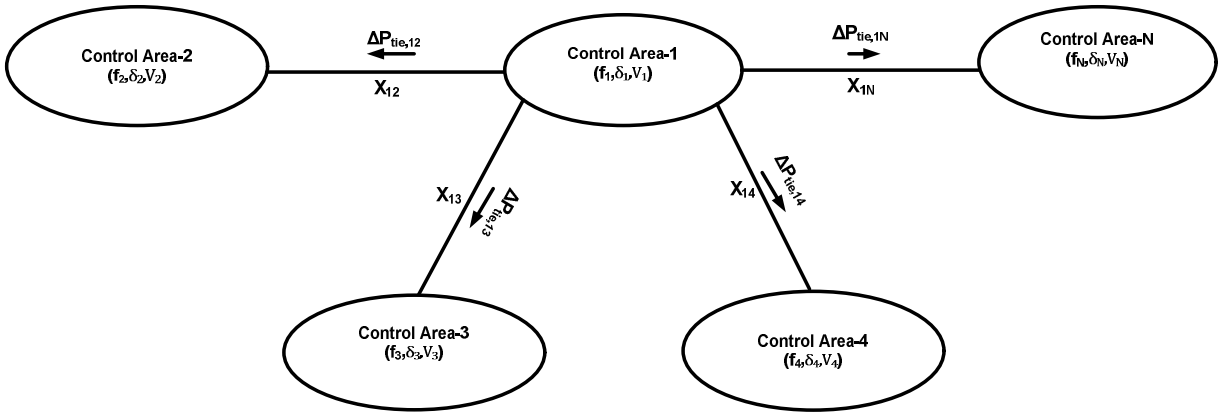

Fig. 1.4 Schematic model of power system with N-control areas

Here, for this thesis requirement, brief mathematical modelling of two-area interconnected power systems has been presented. In general, the tie-line power flow ($P_{tie,12}$) between area-1 and area-2 can be expressed as:

$$P_{tie,12} = \frac{|V_1||V_2|}{X_{12}} \text{Sin } (\delta_1 - \delta_2) \tag{1.11}$$

Where 'X_{12}' is the transmission line reactance between control area-1 and area-2. Each area can be represented by a voltage source ($V_1, V_2 - - - V_N$) with relative load angles ($\delta_1, \delta_2 - - - \delta_N$).

For a small change in δ_1 and δ_2 due to change in load, the change in tie-line power deviation($\Delta P_{tie,12}$) can be expressed as (which is obtained by differentiating Eq. (1.11) w.r.to δ_1 andδ_2):

$$\Delta P_{tie,12} = \frac{|V_1||V_2|}{X_{12}} \cos (\delta_1 - \delta_2)(\Delta\delta_1 - \Delta\delta_2) \tag{1.12}$$

The synchronizing power coefficient (T_{12}) can be defined as:

$$T_{12} = \frac{|V_1||V_2|}{X_{12}} \cos (\delta_1 - \delta_2) \tag{1.13}$$

The tie-line power deviation in terms of synchronizing power can be expressed as:

$$\Delta P_{tie,12} = T_{12}(\Delta\delta_1 - \Delta\delta_2) \tag{1.14}$$

The change in load angle in terms of frequency can be expressed as:

$$\Delta\delta = 2\pi \int_0^t \Delta f \, dt \tag{1.15}$$

By substituting Eq. (1.15) in Eq. (1.14), the tie-line power deviation in terms of frequency deviation can be expressed as:

$$\Delta P_{tie,12} = 2\pi T_{12}(\int_0^t \Delta f_1 dt - \int_0^t \Delta f_2 \, dt) \tag{1.16}$$

Eq. (1.16) can be expressed in Lapalcian form as:

$$\Delta P_{tie,12}(s) = \frac{2\pi T_{12}}{s}(\Delta f_1(s) - \Delta f_2(s)) \tag{1.17}$$

Similarly, the $\Delta P_{tie,21}$ can be expressed as:

$$\Delta P_{tie,21}\,(\mathrm{s}) = \frac{2\pi T_{21}}{s}\left(\Delta f_2(s) - \Delta f_1(s)\right) \tag{1.18}$$

From Eq.(1.16) and Eq. (1.17), $\Delta P_{tie,21}$ can be expressed in terms of $\Delta P_{tie,12}$ as:

$$\Delta P_{tie,21} = -\,\Delta P_{tie,12} \tag{1.19}$$

Likewise, the tie-line power deviation between area-1 and area-3 ($\Delta P_{tie,13}$) can be expressed as:

$$\Delta P_{tie,13} = \frac{2\pi T_{13}}{s}\left(\Delta f_1(s) - \Delta f_3(s)\right) \tag{1.20}$$

Similarly, for the N-area power system, the tie-line interconnection from area-1 can be expressed as:

$$\Delta P_{tie,1j} = \frac{2\pi}{s}\left(\sum_{j=2,3..}^{N} T_{1j}\,\Delta f_1 - \sum_{j=2,3..}^{N} T_{1j}\,\Delta f_j\right) \tag{1.21}$$

By accounting the tie-line power deviations, the ACE as shown in Eq. (1.7) can be modified for the multi-area power system as follows [3]:

$$ACE_1 = \beta_1 \Delta f_1 + \Delta P_{tie,1j} \tag{1.22}$$

For area-2, ACE can be expressed as:

$$ACE_2 = \beta_2 \Delta f_2 + \Delta P_{tie,2j} \tag{1.23}$$

Similarly, for area-N, ACE can be expressed as:

$$ACE_N = \beta_N \Delta f_N + \Delta P_{tie,Nj} \tag{1.24}$$

Fig. 1.5 depicts the mathematical model of the MAPS with tie-line power deviations. In MAPS, besides the load changes, the coherence with neighbour control areas is properly accounted for as two input signals. Each control area should monitor its frequency as well as tie-line power flows at its schedule values with neighbouring control areas.

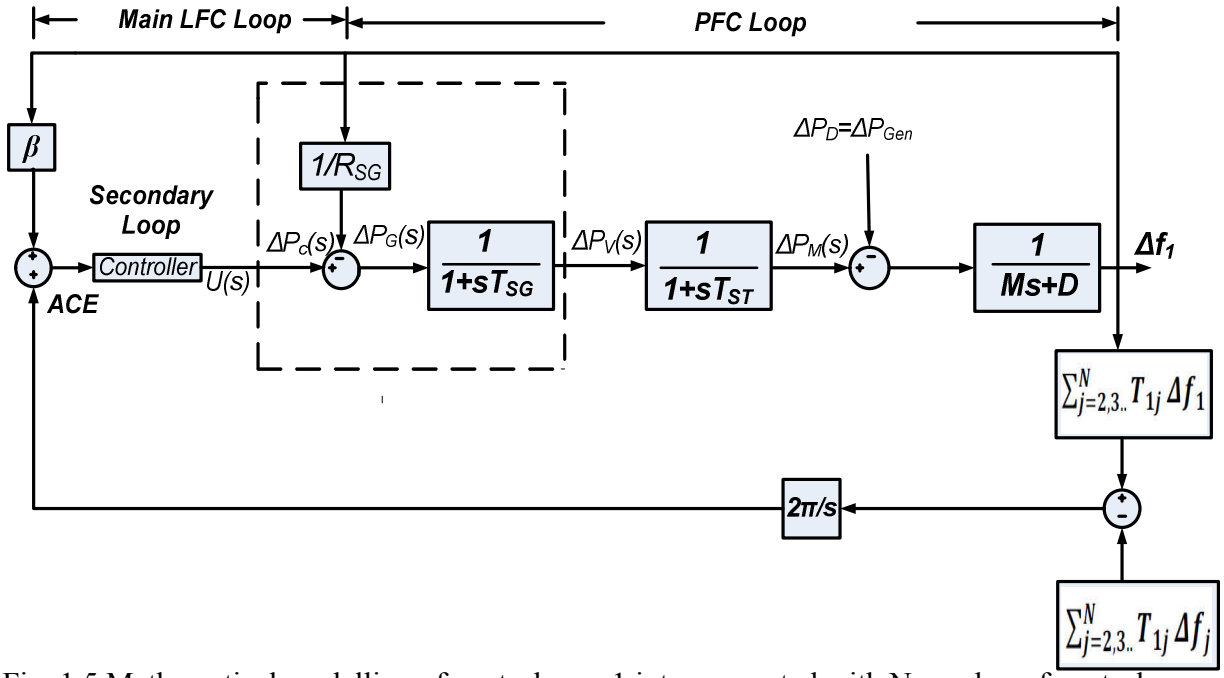

Fig. 1.5 Mathematical modelling of control area-1 interconnected with N number of control areas

1.4 Research Scope

The sizable two difficulties that the world is facing today are environmental changes and management of the dwindling conventional power sources (CPS). To secure the future, for the present and the next generation, the energy consumption from CPS and the emission of greenhouse gasses is to be reduced [5]. Moreover, the CPS has the following drawbacks; first and foremost, most of the CPS depends on fossil fuels, which increases CO_2 emissions. Second, the increasing need for electrical energy to distant locations from long transmission lines can cause voltage drops, power losses, and also it is cost-effective. Third, the CPS may not provide an economically feasible solution to islanded communities. For the aforementioned problems, renewable energy sources (RES) would be a viable alternative solution. With the concern to the above factors, the penetration of RES into the power system is increasing day by day, and it has reached around 12% (excluding hydropower) all over the world by 2017. The United Nations Framework Convention on Climate Change (UNFCCC), Paris has placed urgency for 22% penetration of renewable energy in the electricity market by 2022. From the global energy reports, by 2030, many countries around the world want to replace 50% of their CPS (based on fossil fuels) with RES [6]. The drives for RES in modern power system are:

- ❖ Rapid growth in energy consumption
- ❖ Migration of energy consumption to Electricity
- ❖ Depleting conventional reserves
- ❖ The increasing cost of fuel (to remote locations and islands)
- ❖ Need for reducing emissions (Climate changes and Green earth movements)

Despite the advantages of RES, the increasing penetration of RES into a power system poses new technical challenges and its impacts on power system reliability and stability [7]. This is because their power outputs mainly depend on weather conditions and seasons, which are completely uncontrollable and associated with high forecasting errors. The frequency excursions caused by RES depend on the amount of RES penetration with regards to the total electrical power production of the interconnection. However, for increasing penetration of RES in power systems, the following technical challenges arise for the LFC problem:

1. In RES penetrated power systems, due to the volatile nature of RES power output and gradual changes in load leads to large fluctuations in the system frequency.
2. In addition to the above problem, high penetration of RES reduces the system inertia with the use of more inverter associated generating units, which makes the system frequency more sensitive to the disturbances [8].

Besides the factors mentioned above, the stochastic nature of the load, power system nonlinearities, constraints and uncertainties make the LFC problem more complex in renewable penetrated power systems. Therefore, modern power systems need more robust, efficient, and intelligent LFC approaches to handle such problems [9].

Recently, the application of artificial intelligence to various power system problems has shown that it can improve the dynamic performance of the system. However, the application of AI techniques in particular fuzzy logic based controllers can bring some added advantages under renewable environment and complex power systems, but its strengths are to be exploited. In light of the above, researchers motivated to make application of a more practical and promising form of AI techniques for LFC studies [10]. This is systematic, reliable, and more practical to implement for modern power systems.

Apart from advances in control concepts, from the last decade, there have been many structural changes in power systems like RES in the main power grid, microgrids (MGs) for distant places, ESS penetration in power system has been increased [11]. Most of the works are considered

either hydro or thermal units in a control area. In light of changing power generation scenario, in this research work, it is motivated to include the more realistic combinations of multi generation-sources along with new energy storage options in the control area. This includes different sources of power generations such as thermal, hydro, wind, solar, diesel generators, and various energy storage systems like FCs, RFBs and PHEVs for accurate LFC studies in modern power systems.

1.5 Main Contributions of the Thesis

Although the LFC problem had been broadly addressed by several researchers, by considering the changes in modern power systems, there is still a lot of scope in this area. This thesis has investigated and contributed to the following aspects:

- ☑ Mathematical modelling of autonomous MG with various RES are presented.
- ☑ Mathematical modelling of two-area interconnected power systems with multi-sources of generations including RES and PHEVs are presented. In this study, all possible nonlinearities in the power system like boiler dynamics, governor dead band, generation rate constraint (GRC), and communication delays in PHEVs are also considered.
- ☑ More efficient usage of AI controllers is presented for the LFC study. Different algorithms are presented to solve the problem using MATLAB software.
- ☑ The AI techniques are presented for the LFC of i) MG and ii) Interconnected power systems under different operating conditions. The sensitivity analysis is done for variations in load conditions and RES power output. Besides, the effect of various power system parameters, constraints on the performance of the proposed controllers also studied.
- ☑ The superiority of proposed approaches is compared with some standard and recent controllers published in the literature.

In summary, four controllers have been proposed for MG and interconnected power systems and, they are summarized as follows:

I. **Grasshopper Optimization Algorithm(GOA) Based PID Controller for Frequency Control of An Autonomous Hybrid MG**

a) In this contribution, an efficient LFC method for an autonomous two-area MG system is addressed. GOA has applied to fine-tune the PID controllers.

b) It aims to improve the LFC performance and enhance robustness against various MG internal and external disturbances.

II. **Robust Frequency Control in An Autonomous Microgrid: A Two-stage Adaptive Fuzzy Approach**

a) The proposed controller gains the benefits of both the PI controller and the fuzzy logic controller. The proposed controller able to track the operational changes in MG quickly and tunes the controller according to operating conditions.

b) It is simple in control, preserves the structure of the PI controller and well suited for islanded MG frequency control applications.

c) It is capable of controlling all possible uncertainties and constraints that occur in MG simultaneously.

III. **Coordinated Control of Conventional Power Sources and PHEVs for Frequency Control of A Renewable Penetrated Power System**

a) In this contribution, a new coordinated optimal LFC strategy with a modified control signal to have PHEVs for LFC enhancement of the renewable penetrated power system has been presented.

b) An optimal trade-off is established between PHEVs and CPS with JAYA optimized PID controller.

c) The impact of PHEVs on various levels of frequency control loop has been analyzed. It facilitates that PHEVs can be used as an ancillary service in secondary frequency control with less frequency deviation.

IV. **Design of an Adaptive Fractional Order Fuzzy PID Controller for Frequency Control of Renewable Penetrated Power Systems**

a) In this contribution, a novel controller is proposed by combing the fuzzy logic approach and fractional order PID controller.

b) The proposed combination aims to improve the frequency response under nonlinearities, stochastic variations in load, RES and disconnection of PHEVs and system perturbations.

The work flowchart for the proposed thesis is shown in Fig. 1.3.

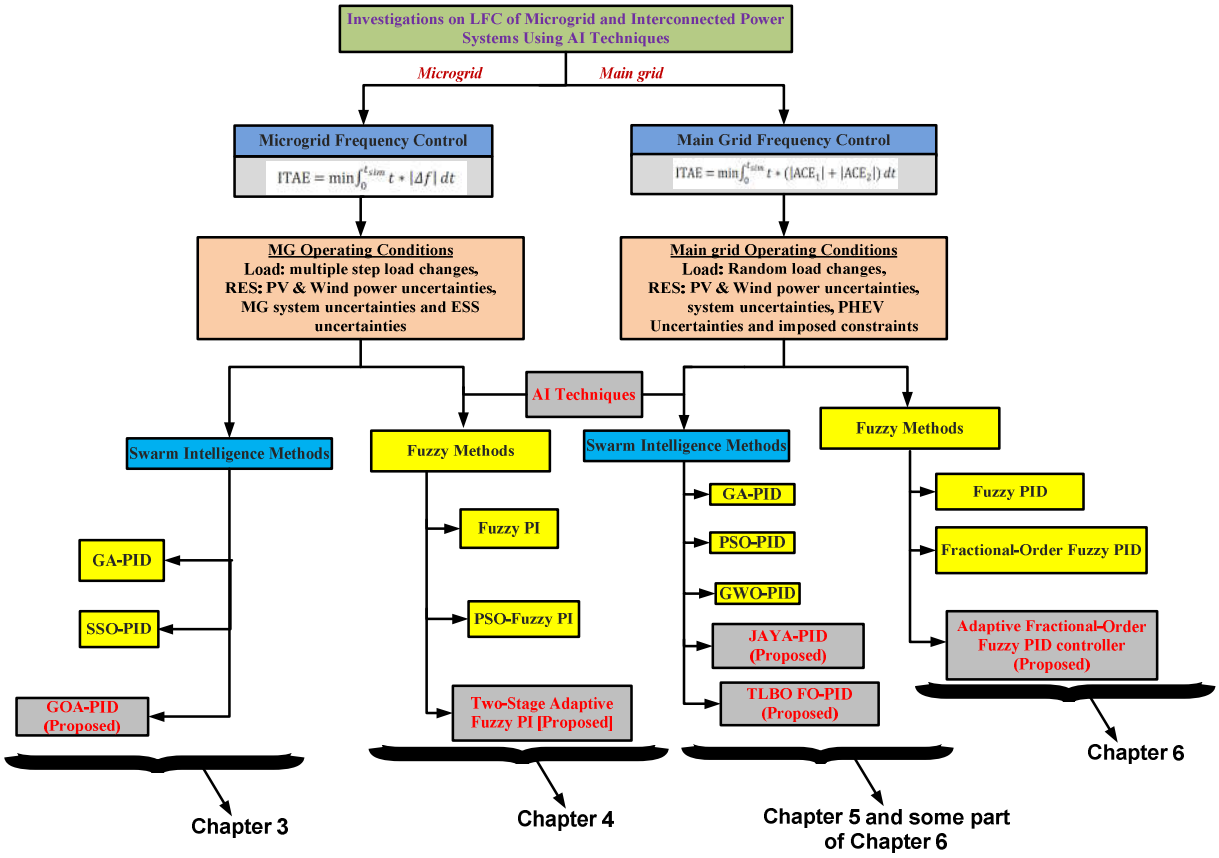

Fig. 1.6 Flow diagram of thesis work

1.6 Organization of Thesis

The thesis is organized as follows:

Chapter 1 describes an overview of the LFC problem in the electric power system and pertinent background to the introduction of RES and their issues in the LFC problem. The scope of the research work and the author's contribution has been summarized.

Chapter 2 presents a comprehensive literature review on various LFC schemes of conventional and modern power systems has been presented. Brief comparisons of different schemes also

given in this chapter based on minimum specifications of good LFC for modern power systems. The literature gives an overview of issues on the development of AI-based LFC schemes. This sets the tone for the development of AI-based LFC schemes for modern power systems.

Chapter 3 begins with the introduction to microgrid and challenges in microgrid frequency control. The mathematical model of a two-area microgrid is developed based on real-time wind and solar power data. The two-area MG investigated consists of a wind turbine generator (WTG), solar photovoltaic (PV) system, conventional diesel engine generator (DEG), and redox flow batteries. To control the MG frequency deviations, a recently developed grasshopper optimization algorithm (GOA) is applied to optimize the parameters of the PID controller. The performance of the proposed GOA-PID controller is demonstrated on a stand-alone microgrid complete with different operating scenarios. The scenarios include load fluctuations, variations in wind speed, and sun irradiance employing real site measurements. The results obtained are compared with the Z-N PID controller, well known GA-PID controller and recently developed SSO-PID controller for validation.

Chapter 4 proposes a novel two-stage adaptive fuzzy logic based PI controller for extensive load frequency control (LFC) analysis of an autonomous MG. As discussed in the literature, due to intrinsic MG characteristics, conventional controls may fail to meet the specified frequency control objective in the MGs. To address the above issues, this chapter proposes a novel adaptive fuzzy PI controller. The feasibility of the proposed controller is demonstrated on BELLACOOLA MG, Canada. The objective function is to minimize the frequency fluctuations against various disturbances and ensures the robustness of the proposed controller under various operating constraints. Time-domain simulations of the proposed controller are compared with that of the conventional PI controller, PSO-PI controller, Fuzzy-PI controller and Adaptive Fuzzy-PI controller.

Chapter 5 proposes a novel coordinated control strategy between CPS and PHEVs for LFC of a renewable penetrated power system. Where, the proposed coordinated control strategy is based on the PID controller, which is optimally tuned by the recently developed JAYA Algorithm (JA) to minimize the frequency deviations of the power system. In this work, an optimal trade-off is established between conventional sources and PHEVs. The feasibility of the proposed methodology is demonstrated on IEE Japan East 107-bus-30-machine power. The Japanese power system includes conventional power sources with inherent nonlinearities, PHEVs, and

RESs (i.e., solar and wind energy). To prove the effectiveness of the proposed coordinated control strategy, the results have been compared with both: the optimal LFC (JA-PID controller) with/without the effect of PHEVs.

Chapter 6 proposes a novel adaptive fractional order fuzzy PID controller for LFC of a renewable penetrated power system. The effectiveness of the proposed controller is demonstrated on the IEE Japan East 107-bus-30-machine power. The performance of the proposed controller is evaluated by using real-world solar radiation data and wind power data. Finally, the extensive studies over different scenarios are presented to prove that the proposed controller tracks the frequency with lower deviation and fluctuation and is more robust in comparison with the prior-art controllers used in all the case studies.

Chapter 7 summarizes the research contribution, findings, and observations on the presented research work. Then it presents the scope for the future work that can be preceded in the topic.

Chapter 2

Literature Survey

2.1 Introduction

In recent times, the load frequency control (LFC) problem under the renewable environment has been addressing by several researchers across the globe with the primary goal of maintaining the power system frequency and net tie-line power flow between each control area to the scheduled values irrespective of power system operating conditions. In modern power systems, finding the operating point is very tedious due to various power system components that constitute high non-linear characteristics. Moreover, as discussed in the earlier chapter, the intrinsic characteristics of renewables make a rapid change in operating points of the power system. The classical controllers may not give an optimal performance under the above conditions due to the fixed gains which are optimally tuned based on predetermined operating conditions. In designing an efficient controller, the following aspects of power systems like non-linear structure, working under deregulation environment, centralized structure/decentralized structure has to be considered while designing the new LFC strategies. Furthermore, various aspects related to the stochastic nature of the load, sensitivity features, and excitation control also to be studied. A considerable amount of research contribution has also been done in LFC design for an autonomous microgrid (MG) and also in interconnected power systems with various control techniques like classical, sub-optimal, and optimal control approaches. Besides these approaches, self-tuning controllers, robust controllers, variable structure controllers and adaptive controllers have been investigated for the LFC literature. Presently advancement in AI techniques like a neural network, swarm-intelligent techniques, and fuzzy logic techniques have found their appliance into the design of new LFC schemes. Introduction of these techniques has been increasing rapidly in various power system applications due to their capability to handle the uncertainties allied with renewable sources, non-linear power system components along with an insufficient mathematical model of the system. In addition to this, the impact of various energy storage systems like SMES, RFBs, PHEVs, BESS and FCs on frequency control of renewable penetrated power systems have also been considered for LFC studies.

2.2 LFC Strategies for MG and Interconnected Power Systems with Renewables

The increasing energy demand from distant places like rural areas and islands from the main grid is becoming complicated, costly, and environmentally hazardous in today's modern power system. For such conditions, an autonomous MG would be an efficient and reliable solution. Diversity in generation/load, functional complexity, variable nature of RES, and continuous change of structure are known as some intrinsic characteristics of the MGs [6]. These characteristics introduce new operational challenges with regards to the stable operation of the MG, particularly in frequency deviation control. Therefore, LFC control strategies may need to modify the different control hierarchies in order to account the intrinsic MG characteristics. Therefore, in the first half of the thesis, the main focus is on the LFC of MG. On the other hand, increasing levels of renewable power in power systems have resulted in an urgent assessment of their impact on the LFC of the main grid. The conventional LFC paradigm may not suite under these circumstances due to large instantaneous variations and uncertainty in RES output power, which limits the controllability of CPS [7]. Moreover, the governors of hydro and thermal units are not adequate to mitigate the frequency fluctuations due to their sluggish response and may make a system more sensitive to disturbances. So, to obtain desired LFC requirements in renewable penetrated power systems, the ESSs have turned into an important part in a RES penetrated interconnected power system. In literature, several authors considered various ESSs like BESS, SMES, RFBs, fuel cells, flywheel energy storage and PHEVs etc., in the design of a modern power system. However, power system and ESS constraints, renewable uncertainties, parametric uncertainties and stochastic nature of the load, challenges the control capability and stability of power systems. Therefore, in the second half of the thesis, the assessment of the impact of these factors of LFC of the main power system is studied.

2.3 Classification of LFC Control Strategies

In literature, various control strategies have been developed for the LFC mechanism of power systems. Besides the type and complexity in the power system, LFC performance highly depends on the proper design of the secondary/supplementary control mechanism. As renewable penetration growing rapidly in modern power systems over the last two decades, to enhance the LFC performance under these scenarios, many control strategies were implemented by various

researchers. In this section, a comprehensive and up-to-date review of various LFC strategies for MG and interconnected power systems are discussed. An endeavour has been made to classify the LFC strategies based on controller design techniques. The subsequent sections discuss few of them viz., section 2.3.1 focuses on the classical controllers, section 2.3.2 focuses on the optimal controllers, section 2.3.3 focuses on self-tuning and adaptive control schemes, section 2.3.4 focuses on model-based controllers, section 2.3.5 focuses on robust LFC techniques and section 2.3.6 focuses on artificial intelligent techniques. A summary of each classification in terms of its merits and demerits are given in their respective tables.

2.3.1 Conventional Control Approaches:

Conventional PI/PID controllers are mostly based on classical control theory and graphical design methods. These controllers are simple, very easy to design as well as in the implementation, particularly for single loops. The earliest works on MG and interconnected power systems were based on these classical control methods [13-22].

Ray et al. [13] proposed a conventional PI controller for frequency control of an MG, where the PI controller gains are selected by trial and error method. *Serban* et al. [14] proposed an aggregate LFC model for an MG with hydro and wind power sources. The LFC model is based on a conventional PI controller where the gains of the PI controller are tuned using the trial & error method. The impact of wind power changes and step load changes on LFC had been analyzed. The impact of BESS on frequency control with the aforementioned test conditions had been analyzed. Similarly, M*allesham* et al. [15] proposed Ziegler-Nicholas tuned PI controller for frequency control of hybrid distributed generation systems. *Datta* et al. [16] proposed an aggregate LFC model for a solar-diesel MG without any ESS. In this paper, the authors proposed a frequency control strategy from the solar side as well as from the DEG side. FLA approach is used on the solar side and a fixed gain integral controller based on the final value theorem is used on the DEG side. The impact of random load disturbances and solar power variations are considered in LFC analysis. Though the proposed controller can manage the frequency control of MG without ESS, the frequency excursions are limited moderately under certain operating conditions. However, a sensitivity analysis of RES on LFC did not perform. Similarly, *Datta* et al. [17] proposed the same control strategy (as stated in 16) for an aggregate LFC model for a wind-diesel MG without any ESS. *Anwar* et al. [18] proposed a novel PID controller based on a direct synthesis (DS) approach for LFC analysis of a single-area and multi-area power system

with nonlinearities. The frequency response matching in between the DS controller and the PID controller is done at two low-frequency points to arrive at a set of linear algebraic equations, the solution of which gives the controller parameters. The proposed method had a small computational burden and mathematical simplicity over a unified tuned PID controller.

In large power systems*, Milan* et al. [19] proposed a PID controller design based on optimal linear regulator theory, *Ota* et al. [20] proposed a PI controller based on Z-N tuned PI controller. *Khodabakhshian* et al. [21] proposed a PID controller design based on constant M-circles of Nicholas chart. The PID controller parameters are tuned such that the open-loop frequency curve follows the corresponding constant-M circle using a predetermined maximum peak resonance. The proposed controller is tested against various levels of load perturbations on a two-area power system. The proposed controller shown its fast response in terms of fast settling times and fewer overshoots compared to the Z-N tuned PI controller. Liu et al. [22] proposed the PI controller based on optimal linear regulator theory for LFC of MAPS.

Table 2.1 Concise analysis of the merits and demerits of the conventional LFC schemes

Technique	Merits	Demerits
Conventional LFC Schemes [13-22]	• These schemes are simple in structure, easy to understand, maintain and design.	• They are single-input and single-output (SISO) based and could perform poorly under MIMO based systems. Also, its capability to cope up with power system non-linearities is poor due to its fixed gains on predetermined operating conditions.

Despite the advantages of structural features and ease of implementation, these methods may not well enough for multivariable systems. Moreover, most of the conventional controllers consist of fixed gains and these gains are obtained by considering predetermined operating conditions of the system. So, for rapid change in operating conditions, conventional controllers may not provide satisfactory performance in some critical operating scenarios. A brief key summary of the merits and demerits of the conventional LFC schemes are given in Table 2.1.

2.3.2 Optimal Control Approaches

Optimal LFC control schemes are based on the optimal control theory, the main philosophy under this type of control framework is to establish a suitable control strategy that can drive the dynamic systems towards the minimal cost. These control techniques use an objective function to specify the objectives of the plant and this objective function is optimized assuming a known dynamical model of the plant. Further, a set of solutions is obtained based on the cost function minimization, which resembles the optimal gains of the controller suitable to attain the specified objectives of the LFC. The optimal control schemes have been successfully applied to LFC problems both in the MG [23-27] and the main power grid [28-32].

Yang et al. [23] proposed a dynamic event-triggered based frequency control for an autonomous MG. In this work, the impact of communication delays of various networks on LFC performance was studied. The proposed method does not require a full state matrix for LFC evaluation compared to static event-triggered frequency control. The communication intervals are enlarged with the proposed method compared to static event-triggered frequency control. Moreover, the proposed control method provided a better dynamic performance over H-∞ control method and the conventional PI control method. *Mu* et al. [24] proposed an observer-based integral sliding mode controller, *Wang* et al. [25] proposed Equivalent-Input-Disturbance method, Mehrizi et al. [26] proposed Potential-function based control for MG frequency control. *Diambomba* et al. [27] proposed an optimal controller for minimization of tie-line power flow and frequency deviations between interconnected MGs. The optimization control is based on the fmincon toolbox approach in MATLAB which is based on sequential quadratic programming (SQP) approach. The SQP is a class of iterative algorithms for solving the nonlinearly constrained optimization problem. The proposed approach attempts to solve the nonlinearities and complexities associated with the LFC of interconnected two-area MG. *Mandal* et al. [28] proposed a linear quadratic regulator(LQR) based integral controller for LFC analysis of an islanded hybrid MG.

Hanwate et al. [29] proposed an optimal PID controller design for LFC analysis. Where the PID controller design is based on quadratic regulator augmented with compensated pole approach. In the proposed approach, the compensating pole for each subsystem is derived. Based on this, the PID controller gains are obtained through quadratic regulator optimization. The

proposed controller is tested on single-area and two-area power system against step load perturbations and power system nonlinearities. *Saxena* et al. [30] proposed a PID controller for LFC analysis of a multi-area power system under different perturbation conditions. In the proposed approach, by using Kharitonov's theorem, the stability boundary locus is defined. Based on this, the optimal PID controller parameters are designed for each area. The proposed controller is tested on four area power system under different load perturbations and parametric uncertainties. Similarly, *Ray* et al. [31] designed a decentralized optimal PID controller based on the Lyapunov stability theory, *Rakhshani* et al. [32] proposed an optimal LFC strategy with a combination of output feedback control and state observer method. *Parmar* et al. [33] proposed an optimal feedback controller for LFC analysis of a multi-area power system under a deregulated environment. Unlike the other optimal controllers in literature, where the proposed controller uses few states for feedback as measurements of all state variables of the large power system is impossible to measure. The application of the proposed output feedback controller is simple, economic and pragmatic as fewer sensors are required.

Table 2.2 Concise analysis of the merits and demerits of the optimal LFC schemes

Technique	Merits	Demerits
Optimal LFC Schemes[23-33]	• Optimal schemes are systematic, simple and straight forward. These schemes have also been considered in the renewable penetrated power systems and can cope with the multivariable structure of the power systems.	• The optimal schemes are little insufficient in constraint handling capabilities hence may give an underrated performance in the presence of renewable and power system nonlinearities. Moreover, an optimal LFC scheme does not consider the system uncertainty explicitly.

Several LFC schemes proposed based on optimal control theory had been proposed in the literature to achieve better dynamic response in MG and interconnected power systems. These schemes are simple in structure, systematic in procedure, computationally efficient and less cost for real-time implementation. Nevertheless, these schemes also have several demerits. These controllers may not give optimal performance for parametric uncertainties and unmodelled dynamics. Moreover, the explicit constraint handling capabilities of these schemes are poor. A brief key summary of the merits and demerits of the optimal LFC schemes is given in Table 2.2.

2.3.3 Model Control based LFC Schemes

Model control based LFC schemes has relied on a fact that, if a controller extracts the exact dynamic model of the process to be controlled (explicitly or implicitly), at that point a superior control can be plausible. In recent times, these model-based schemes are successfully applied for power system problems like voltage control, direct torque control (DTC) and ESSs control, etc. The model control based LFC schemes like Internal Model Control (IMC) and Model Predictive Control (MPC) are also successfully applied to LFC problems both in MG and the main power grid [34-43].

Jeya Veronica et al. [34] proposed an IMC based LFC scheme for an islanded hybrid MG. The principle of IMC is based on the fact that if the control network encapsulates the model of the plant to be controlled, then a better control can be achieved. The IMC mainly classified into two modes either in disturbance rejection mode or setpoint tracking. To obtain overall control, this was approximated with a PID controller. In this work, set point tracking based IMC is used. The proposed controller is tested against various RES and load perturbations. *Jeya Veronica* et al. [35] proposed an IMC based LFC scheme for an islanded hybrid MG. In this work, the disturbance rejection mode approximation based FOPI controller is proposed. The proposed controller is tested against various RES and load perturbations. The proposed controller is compared against IMC based PI controller and Z-N tuned PI controller. *Yang* et al. [36] proposed microgrid frequency control with EVs in primary frequency control using generalized predictive theory.

Pahasa et al. [37] proposed a coordinated control of blade pitch angle of wind turbine generators and PHEVs for LFC of MG using model predictive controls (MPCs). The proposed approach reduces the number of electric vehicles to have participated in frequency control over other methods. In the proposed approach, the participation of diesel engine generators on frequency is curtailed significantly with the effective utilization of the MPC controller. *Kayalvizhi* et al. [38] proposed an adaptive MPC for LFC analysis of standalone MG. In the proposed controller, the cost function regulation factor (R) is optimized by using FLA. Various operating scenarios are considered to demonstrate the impact of the proposed controller on MG frequency control. The superiority of the proposed controller in the frequency control was compared with conventional MPC and optimal PI controllers. *Chen* et al. [39] proposed a FOMPC for LFC

analysis of MG. In the proposed controller, to obtain optimal frequency control of islanded MG, the integer order cost function in MPC is replaced with fractional order cost function in MPC. The proposed controller able to enhance the frequency response of MG under various operating scenarios such as RES fluctuations, load disturbances and parametric uncertainties compared to integer-order MPC.

Tan et al. [40] proposed a unified tuning of the PID controller based on the IMC method for the LFC problem of MAPS. *Elsisi* et al. [41] proposed a coordinated control of CPS and PHEVs for frequency control of a renewable penetrated power system. An efficient MPC is proposed for frequency regulation in a smart three-area power system comprising RES and PHEVs. Two MPCs in each area are considered to adjust the input signals of the governor and PHEV to tolerate frequency perturbations subject to RES fluctuations, load disturbances and various power system nonlinearities. To obtain a better performance, the internal parameters of MPC are optimized by using the Imperialist Competitive Algorithm (ICA). Besides, the adding of PHEV has a powerful effect on the improvement of the frequency response under a renewable environment. *Mir* et al. [42] proposed an adaptive MPC for LFC, where the operational constraints for SMES for frequency control are determined with the proposed controller, and the impact of SMES in frequency control of complex MG had been analyzed. To overcome the drawbacks in generalized MPC and certain adaptive MPCs, *Mohamed* et al. [43] proposed a novel adaptive MPC for LFC analysis of power system with high penetration of wind energy. In the proposed controller, a combination of MPC and recursive polynomial model estimator (RPME) is used. In each control duration, the RPME is identifying a discrete-time online autoregressive exogenous model and MPC has to be updating the interior plant model to achieve successful nonlinear control. The proposed controller is tested on a single-area wind farm penetrated power system and simulation results revealed that proposed adaptive MPC has fast oscillation damping, decreasing variations and effective response. Moreover, the proposed controller able to handle wind energy vulnerabilities and load variations effectively compared to conventional MPC. However, in this work, conventional MPC is robust particularly in the instances of no parametric variations.

Diverse LFC schemes based on the model control approach had been proposed in the literature to achieve better dynamic response in MG and interconnected power systems. These schemes are

open, flexible and intuitive formulation in the time domain. MPCs can handle the multi-variable systems in a good manner and can handle the nonlinear systems up to some extent without modification of the controller formulation. However, these controllers associate with certain drawbacks like needs an exact mathematical model, high computational cost when more uncertainties in the systems. A brief key summary of the merits and demerits of these schemes is given in Table 2.3.

Table 2.3 Concise analysis of the merits and demerits of the model-based LFC schemes

Technique	Merits	Demerits
LFC Schemes Based on Model Control Schemes [34-43]	• Can handle the nonlinear and multivariable systems without changing the controller formulation. • Uses an optimal cost function.	• It requires an accurate dynamic model of the system. • Uncertainties and the constraints imposed on the system makes the problem very difficult to resolve. • Till now, model based controllers have not guaranteed its stability.

2.3.4 Self-Tuning and Adaptive Control based LFC schemes

Self-tuning and adaptive control methods are the few methods that have a good track record in handling parametric uncertainties in various engineering problems. Adaptive control takes advantage of *a posteriori* estimates of parameter values and adapts the control law according to operating conditions of the system. Based on self-tuning and adaptive control methods, numerous LFC solutions [44-52] have been presented in the literature.

Mahdi et al. [44] proposed a model reference adaptive controller (MRAC) for LFC analysis of a hybrid MG. This paper proposed two control schemes based on the adaptive controller to track sudden load changes and smooth transfer of MG from grid-connected mode to islanded mode. First, the classical MRAC based PI controller is proposed in the DEG side. Further, neural networks are employed for further reduction in the error signal and to improve the performance of MG. *Khalghani* et al. [45] proposed a novel self-tuning PI controller for LFC analysis of MG. This proposed controller is based on the emotional learning process of the human brain. The beauty of the proposed controller is unlike other techniques intelligence is not given to the system from the outside but is acquired by the system itself. The proposed controller is tested on

MG with load disturbances and parametric uncertainties and the results are compared with fuzzy and conventional PI controllers. *Qudaih* et al. [46] proposed a coefficient diagram method (CDM) technique to enhance MG frequency response and robustness of controller tested against various uncertainties. In the proposed controller scheme, CDM and PI controllers works in parallel and parameters of the PI controller are updated according to operating conditions. Furthermore, the impact of EVs in frequency control of MG had been analyzed. Various operating scenarios had been simulated to demonstrate the effectiveness of proposed parallel CDM and PI controllers. *Hu* et al. [47] proposed a coordinated control scheme for frequency and voltage control of MG with RES and loads. First, a local-level coordinated control strategy of distributed converters is presented. Later, self-organized energy management scheme is developed to ensure smooth power transfer between the dc and ac sub-grids, power balance and stable operation of the grid. *Liu* et al. [48] proposed Linear Active disturbance rejection control (LDRC) for frequency control of islanded microgrid.

Rubaai et al. [49] proposed a self-tuning regulator for the multi-area LFC problem. In this technique, each area controller parameters are estimated by using a recursive least-squares method. The proposed controller is tested on a two-area power system under different load perturbations and parametric uncertainties. The proposed controller can reject the load disturbances with fast settling times and less overshoot compared to classical and optimal controllers. *Padhan* et al. [50] proposed a novel self-tuning PID controller for LFC analysis of a single area and multi-area power systems. The parameters of the PID controller are obtained by expanding the controller transfer function using the Laurent series and relay-based identification technique is used to estimate the power system dynamics. The proposed controller is applied on a single area power system, later extended to four area power system and tested against load disturbance along with different plant parameters uncertainty scenarios. *Hanwate* et al. [51] proposed a novel adaptive policy for LFC analysis of a single area power system. In this work, two optimal controllers are selected based on their practical LFC performance. One controller is good in overshoot reduction and the other one is good in improving settling time. The proposed adaptive policy incorporates the concept of enhancing and lowering both controller's activity by assigning them weights at every instance throughout the operation. The proposed policy provided an optimal performance with a compromised overshoot and settling time. *Grover* et al.

[52] proposed Model Reference Adaptive Controller (MRAC) for frequency control of renewable penetrated power systems.

A voluminous of LFC schemes based on these techniques proposed until now is well in meeting the desired objectives of LFC, particularly in handling the parametric uncertainties. Nonetheless, a common attribute of the schemes above is the online parameter estimation, which could be computationally time-consuming, and hence slow for complex power systems control. Moreover, biased parameter estimation or failure in parameter estimation can be detrimental for stringent power systems like MGs and renewable penetrated power systems. Furthermore, most of the proposed optimal control schemes mainly focused on driving the steady-state error to zero without accounting the transient performance, during which large frequency excursions can occur. A concise analysis of the key merits and demerits of these schemes is given in Table 2.4.

Table 2.4 Concise analysis of the merits and demerits of the self-tuning and adaptive LFC schemes

Technique	Merits	Demerits
LFC Schemes Based on Self-tuning and Adaptive control Mechanisms [44-52]	• Self-tuning and adaptive schemes work quite well for some limited conditions in terms of coping with parameter uncertainties.	• For large scale power systems with RES penetration and nonlinearities, the online parameter estimation is time-consuming and difficult. Moreover, a biased estimation may be baleful to the frequency control.

2.3.5 LFC Schemes based on Robust Controllers

Power system engineers are always concerned for the controller robustness concerning the perturbations and plant uncertainties. In modern power systems, on one hand, due to the variations in system parameters, there are a lot of disturbances and uncertainties. On the other hand, the power system operating scenarios may also change randomly during a daily cycle. Concerning this, various researchers have been proposed different robust control techniques with enhanced LFC performance to cope up with disturbances and uncertainties [53-61].

Singh et al. [53] proposed a Robust H-infinity controller for LFC analysis of a hybrid MG. In the proposed controller, the PSO algorithm is used to optimize the parameters of the controller like compensator gain and high pass filter time constants. In the proposed controller unstructured load, wind power and system parameters are considered as system uncertainties. The proposed

controller is tested against various loads, RES disturbances and parametric uncertainties. Moreover, the supremacy of the proposed controller is tested against GA based loop shaping of the H-infinity controller and H-infinity droop controller. Similarly, *Sedhom* et al. [54] proposed an H-∞ controller with loop shaping through the harmony search algorithm for LFC analysis of autonomous MG. *Shashi* et al. [55] proposed a new LFC scheme based on linear matrix inequalities (LMI). The parameters are tuned by using PSO, which is a new contribution to earlier studies. The robustness of the proposed controller is demonstrated with different operating conditions and parametric variations. *Pandey* et al. [56] proposed an iterative LMI approach to tune PID controller parameters subjected to H-∞ constraints in terms of iterative matrix inequality. *Bevrani* et al. [57] proposed a novel H-∞ and μ-synthesis approaches for frequency control of an islanded MG. The proposed robust approaches are flexible enough to include uncertainties in the MG model and control synthesis procedure. For both *H*-∞ and *μ-synthesis* methods, Linear Fractional Transformation (LFT) is used. In the μ-synthesis approach, the parametric perturbation is considered as both unstructured uncertainty and structured uncertainty. Whereas in *H*-∞ approach, the parametric perturbation is considered as unstructured uncertainty. The proposed controller is tested against various critical operating scenarios. Simulation results have proven that the proposed μ-synthesis approach with structured uncertainty provided a better dynamic response compared to both *H*-∞ and *μ-synthesis* unstructured uncertainty models.

Qian et al. [58] proposed an SMC for LFC analysis of a multi-area power system, where the uncertainty due to the wind energy penetration was considered; GRC nonlinearity and power system delays were also considered and represented as part of system uncertainties. The total system uncertainty was captured by a radial basis function network. The proposed controller is effective in minimization of time delays, load disturbances and wind power fluctuations. Furthermore, the proposed controller was able to maintain a stable performance against change in operating points and different levels of wind power penetration. *Pham* et al. [59] proposed a robust output feedback H-∞ controller with multiple time delays in input for LFC analysis of smart grid with RES and EVs. In this work, a new mathematical model developed which contains the dynamic interactions of electric vehicles and multiple network-induced time delays. Later, dynamic output feedback H-∞ controller for LFC of power systems with multiple time delays in the control input is proposed. In the work, unmodelled dynamics, undesirable tie-line

flows and system nonlinearities were represented as a bounded sector of uncertainties. *Shendge* et al. [60] proposed robust LFC strategy based uncertainty and disturbance estimator, *Sebastian* et al. [61] proposed second-order SMC for LFC of renewable and nonlinear power systems.

A common attribute among these techniques is their competency to cope up with multi-variable systems. Besides, these schemes work well under the bounds of uncertainty defined as delay margins for robustness against time delays or the range of parametric uncertainties. However, these techniques may preclude some practical implementation for rapidly growing modern power systems. Moreover, the controllers presented above suffer from the disadvantage of being complex and can perform optimally only when the exact mathematical model of the power system is available. Furthermore, the impact of ESS on the robustness of the controller not yet considered. A concise analysis of the merits and demerits of these schemes is given in Table 2.5.

Table 2.5 Concise analysis of the merits and demerits of the robust LFC schemes.

Technique	Merits	Demerits
Robust LFC considering either parameter uncertainty and/or system uncertainty [53-61]	• Works well under the uncertainties within the design bounds and can handle the multivariable system effectively.	• Some lead to high order fixed-gain controller hence may be impractical for large rating power systems. • Generally, these schemes are hugely conservative and hence control performance may be underperformed under certain operating conditions.

2.3.6 Artificial Intelligent Based Control Schemes

In the last two decades, Artificial Intelligent (AI) based control system design has gained considerable attention from researchers around the world due to its advantages. It offers the guarantee of a solution, low solution costs, and their practicabilities are the key features of the AI controllers. They can handle technical issues such as nonlinearities, uncertainties, and complexities effectively over other methods particularly when the exact mathematical model is not available. To achieve fast control and better dynamic performance, AI techniques have been used for optimizing the LFC parameters. More recently, with the advancement of soft

computational techniques, these objectives are effectively accomplished using AI control schemes.

AI is a type of humanly created software or machine intelligence that substantially decreases the workload of humans [62]. AI can be broadly defined as the automation process based on human wisdom, such as problem-solving, decision making, perception, reasoning and learning [63]. It is established from the literature that; AI techniques outperform conventional techniques in terms of controllability and response time. Furthermore, they are also found effective in multi-mode operation by switching between different operational modes according to the situation. It is projected that AI would stand far long in the future control architectures as it can adapt to different situations without acquiring a large amount of information. Although AI seems to outperform advanced conventional methods in terms of durability, response time, and feasibility, yet unlike conventional techniques, it needs memory to achieve the aforementioned performance. As such, the inclusion of these parameters in AI controllers makes them more expensive than other conventional techniques [62]. The AI tools of interest to the electric power research community include FLA, ANNs, ANFIS, GAs, and PSO [64]. Each of these AI techniques and algorithms has to be extensively explored in addressing LFC issues of modern power systems. The AI Techniques are mainly classified into three categories like evolutionary methods, neural networks, and fuzzy logic approach as shown in Fig.2.1. A detailed literature survey on each method is discussed in the subsequent sections.

2.3.6.1 Evolutionary Methods

Evolutionary methods (mainly swarm intelligence algorithms) are one of the main groups in AI techniques. The main objective of these methods is to find the optimal combination of variables for a particular problem to maximize or minimize the objective function. To achieve the best solution, the following steps are required to be performed. The first one is the identification of the parameters to be optimized. Second, based on the type of the problem and parameters, identify the suitable fitness function (FF), and impose if any constraints are present. Third, the objectives of the given problem should be considered and investigated. Finally, the number of objectives, identified parameters, and constraints, a suitable technique is employed to solve the optimization problem. Fig. 2.2 depicts the generalized flow chart for tuning the process of evolutionary methods.

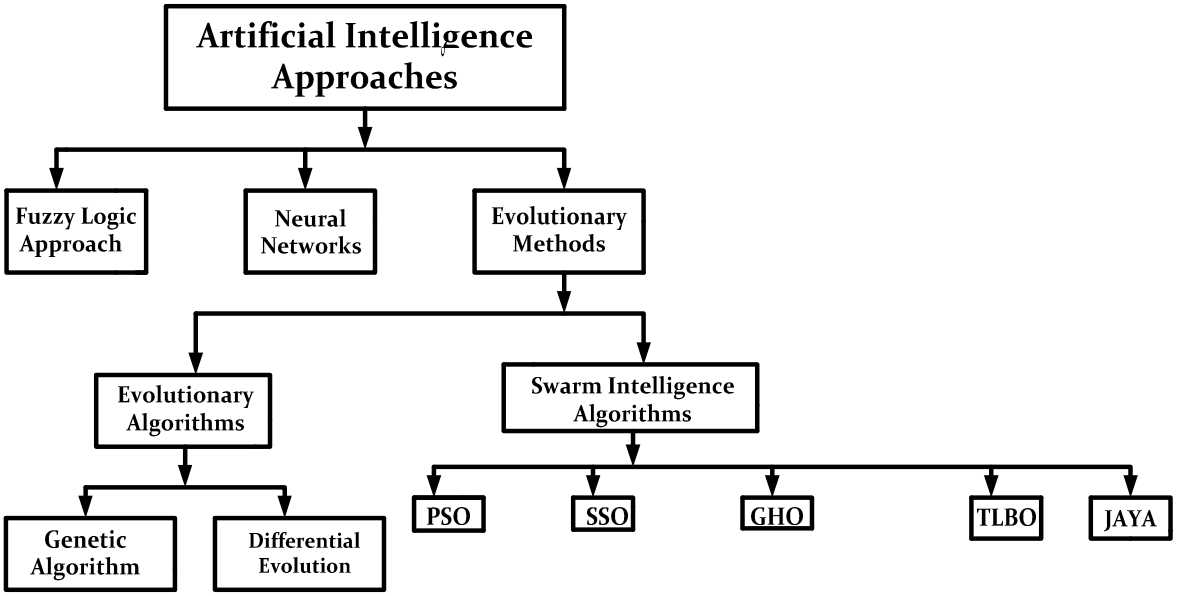

Fig. 2.1 AI-based optimization technique used to solve power quality issues in power system

In this type of method, the parameters of the selected optimization algorithm are defined ahead of the application of the optimization. Which includes population size, number of iterations, number of variables to be optimized, etc. is required to perform smooth execution. Later, based on defined FF maximize or minimize the objective function according to constraints. Based on the best solution in the population update the rest of the population and finds the best solution amongst all workable solutions in each iteration. The process of identifying the best combination of variables for a particular problem continues until it attains a suitable value or algorithm completes the maximum number of iterations. In literature, numerous evolutionary methods are available for various complex engineering problems but all may not be suitable for optimizing a particular system [65]. Therefore, the choice of an appropriate optimization algorithm for solving a particular optimization problem is also another vital issue in this regard.

Recently, various EMs are considered for LFC of modern power systems and MGs. Compared to several LFC schemes as stated in the literature above, these schemes are well coping up with modern power system LFC issues. Particularly, when time constants and gains of the power system changes due to ageing and operating conditions. The classical, optimal, and model-based controllers are not well enough to handle these uncertainties.

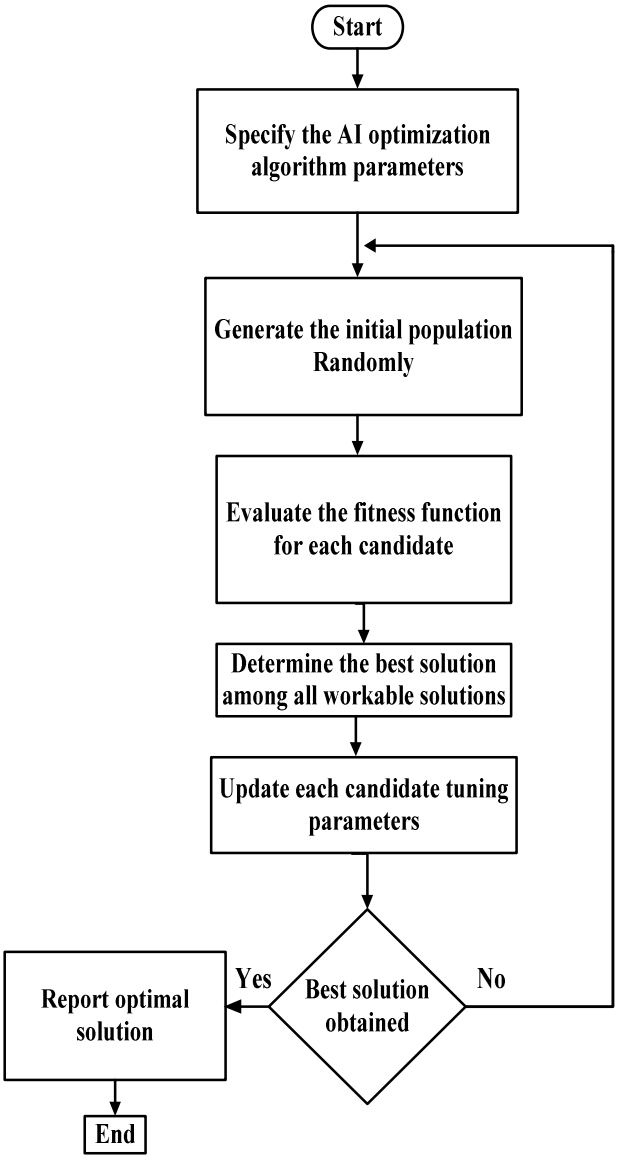

Fig 2.2 Generalized flowchart of evolutionary methods to obtain the optimal solution for a given problem

Moreover, adaptive and robust controllers can handle the uncertainties up to a level where the boundaries are well defined and may preclude some practical implementation for rapidly growing modern power systems. Therefore, to design LFC controllers substantial attempts have been made with better performance to cope up with the uncertainties and disturbances using various EMs.

- ☑ *Das* et al. [66] proposed a genetic algorithm (GA) based PID controller for frequency control of an islanded MG. Where the proposed GA-PID controller robustness against

generation and load uncertainties are shown in with different operating scenarios. Moreover, the superiority of the proposed controller in improving dynamic response in terms of settling time, overshoot reduction, and overall mean error reduction has been proven by comparing with classical and optimal controllers. However, the MG internal parameters impact did not consider in frequency response analysis. The sensitivity analysis of renewables is not considered in this work.

- ☑ *Shankar* et al. [67] proposed a quasi-opposition harmony search algorithm (QOHSA) based PID controller for frequency control of a hybrid MG. Where the proposed GA-PID controller robustness against generation and load uncertainties are shown in with different operating scenarios. The proposed controller achieved superior dynamic response over the GA-PID controller. The sensitivity analysis of renewables is not considered in this work. Moreover, the proposed algorithm associated with more algorithmic specific parameters and improper selection of these may lead to poor solutions.
- ☑ *Abdel-Hamed* et al. [68] proposed a firefly algorithm optimized PID controller for frequency control of an autonomous MG. In this paper, a novel weighted goal attainment method is proposed for fitness function by splitting the fitness function into two sub-sections. The proposed approach is to maximize the fault-tolerant operation of MG under various disturbances of MG (solar, wind, and load disturbances) individually as well as simultaneously. It improved the dynamic response of MG effectively based on the type and magnitude of disturbance. However, the computational complexity is high and the improper selection of weighting factors may move the solution from the desired target.
- ☑ *El-Fergany* et al. [69] proposed an efficient frequency controller for two-area hybrid MG using a social-spider optimizer (SSO) based PID controller. The impact of load fluctuations, variations in wind speed, and sun irradiance employing real site measurements on MG frequency control are analyzed. Sensitivity analysis of renewables had been performed and parametric uncertainties of MG also considered in the design of the proposed controller. The proposed controller does not consider the uncertainties in ESS on MG frequency control. Moreover, the number of PID controllers to be optimized are high (for two-areas: four PID controllers) and the proposed algorithm depends on its algorithm-specific parameters.

- ☑ *Ray* et al. [70] and *Sreenivsaratnam* et al. [71] proposed a firefly optimized and grey wolf optimized PID controller for robust frequency control of a hybrid MG. However, the aforementioned drawbacks in [69] are not considered in their studies.

Similarly, the evolution of PID/FO-PID controllers for the renewable penetrated power system using swarm-intelligence techniques is as follows:

- ☑ *Daneshfar* et al. [72] proposed the GA-PID controller for frequency control of IEEE 10 Generators 39 Bus System as a non-linear test case study for the large load disturbances. The impact of RES is not considered in the analysis, however, all the possible nonlinearities in the power system are considered in the studies.
- ☑ *Magdy* et al. [73] proposed the PSO-PI controller based coordinated control strategy for LFC enhancement of the Egyptian power system. In this work, the authors proposed a coordinated control strategy between CPS and SMES in a renewable penetrated power system. The proposed strategy ensured a good dynamic response owing to high-level RESs integration. In this analysis, all the possible nonlinearities in the power system are considered, however, sensitivity analysis (with different levels of RES penetration) of the proposed controller was not considered.
- ☑ *Kouba* et al. [74] proposed the GWO-PID controller based coordinated control strategy for LFC enhancement of the Japanese power system. In this work, the authors proposed a coordinated control strategy between CPS and RFBs in a renewable penetrated power system. The impact of wind farm penetration on power system frequency control has been analyzed and the effectiveness of RFBs in secondary frequency was reported. Sensitivity analysis was performed with different levels of wind power penetration.

Power system engineers always concern with improvement in system performance, robustness, and stability against various disturbances. Concerning this, fractional-order (FO) PID controllers are gaining popularity in renewable penetrated power systems, due to its added flexibility and design methodology over traditional PID controllers. In [16-21] authors proposed various EMs for tuning FO-PID controllers for LFC of renewable penetrated power systems. The FO-PID controllers have superior performance over traditional PID controllers due to its additional degree of freedom in tuning the two additional non-integer knobs (i.e. λ & μ). Therefore, FO-PID controllers can handle the power system non-linearities in a better way over PID controllers.

- ☑ *Debbarma* et al. [75] proposed a flower pollination algorithm optimized FO-PID controller for a deregulated power system by utilizing the PHEVs in the PFC loop. The impact of PHEVs had been analyzed on the PFC of the deregulated power system. The advantage of the FO-PID controller over integer-order PID controllers had been demonstrated in this work.
- ☑ *Khezri* et al. [76] proposed a sine-cosine algorithm optimized FO-PID controller based coordinated control strategy for frequency control of the renewable power system. Where heat pumps and PHEVs are utilized in primary frequency control of the smart power system. Similarly, *Saha* et al. [77] proposed a whale optimization algorithm tuned FO-PID controller based coordinated control strategy by including SMES in the PFC loop, *Shayeghi* et al. [78] proposed social spider optimization(SSO) based coordinated control strategy by including distributed generators(DGs) in PFC loop. *Mahoo* et al. [79] proposed a PSO based FO-PID controller for the LFC of renewable penetrated power systems.

The LFC schemes based on EMs until now are well in meeting the desired objectives of LFC in modern power systems. However, a common attribute of the schemes is the performance of these methods highly depends on its algorithm-specific parameters. Improper selection or tuning of these parameters may lead the solution towards the divergence or increases the computational complexity of the algorithm. A limited degree of freedom in tuning when compared to other AI techniques like FLA. A brief key summary of the merits and demerits of these schemes is given in Table 2.6.

Table 2.6 Concise analysis of the merits and demerits of the EMs-based LFC schemes

Technique	Merits	Demerits
LFC Schemes based on EMs[66-79]	• Flexible in tuning • EMs can handle MIMO systems(multi-variable optimization)effectively over previous methods	• Most of the algorithms depend on their algorithm-specific parameters • A limited degree of freedom in tuning

2.3.6.2 Artificial Neural Network (ANN) based LFC Schemes

ANN-based schemes mimic the human brain model, which has the natural ability to learn certain patterns, store them and make them use decisions certainly a similar pattern is presented. These controllers are proficient in handling the parametric uncertainties, nonlinearities, incomplete and noisy data. These techniques are extensively applied in robotics, manufacturing, pattern recognition, medicine, processing, control, and power systems [80]. A typical flowchart for the ANN-based control scheme for the LFC of the renewable penetrated power system is shown in Fig. 2.3 (a) & (b). The input variables are measured frequency and its error and output variables are usually optimized parameters of K_P, K_I or K_P, K_I, and K_D.

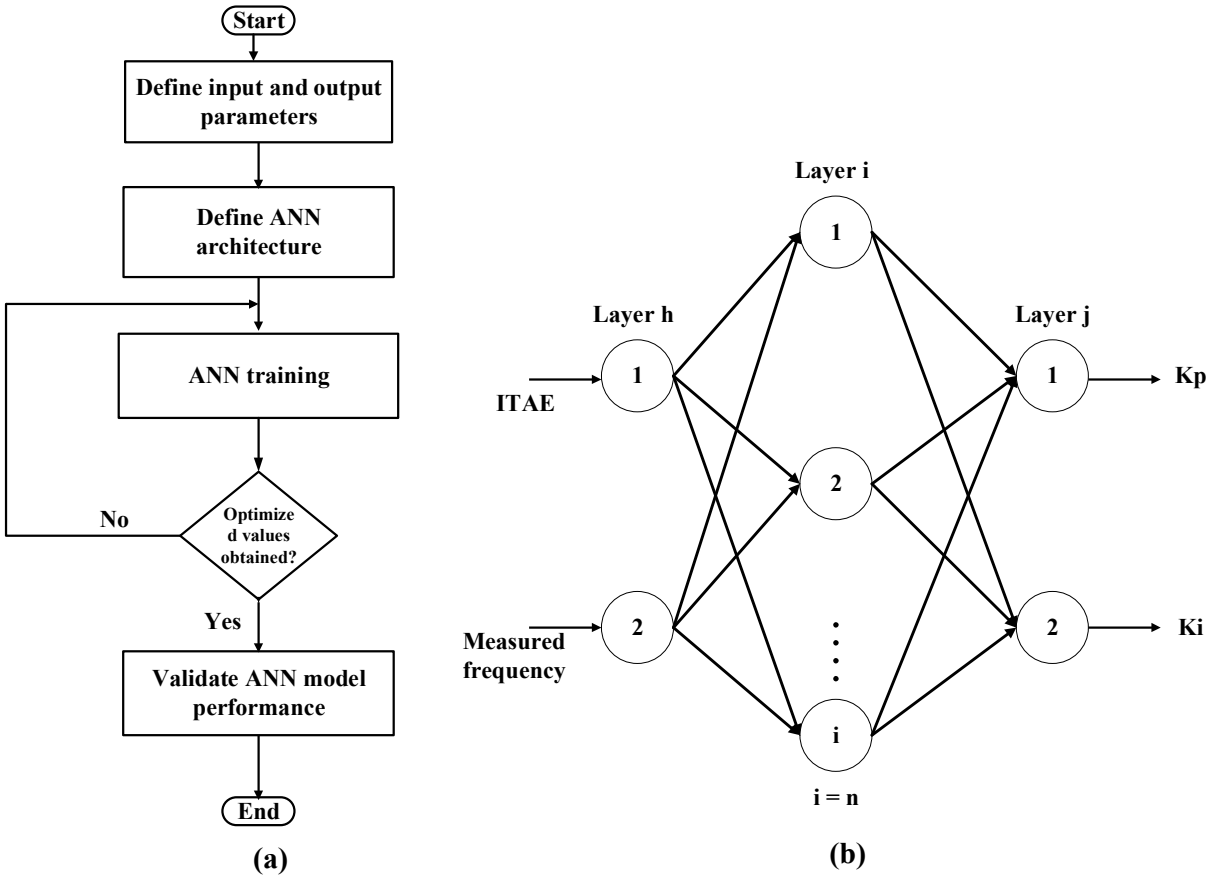

Fig. 2.3 ANN optimization Methodology: (a) A generalized ANN modelling flowchart for optimization. (b) A typical ANN structure for voltage and frequency control of islanded MG.

Recently, various ANN-based methods are considered for LFC of MGs and main grids [81-86]. *Sekhar* et al. [81] proposed an ANN-PI technique based novel frequency control method for an

MG. The proposed controller can handle both transient and steady-state frequency regulation based on load demand under different operating scenarios. *Safari* et al. [82] proposed PSO tuned ANN-based PID for an islanded MG. To enhance the performance of the proposed ANN-PID, the weights and bias-coefficients in each layer are tuned with PSO. *Bevarani* et al. [83] suggested various adaptive neural networks for robust MG frequency control which extensively used by various researchers.

Similarly, *Kumari* et al. [84] proposed a generalized ANN-PID controller for frequency control of a nonlinear power system. *Qian* et al. [85] proposed an ANN terminal-based SMC for renewable power systems. In the proposed approach, T-SMC and the radial basis function ANN works in parallel to solve the LFC problem. *Ghafouri* et al. [86] proposed a coordinated control strategy between CPS and distributed energy sources. Where the coordinated control strategy is based on an adaptive neuro-fuzzy inference system(ANFIS). In the proposed controller, neural networks are used to estimate the future behaviour of frequency based on current frequency deviation and tunes the parameters of FLC to provide an appropriate control signal.

A common attribute in ANN-based schemes mentioned above is their proficiency to ensure a good dynamic response against power system nonlinearities and parametric uncertainties. However, a general limitation with these techniques is, it operates the system as a black box and analyzes it functionally. Moreover, for each problem, it has to be trained separately and a large number of tests are performed to define the adequate algorithm architecture. Finally, for complex large scale power systems, a huge number of neurons in the hidden layers are required to capture the system complexity. A concise analysis of key merits and demerits of these schemes is given in Table 2.7.

Table 2.7 Concise analysis of the merits and demerits of the ANN-based LFC schemes

Technique	Merits	Demerits
LFC Schemes based on ANNs [89-95]	• Storing information on the entire network • Having fault tolerance • Gradual corruption	• Unexplained behaviour of the network • The difficulty of showing the problem to the network • The duration of the network is unknown (The system is reduced to a particular error value on given sample means that the training has been ended. This value may or may not give an optimal value).

2.3.6.3 Fuzzy Logic Approach (FLA) Based LFC Schemes

FLA utilizes a mathematical calculus to decode the subjective knowledge of humans for the real processes [87]. The fuzzy logic theory was introduced by L. Zadeh in 1965. The behaviour of such systems is defined through a set of fuzzy-based rules, which uses linguistics variables with symbolic terms to formulate the solution of a given problem. A typical structure of FLA is shown in Fig. 2.3. From Fig 2.3, it can be observable that FLA is trisected as a fuzzifier, inference engine, and defuzzifier. The fuzzifier assigns the membership functions (MFs) to input and output variables where MFs maps the crisp values into fuzzy variables. The second section is the inference engine (IE) and IE consists of a database and rule base. They contain information on control rules, linguistic labels and the decision making is inferring control action from the rule base. The third section is the defuzzification, which converts the sum of fuzzy singleton outputs into a crisp value which is the required frequency restorative control command to the plant model.

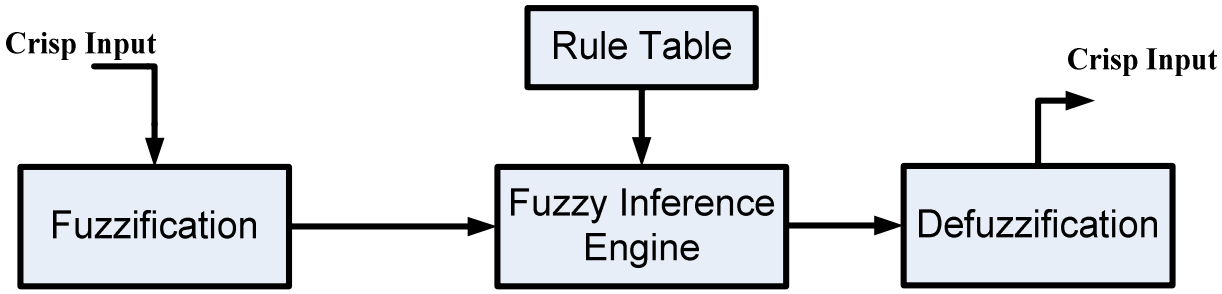

Fig. 2.4 The basic structure of fuzzy logic

The FLA has been broadly applied to various complex engineering problems due to ease of interpreting the results, simplicity, approximate reasoning, and provision to change in FLA parameters online according to operating conditions. Furthermore, this approach is well coped up with system nonlinearities and parametric uncertainties. Unlike the other control schemes, this approach able to provide an acceptable performance even though the exact mathematical model of the plant/system is unavailable [88]. Moreover, it can easily adaptable for small, large scale power systems as well for rapidly growing power systems. The FLA applications in the LFC problem of MGs and MAPS are reported by various authors in the literature, out of which few important studies are reviewed and briefly discussed as follows:

- ☑ *Marzband* et al. [89] proposed the FLA-PID controller for LFC of an islanded MG. Where the gains of the PID controller are scheduled using the fuzzy logic controller. In

this work, the robustness of the fuzzy logic controller proven against wind power changes and load changes simultaneously. The shortcoming of the proposed approach is proposed controller performance can be improved with fine-tuning of FLC according to operating conditions online.

- ☑ *Bevrani* et al. [90] proposed PSO tuned adaptive fuzzy PI controller for frequency control of an autonomous MG. Where the MFs of FLC are tuned in online using the PSO algorithm. The proposed controller robustness proved against all possible uncertainties like load changes, solar, and wind power changes individually. The impact of parametric uncertainties of MG on frequency control also analyzed. The proposed controller exhibits the superiority over FLC-PI due to its fine-tuning of MFs in online according to operating conditions. Similarly, Khooban et al. [91] proposed a modified harmony search algorithm tuned type-II fuzzy logic controller for frequency control of an autonomous MG. Where the effectiveness of the proposed controller over FLC and swarm-intelligence tuned PI controller is proven through different critical operating scenarios.

Similarly, the evolution of fuzzy-based PI/PID controllers for modern power systems is as follows:

- ☑ *Bevrani* et al. [92] proposed new decentralized FLA based LFC schemes for MAPS with high penetration of wind power. The performance of the proposed controller is tested on a practical New England test system. The simulation outcomes are compared with an optimal controller for the different rates of wind power penetrations and serious load disturbances.
- ☑ *Khooban* et al. [93] proposed a new optimized FLA based PI controller for an interconnected power system. Where the proposed controller is a combination of the BAT algorithm and FLC which is used to optimize both fuzzy MFs ranges and PI controller. Similarly, *Abazari* et al. [94] proposed an optimal FLA based LFC scheme for MAPS with high penetration of wind power. Where the proposed controller is a combination of the ABC algorithm and FLC which is used to optimize both fuzzy MFs ranges and PI controller. The test results reveal how effectively the proposed controller handling the frequency control concerning dynamic plug-in and plug-out of a large scale wind farm.

☑ For further improving the performance of modern power systems, recently, *Arya* et al. [95] proposed a fractional-order fuzzy PID controller for nonlinear MAPS with governor dead-band and GRC. Where authors used a combination of the Fuzzy and FO-PID controller for frequency control of the power system.

A concise analysis of the merits and demerits of these schemes is given in Table 2.8.

Table 2.8 Concise analysis of the merits and demerits of the FLA based LFC schemes

Technique	Merits	Demerits
LFC Schemes based on FLCs [89-95]	• FLC has advantages over the mathematical (numerical) approach or pure symbolic approaches because very often system knowledge is available in such a combination. • Fuzzy algorithms are often robust, in the sense that they are not very sensitive to changing environments and erroneous or forgotten rules. • Problems for which an exact mathematically precise description is lacking or is only available for very restricted conditions can often be tackled by fuzzy logic.	• The proper construction of rules and MFs ranges tuning is required for large-scale systems.

2.4 Problem Formulation

After reviewing the literature on various techniques in LFC of MG and interconnected power systems, the following observations have been made by considering all possible specifications of an efficient LFC design in modern power systems.

- S_1: Systematic, simple and reliable in design
- S_2: Constructive and effective in constraint handling capabilities including ESSs
- S_3: Multivariable handling capability
- S_4: Distributed control architecture
- S_5: Robust against various system uncertainties including RES uncertainties
- S_6: Adaptable and flexible in tuning according to system operating conditions in online

Based on the evaluation of various techniques in the literature, a simplified comparison of various schemes based on the specifications (S_1 - S_6) as mentioned above are summarized in Table 2.9. Where tick mark (☑) indicates its strengths, cross mark (x) indicates its weakness and asterisk (*) indicates a technique whose strength and weakness concerning a given LFC specification is subjective.

Table 2.9 Comparison of various LFC schemes based on specifications S_1- S_6

LFC Schemes	Specifications of good LFC					
	S_1	S_2	S_3	S_4	S_5	S_6
Conventional Schemes	☑	x	x	x	x	x
Optimal Schemes	☑	x	☑	x	x	x
Model-based Schemes	x	x	☑	☑	☑	x
Adaptive & Self-tuning Schemes	x	x	☑	x	☑	*
Robust Schemes	x	x	x	☑	☑	x
AI Schemes	*	*	☑	☑	☑	*

From Table 2.9, it can be observed that no single control technique meets all specifications for modern power systems. For an instant, apart from AI techniques, other LFC schemes also lack in constructive and effective constraints handling capability. Moreover, those schemes effective in handling system uncertainties (self-tuning schemes, model-based schemes, and robust schemes) could be too complex for large renewable penetrated power systems. Furthermore, these schemes perform effectively when the exact mathematic model of the system is available. However, most of the AI techniques concentrated on the conventional power system; hence further work is required in exploiting new combinations of AI techniques in modern power systems.

The proposed research work focuses on the development of new LFC schemes based on AI techniques for MG and interconnected power systems with RES. It aims to provide a good dynamic response (in terms of fast settling times, fewer overshoots/undershoots, and lower error value) under the renewable environment. Besides, the proposed control schemes are designed in a way to meet all possible specifications of good LFC design of modern power systems such as systematic and reliable design, distributed architecture, effective constraints handling capability, and robust to various system uncertainties.

2.5 Objectives of the Proposed Research Work

The main objectives of this thesis are:

i. To develop a mathematical model of the WTG, solar array, and microgrid.
ii. To develop a mathematical model of a two-area interconnected system with various power system constraints, RES, and PHEVs.
iii. To develop some efficient and meticulous control approaches for LFC enhancement of MG and interconnected power systems.
iv. To validate the control schemes on standard test systems.

Specifically, the following perspectives are considered and examined in this work for the improvement of proposed approaches in taking care of the LFC issue.

a) *The accomplishment of specific goals of LFC:* The main objectives of LFC are, firstly, minimizing the frequency deviations from the nominal frequency (50 or 60 Hz) during the disturbances, and return the frequency to the nominal value at steady-state is the primary objective. Secondly, tie-line power deviations are also to be made zeros as fast as possible.
b) *Constraints and uncertainties*: In this research, non-reheat turbines, governor dead band, generation rate constraints, boiler dynamics, and communication delays in electric vehicles are considered as constraints to resemble the real power system. In addition to that, the uncertainties caused by renewable penetration like the intermittent nature of renewable power output, reduction system inertia, uncertainty in governor time constant, etc. are also considered.
c) *Preserving the controller structure and fine-tuning:* As a technical obstacle upon the overall generality of the various robust approaches in the literature, the structure of the conventional PI/PID controllers would be changed following the system specification changes. This will affect the system dynamic response. This thesis aims to recruit the fuzzy logic approach to sketch a new LFC technique, called the robust fuzzy logic-based fine-tuning (RFLFT) approach, which is intended to fulfill the declared technical gaps. To do so, the supplementary fuzzy logic corrective loop is suitably superimposed to the principal foundation of the PI/PID/FOPID controllers for adapting gain values encountered with various operating scenarios. Consequently, through prudent RFLFT

design, the conventional PI/PID controller structure has been preserved as valid for steady-state conditions.

d) *Robustness*: The Robustness level of proposed controllers using different intelligent techniques are examined with a wide range of variation in the level of renewable penetration, load perturbations, and system parameters.

e) *Different sources and environment*: In modern power systems, the amount of renewable penetration has been increasing day by day. Considering the present scenario, renewable energy sources along with thermal and hydro units with all possible nonlinearities are considered as a control area. In remote and islanded locations, as there is a transition from the main grid to the microgrid, the LFC problem with microgrid is also studied.

Chapter 3

Frequency Dynamics Control in an Autonomous Hybrid MG: Grasshopper Optimization Tuned PID Controller Approach

3.1 Introduction

In today's modern power systems, the increasing energy demand from distant places like rural areas and islands from the utility grid is becoming costly, complicated and environmentally hazardous. For such conditions, a stand-alone MG would be an efficient and reliable solution. The MG comprises various RES, which are intermittent by nature, and this intermittency of RES introduces new technical challenges concerning the secure operation of the MG, particularly in frequency deviation control, as clearly reported in chapter 2. Therefore, in this chapter, a new grasshopper optimization algorithm (GOA) tuned PID controller is proposed for MG frequency control. The proposed controller is an upgrade of a swarm-intelligence group with significant advantages of fast computation time, adaptable, and flexible as compared to other swarm-intelligence techniques [96]. Besides, the proposed controller can adapt to a wide range of internal MG disturbances. The effectiveness of the proposed GOA-PID controller is tested on two-area hybrid MG through the simulation with different MG operating conditions. Moreover, a brief comparative assessment of the proposed controller with the existing controllers in literature is also carried out to show the merits of the proposed controller.

3.2 Mathematical Modelling of Two-Area Hybrid Microgrid

The simplified mathematical model of two-area hybrid MG under investigation is shown in Fig. 3.1. This model consists of diesel engine generator (DEG) with a control mechanism, the output power of real-time PV and WTG models, load fluctuations along with energy storage systems like redox flow batteries (RFBs). In detail explanation regards to each MG component is explained in the subsections. In each area, the change in frequency deviation due to load and RES output power changes can be given as:

$$\Delta f_1 = \frac{1}{M_1 s + D_1}(\Delta P_{DEG1} + \Delta P_{WTG} - \beta_1 \Delta f_1 - \Delta P_{RFB1} - \Delta P_{L1})$$

$$\Delta f_2 = \frac{1}{M_2 s + D_2}(\Delta P_{DEG2} + \Delta P_{PV} - \beta_2 \Delta f_2 - \Delta P_{RFB} - \Delta P_{L2}) \quad (3.1)$$

The $\Delta P_{tie,12}$ is defined as:

$$\Delta P_{tie,12} = \frac{T_{12}}{s}(\Delta f_1 - \Delta f_2) \tag{3.2}$$

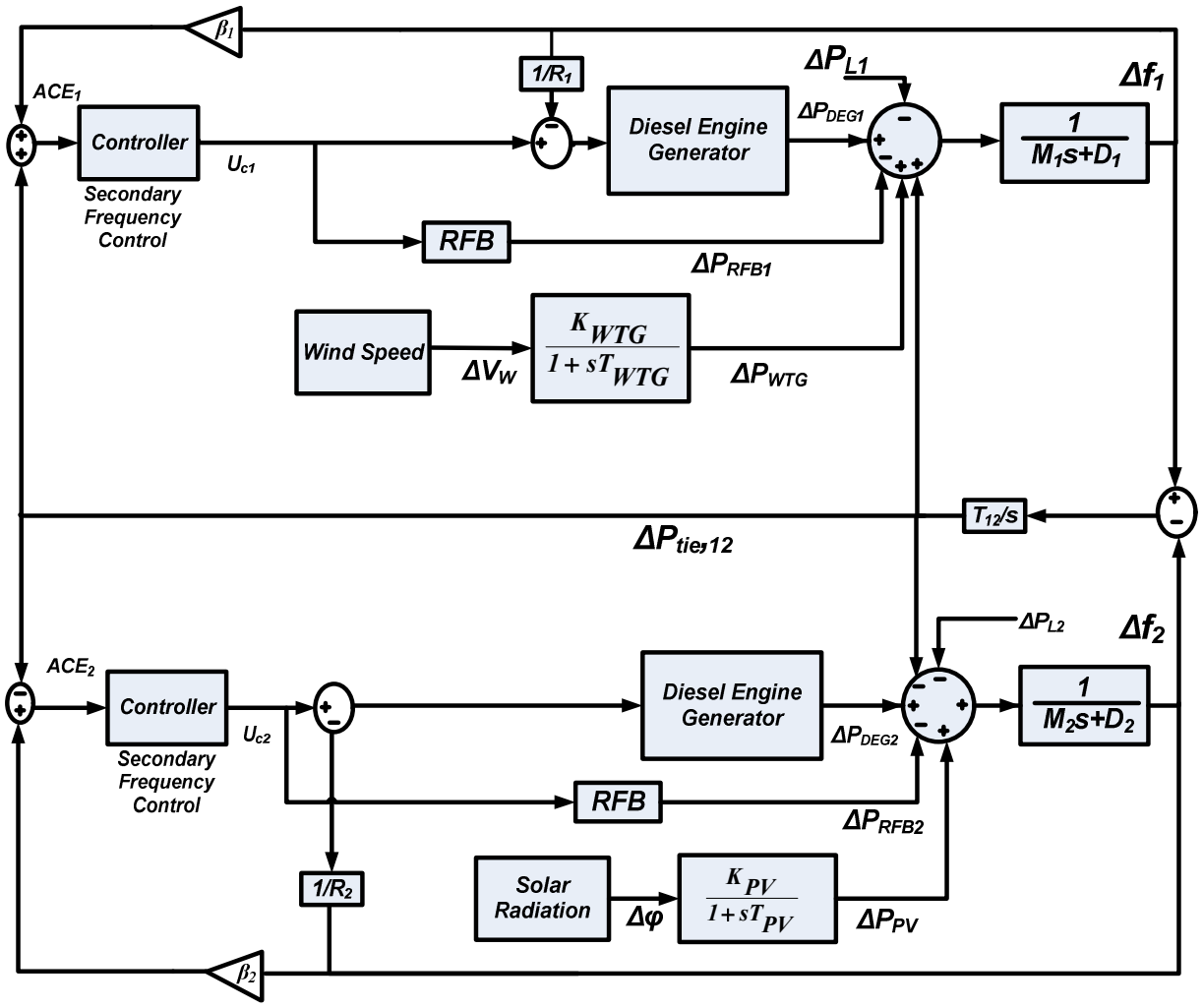

Fig. 3.1 Mathematical model of investigated microgrid

In the interconnected MG, The ACE of each area can be defined as:

$$ACE_1 = \beta_1 \Delta f_1 + \Delta P_{tie,12}$$

$$ACE_2 = \beta_2 \Delta f_2 + \Delta P_{tie,21} \tag{3.3}$$

The control signal fed to DEGs of each area (U_{ci}) can be expressed as:

$$U_{ci} = (K_P + \frac{K_I}{s} + s * K_D) * ACE_i \quad \text{where i=1,2} \tag{3.4}$$

The objective of the proposed GOA-PID controller is to minimize the frequency and tie-line power deviations to scheduled values by minimizing the ACE.

3.2.1 DEG

Due to inherent features of DEG including high efficiency, low maintenance and fast starting speed, it is a very good backup option in autonomous MGs. The properly controlled DEG can quickly track the load changes through its power control mechanism. Moreover, the fluctuation of uncontrollable RES and loads can be effectively compensated by the DEGs.

DEG can be represented by a combination of speed governor and diesel engine, as shown in Fig. 3.2 [97]. DEG takes care of the generation-demand imbalance in the MG by supplying deficient power to load depending on PV, WTG, and various ESSs output power. In Fig. 3.2, U_f and Δf represent the LFC control signal for DEG and frequency deviation of MG respectively. Based on this signal, the governor adjusts the valve position (ΔX) to accommodate the load changes (ΔP_L). 'Δf' is the frequency deviation of MG due to generation-load imbalance, ΔP_{DEG} is the change in generator power to accommodate the load changes.

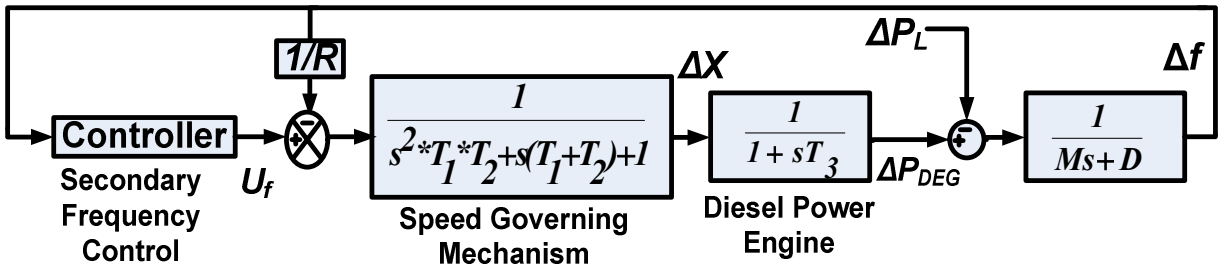

Fig. 3.2 Mathematical Model of DEG

3.2.2 WTG Model

Due to the volatile nature of wind speed, the WTG output power changes nonlinearly according to wind speed and the wind directions. In connection to MPPT limitation and intermittency in RES output power, these RES are not considered in LFC. In this work, only DEG and FCs can take care of LFC duties. Therefore, the WTG can be modelled as an uncontrolled power source and considered as a disturbance in LFC analysis. Fig.3 shows the mathematical model for the random wind velocity generation pattern.

In general, the windmill output power can be expressed as:

$$P_{wm} = 0.5\rho A V_w^3 C_p(\beta, \lambda) \tag{3.5}$$

Where 'V_w' is the wind velocity, 'ρ' is the air density, 'A' is the swept area, and C_p is power coefficient which is a function of Pitch angle (β) and tip speed ratio (λ) and it can be expressed as:

$$C_p(\beta,\lambda) = exp^{-125/\gamma} * (\frac{25.52}{\gamma} - 1.1 - 0.088\beta)$$

$$\gamma = 1 \Big/ [\frac{1}{\lambda + 0.08\beta} - \frac{0.035}{1+\beta^3}]$$

$$\lambda = \frac{R\omega}{V_w} \tag{3.6}$$

Where 'ω' is the angular velocity of the induction generator and 'R' is the radius of the blade. In present research work, GAMESA Company manufactured WTG data is utilized for LFC analysis and the details and ratings of WTG is given in APPENDIX. Based on windmill output power (P_{wm}) at various wind speeds (V_W), by utilizing the curve fitting technique, an equation for P_{wm} is developed in terms of V_W.

$$P_{wm} = \begin{cases} 0.0013V_w^6 - 0.046V_w^5 + 0.33V_w^4 + 3.68V_w^3 - 51V_w^2 + 2.33V_w + 366, & V_{cutin} \le V_w \le V_{rated} \\ P_{rated}, & V_{rated} \le V_w \le V_{cutout} \\ 0, & > V_{cutout} \end{cases} \tag{3.7}$$

LFC analysis is related to the small-signal stability analysis, hence, change in 'P_{wm}' is needed. It can be obtained by differentiating Eq. (3.7), which is expressed as:

$$\Delta P_{wm} = \begin{cases} (0.0078V_w^5 - 0.23V_w^4 + 1.32V_w^3 + 11.04V_w^2 - 102V_w + 2.33) * \Delta V_w, & V_{cutin} \le V_w \le V_{rated} \\ 0, & V_{rated} \le V_w \le V_{cutout} \\ 0, & > V_{cutout} \end{cases} \tag{3.8}$$

The transfer function model of the WTG system can be expressed as:

$$TF_{WTG} = \frac{\Delta P_{WTG}}{\Delta P_{wm}} = \frac{K_{WTG}}{1+sT_{WTG}} \tag{3.9}$$

3.2.3 PV Model

The PV array is the combination of modules is in series and parallel and this combination relies on the desired voltage and current ratings of the MG. The output power of the PV array is volatile by nature and it depends on solar irradiation and temperature. The output power of the PV array (P_{PV}) can be given as [69]:

$$P_{PV} = P_{solar} * \frac{\varphi}{\varphi_{STC}} * (1 + K_t * [T_a + 0.0256 * \varphi * \Delta\varphi - T_{STC}]) \quad (3.10)$$

The ΔP_{PV} based on the change in irradiation can be computed using the Eq. (3.11):

$$\Delta P_{PV} = \frac{P_{solar}}{\varphi_{STC}} * (\Delta\varphi + K_t[\Delta\varphi * T_a + \varphi * \Delta T_a + 0.0512 * \varphi * \Delta\varphi - T_{STC} * \Delta\varphi]) \quad (3.11)$$

The first-order model of the PV system can be expressed as:

$$TF_{PV} = \frac{\Delta P_{PV}}{\Delta\varphi} = \frac{K_{PV}}{1+sT_{PV}} \quad (3.12)$$

K_{PV} denotes the gain of the PV array and T_{PV} indicates the time constant of PV array including converter time delay also.

3.2.4 RFB Model

Conventional LFC regulating units like DEGs are quite sluggish for short-term frequency deviations due to lethargic time constants involved in DEGs. The unanticipated changes in PV and wind output power cause short-term transients in frequency deviations of MG. To conquer these problems, the ESSs have turned a vital part in LFC of MG and one of the most promising ESS to meet the LFC requirements are RFBs. The RFBs offer several attracting features such as full discharging capabilities, low cost, high energy efficiencies and relatively easy to maintain compared to other ESSs [74]. The mathematical model of RFBs for LFC studies is shown in Fig. 3.3. The change in RFB output power (ΔP_{RFB}) against frequency deviations can be given as:

$$\Delta P_{RFB} = \left(\left[U_{fi} * K_{RFB}\right] - \left[\frac{K_{ri}}{1+sT_{ri}}\right]\right) * \left(\frac{1}{1+sT_{di}}\right) \text{ - set value} \quad (3.13)$$

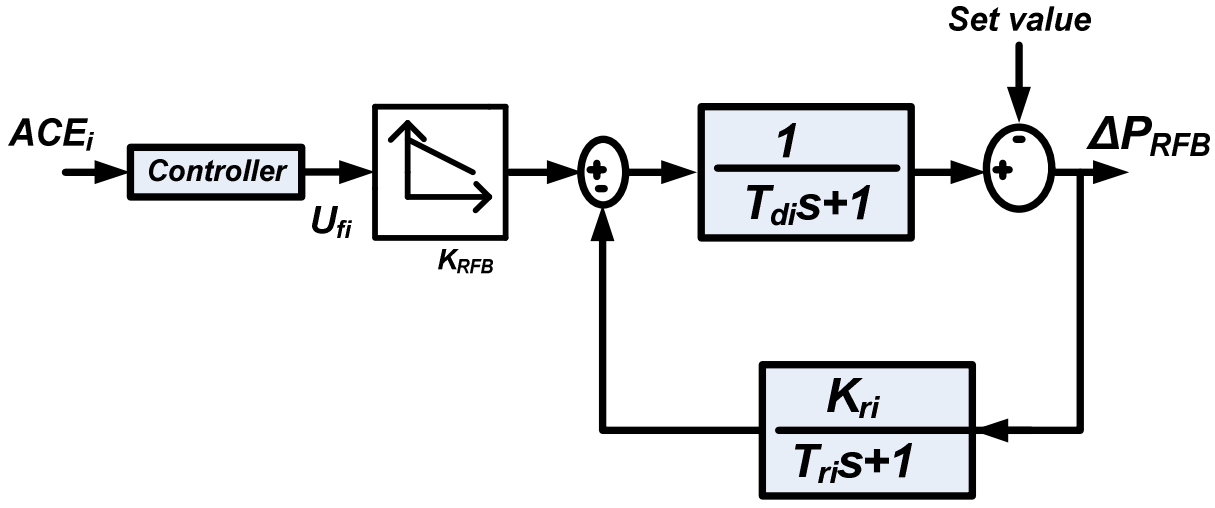

Fig. 3.3 Mathematical model of RFB

3.3 Grasshopper Optimization Algorithm

The increasing complexity of power systems needs an accurate and fast tuning of control parameters for a better LFC response. In light of this issue, in literature, several authors proposed various swarm-intelligent techniques for PI/PID controller tuning process. The inherent features of these algorithms are; independent on the model of the plant and derivative-free. Few of them like BFO, FPA, CSO, FA, DE, GA and PSO [96]. According to No Free Lunch (NFL) theorem, no single metaheuristic technique is suitable for solving all engineering optimization problems and scope of improvement is always persists. Thereupon, a recently developed and powerful GOA is presented for fine-tuning of PID controller. GOA was developed by Mirjali et al.. in 2017, which mimics the collective behaviour of grasshoppers. This algorithm was benchmarked on various standard test problems and verified its performance quantitatively and qualitatively. Due to advantages in less number of controlling parameters, easy implementation structure, fast convergence and simplicity, this algorithm successfully implemented to various engineering problems [100-101].

3.3.1 Mathematical Modelling of GOA

Grasshoppers are insects, but they are considered as pests due to their damage in agriculture and farming crops. Though they are seen individual by nature, in food searching process they form one of the largest swarm. The group size may be of large scale and a nightmare for farmers. The unique feature of these grasshoppers is, the swarming behaviour is found in both nymph (larval phase) and adulthood stages. In the larval stage, millions of grasshoppers move and jump like rolling cylinders and eat all most all crops in their path. In adulthood stage, they form swarm in air and migrate over large distances.

In the nymph stage, the grasshoppers' movement is slow and in small steps. In adulthood stage, they are encouraged to move abruptly over long distances. However, in both stages the grasshoppers in food-seeking process. Any swarm-intelligence algorithm divides the search process into two categories viz., exploration and exploitation. In exploitation, grasshoppers are tending to move locally, while they are encouraged to move expeditiously during exploration. The mathematical model followed to simulate the swarming behaviour of grasshoppers can be expressed as follows:

The initialization of the population for the first iteration is as follows:

$$X_{i,0} = lb + randomno(1, N_{pop}) * (ub - lb) \tag{3.14}$$

where $X_{i,0}$ denotes the position of an i^{th} grasshopper for the first iteration, the position of the i^{th} particle in the k^{th} iteration is modified based on the following equation [100]:

$$X_{i,k} = r_1 * S_i + r_2 * G_i + r_3 * A_i \tag{3.15}$$

where r_1, r_2 and r_3 are the random numbers between 0 and 1.

S_i function denotes the social force on i^{th} grasshopper, which can be calculated as [100]:

$$S_i = \sum_{j=1,\neq i}^{Npop} s(D_{ij}) * \widehat{D_{ij}} \tag{3.16}$$

Where $s(D_{ij}) = 0.5e^{-D_{ij}}\left(e^{-\frac{2}{3}} - 1\right), D_{ij} = |X_j - X_i|$ & $\widehat{D_{ij}} = \frac{X_i - X_j}{D_{ij}}$

G_i denotes gravitational force on i^{th} grasshopper, which can be calculated as:

$$G_i = -G * \widehat{e_g} \tag{3.17}$$

A_i denotes wind advection of i^{th} grasshopper, which can be calculated as:

$$A_i = u * \widehat{e_w}; \tag{3.18}$$

To attain the proper balance between exploitation (in the nymph stage) and exploration (in the adulthood stage), an adaptation factor (c) is introduced as follows:

$$c = c_{max} - i * \left(\frac{c_{max} - c_{min}}{\mathrm{i_{max}}}\right) \tag{3.19}$$

With this adaptation factor, a modified version of the population updating equation to solve optimization problems can be expressed as:

$$X_{i,k}^{d} = \widehat{T_d} + c * \left(\sum_{i=1,j\neq i}^{Npop} c * \left(\frac{ub_d - lb_d}{2}\right) * s(D_{ij}) * \widehat{D_{ij}}\right) \tag{3.20}$$

Where lb_d , ub_d lower and upper bounds in the Dth dimension. $\widehat{T_d}$ is the target vector in the Dth dimension (best solution in the population-based on fitness function), and 'c' helps to reduce the area of the comfort zone, attraction zone, and repulsion zone to move close towards the optimal global solution. In the modified equation i.e., (Eq. 3.20), the wind advection is not considered and assumed that wind direction is towards the target vector ($\widehat{T_d}$). The first part of Eq. (3.20) represents the position of current grasshopper with respect to other grasshoppers.

In this work, ITAE is chosen as an objective function (FF). The objective function can be minimized with the help of optimal PID gains as variables.

3.3.2 Reason for Selecting ITAE as the Objective Function

The selection of objective function is one of the key factors for improving the system dynamic response in the time-domain analysis. In general, three types of error criteria, such as integral time multiplied absolute error (ITAE), integral absolute error (IAE), and integral square error (ISE) are used to define the objective functions. If the magnitude of error is small and persists for a short duration, IAE is found to be a better objective function than ISE. If the magnitude of error is large and persists for a short duration, ISE is found to be a better objective function than IAE. On the other hand, if the magnitude of error is small and persist for a long time (which is identical to this problem stated in this work), ITAE is the best option, because as 't' term amplifies the small persisting error which exists for a long duration. For the case mentioned above, ITAE produces small overshoots and fast settling time over IAE or ISE [102]. Hence, ITAE is selected as the objective function. The ITAE criteria can be expressed as follows:

$$\text{ITAE= minimization of } \int_0^{t_{sim}} t * \left((K_P + \frac{K_I}{s} + s * K_D) * (|ACE_1| + |ACE_2|)\right) \text{dt} \qquad (3.21)$$

Where $|ACE_1| = |\Delta f_1| + |\Delta P_{tie,12}|$, $|ACE_2| = |\Delta f_2| + |\Delta P_{tie,21}|$, t_{sim}= Total simulation time

t = Time at which error sample collected.

The sequential steps for tuning the proposed PID controller with GOA are explained in detail below:

Step 1: **Initialization:** A random population is generated by initializing the controller parameters (K_P, K_I, K_D) within the limit 0.01 and 5.0. As there are 6 controller parameters related to two PID controllers, so the population size is considered as 50×6.

Step 2: **Fitness Evaluation:** The designed Simulink model is run by implementing the ITAE as fitness function Eq. (3.21) to assess the fitness values of the defined population.

Step 3: **Selection:** After evaluating all the solutions in the population, the overall best solution in the population is assigned as a target value ($\widehat{T_d}$).

Step 4: **Updating the decreasing coefficient parameter:** At each iteration, the coefficient parameter 'c' is updating to shrink the attraction, repulsion and comfort zone as shown in Eq. (3.19)

Step 5: **Estimation:** Estimate the social forces between two grasshoppers, gravitational force and wind advection using the Eq. (3.16 - 3.18).

Step 6: **Update the position of each grasshopper:** Based on the above three forces and the best solution in the population(T_d), update the position of each grasshopper using Eq.(3.20).

Step 7: **Termination criteria:** if iterations = iterations_maximum, the best member of the population will be treated as the best set of controller parameters.

Fig. 3.4 shows the flow chart for the proposed GOA based tuning of the PID controller.

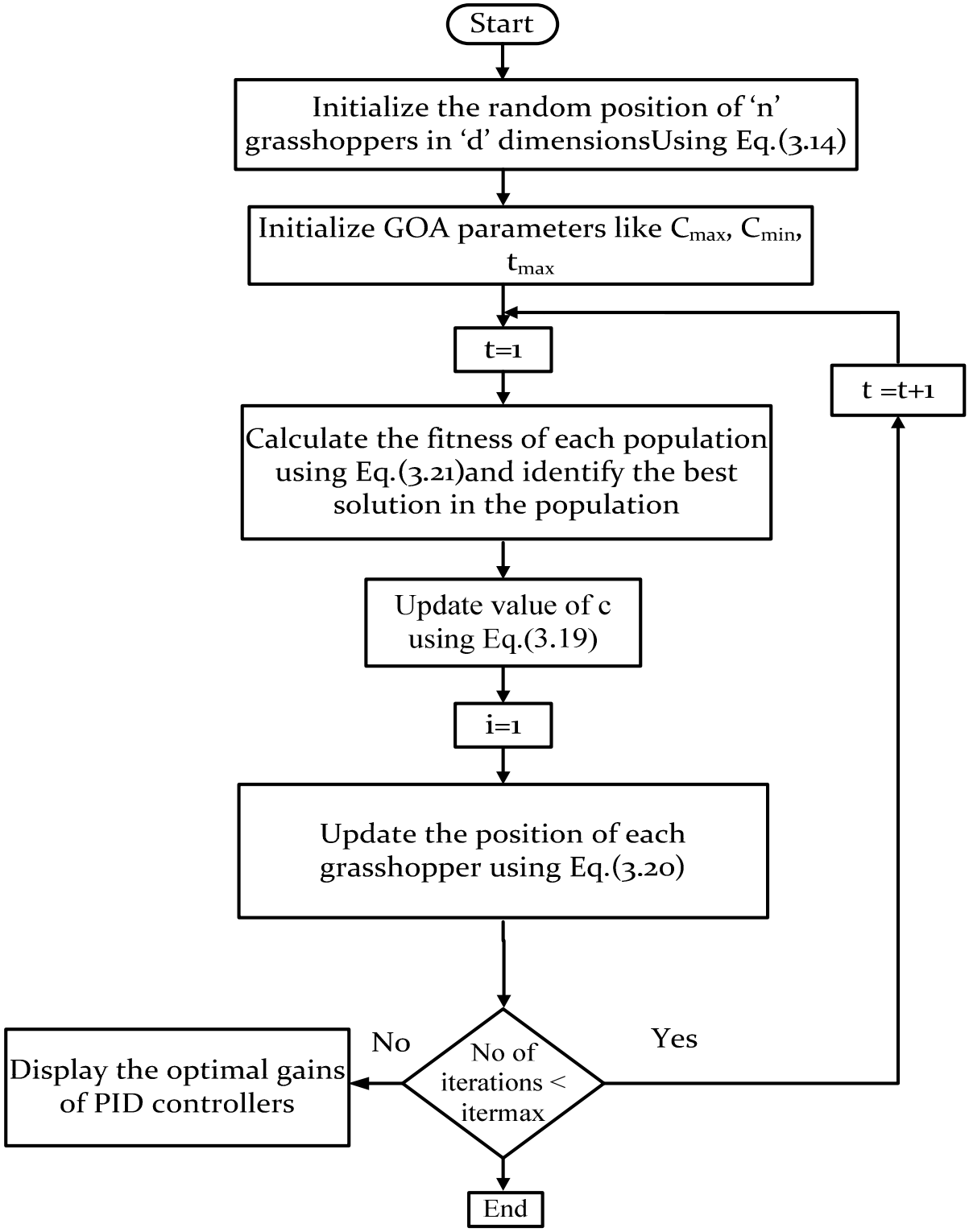

Fig. 3.4 Flow-chart for the proposed GOA-PID controller tuning process

3.4 Results & Discussion

In this section, to examine the proposed controller, LFC analysis on BELLACOOLA MG has been performed under different operating scenarios. The test system is shown in Fig. 3.1 is simulated in MATLAB/Simulink 2015 environment. The simulation parameters of the test system are given in Table 3.1. The performance of the proposed GOA-PID controller is compared with that of Z-N PID controller, GA-PID controller and SSO-PID controller. To assess the performance of the proposed controller, the test system is subjected to various disturbances like load, RES output power variations and various uncertainties in MG and ESSs. To demonstrate the effectiveness of the proposed controller, time-domain simulations of the proposed controller and other controllers are compared case by case in each scenario.

Table 3.1 Simulation parameters of two-area hybrid MG

Parameter	**Value**	**Parameter**	**Value**
M_1, M_2 (s)	0.1667	T_2(s)	2
D_1, D_2 (puMW/Hz)	0.015	T_3(s)	3
R_1, R_2 (Hz/puMW)	2.4	$K_{RFB,}$ K_r	0.5,1
β_1, β_2 (puMW/Hz)	0.426	T_r(s)	1.8
$K_{PV,}$ K_{WTG}	1	T_{PV}(s)	1.5
T_1(s)	0.025	T_{WTG}(s)	2

Scenario 1: Performance evaluation of the controllers under multiple disturbances

In this scenario, area-1 alone is considered as an isolated area and all the possible disturbances in MG (i.e., ΔP_L, ΔP_{WTG} and ΔP_{PV}) are considered simultaneously. Besides the multiple

disturbances, the internal MG uncertainties like a 50% reduction in inertia (M) and 50%reduction in damping coefficient (D) are also considered.

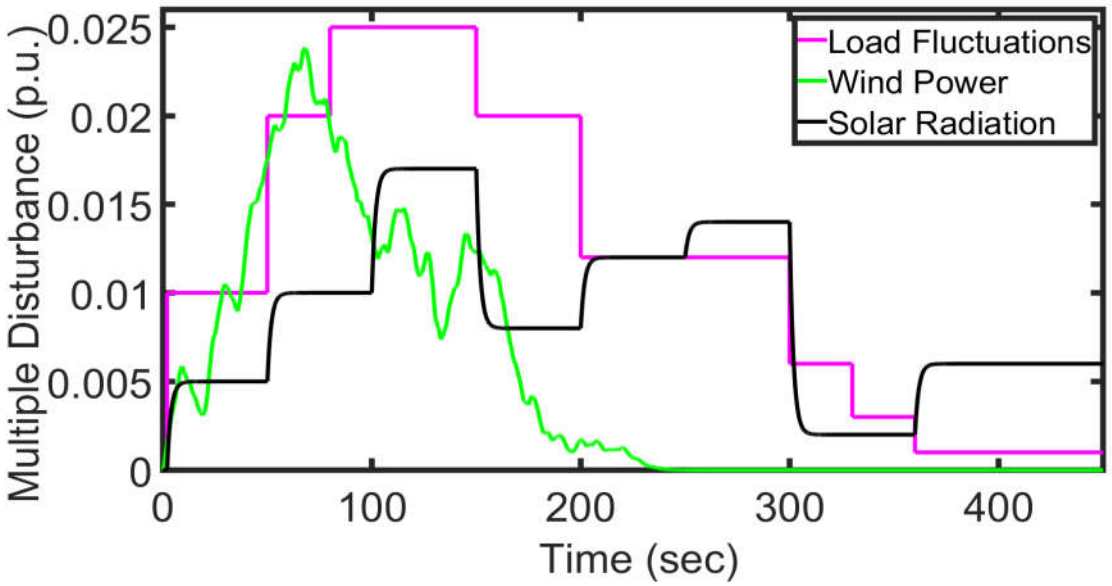

(a)

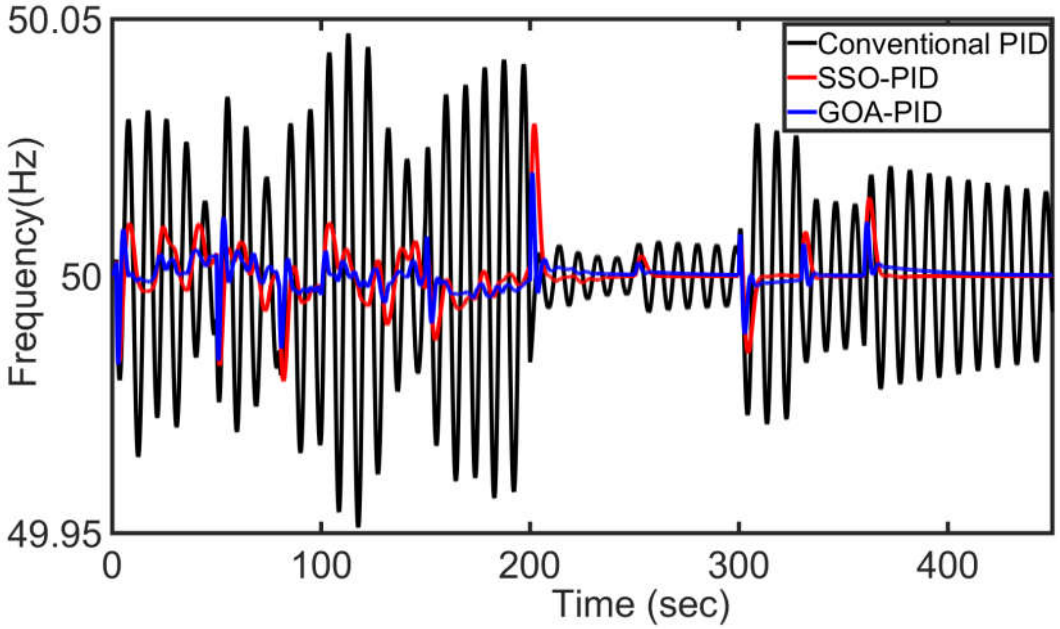

(b)

Fig. 3.5 (a) Concurrent disturbances in MG (b) Frequency response of the MG for scenario 1 conditions

Fig. 3.5 (a) shows the concurrent disturbances in MG and Fig. 3.5 (b) depicts the frequency deviation response of MG with various controllers. For this test scenario, as the results obtained in Fig. 3.5(b), the conventional Z-N PID controller fails to stabilize the frequency fluctuations in MG against multiple disturbances. However, the other controllers can provide quite better performance.

Scenario 2: Performance evaluation of the controllers under step load disturbances

In this scenario, the load in area-1 of MG is increased suddenly by 10% and respective Δf_1, Δf_2 and $\Delta P_{tie,12}$ are depicted in Fig. 3.6 (a) – (c). It has been observed that the increase in load demand causes the decrease in frequency deviation, due to controller action the frequency and tie-line power deviations attained the steady-state value after some time. The quantitative analysis of Fig. 3.6 (a) – (c) in terms of overshoots and settling times are given in Table 3.2. The heuristic gains of the PID controller with various swarm-intelligence methods are given in Table 3.3.

Table 3.2 Dynamic response analysis of MG for scenario 2 conditions

Techniques	Area-1 Dynamics		Area-2 Dynamics		$\Delta P_{tie,12}$ Dynamics	
	PUS (Hz)	T_s (sec)	PUS (Hz)	T_s (sec)	PUS (puMW)	T_s (sec)
GA-PID [66]	49.902	33	49.9135	33.5	0.0403	26
SSO-PID [69]	49.916	24.5	49.924	27	0.0346	18
GOA-PID	49.914	19	49.926	20	0.0342	13

*PUS: Peak Undershoot, Ts: Settling Time

Table 3.3 Heuristic gains of PID parameters for different swarm techniques

Methods	Area-1			Area-2		
	K_{P1}	K_{I1}	K_{D1}	K_{P2}	K_{I2}	K_{D2}
GOA-PID	4.9	0.844	2.99	0.7189	0.09	4.5494
SSO-PID [69]	4.7781	0.9741	3.60	3.0540	0.5877	2.9625
GA-PID [66]	3.231	2.4032	5	2.7613	0.3081	3.5061

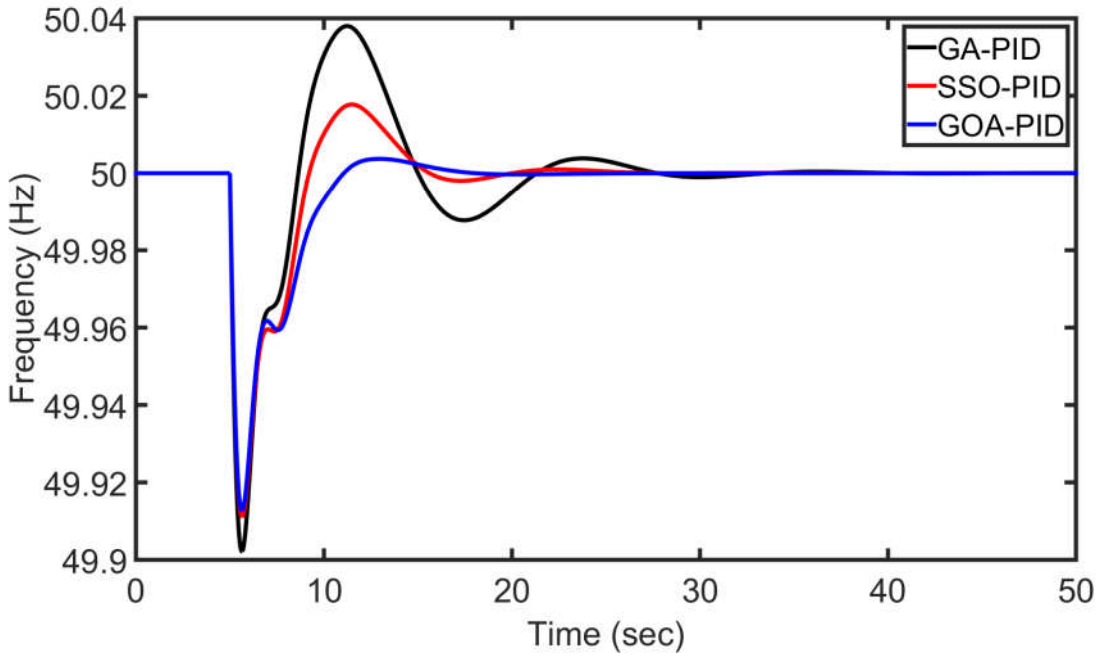
50.04
50.02
50
49.98
49.96
49.94
49.92
49.9
Frequency (Hz)
0
10
20
30
40
50
Time (sec)
GA-PID
SSO-PID
GOA-PID

(a)

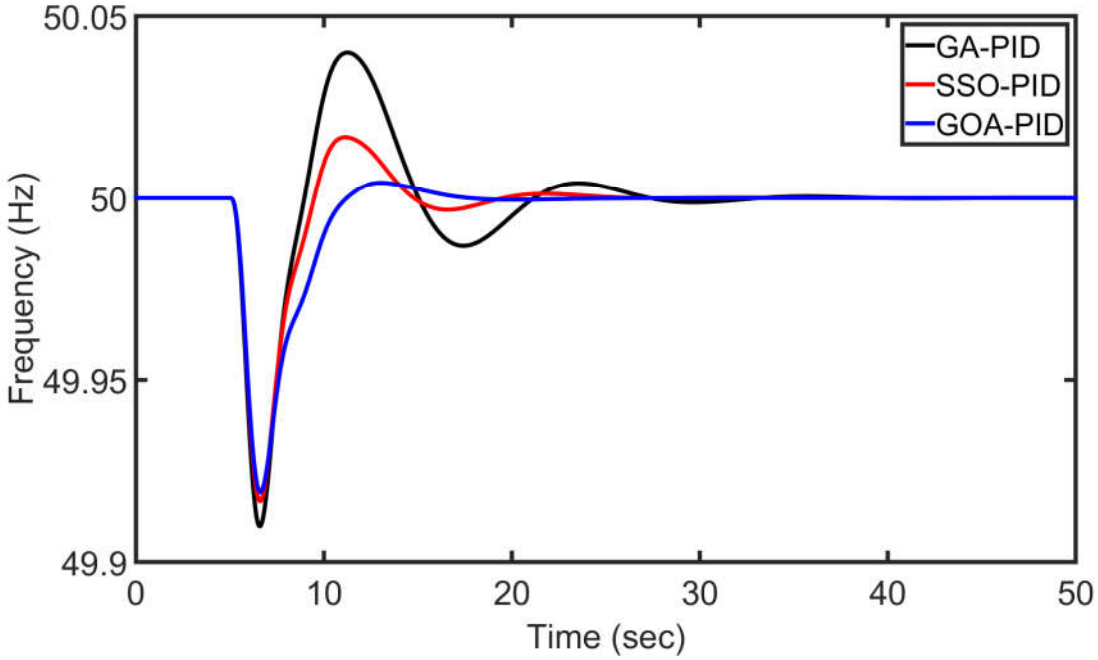
50.05
50
49.95
49.9
Frequency (Hz)
0
10
20
30
40
50
Time (sec)
GA-PID
SSO-PID
GOA-PID

(b)

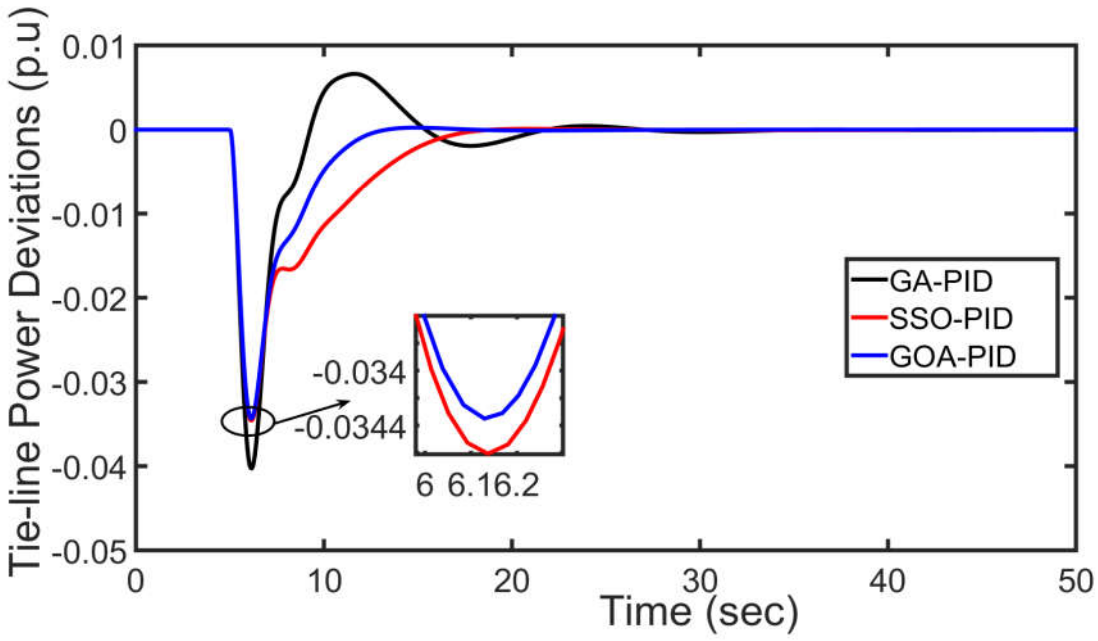

(c)

Fig. 3.6 a), b) Δf_1 and Δf_2 of MG for scenario 2 conditions c) $\Delta P_{tie,12}$ of MG for scenario 2 conditions

Scenario 3: Robustness analysis of the proposed controller subject to RES disturbances and MG uncertainties

In this scenario, to analyze the two-area MG LFC dynamics, the following test conditions are considered:

- Random wind power disturbances and multi-step load disturbances are considered in area-1
- Solar power disturbances are considered in area-2. In addition to these, following uncertainties in MG are considered as mentioned in Table 3.4.
  - Table 3.4 Parametric uncertainties in MG

Parameters	Percentage variation
R_1, R_2	+30
M_1, M_2	-50
D_1, D_2	-50

The wind power, solar power and load disturbance conditions are similar as shown in Fig. 3.5 (a).

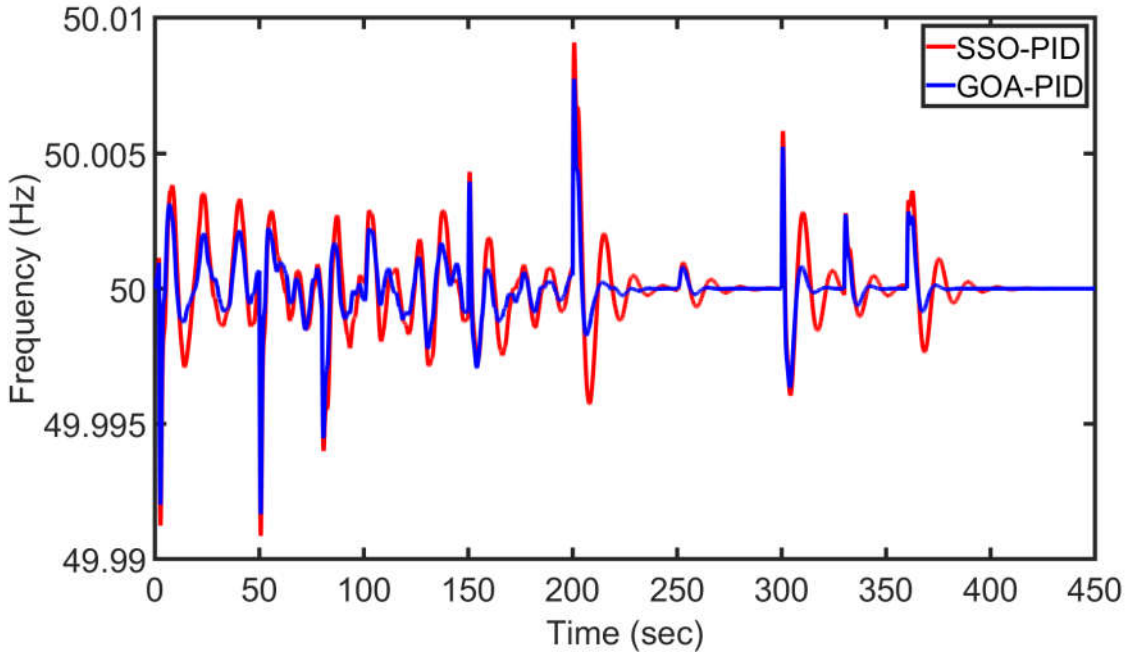

(a)

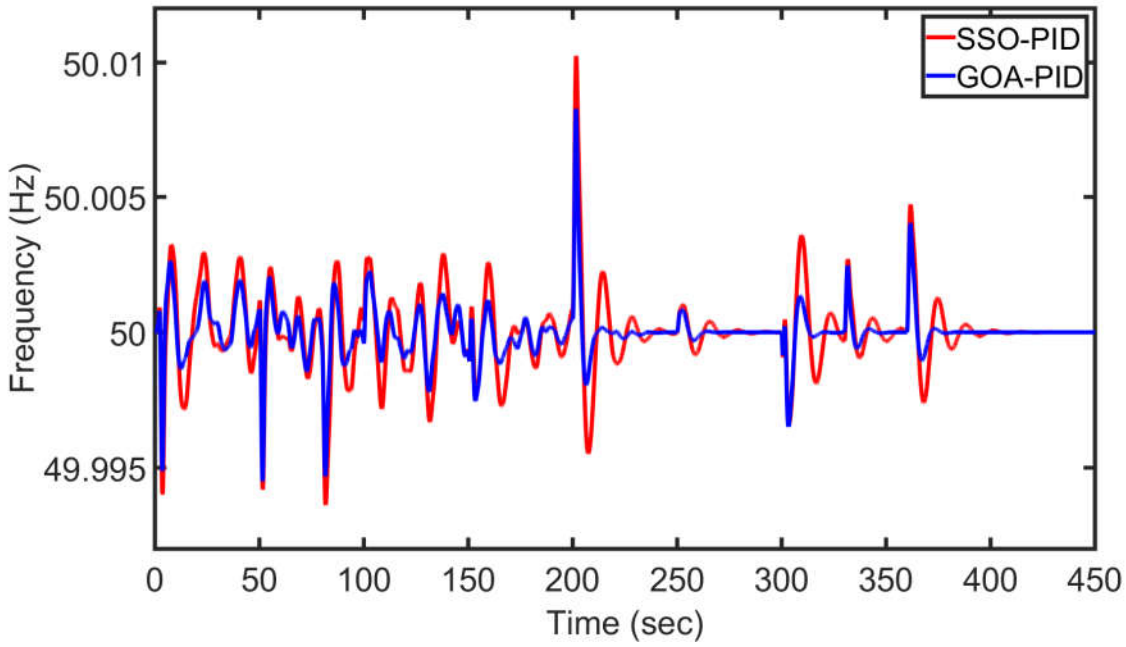

(b)

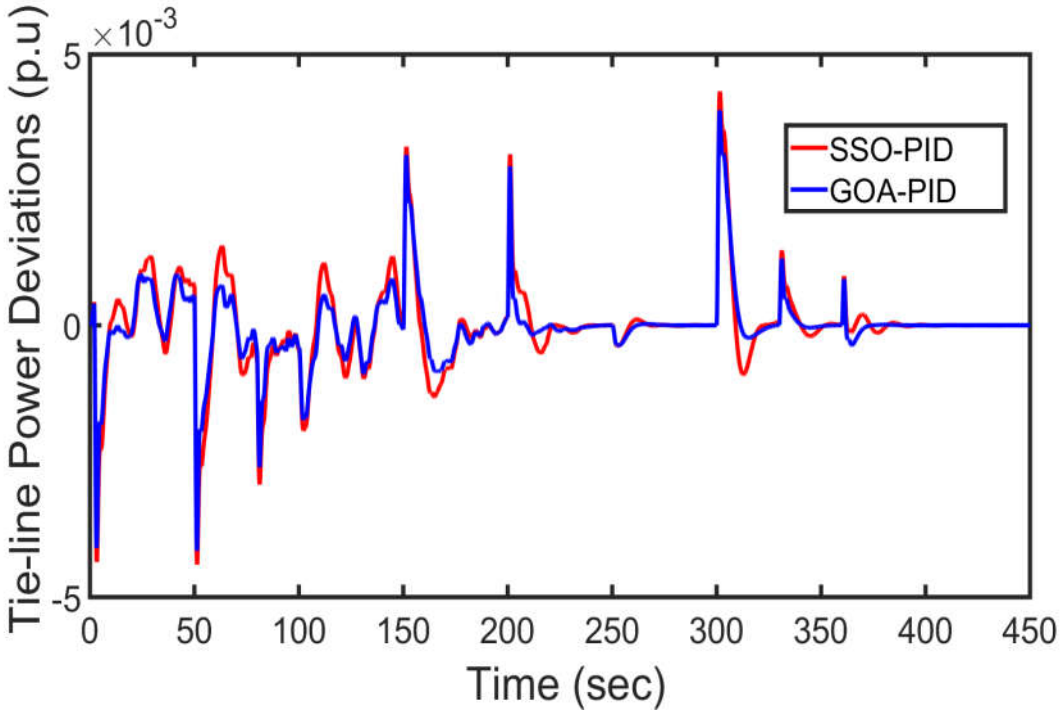

(c)

Fig. 3.7 a), b) Δf_1 and Δf_2 of MG for scenario 3 conditions c) $\Delta P_{tie,12}$ of MG for scenario 3 conditions

Fig. 3.7 (a)-(c) depicts the Δf_1, Δf_2 and $\Delta P_{tie,12}$ of the MG respectively. From the scenario 3, it can be observable that both the controllers are shown its capabilities against RES disturbances and MG uncertainties. However, the proposed GOA-PID controller shows a better frequency response and low ITAE value over the recently developed SSO-PID controller. The ITAE values of different optimized controllers under various operating scenarios are given in Table 3.5. The ITAE performance for scenario 3 is shown in Fig. 3.8.

In this work, hybrid two-area MG with diverse operating scenarios are considered for performance evaluation of various controllers in the literature. The simulation outcomes divulge that proposed controller enhances the frequency response of MG as compared to other controllers in terms of various performance indices and hence satisfies the LFC requirements. Moreover, when the MG is subjected to robustness against internal uncertainties, the proposed controller shows a laudable performance.

Table 3.5 The ITAE performance index of controllers for various operating scenarios

Scenario	Z-N PID[14]	GA-PID [66]	SSO-PID [69]	GOA-PID
Scenario 1	Oscillatory	5.63 e-04	4.71 e-04	3.96 e-04
Scenario 2	1.2e-04	6.2e-05	5.15e-05	4.9e-05
Scenario 3	Oscillatory	1.58 e-03	1.03 e-03	9.62 e-04

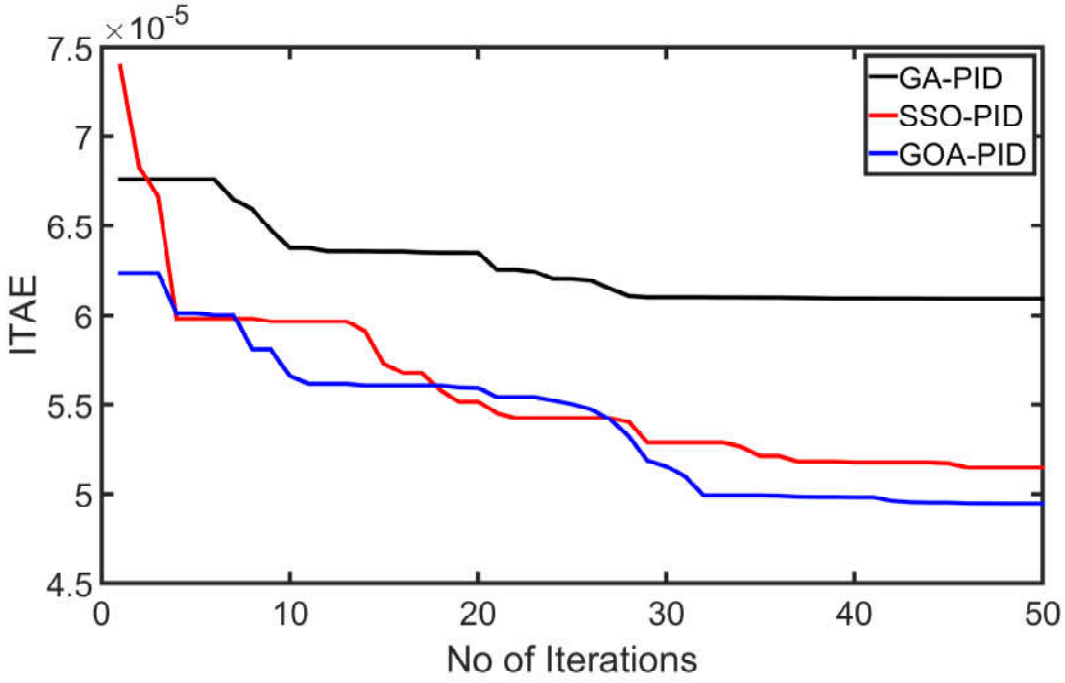

Fig. 3.8 ITAE characteristics for scenario 2

3.5 Summary

In this chapter, a maiden application of GOA optimized PID controller is proposed for frequency control of an autonomous microgrid. As discussed in the introduction, the robustness feature of the proposed controller is obtained through the effective utilization of the PID controller and fine-tuning capabilities of GOA. Furthermore, the level of robustness of the proposed controller is compared with three standard controllers in literature viz., Z-N PID controller, GA-PID controller and recently proposed SSO-PID controller. Besides, the simulations outcomes and quantitative results proved that the proposed controller shows a better frequency response in terms of fast settling times, less over/undershoots and low ITAE value.

Moreover, the proposed controller is more stubborn to RES intermittencies and load disturbances. As the concluding remark, the better frequency responses of all operating scenarios certified that the proposed controller is a suitable choice for LFC control purposes in MG.

Chapter 4

Robust Frequency Control in an Autonomous Microgrid: A Two-Stage Adaptive Fuzzy Approach

4.1 Introduction

The proposed GOA-PID controller in the previous chapter has the advantages of efficient dynamic response and more robust to load and renewable intermittencies compared to various standard and recent optimization techniques in the literature. However, the performance of most of the swarm intelligence techniques including GOA depends on their algorithm-specific parameters. Improper tuning or selection of these parameters may lead the solution towards the divergence, or it increases the computational complexity. Moreover, the proposed controller had a limited degree of freedom in its tuning process and provided optimal performance when the exact mathematical model of the system is available. To address the above-said problems encountered by the optimized PID controllers in MG frequency control, this chapter presents a novel two-stage adaptive fuzzy PI controller for MG frequency control.

The proposed controller is derived from a combination of a fuzzy logic approach and a conventional PI controller. Consequently, in the proposed controller, the conventional PI controller structure has been preserved as valid for steady-state conditions. Hence, there would be no structural changes for the primary PI controller that is, the supplemented fuzzy logic corrective loop merely influences the PI performance when faced with various disturbances. This approach is, in essence, deploying the cooperation of fuzzy logic features and conventional PI controllers to improve the extensibility of the control space investigated in the LFC problem. This controller is suitable for MG frequency control applications and capable of handling the intrinsic characteristics of renewables and uncertainty in MG system parameters simultaneously. The dynamic performance of the MG with the proposed controller is investigated for random changes in load, wind, and solar power through simulations. Besides, the robustness of the proposed controller against concurrent changes in all possible disturbances, energy storage systems, and inertia uncertainties are tested in a single controller framework. Finally, in this chapter, a brief comparative assessment is formulated with other controllers to show the merits of the proposed controller.

4.2 System Configuration and Mathematical Modelling

Fig. 4.1 illustrates a schematic diagram of BELLA-COOLA MG. This model consists of DEG, RES like wind turbine generator (WTG), photovoltaic (PV) model, battery energy storage system (BESS), fuel cell (FC), and load model. Fig. 4.2 depicts the mathematical model of BELLA-COOLA MG. In detail, an explanation regards to each MG component is explained in the previous chapter. The MG components which are not presented in chapter 3 are presented in chapter 4. The simulation parameters of the MG are given in Table 4.1.

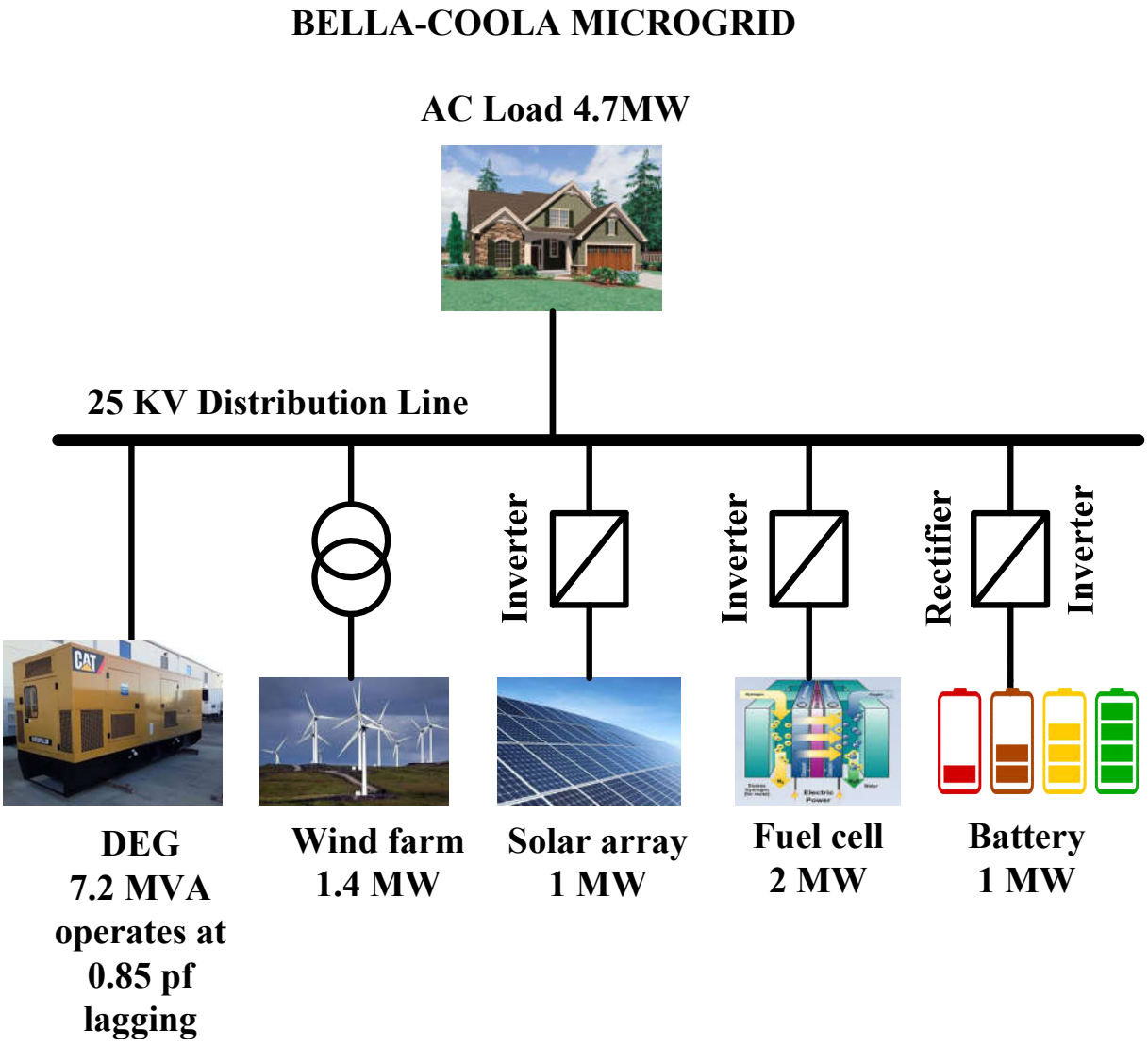

Fig. 4.1 Schematic model of BELLA-COOLA MG

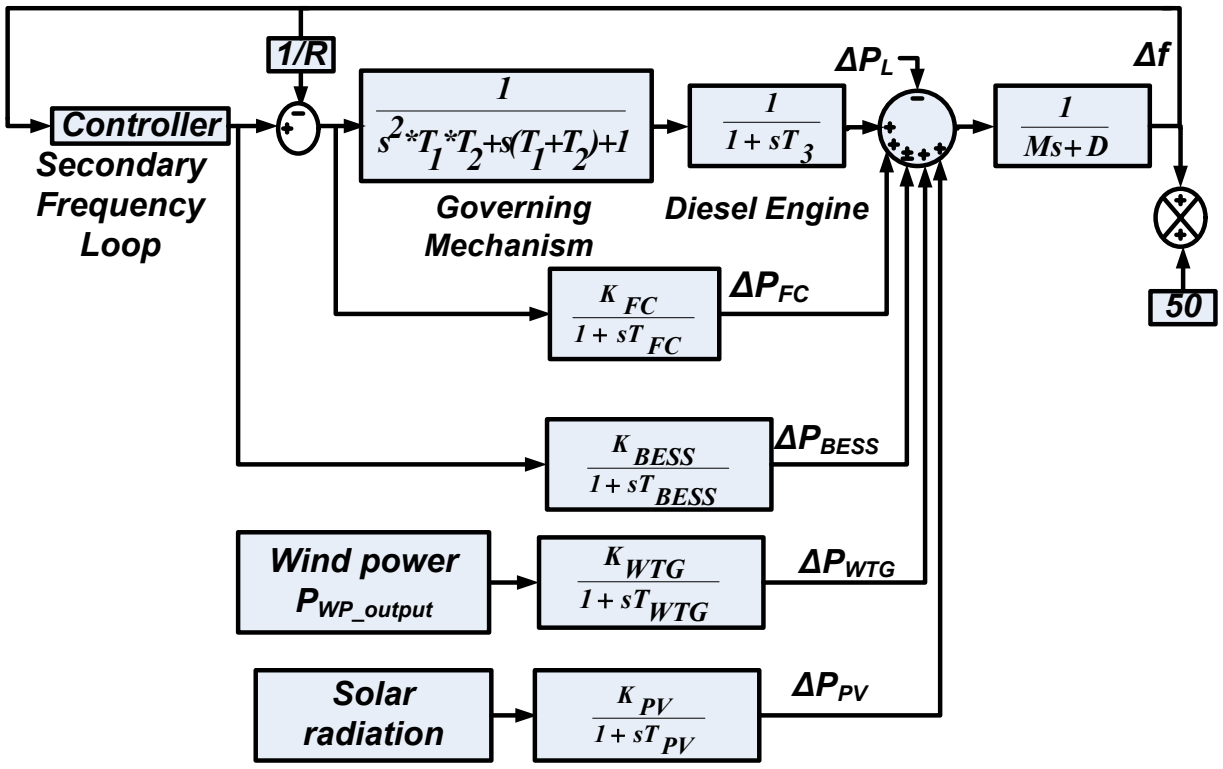

Fig. 4.2 Mathematical model of BELLA-COOLA MG

Table 4.1 Simulation parameters of MG [57]

Parameter	Value	Parameter	Value
M(s)	0.1667	T_2(s)	2
D(puMW)	0.015	T_3(s)	3
K_{BESS}	1.5	T_{BESS}(s)	0.1
K_{WTG}	1	T_{FC}(s)	0.1
K_{PV}	1	T_{PV}(s)	1.5
T_1(s)	0.025	T_{WTG} (s)	2

Due to uncertainty in the output power of RES (PV and WTG), the RES are not considered in the frequency control loop. Only DEG and FC are considered in the frequency control problem. The expression for the change in power can be written as [98]:

$$\Delta P_{DEG} + \Delta P_{WTG} + \Delta P_{PV} + \Delta P_{FC} \pm \Delta P_{BESS} = \Delta P_{LOAD} \quad (4.1)$$

$$\Delta P_e = \Delta P_{MG} - \Delta P_L \quad (4.2)$$

where, $\Delta P_{MG} = \Delta P_{DEG} + \Delta P_{WTG} + \Delta P_{PV} + \Delta P_{FC} \pm \Delta P_{BESS}$, ΔP_e is the residual power (or) power indicates the generation-load imbalance. If ΔP_e=0 then, the frequency deviation in the MG is zero.

4.2.1 Battery Energy Storage System (BESS)

BESS is used to improve the primary frequency regulation of an autonomous MG. In general, the primary frequency control task is taken care of by DEG. Due to its high time constant, it responds slowly to frequency variations, which creates significant overshoot. To overcome this problem and to enhance the primary frequency response, BESS is incorporated. The first-order transfer function (TF) model of BESS can be expressed as [98]:

$$TF_{BESS} = \frac{\Delta P_{BESS}}{\Delta f} = \frac{K_{BESS}}{1+sT_{BESS}} \quad (4.3)$$

Depending on Δf of MG, BESS works either in charging or discharging mode.

- If Δf is positive, then BESS is in charging mode.
- If Δf is negative, then BESS is in discharging mode.

4.2.2 Fuel Cell

Uncertainty in output power of PV and wind due to solar radiation and wind speed may reduce the capacity of BESS. Hence, the fuel cells are integrated with BESS to overcome the stability related issues. The first-order TF model of FC can be expressed as [98]:

$$TF_{FC} = \frac{\Delta P_{FC}}{U_c} = \frac{K_{FC}}{1+sT_{FC}} \quad (4.4)$$

4.3 Fuzzy Logic Approach based PI Controller

The conventional PI controller consists of fixed gains, and these gains are obtained by considering predetermined operating conditions of MG. Due to intermittency in RES output, operating conditions of MG changes rapidly. Fixed gain PI controllers may not be able to track these rapid changes, which results in MG losing its stability. If the PI controller can track the changes that occurred in the MG continuously, the optimum performance will be ensured. This continuous tracking of a PI controller can be realizable with FLA [103].

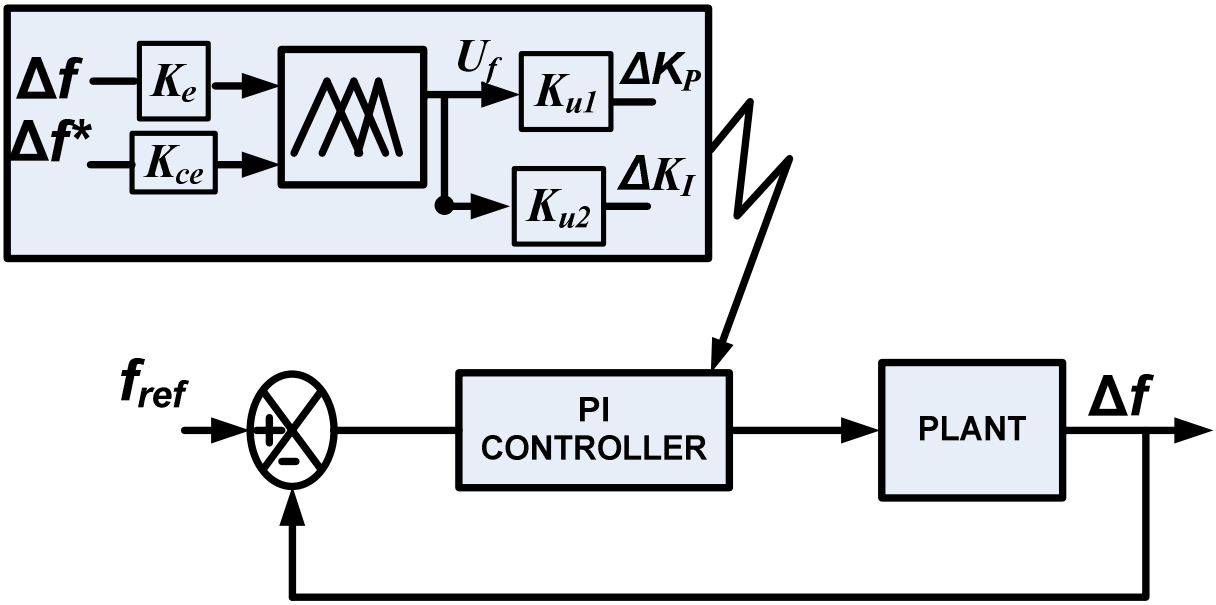

Fig. 4.3 FLA based PI controller for Autonomous MG

Fig.4.3 shows FLA based fine-tuning of the conventional PI controller. The inputs and output of FLA are $\Delta f, \Delta f^*$and U_f. As depicted in Fig.4.3, it comprises of two levels, conventional PI controller and fuzzy system. The fuzzy system tunes the gains of the PI controller as shown in the following expression:

$$\Delta K_P = K_{u1} U_f$$

$$\Delta K_I = K_{u2} U_f \tag{4.5}$$

With these gains, the modified PI controller can be expressed as:

$$U_c = (K_P + \Delta K_P) + (K_I + \Delta K_I)\,/s \tag{4.6}$$

where U_c is corrective control command to the governor summing point. Inputs, output and rule base of FLA are described below.

Input and output parameters

The FLA is formulated using MFs for the input parameters such as frequency deviations (Δf) and the rate of change in frequency deviations (Δf^*) which are defined as:

$$\Delta f = f_{ref} - f \qquad (f_{ref} = 50)$$

$$\Delta f^* = \Delta f(k) - \Delta f(k-1) \tag{4.7}$$

The above-mentioned input parameters of FLA are transformed into fuzzy set notations with the help of MFs. The output of fuzzy logic is updating factor U_f. The MFs for the inputs and outputs of FLA are shown in Fig.4.4 [104].

Linguistic variables of fuzzy parameters

Linguistic variables of fuzzy parameters are used to describe the states of the system. Seven linguistic terms are used for defining two inputs i.e. frequency deviation (Δf) and rate of change in frequency deviation (Δf^*) and one output i.e. updating factor (U_f) of the FLA. The MFs range from negative big to positive big having centroids at -1,-0.5,-0.25, 0, 0.25, 0.5,1 respectively.

Fuzzy rule base Design

Two inputs with seven fuzzy sets (7^2), hence, FLA consists of 49 rules to represent possible operating conditions, which are given in Table 4.2. The few control rules in Table 4.2 are described as [104]:

If Δf is PB and Δf^* is PB then U_f is NB

If Δf is PB and Δf^* is NB then U_f is Z

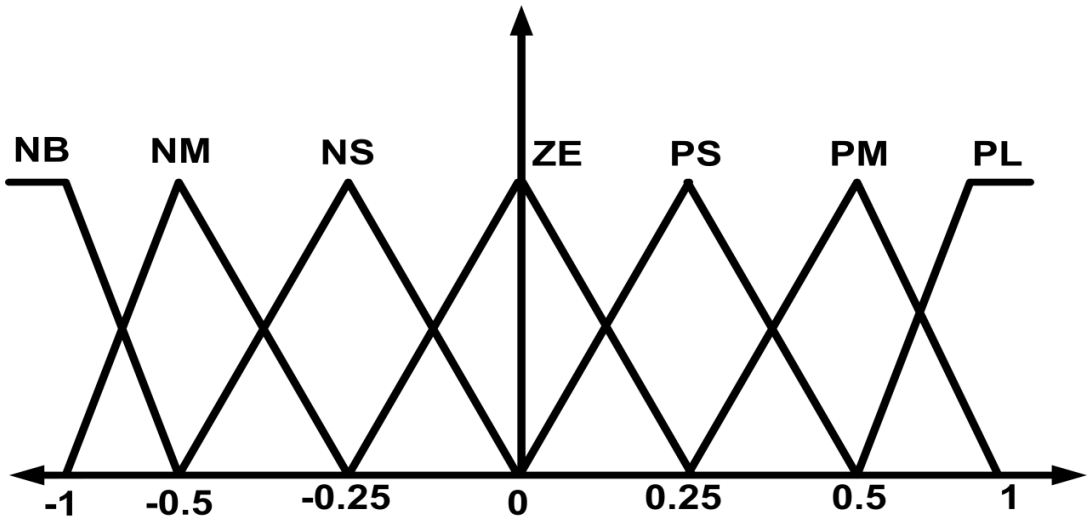

Fig. 4.4 Membership functions for Δf, Δf^* and U_f

Defuzzification

Transformation of the sum of fuzzy singleton outputs to an equivalent crisp control action U_f. Here centroid method is used for defuzzification. The defuzzified output is expressed as:

$$U_f = \frac{\sum_{j=1}^{f} A_i Q_l}{\sum_{j=1}^{f} Q_l} \tag{4.8}$$

where A_i represents the total firing area of j rules, 'f ' represents the total number of partitions of the fired area and Q_l represents the centre of an area.

Table 4.2 Fuzzy logic rules for updating factor U_f

Δf	Δf^*						
	NB	**NM**	**NS**	**ZE**	**PS**	**PM**	**PB**
NB	PB	PB	PB	PB	PM	PS	ZE
NM	PB	PB	PB	PM	PS	ZE	NS
NS	PB	PB	PM	PS	ZE	NS	NM
ZE	PB	PM	PS	ZE	NS	NM	NB
PS	PM	PS	ZE	NS	NM	NB	NB
PM	PS	ZE	NS	NM	NB	NB	NB
PB	ZE	NS	NB	NB	NB	NB	NB

As will be shown in the results and discussion section, the FLA based controller has superior performance over the conventional controller. The crucial factor about the FLA is, its performance is highly dependent on its parameters (i.e., rule base and MFs). The proper selection of these parameters depends on the availability of precise information about the system, without which the designed FLA based PI controller may not provide optimal performance over a wide range of operating conditions. To conquer this, a two-stage fuzzy logic controller is proposed for the online regulation of fuzzy parameters (MFs and rule base).

4.4 Two-Stage Adaptive Fuzzy Logic Approach based PI controller

There are several approaches to tuning fuzzy parameters [90-91,105]. In [90-91], the authors have proposed various optimization techniques to tune the MFs of FLA. In [105], the authors proposed optimal control theory for online tuning of the fuzzy rule base. Up to now, several researchers are interested in either tuning of MFs or the rule base of an FLA for frequency control of MG, but not both of them simultaneously. Based on the complexity and requirements in frequency control of MG, this work addresses a novel two-stage AFLA based PI controller for frequency control of MG. Fig. 4.5 shows the framework for the proposed controller.

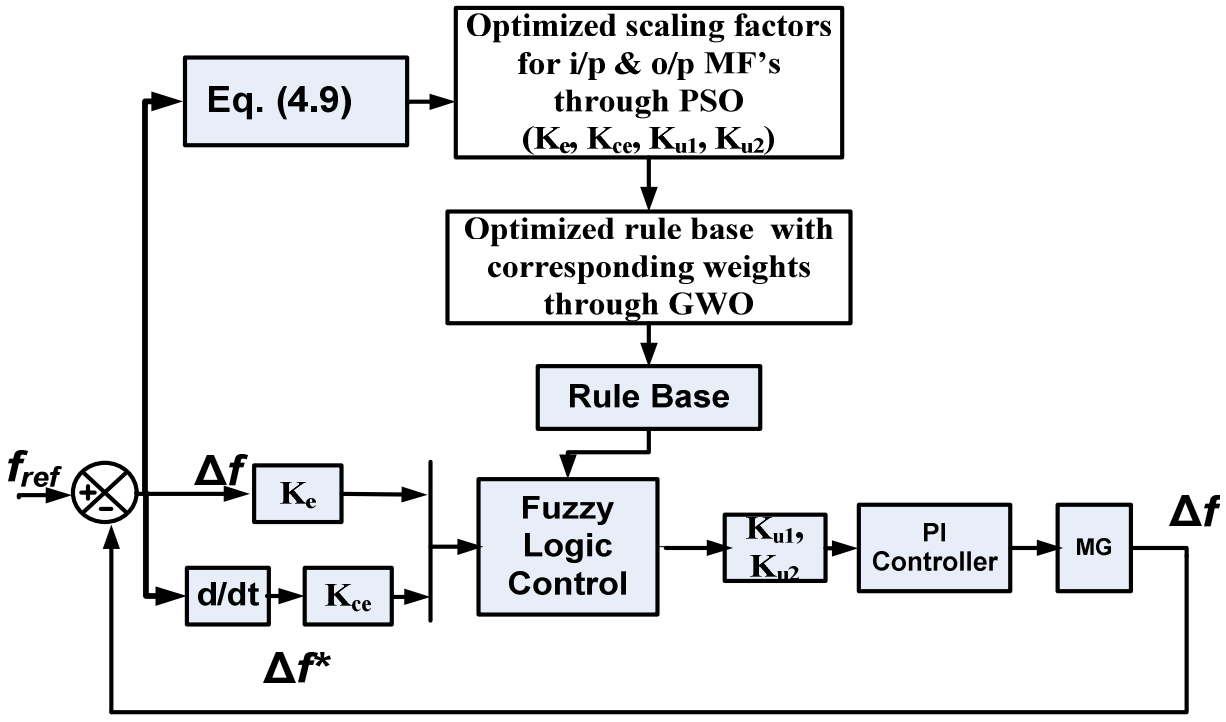

Fig.4.5 Block diagram for the proposed two-stage fuzzy logic controller

As depicted in Fig. 4.5, to design the proposed controller, two steps are needed to be performed: 1) tuning the scaling factors of MFs of FLA, 2) to design the optimal rule base with corresponding weights. To perform these steps, two metaheuristic techniques such as PSO, GWO are employed in this work. Here, in the first stage, the PSO technique is adopted to optimize the scaling factors of fuzzy parameters. Then the GWO technique is used to optimize the rule base in the second stage. With this two-stage processing, a new optimal fuzzy PI controller is obtained, and it is termed as a two-stage AFLA based PI controller. Hence, this controller is used for injecting a corrective control signal to the governor summing point. The ITAE criterion is selected as the objective function. The ITAE criteria can be expressed as follows:

$$\text{ITAE} = \min \int_0^{t_{sim}} t * |\Delta f| \, dt \tag{4.9}$$

4.4.1 PSO Algorithm to Optimize the Scaling Factors of MFs

Recently, meta-heuristic techniques became more popular because of simple implementation, non-mathematical, avoiding local minima, etc. In these techniques, PSO (standard one) and GWO (the recent one) became the most promising techniques for optimization problems. Here, these two techniques are utilized for implementing the proposed two-stage adaptive fuzzy logic controller.

PSO technique was introduced in 1995 by Kenedy et al.. inspired by the social behaviour of a group of birds flocking in the sky and searching for food [106]. In this technique, a group of birds searching for food in a specific region randomly. In that specific region, there is only one sub-region that has food, a group of birds is not aware of this sub-region, but they know their distance at each step of the searching process. In that group, one of the birds is close to food and the rest of the birds follow this bird. In this technique, swarm means the group of birds, each bird is a particle and each particle consists of two vectors X_i^K & V_i^K represents the position and velocity of each particle at the current iteration. After pre-defined iterations or maximum tolerance limit, X_i is considered as the solution to the problem. The advantage of PSO is all the particles regulate their position and velocity from previous experiences and other particle experiences. In D-dimensional search space, velocity and position of i^{th} particle at k^{th} iteration is given as:

$$V_i^K = [V_{i1}^K,\ V_{i2}^K, - - - - V_{iD}^K]$$

$$X_i^K = [X_{i1}^K,\ X_{i2}^K, - - - - X_{iD}^K] \tag{4.10}$$

In each iteration for swarm size of *'N'* in D-dimension this algorithm experiences p_{best} of each particle and overall best g_{best} represented in equation (4.11) & (4.12)

$$p_{best}^K = [p_{best,i1}^K, p_{best,i2}^K, - - - - p_{best,iD}^K] \tag{4.11}$$

$$g_{best}^K = [g_{best,1}^K, g_{best,2}^K, - - - - g_{best,D}^K] \tag{4.12}$$

With this data, the velocity and the position of each particle for the next iteration can be updated as:

$$V_{i,j}^{K+1} = w * V_{i,j}^K + c_1 * r_1 * (p_{best\ i,j}^K - X_{i,j}^K) + c_2 * r_2 * (g_{best,j}^K - X_{i,j}^K) \tag{4.13}$$

$$X_{i,j}^{K+1} = X_{i,j}^K + V_{i,j}^{K+1} \tag{4.14}$$

Where c_1 and c_2 are accelerating factors; W is inertial weight; r_1 and r_2 are random numbers between [0-1]; $X_{i,j}$ denotes the position of i^{th} particle in j^{th} dimension; $V_{i,j}$ denotes the velocity of i^{th} particle in j^{th} dimension; where *i =1,2,3-------N* and *j=1,2,3------D*. The flowchart for the PSO - based fuzzy scaling factors optimization is shown in Fig. 4.6. The sequential steps as shown in Fig. 4.6 can be summarized as follows:

Step 1: Select the PSO parameters, like population size, inertial weight, acceleration factor, number of iterations etc.

Step 2: Initialize the PSO parameters i.e. position and velocity of each particle and set $\overrightarrow{lb}$ = [0 0 0 0]; $\overrightarrow{ub}$ = [1 1 1 1]. These vectors are mandatory to implement PSO mechanism. Since optimized values lie in between [0-1].

Step 3: Evaluate the fitness function using Eq. (4.9)

Step 4: Determine p_{best} of each particle, g_{best} of each iteration based on the fitness function.

Step 5: Update the velocity and position of each particle based on Eq. (4.13) & Eq. (4.14) respectively.

Step 6: Update p_{best} and g_{best} ; if $g_{best}^{K+1} < g_{best}$ then $g_{best}^{K+1} = g_{best}$

Step 7: If the stop condition is met, display optimal scaling factors, else go to step 3.

4.4.2 GWO Algorithm to Optimize the Fuzzy Rule Base Weights

In the second stage of the proposed controller, the GWO technique is used to optimize the rule base weights of FLA. GWO technique was introduced in 2014 by Mirjalili et al., inspired by the hunting mechanism of grey wolves in nature. Average grey wolves in a group vary between 5-12, in each group four types of grey wolves such as alpha (α), beta (β), delta (δ) and omega (Ω) are employed for simulating the leadership hierarchy [74]. In hierarchy topmost level is 'α' category wolves; these are predominant in decision making, and all other wolves in the pack will follow these wolves. The second level in the hierarchy is 'β' category wolves, these wolves will help in decision making for 'α' category wolves, and these wolves will be turned into 'α' category wolves after 'α' wolves became old or passed away. The third level in the hierarchy is 'δ' category wolves have to submit themselves to 'α' and 'β' category wolves but they dominate omega. The scouts, elders, caretakers belong to these groups. The fourth level in the hierarchy is the omega (Ω) category wolves; these play the role of scapegoat. These wolves are subordinate to the all-dominating wolves. In order to design GWO to perform optimization problems, the hierarchy of wolves is modelled mathematically as shown below:

Social hierarchy

In these top-level wolves (α) are considered as the fittest solutions followed by β and δ. The rest of the solutions are considered as omega (Ω) category wolves.

Encircling Prey

Grey wolves encircle prey during hunting mathematically can be represented as:

$$\vec{D} = \left|\vec{c}.\ \vec{X}_P^K - \vec{X}^K\right| \tag{4.15}$$

$$\vec{X}_P^{K+1} = \vec{X}_P^K + \vec{A}.\vec{D} \quad (4.16)$$

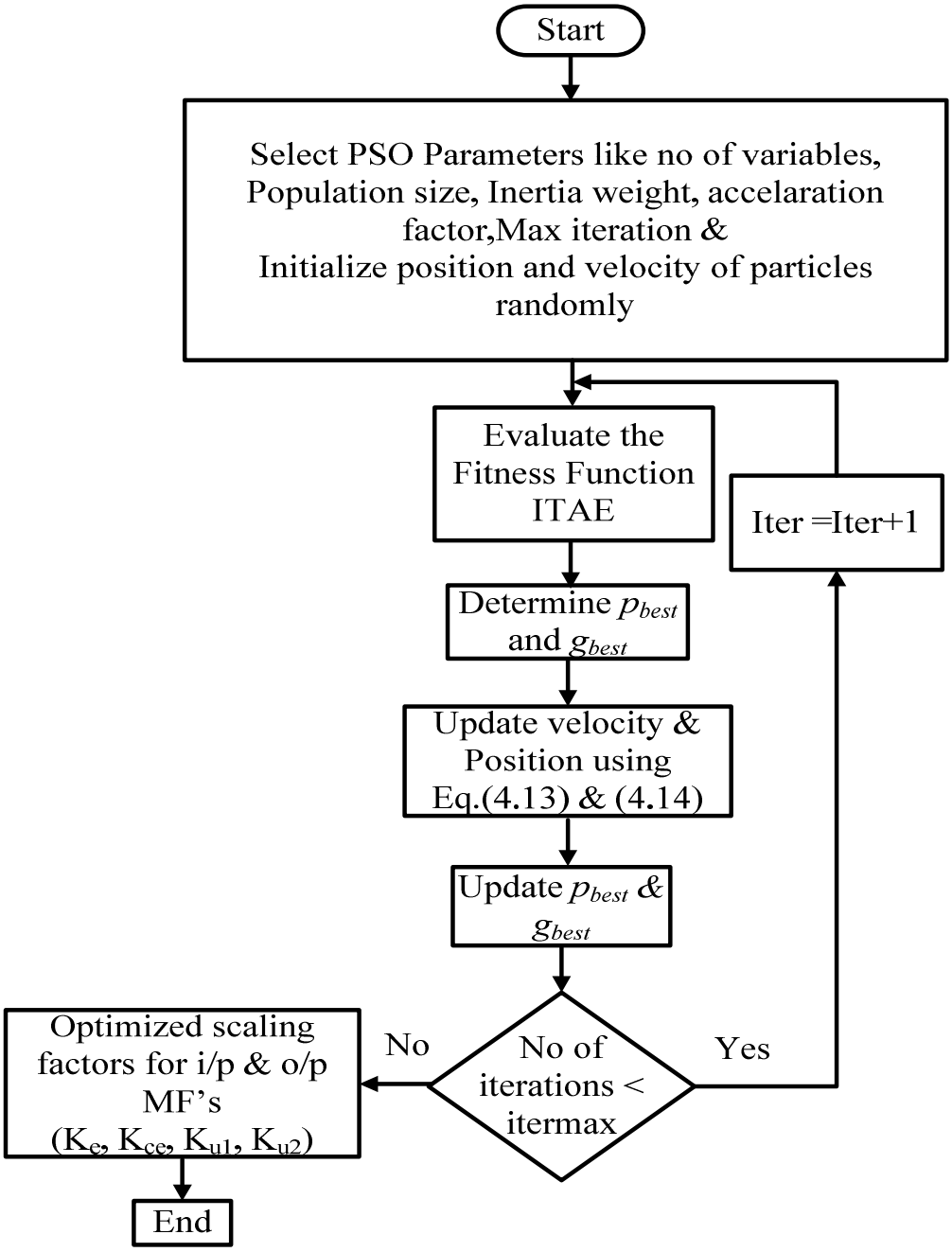

Fig. 4.6 Flowchart of PSO algorithm for optimizing scaling factors

'k' indicates the current iteration; $\vec{A}$ & $\vec{C}$ are the coefficient vectors; $\overrightarrow{X_P}$ is the position vector of prey; $\vec{X}$ the position vector of the grey wolf. $\vec{A}$ & $\vec{C}$ are calculated as follows:

$$\vec{A} = 2.\vec{a}.\overrightarrow{r_1} - \vec{a} \tag{4.17}$$

$$\vec{c} = 2.\overrightarrow{r_2} \tag{4.18}$$

$\vec{a}$ decreases linearly from 2 to 0 over a defined number of iterations, r_1 and r_2 are random vectors. A grey wolf can update its position inside the space around the prey from any initial random location.

Hunting

After encircling along with the first three best solutions all other agents update their positions according to the best search agent.

$$\overrightarrow{D_\alpha}=\left|\overrightarrow{C_1}.\overrightarrow{X_\alpha} - \vec{X}\right|;\ \overrightarrow{D_\beta}=\left|\overrightarrow{C_1}.\overrightarrow{X_\beta} - \vec{X}\right|;\ \overrightarrow{D_\delta}=\left|\overrightarrow{C_1}.\overrightarrow{X_\delta} - \vec{X}\right|$$

$$\overrightarrow{X_1} = \overrightarrow{X_\alpha} - \overrightarrow{A_1}.(\overrightarrow{D_\alpha});\ \overrightarrow{X_2} = \overrightarrow{X_\beta} - \overrightarrow{A_1}.(\overrightarrow{D_\beta});\ \overrightarrow{X_2} = \overrightarrow{X_\delta} - \overrightarrow{A_1}.(\overrightarrow{D_\delta});$$

$$\vec{X} = \frac{\overrightarrow{X_1}+\overrightarrow{X_2}+\overrightarrow{X_3}}{3} \tag{4.19}$$

α, β and δ estimate the prey other wolves in pack update their position around the prey and final position randomly within the circle. If $|A|>1$ grey wolf divergence from prey. If $|A|<1$ convergence toward prey and attack it. 'A' is a random value between [-a a] this process is known as exploitation. The flowchart for the GWO based fuzzy rule base optimization is shown in Fig.4.7. The sequential steps as shown in Fig. 4.7 can be summarized as follows:

Step 1: Initialize the grey wolf population size using the equation:

$$\overrightarrow{X_{ij}} = \overrightarrow{lb} + rand * (\overrightarrow{ub} - \overrightarrow{lb}) \tag{4.20}$$

where, $\overrightarrow{lb}$ = [Zeros (1, 49)] and $\overrightarrow{ub}$= [Ones (1, 49)].

Step 2: Calculate the fitness of each wolf using Eq. (4.9).

Step 3: Based on fitness function value, prepare the wolf's list in descending order. Select the top three wolves in the population as α, β, and δ.

Step 4: Initialize the values of 'a', 'A' and 'c'.

Step 5: Update the position of wolves using the equations (4.19).

Step 6: Decrease the value of '*a*' linearly.

Step 7: If the termination condition is achieved display optimal rule base with corresponding weights. Otherwise, return to step 2.

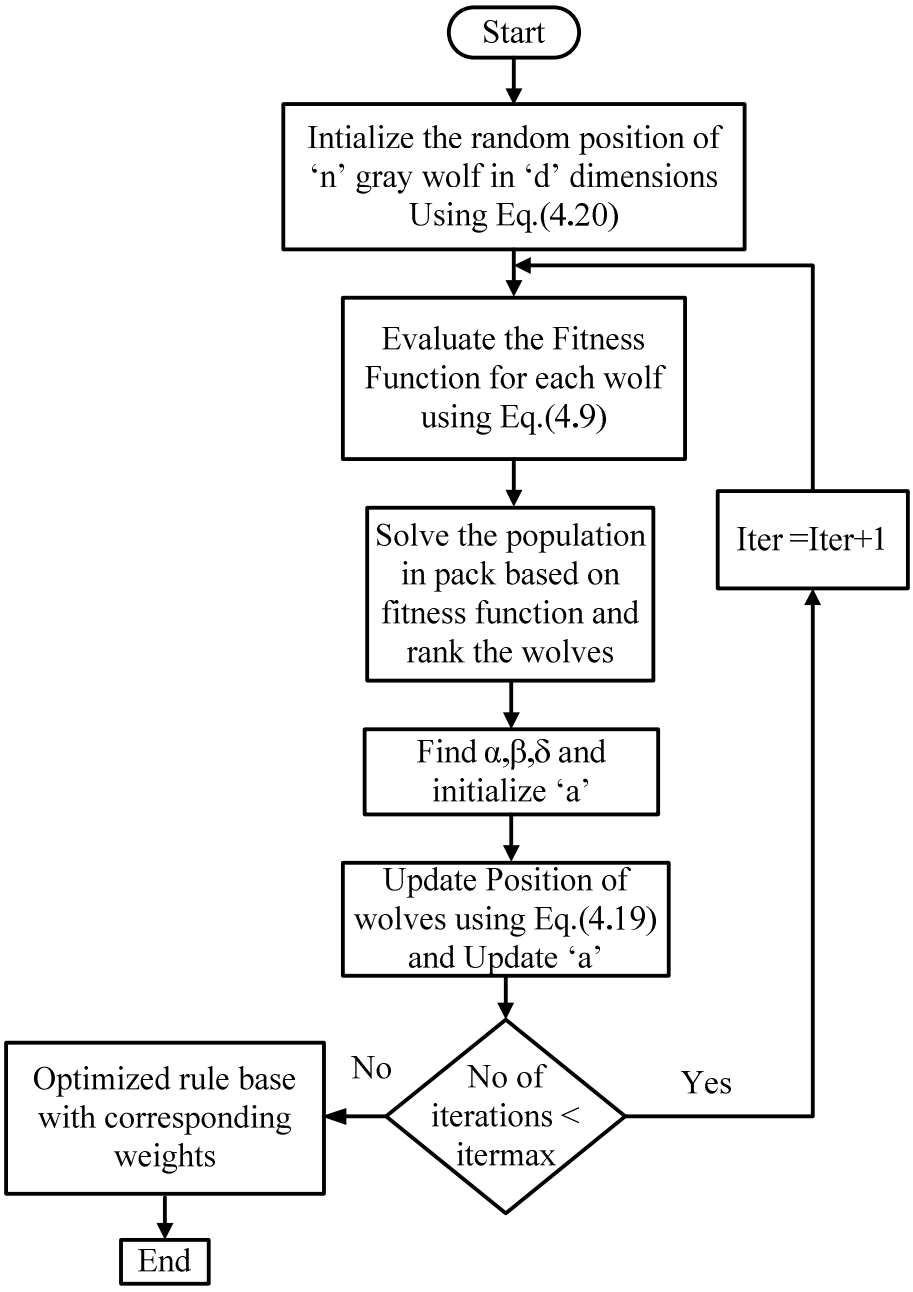

Fig. 4.7 Flowchart of GWO algorithm for optimizing the rule weights

4.5 Results and Discussion

The simulated model of the selected test system has been formulated with the help of MATLAB (R2015a) software, a core i7 processor with 8 GB RAM computer. The test system parameters are listed in Table 4.1. Time-domain simulations of MG frequency response, in the presence of disturbances likeΔP_L,ΔP_{WP}, ΔP_{φ} are presented. To show the supremacy of the proposed two-stage adaptive FLA based PI controller, results are compared with conventional PI [14], FLC PI [103], and PSO tuned FLC PI [90]. Six scenarios are considered in order to demonstrate the effectiveness of the proposed controller. In this study, to get better clarity of results, the first three controllers (PI, Fuzzy, PSO tuned Fuzzy) are compared. Out of these three controllers, the better one is chosen and compared with the proposed controller.

Scenario 1: Only with Load disturbance (ΔP_L) in MG

Multi-step load deviations are considered as shown in Fig. 4.8 (a). Fig. 4.8 (b) and Fig. 4.9 (c) represent the output frequency deviation response of MG for scenario 1.

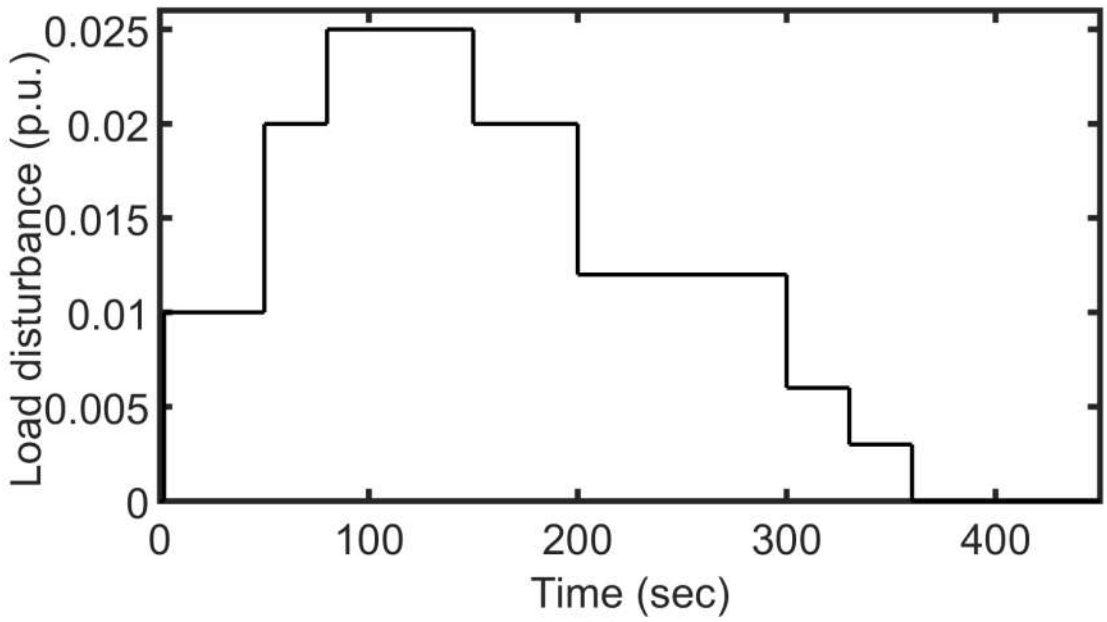

(a)

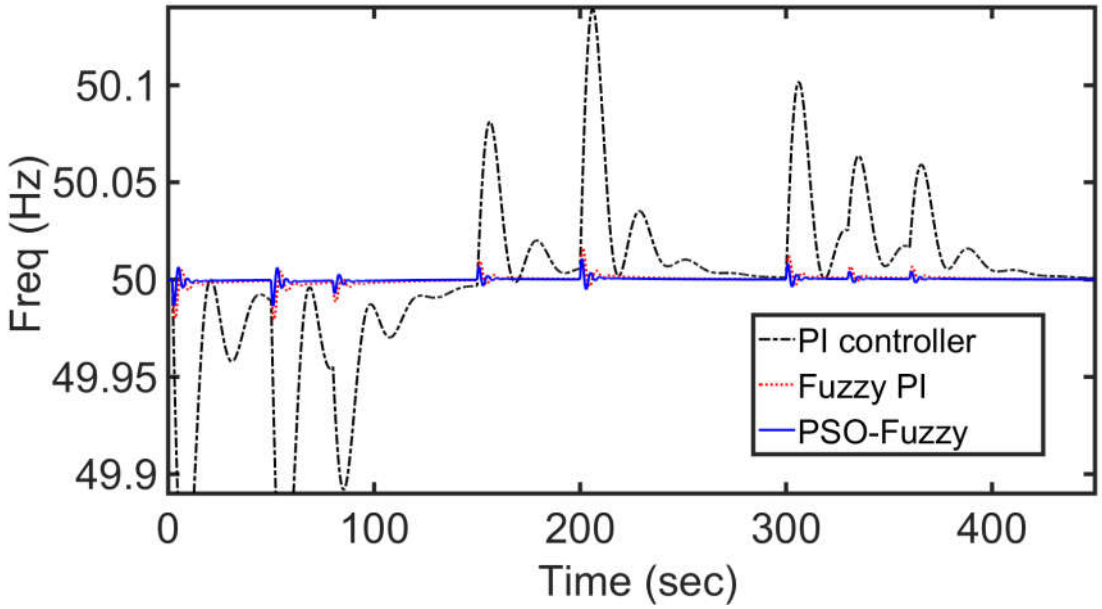

(b)

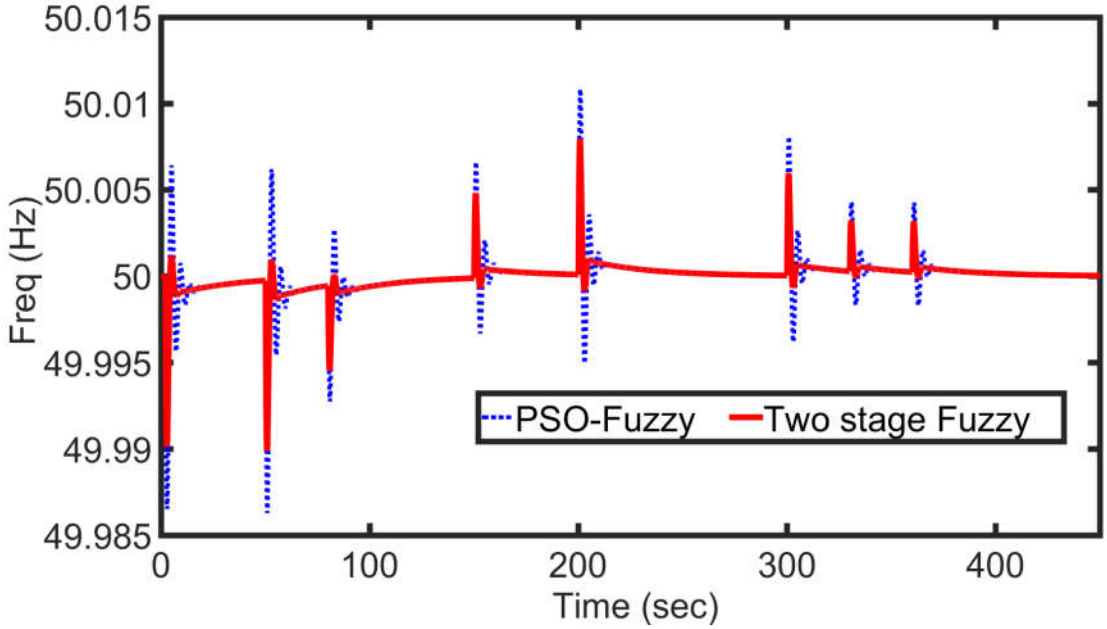

(c)

Fig. 4.8 (a) Load fluctuations b) MG frequency response (with PI, Fuzzy and PSO-Fuzzy) c) MG frequency response (with PSO- Fuzzy and Two-stage fuzzy controller)

Scenario 2: Only with wind power fluctuations (ΔP_{WP}) in MG

Fig. 4.9 (a) shows the randomly fluctuating wind power deviations. Fig. 4.9 (b) and Fig. 4.9 (c) represents the output frequency deviation response of MG for scenario 2.

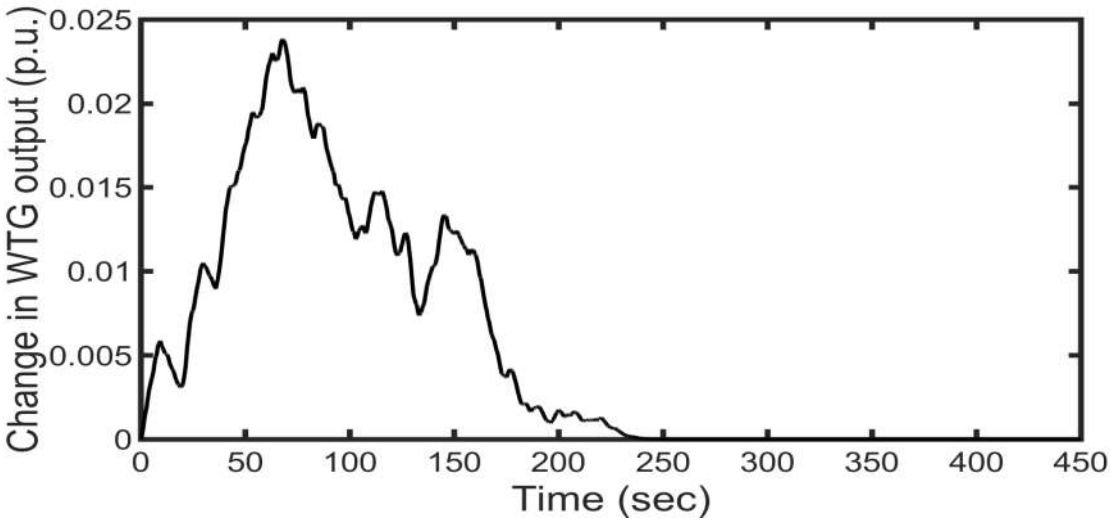

(a)

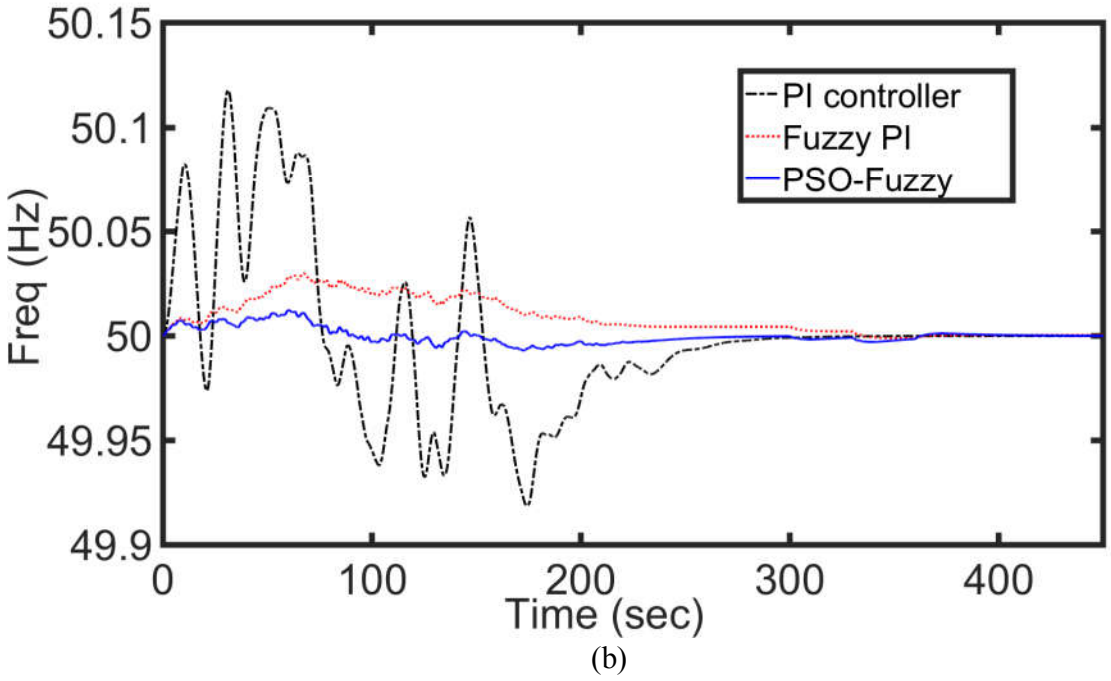

(b)

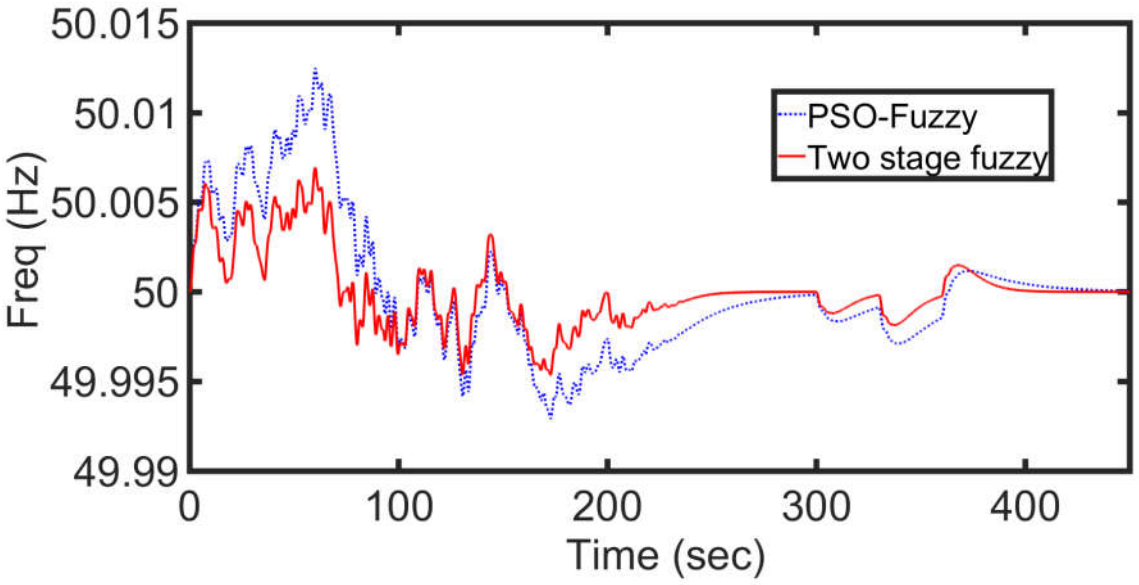

(c)

Fig. 4.9 a) Wind power fluctuations b) MG frequency response (with PI, Fuzzy and PSO-Fuzzy) c) MG frequency response (with PSO- Fuzzy and Two-stage fuzzy controller)

Scenario 3: Only with solar radiation changes (ΔP_{φ}) in MG

Fig. 4.10 (a) shows the solar radiation changes at different time instants. Fig. 4.10 (b) and Fig. 4.10 (c) represent the frequency deviation response of MG for scenario 3.

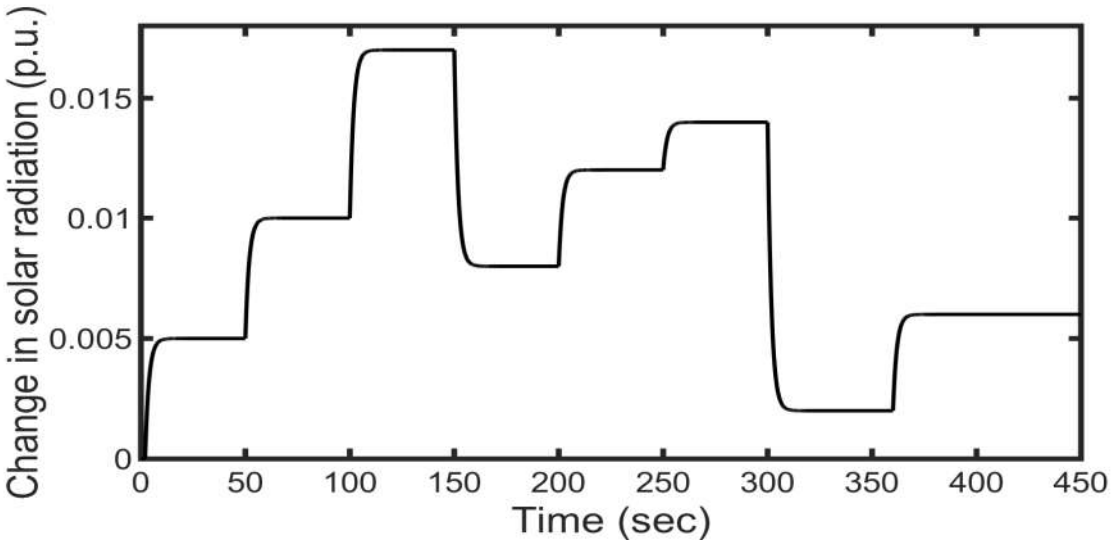

(a)

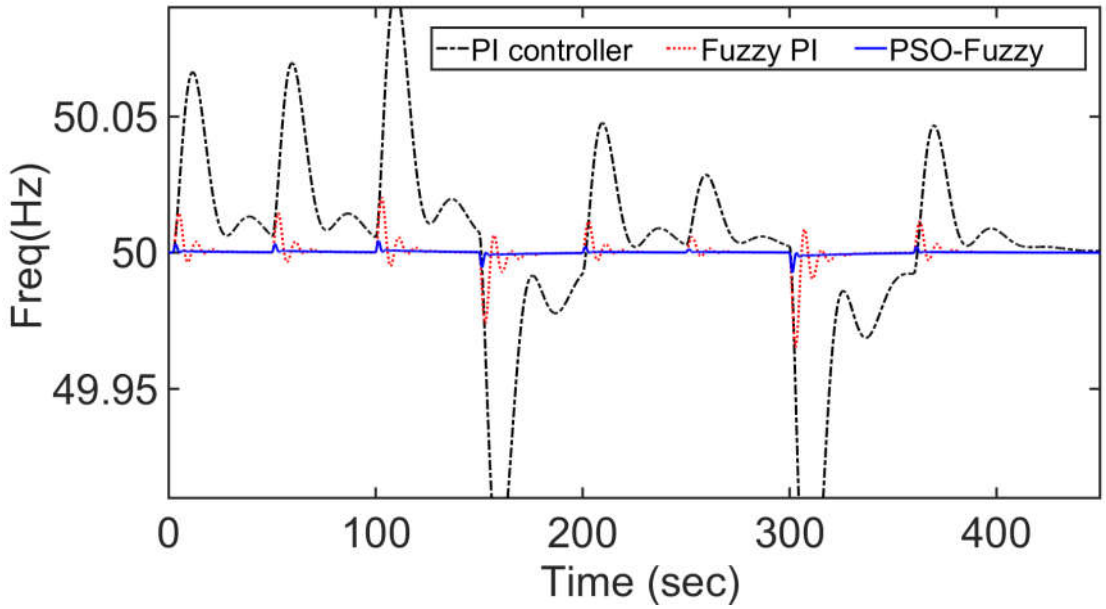

(b)

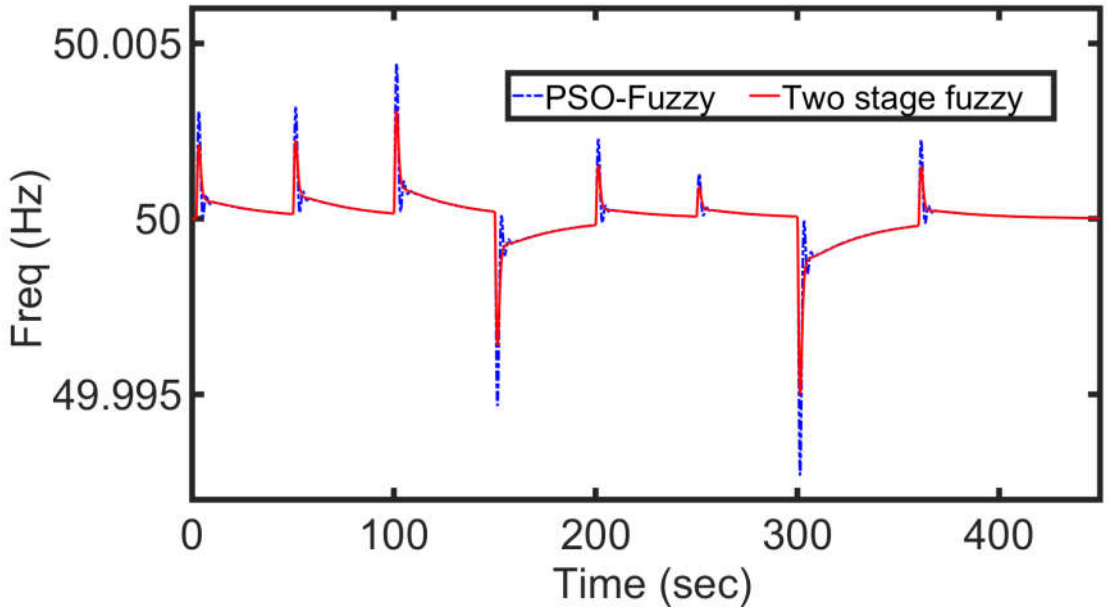

(c)

Fig. 4.10 a) Solar radiation changes b) MG frequency response (with PI, Fuzzy and PSO-Fuzzy) c) MG frequency response (using PSO- Fuzzy and Two-stage fuzzy controller)

Scenario 4: Robustness against Concurrent changes $(\Delta P_L, \Delta P_{WP}, \Delta P_{\varphi})$ in MG

Fig. 4.11 (a) shows multiple disturbances occurring simultaneously. Fig. 4.11 (b) and Fig. 4.11 (c) represent the output frequency deviations of MG for scenario 4.

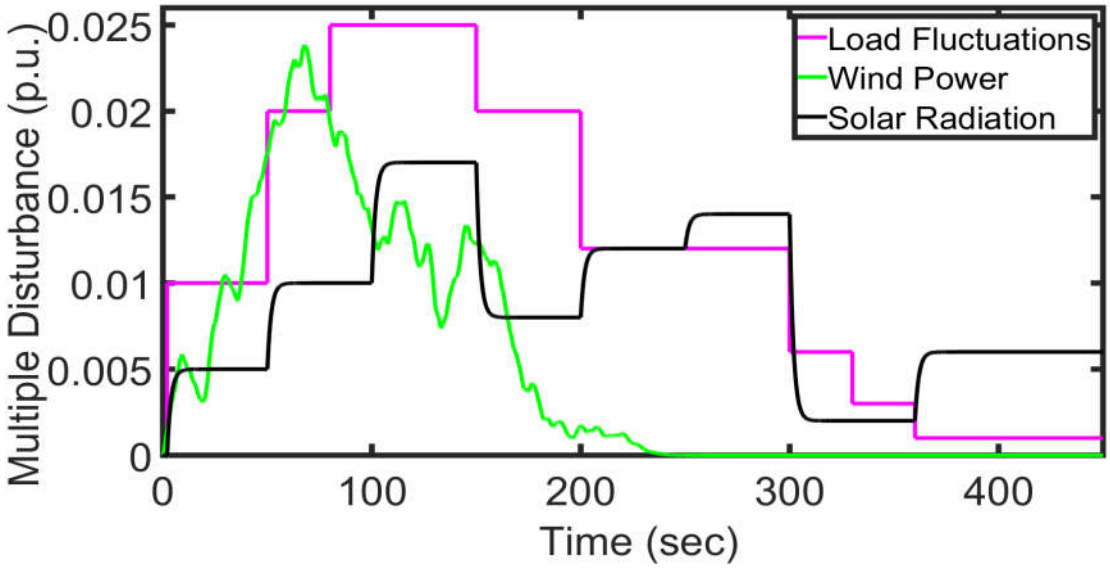

(a)

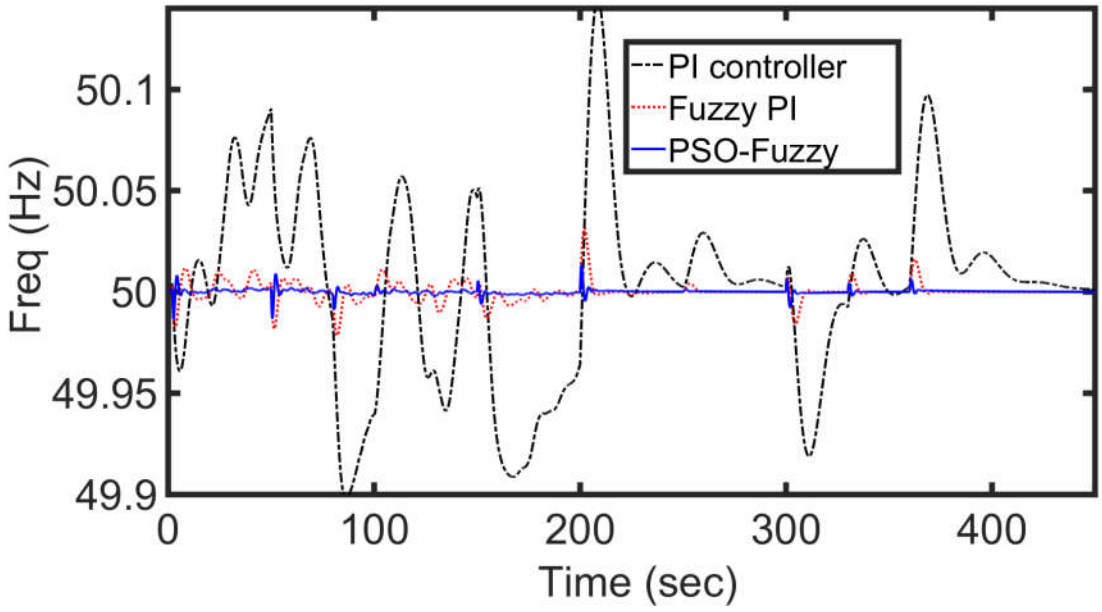

(b)

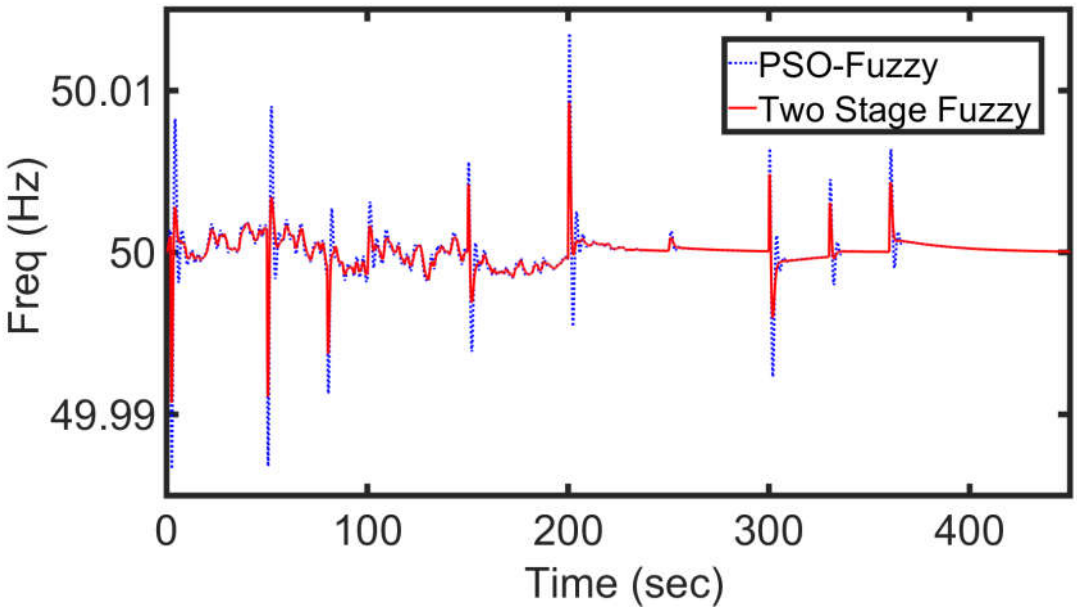

(c)

Fig. 4.11 a) Simultaneous disturbances in MG b) MG frequency response (with PI, Fuzzy and PSO-Fuzzy) c) MG frequency response (with PSO- Fuzzy and Two-stage fuzzy controller)

Scenario 5: Robustness against concurrent changes in ($\Delta P_L, \Delta P_{WP}, \Delta P_{\varphi}$) in MG (Scenario 4 conditions) along with parametric uncertainties (50% reduction in M & D).

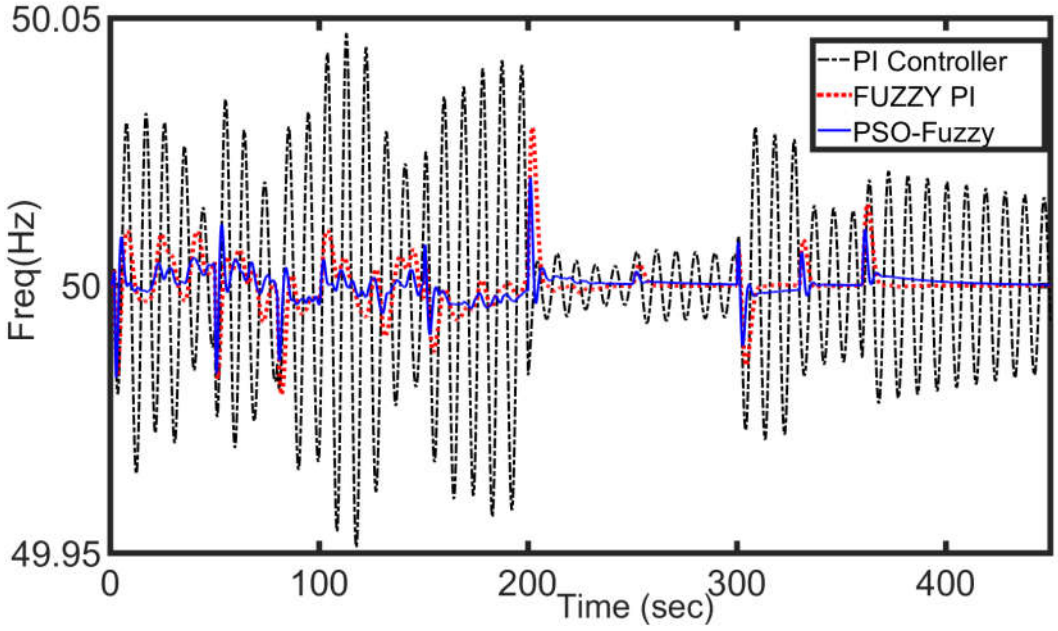

(a)

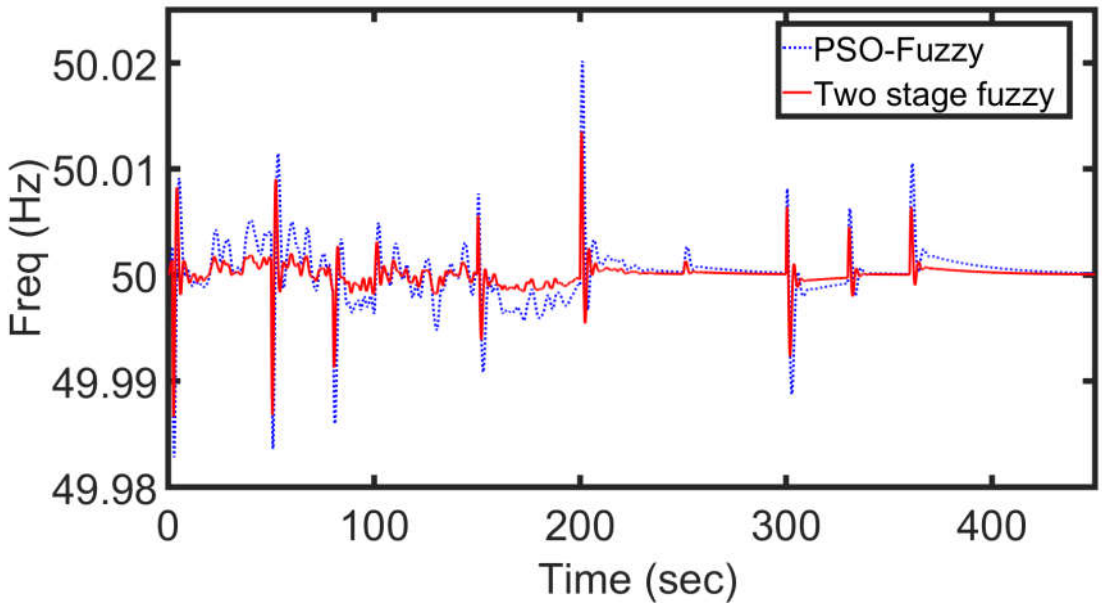

(b)

Fig. 4.12 a) MG frequency response (with PI, Fuzzy and PSO-Fuzzy) b) MG frequency response (using PSO- Fuzzy and Two-stage fuzzy controller)

Fig. 4.12 (a) & (b) represents the output frequency deviations of MG with multiple disturbances and parametric uncertainties (i.e., 50% reduction in M & D).

Scenario 6: Robustness against ESS uncertainties along with scenario 5 conditions.

Finally, to explore the robustness of the proposed controller at the next level, the fuel cell is disconnected from the MG at t=100s with scenario 4 conditions. Fig. 4.13 illustrates the simulation results for this scenario. It also shows that the proposed controller enhances the frequency response of the MG in comparison to other controllers in the literature, especially where the overshoots are concerned. Certainly, from Fig 4.13, despite the fuel cell disconnection, the proposed controller shows its robustness over the other three controllers. Whereas, GOA optimized PI controller fails to stabilize the frequency deviations within the tolerable limits due to its limited degree of freedom in tuning and also due to unpredictable change in operating conditions of the MG.

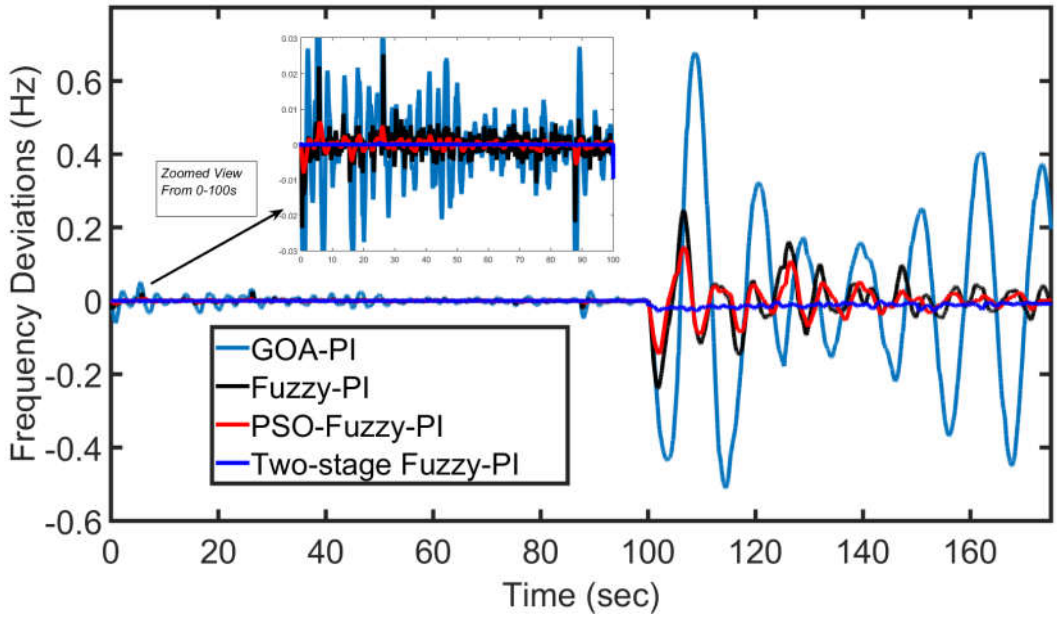

Fig. 4.13 Frequency deviation response of MG for scenario 4 conditions

From the simulation results of the scenarios mentioned above, it is evident that the proposed controller minimizes the frequency deviations significantly when compared to the other controllers. A sudden change in operating condition due to highly uncertain RES power and continuous change in MG structure, conventional PI controller fails to stabilize the frequency deviations of MG, as shown in Fig. 4.13. The characteristics as mentioned above demand the need for an efficient and intelligent controller. The proposed controller is a reliable solution for the MG frequency control problem. To assess the performance of the proposed controller quantitatively from the simulation results, three performance indices are considered. These are ITAE, settling time, and peak overshoot/undershoot. The ITAE performance index is evaluated for five scenarios, and the results are tabulated in Table 4.3.

In this work, each type of disturbance is considered with multiple-step deviations, except in scenario 2. In scenario 2, continuously fluctuating power is considered. For performance analysis in scenario 2, overall peak overshoot and settling time are considered. For the rest of the scenarios, the analysis is done with step load disturbance at 200sec. The settling times and peak overshoots of various controllers are given in Table 4.4.

Table 4.3 The ITAE performance index (Eq. (4.9)) for different scenarios

Scenario	**PI [14]**	**FUZZY PI [90]**	**PSO-FUZZY PI [103]**	**Two-Stage Fuzzy PI**
Scenario 1	0.00751	0.00314	0.000329	0.000216
Scenario 2	0.00683	0.001364	0.000651	0.0002445
Scenario 3	0.00432	0.001298	0.000423	0.0001609
Scenario 4	0.00956	0.000372	0.000160	0.000122
Scenario 5	Unstable	0.000618	0.000392	0.000277

As shown in Table 4.3 and 4.4, the performance indices of various scenarios evident that the proposed controller is robust and efficient to various operating conditions. In fact, with the proposed controller, in all scenarios, overshoot and settling time reduces to a minimum of 43.75% and 37.5% compared to Fuzzy PI [90], 18.18%, and 20% compared to PSO-Fuzzy PI [103].

Table 4.4 Dynamic response comparative study

Scenario	PI Controller [14]		Fuzzy PI [103]		PSO-Fuzzy PI [90]		Two-stage Fuzzy PI	
	Peak over/under shoot (Hz)	Settling Time (Sec)	Peak over/under shoot	Settling Time (Sec)	Peak over/under shoot	Settling Time (Sec)	Peak over/under shoot	Settling Time (Sec)
Scenario 1	50.14	65	50.016	28	50.011	20	50.009	14
Scenario 2	50.11	290	50.018	255	50.0116	250	50.0075	242
Scenario 3	50.15	50	50.0045	25	50.003	15	50.0017	12
Scenario 4	50.138	50	50.03	32	50.014	25	50.01	20
Scenario 5	Unstable		50.031	40	50.0205	34	50.013	25

Fig. 4.14 (a) shows the ITAE characteristics of proposed two-stage FLC PI and PSO tuned FLC PI for scenario 4. Fig. 4.14 (b) shows the ITAE characteristics of two-stage FLC PI, PSO tuned FLC PI and GOA-PI controller for scenario 6.

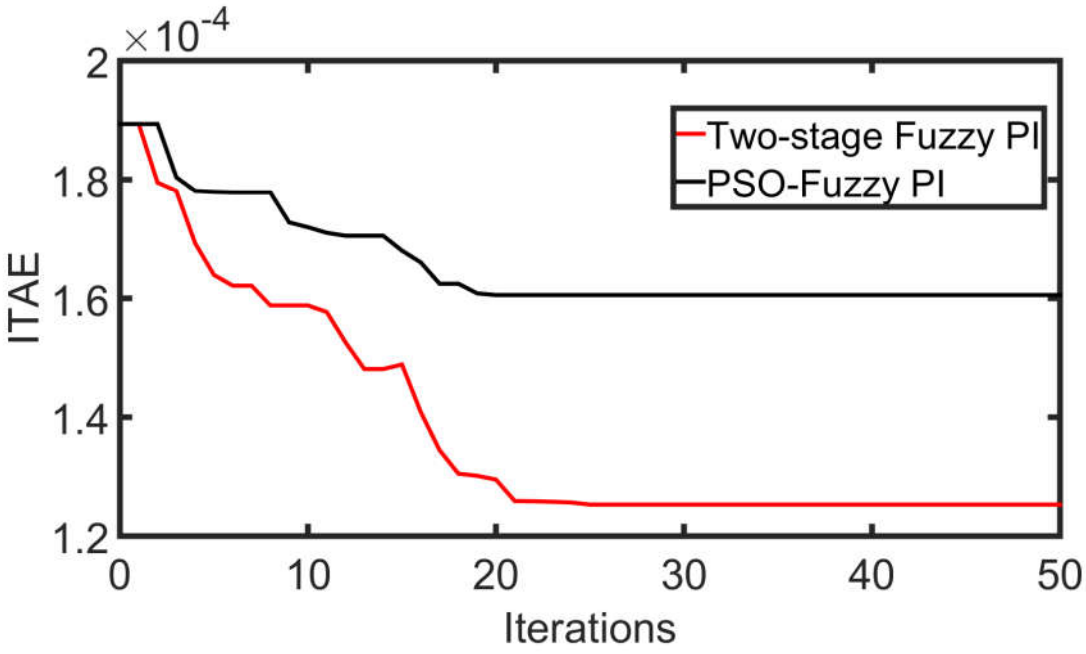

(a)

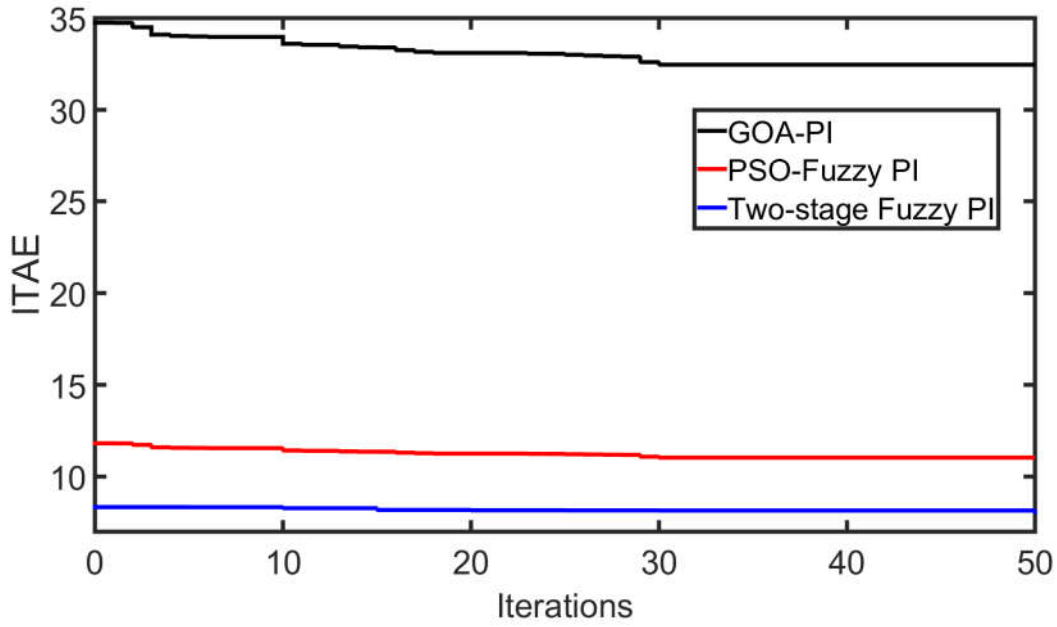

(b)

Fig. 4.14 a) ITAE Characteristics for scenario 4 b) Characteristics for scenario 6

4.6 Summary

In this chapter, a novel two-stage adaptive fuzzy logic based PI controller is presented for the LFC problem of an autonomous MG. In practice, the conventional PI controller fails to provide better performance in the presence of multiple disturbances and parameter uncertainties. Moreover, the GOA-PI controller fails to provide acceptable performance in the presence of multiple disturbances and ESS uncertainties. In response to this problem, the proposed approach is designed in a way to minimize the effects of disturbances **(**ΔP_L, ΔP_{WP}, ΔP_{φ}**)** and parameter uncertainties MG and ESSs in frequency control of MG. Six scenarios are considered for testing the effectiveness of the proposed controller under steady-state and dynamic conditions. From the results, it is found that the proposed method has the inherent advantages of independent control, reduced overshoots, better settling times, and an increased level of robustness. Compared to other controllers, the proposed controller has better performance than the PSO-Fuzzy PI controller and Fuzzy PI controller due to its simultaneously tuning capability of fuzzy parameters.

Chapter 5

Coordinated Control of Conventional Power Sources Along with PHEVs for Load Frequency Control of Renewable Penetrated Power System

5.1 Introduction

A high amount of RES penetration (instead of CPS) reduces the system inertia with the use of more number of inverter associated generation units, which makes the system more sensitive to disturbances. The governors of the hydro and thermal units are not adequate to mitigate the frequency disturbances due to their sluggish response [107]. So, the CPS needs an additional energy source with immediate response to discharge or store the energy for frequency control of the power systems. Among all the ESSs, plug-in hybrid electric vehicles (PHEVs) form an excellent option for frequency stability studies due to its inherent distributed availability, fast-acting capability, and slow discharge rate during the idle condition [108]. Therefore, in this chapter, an aggregated model of PHEVs is developed and its impact on frequency control of renewable penetrated power systems has been analyzed. Moreover, a coordinated control scheme for CPS along with PHEVs is required to enhance the frequency response for such a renewable penetrated power system.

Hence, in this work, a coordinated control strategy between CPS and PHEVs is proposed. Where, the proposed coordinated control strategy is based on the PID controller, which is optimally tuned by the recently developed JAYA Algorithm (JA) to minimize the frequency deviations of the power system. The proposed strategy is tested on IEE Japan East 107-bus-30-machine power system. The dynamic performance of the test system with the proposed strategy is investigated through simulations against random changes in load, wind power and solar power. Furthermore, the proposed coordinated LFC strategy with the JAYA algorithm is compared with the JAYA LFC strategy with CPS alone and LFC strategy with CPS along with PHEVs in the PFC loop. Besides, a brief comparative assessment of the proposed JA in improving dynamic response in terms of overshoots, settling time and ITAE over with the existing controllers in literature is also carried out to show the merits of the proposed controller.

5.2 Modelling of the Interconnected Power System

This chapter focuses on frequency control of the IEE Japan East 107-bus-30-machine power system, including CPS, solar power, wind power, and PHEVs. Fig. 5.1 illustrates a schematic diagram of the Japanese power system with RES and PHEVs. Fig. 5.2 illustrates a mathematical model of the IEE Japan East 107-bus-30-machine power system, which is modelled as a two-

area interconnected power system. There are two types of CPS in each area, which are thermal and hydro generators with an aggregated speed control mechanism. In area-1, CPS and PHEV aggregator are responsible for generation-load balance, and in area-2, CPS are only responsible for the generation-load balance. These two areas are interconnected through an AC tie-line with a maximum allowable capacity of 500 MW.

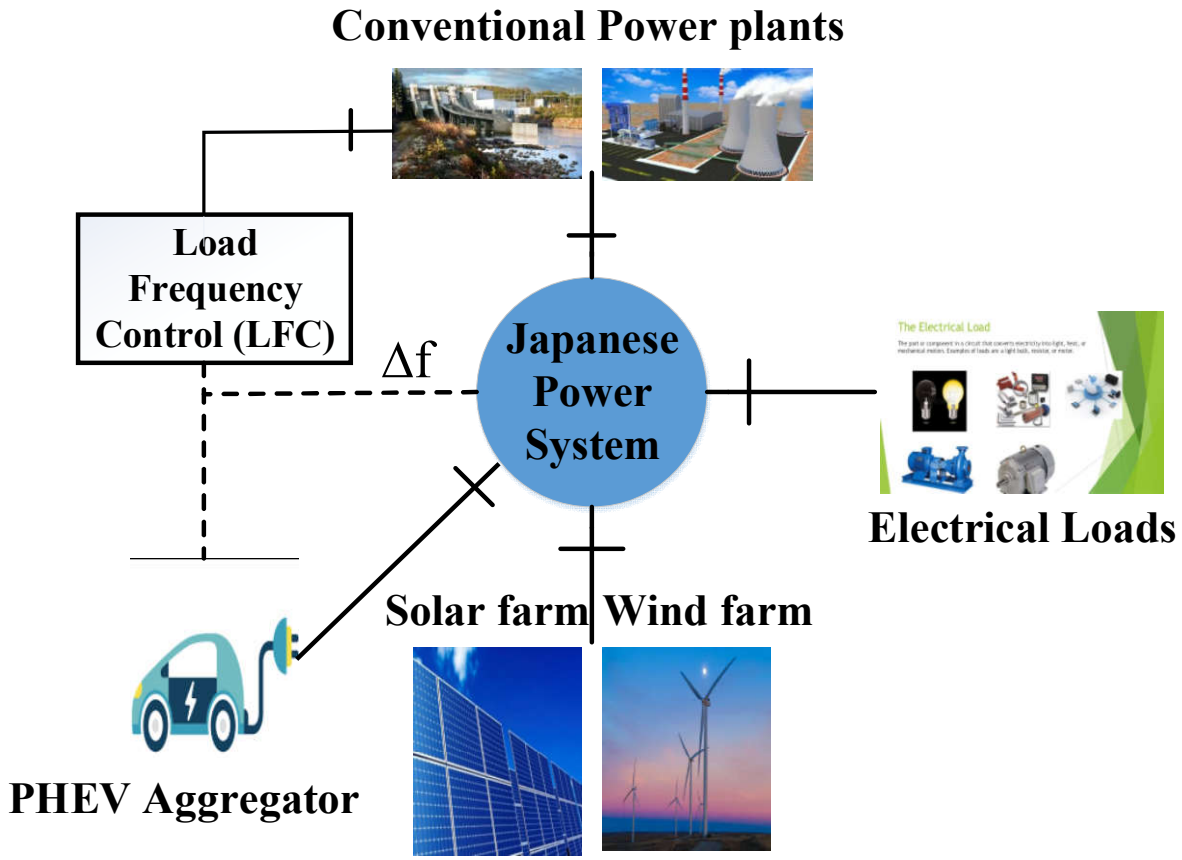

Fig. 5.1 Schematic model of the Japanese power system with PHEVs and RES

In interconnected power systems, the disparity between the actual and scheduled generation is termed as Area Control Error (ACE):

$$ACE_1 = \beta_1 * \Delta f_1 + \Delta P_{tie,12}$$
$$ACE_2 = \beta_2 * \Delta f_2 + \Delta P_{tie,21} \quad (5.1)$$

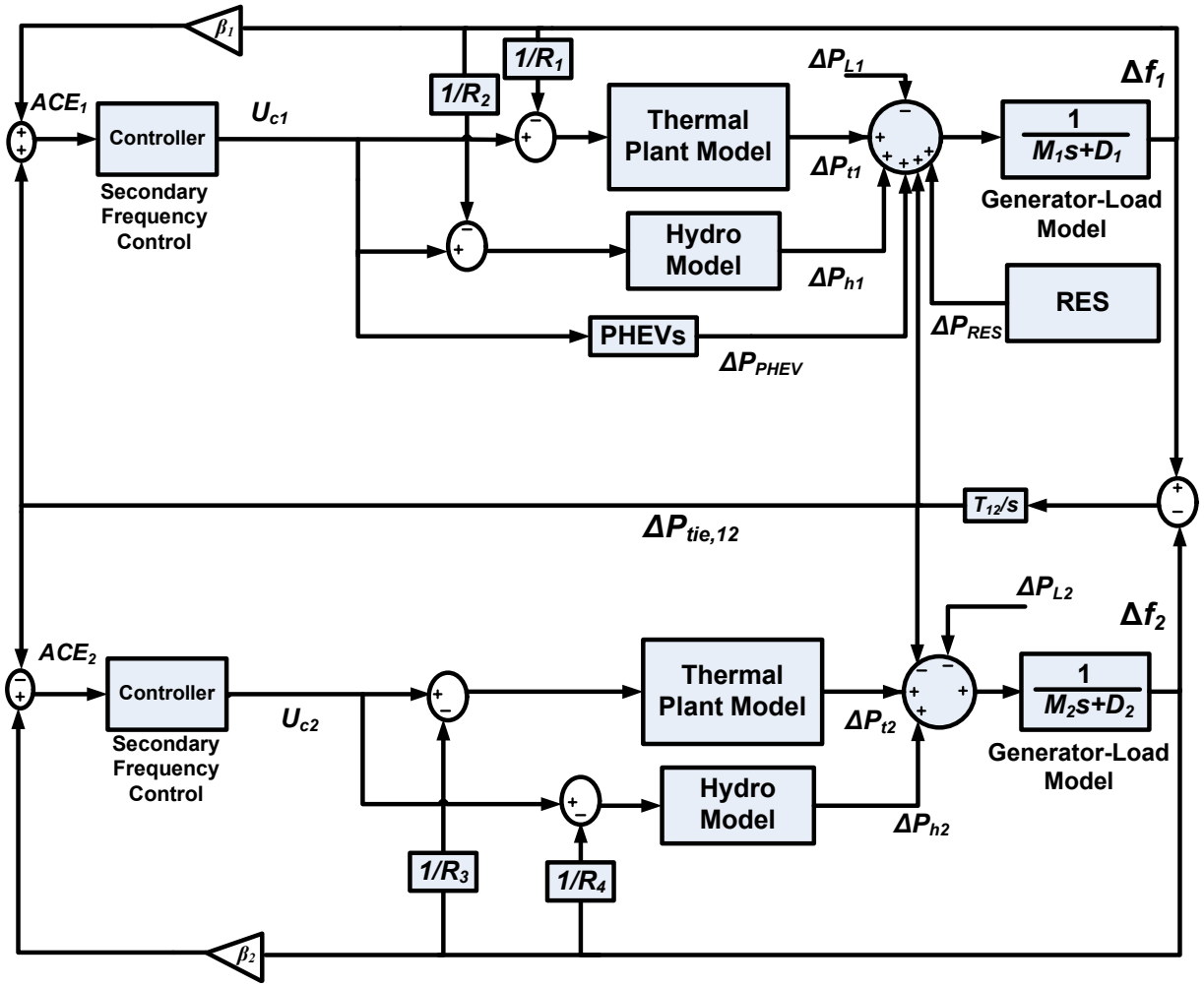

Fig. 5.2 Mathematical model of two-area power system with RES and PHEVs

where, $\Delta f_1 = \frac{1}{M_1 s + D_1}(\Delta P_{t1} + \Delta P_{h1} + \Delta P_{RES} + \Delta P_{PHEV} - \beta_1 \Delta f_1 - \Delta P_{L1})$; $\beta_1 = (\frac{1}{R_1} + \frac{1}{R_2} + D_1)$ &

$$\Delta f_2 = \frac{1}{M_2 s + D_2}(\Delta P_{t2} + \Delta P_{h2} - \beta_2 \Delta f_2 - \Delta P_{L2}); \quad \beta_2 = (\frac{1}{R_3} + \frac{1}{R_4} + D_2); \tag{5.2}$$

$$\Delta P_{tie,12} = \frac{T_{12}}{s}(\Delta f_1 - \Delta f_2) \text{ and } \Delta P_{tie,21} = -\Delta P_{tie,12} \tag{5.3}$$

Finally, the corrective signal from the controller to PHEV aggregator and governors of each area can be expressed as:

$$U_{ci} = (K_P + \frac{K_I}{s} + s * K_D) * ACE_i \text{ where } i=1,2 \tag{5.4}$$

The objective of the proposed controller is to minimize the ACE, such that the frequency deviations in each area and tie-line power deviation between two areas are to be restored within the scheduled limit.

5.2.1 Thermal and Hydro Generator Models

Fig. 5.3 (a)-(c) shows the mathematical models of the thermal generator, boiler dynamics, and hydro generator with all possible nonlinearities. This model includes all constraints for LFC studies, i.e., speed governor mechanism, boiler dynamics, reheat-turbine system and generator-load model [108]. In this study, the dead-band effect of the governor is about 0.02% for the hydro system and 0.04 % for the thermal system. The GRC for hydro and thermal units is about 3.5% and 1.7e-02 puMW per second respectively.

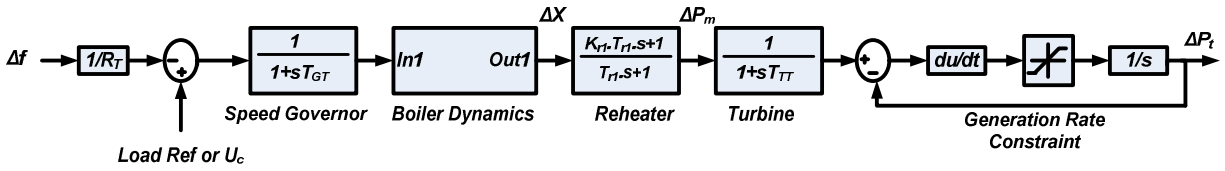

R_T: Droop coefficent of thermal unit; T_{GT},:Governor time constant; ΔX: Change in valve position for steam turbine; K_{r1}: Coefficient of re-heat; T_{r1}: Turbine reheat time constant; T_{TT}: Time constant of turbine; ΔP_m: Change in mechanical power; ΔP_t: Change in output power of thermal unit

(a)

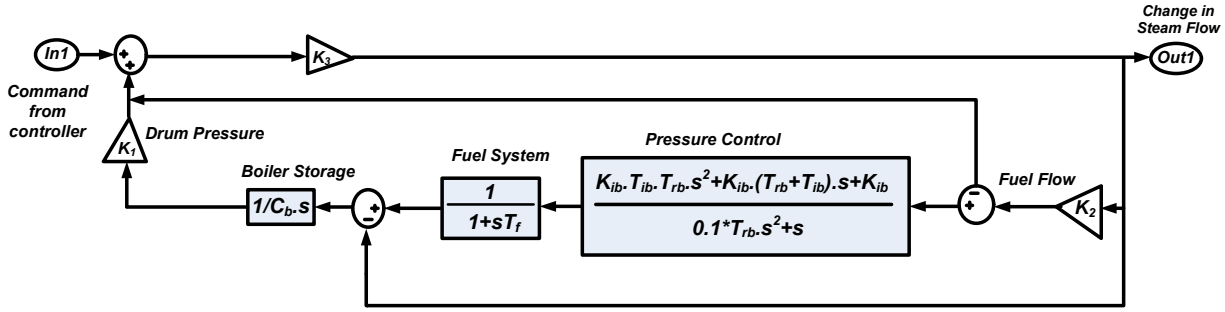

K_1: Drum pressure constant; K_2: Throttle pressure constant; K_3: Steam flow constant; C_b: Boiler storage constant; T_f: Fuel system time constant; T_{rb}: Lead-Lag compensator time; T_{ib}: Pressure controller time constant; K_{ib}: Super heater friction drop coefficent

(b)

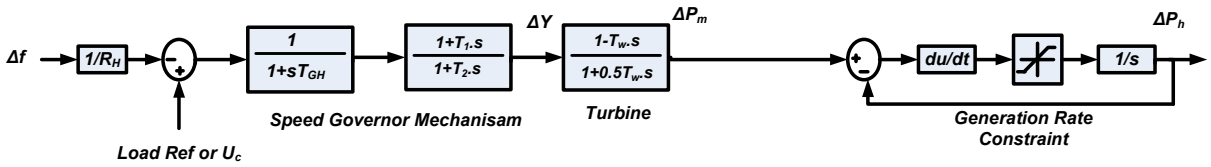

R_H: Speed regulation constant of hydro unit; T_{GH}: Governor time constant of hydro unit; ΔY: Change in valve position for hydro turbine; ΔP_m: Change in mechanical power; T_1:Hydro governor rest time; T_2:Transient droop time constant; T_W: Water turbine time constant; ΔP_h: Change in output power of hydro unit

(c)

Fig. 5.3 Mathematical model of (a) Thermal unit, (b) Boiler dynamics and (c) Hydro unit

As shown in Fig 5.3 (a) & (c), the governors of thermal and hydro units adjust their respective valve positions (ΔX and ΔY) according to the control signal (U_c) to meet the load changes. The ΔP_t and ΔP_h indicates the corresponding change in thermal and hydro-generator powers concerning to the load changes.

5.2.2 PHEVs

A bi-directional vehicle-to-grid (V2G) power control PHEV aggregator is chosen for this study [109]. Fig. 5.4 depicts the mathematical model of the PHEV aggregator. The output power of PHEV aggregator for discharging or charging is selected based on the control signal (U_{c1}) from the controller. In the present work, the U_{c1} is determined by using the JA-PID controller. In Fig. 5.4, the EV aggregator model consists of PFC, LFC and battery charger. e^{-sT} denotes the time delay in the system due to communication delays between the LFC control centre and EV aggregator. $T_{EV,i}$ denotes the battery time constant; R_{AG} denotes the droop coefficient of EV aggregator. $K_{EV,i}$ denotes the individual EV's participation factor in the frequency control. The EVs participate in LFC only when they are in charging mode or in idle mode. The participation factor ($K_{EV,i}$) of each EV depends on their respective battery State-Of-Charge (SOC) level.

Fig. 5.5 (a) & (b) shows the $K_{EV,i}$ vs. Battery SOC for discharge mode and idle mode respectively. If the EVs are disconnected from the aggregator, $K_{EV,i}$= 0. Detailed information regarding the aggregated PHEV model and participation factors is available in [110]. ΔP_{PHEV} represents the change in output power of the PHEV aggregator.

The ΔP_{PHEV} is controlled based on a control signal (U_{c1}), which is based on Δf of each area can be expressed as [107]:

$$\Delta P_{PHEV} = \begin{cases} -\Delta P_{max}, & U_{c1} < -\Delta P_{max} \\ \Delta P_{max,} & U_{c1} > \Delta P_{max} \\ U_{c1}, & |U_{c1}| \leq \Delta P_{max} \end{cases} \tag{5.5}$$

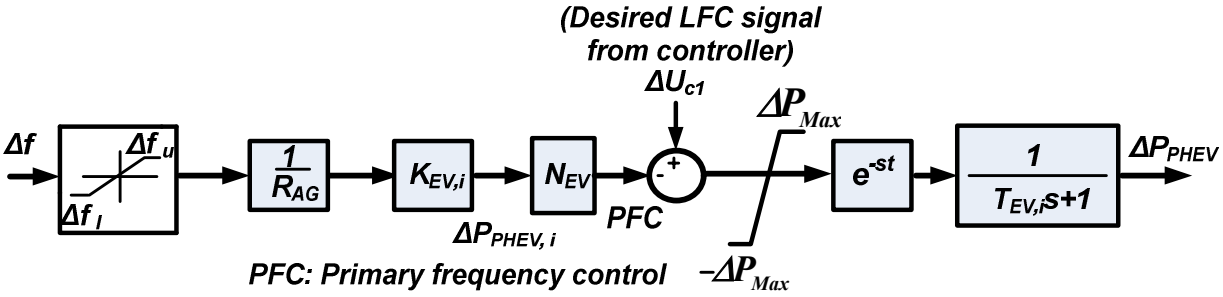

Fig. 5.4 PHEV aggregator model

The maximum upward (ΔP_{AG}^{max}) and downward power (ΔP_{AG}^{min}) from the PHEV aggregator can be expressed as:

$$\Delta P_{AG}^{max} = +\left(N_{EV} * \Delta P_{PHEV,i}\right)$$

$$\Delta P_{AG}^{min} = -\left(N_{EV} * \Delta P_{PHEV,i}\right) \tag{5.6}$$

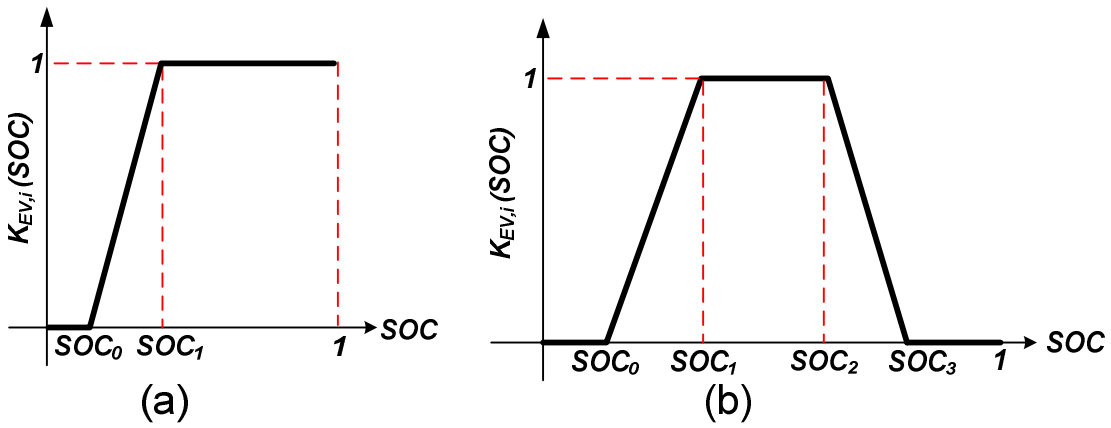

Fig. 5.5 SOC *vs.* $K_{EV,i}$ a) In idle mode b) In discharge mode

5.2.3 Wind Farm Model

Fig. 5.6 depicts the aggregated wind turbine generators (WTGs) based wind farm model. In this wind farm, the total number of wind generators (N) are divided into different groups (N_{g1}, N_{g2}---N_{gn}). Each group follows a different wind pattern. Finally, ΔP_{WF} can be expressed as:

$$\Delta P_{WF} = \sum_{k,j=1}^{N} \Delta P_{WTGk} * N_{gj} \tag{5.7}$$

As discussed in chapter 3; Eq. (3.8), the change in 'ΔP_{WTG}' of WTG can be expressed as:

$$\Delta P_{WTG} = \begin{cases} 0\,, & V_{rated} \le V_w \le V_{cutout} \\ 0\,, & \ge V_{cutout} \\ (0.0078V_w^5 - 0.23V_w^4 + 1.32V_w^3 + 11.04V_w^2 - 102V_w + 2.33) * \Delta V_W, V_{cutin} \le V_w \le V_{rated} \end{cases} \tag{5.8}$$

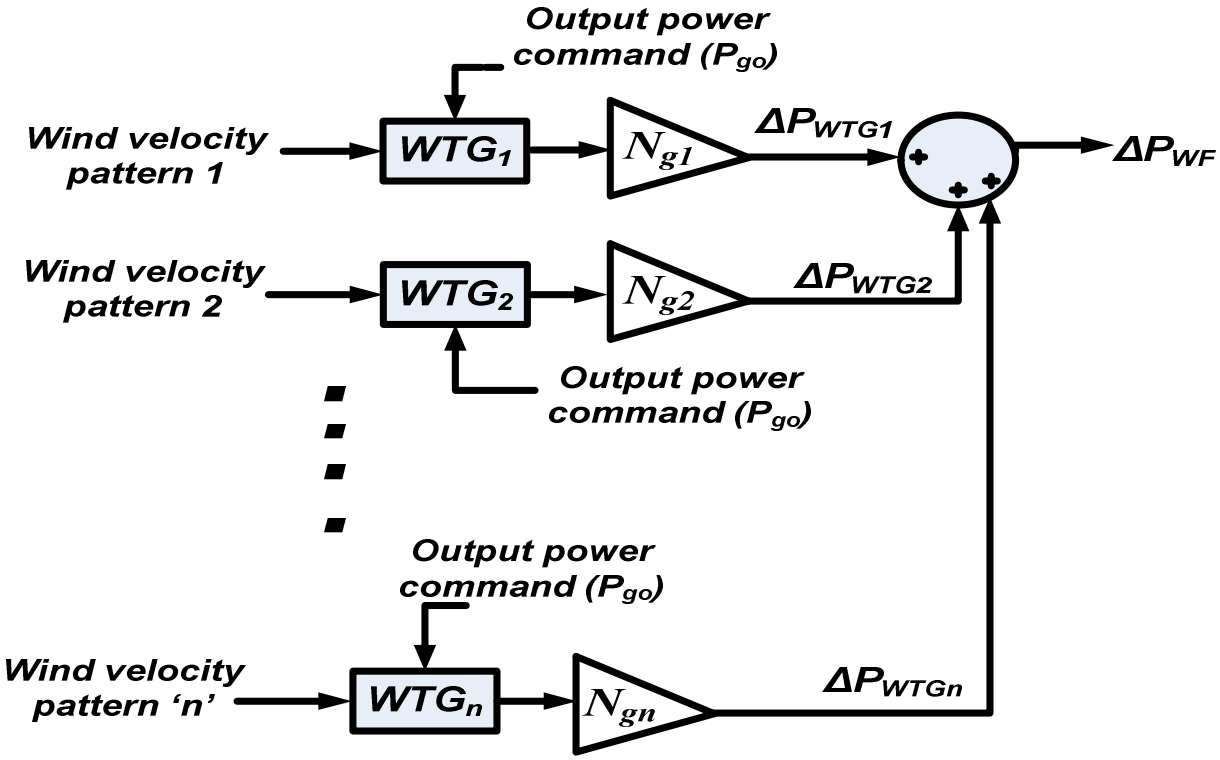

Fig. 5.6 Aggregated model of the wind farm

5.2.4 Solar Farm Model

The PV array consists of a combination of modules in series and parallel, this combination depends on the required voltage and current ratings of the solar farm. The P_{PV} varies due to either change in irradiation (or) load current. In present LFC studies, it is assumed that the P_{PV} changes only due to irradiation. P_{solar} can be computed using Eq. (5.9).

$$P_{solar} = P_{PV} * \frac{\varphi}{\varphi_{STC}} * (1 + K_t * [T_a + 0.0256 * \varphi * \Delta\varphi - T_{STC}]) \quad (5.9)$$

The ΔP_{solar} is based on the change in irradiation can be computed using the Eq.(5.10):

$$\Delta P_{solar} = \frac{P_{PV}}{G_{STC}} * (\Delta\varphi + K_t[\Delta\varphi * T_a + \varphi * \Delta T_a + 0.0512 * \varphi * \Delta\varphi - T_{STC} * \Delta\varphi]) \quad (5.10)$$

$$\Delta P_{SF} = \Delta P_{solar} * N_A \quad (5.11)$$

where 'N_A' denotes the total number of arrays in the form. Also, the total change in RES output power can be expressed as:

$$\Delta P_{RES} = \Delta P_{WF} + \Delta P_{SF} \quad (5.12)$$

5.3 Proposed JAYA Algorithm for Tuning the PID Controller

In the literature, several authors have proposed various swarm-intelligence techniques for the LFC problem [73-79]. But the performance of most of these swarm-intelligence techniques highly depends on their algorithm-specific parameters. For example, cognitive parameters (c_1,c_2) and inertia weight (w) in the case of PSO; crossover, mutation and parent selection in the case of GA. Likewise, the other algorithms, such as flower pollination algorithm (FPO), backstepping algorithm, differential evolution (DE) algorithm, bat algorithm, grey wolf optimization, etc., need the tuning of their respective parameters. Improper selection or tuning of these parameters may not give the optimal solution. To overcome this drawback, in this research work, an algorithm-specific parameters free technique (Jaya algorithm (JA)) is adopted to tune the parameters of the PID controller.

Jaya algorithm was introduced by R.V. Rao in the year 2016 [111], inspired by the humanoid or animal activities. By a biological nature, all humans or animals in a population are different in many cases. But, all of them are inspired by the elite or firm members of the population and try to move away from the lazy or weak member of the population. By mimicking this nature, throughout this algorithm, a candidate solution moves away from the worst solution and in the meantime, it moves towards the best solution. This algorithm has been successfully applied to several engineering problems, because of its fast convergence and simplicity [112-114].

Let p be the population size (m=1,2--p), n be the number of variables (v=1,2--n) and ITAE (Eq.(5.15)) is the fitness function to be minimized. Based on the ITAE, the best solution in the

population is considered as X_{best} and the worst solution is considered as X_{worst}. $X_{v,m,\,i}$ is the value of v^{th} variable for the m^{th} candidate in the i^{th} iteration. Then the updated value of each variable $X'_{v,m,i}$ in the population can be expressed as [111]:

$$X'_{v,m,i} = X_{v,m,i} + r_1 * \left(X_{v,best,i} - \left|X_{v,m,i}\right|\right) - r_2 * \left(X_{v,worst,i} - \left|X_{v,m,i}\right|\right) \quad (5.13)$$

In Eq.(5.13), it is observable that all the members of the population are always moving towards the best solution ('+' indication) and away from the worst solution('-' indication). Moreover, from the equation, it is clear that the proposed algorithm doesn't depend on any algorithmic specific parameters, unlike other algorithms. The updated value of the member of the population ($X'_{v,m,i}$) is accepted only when its value is better than the old value ($X_{v,m,i}$). r_1 and r_2 indicates the random numbers between 0-1.

$$X'_{v,m,i} = \begin{cases} X_{v,m,i}, & ITAE\left(X_{v,m,i}\right) > ITAE(X'_{v,m,i}) \\ X'_{v,m,i}, & Otherwise \end{cases} \quad (5.14)$$

5.3.1 Sequential Algorithmic Steps to Tune the Proposed PID Controller with JAYA Algorithm

Step 1: A random population is generated by initializing the controller parameters (K_P, K_I, K_D) within the limits of 0.01 and 5.0. There are 6 controller parameters related to two PID controllers, so the population size is considered as 50×6.

Step 2: The designed simulink model is run by implementing the integral absolute error (ITAE) as the fitness function (Eq (5.15)) to assess the fitness values of the defined population.

$$\text{ITAE= minimization of } \int_0^{t_{sim}} t * \left((K_P + \frac{K_I}{s} + s * K_D) * (|ACE_1| + |ACE_2|)\right) \text{dt} \quad (5.15)$$

where, $|ACE_1| = |\Delta f_1| + \left|\Delta P_{tie,12}\right|$, $|ACE_2| = |\Delta f_2| + \left|\Delta P_{tie,21}\right|$ & t_{sim}= Total simulation time.

Step 3: In the population, identify the best and worst candidates using Eq.(5.15)

Step 4: Update each candidate position with respect to the best and worst candidates using Eq.(5.13).

Step 5: If the updated candidate ($X'_{v,m,i}$) is better than the old one ($X_{v,m,i}$); replace the old one or else keep the old one using Eq.(5.14).

Step 6: Repeat steps (2) to (5) until the maximum number of iterations (50) is achieved.

Step 7: if iterations = iterations_maximum, the best member of the population will be treated as the best set of controller parameters.

Fig. 5.7 illustrates the flow chart for the summarized steps (1-7) of the proposed JA-PID controller.

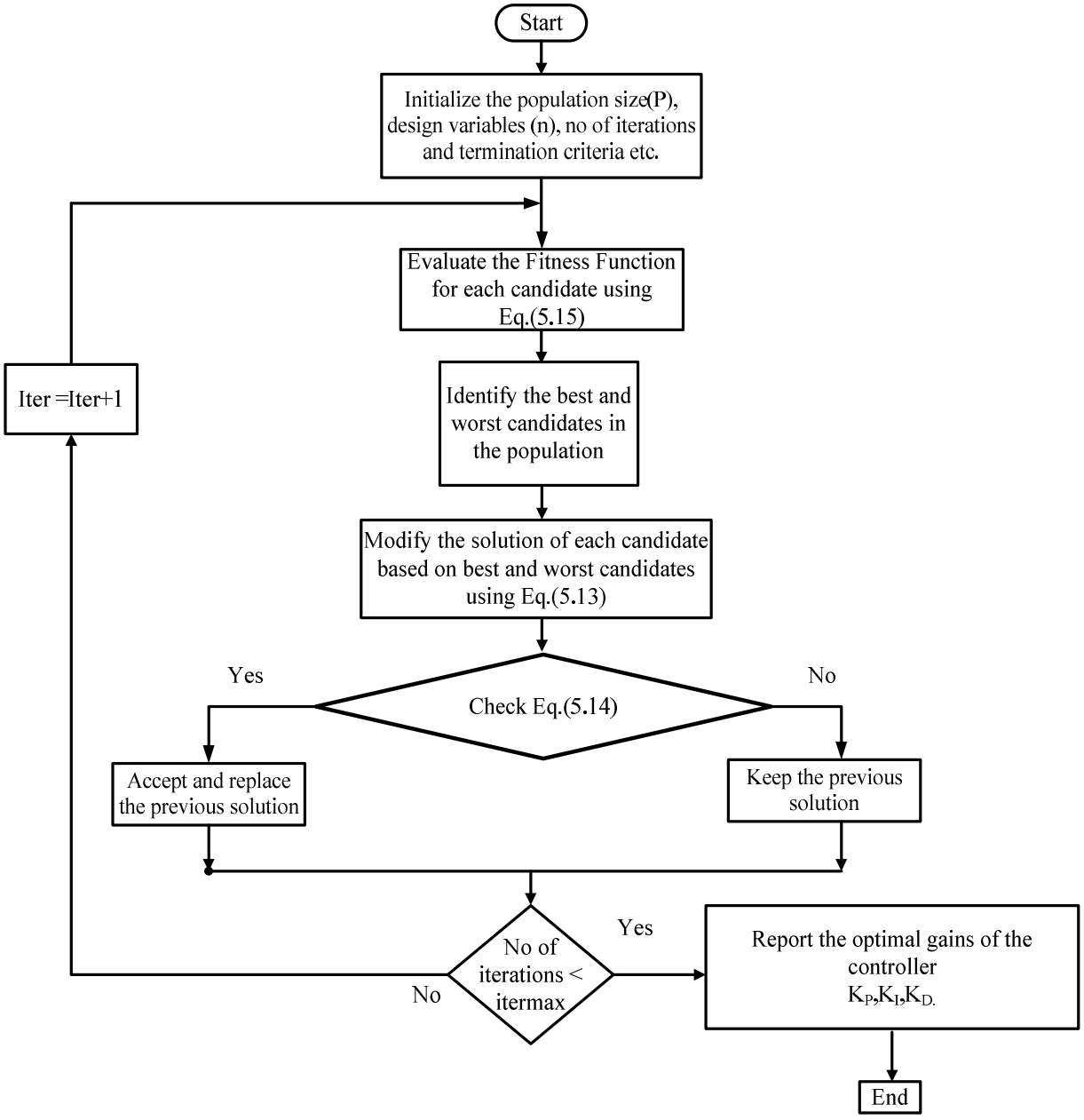

Fig. 5.7 Complete flowchart of the JA-PID controller

5.4 Results and Discussion

The simulated model of the selected test system has been formulated with the help of MATLAB (R2015a) software, a core i7 processor with 8 GB RAM computer. The test system parameters are listed in Appendix (B.1). As already stated, the main contribution of this research is to design an optimal LFC scheme coordinated with PHEVs, which allows the integration of a high renewable penetration in the electric network with minimum frequency fluctuations. Therefore, the test system was updated by adding renewable energy sources to area-1. To analyze the system stability and to compare the efficiency of the proposed control strategy, a set of simulation tests have been carried out.

This section presents the simulation results of the proposed control strategy involving the optimized PID controller based on JA and coordinated with PHEVs by comparison with some powerful published techniques in the literature. To prove the capability of the suggested LFC scheme, four scenarios are hence considered. The main theme of the first and second scenarios is to explore the superiority of the proposed JA based PID controller in the dynamic response enhancement over some recent controllers published in the literature. For these scenarios, the disturbance of step changes in load and RES power are only considered. In the third scenario, the real-time disturbances of RES perturbations and random load changes are considered in area-1, where the LFC capacity was compensated by PHEVs and CPS by coordinating with each other. In the fourth scenario, the PHEV aggregator is placed in the PFC loop (noncoordinated approach) and LFC loop (proposed coordinated approach) and its impact on the frequency response of the power system was analyzed.

Scenario 1 (In Fig 5.2, area-1 is assumed to operate in an islanded mode)

The objective of this scenario is to demonstrate the superiority of the proposed JA-PID controller in improving the dynamic response of the system against the load and RES perturbations. For this, the following test conditions are considered:

A step change of 0.025 p.u. in the load demand & 0.1 p.u. in the RES output power at the instants of 20 seconds and 130 seconds are respectively applied.

Fig. 5.8 shows the dynamic response of area-1 (as an isolated area) with various controllers for scenario 1. The quantitative analysis of Fig. 5.8 is given in Table 5.1.

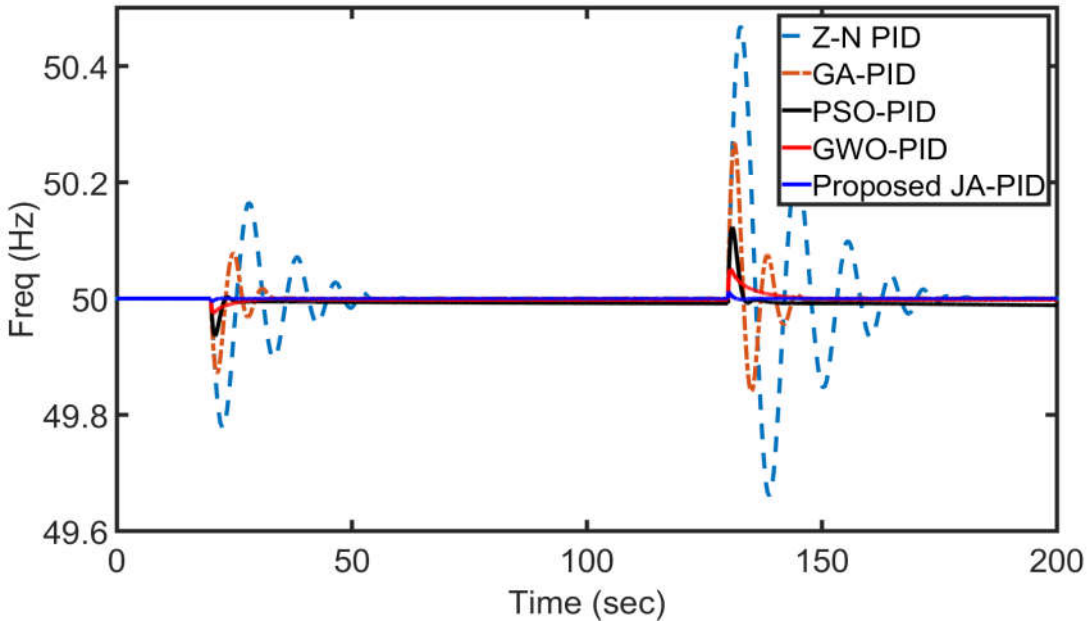

Fig 5.8 Frequency deviations of area-1 for scenario 1 conditions

Table 5.1 Dynamic response performance indices with various controllers for scenario 1

Methods	Performance indices			
	Peak undershoot (Hz)	Settling time (sec)	Peak overshoot(Hz)	Settling time (sec)
Z-N PID	49.79	30	50.4	33
GA-PID[66]	49.85	20	50.2	21
PSO-PID[73]	49.93	17	50.12	18
GWO-PID[74]	49.975	15	50.08	15
JAYA-PID	49.99	10	50.05	11.5

Scenario 2 (In Fig. 5.2, simultaneous load perturbations are considered in area-1 & area-2)

The objective of this scenario is to demonstrate the superiority of the proposed JA-PID controller in improving the settling time and overshoot for step-changes in the disturbances of area-1 and area-2 simultaneously. For this scenario, the following test conditions are considered: A step change of 0.1 p.u. and 0.08 p.u.in the load demand of area-1 and area-2 at 5 seconds is applied.

Fig. 5.9 (a), (b) & (c) show the frequency response of area-1, area-2 and tie-line power deviations between area-1 and area-2 respectively. The quantitative analysis of Fig. 5.9 (a)-(c) is given in Table 5.2. For a better view of the results, the performance of the proposed controller is

also compared with recent approaches available in the literature. The optimized PID parameters with various optimization techniques are given in Table 5.3.

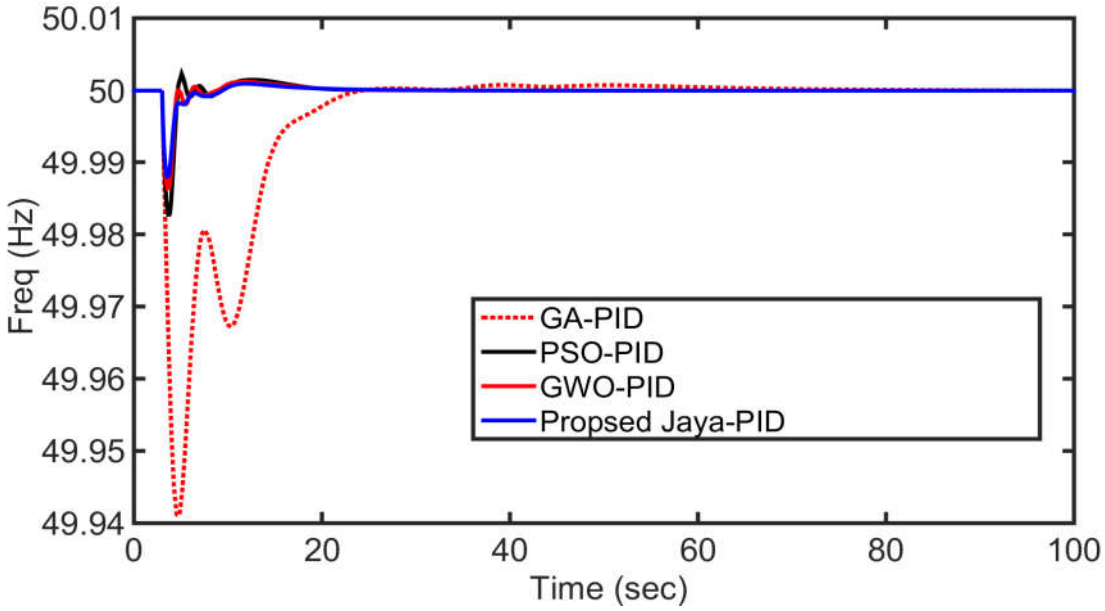

(a)

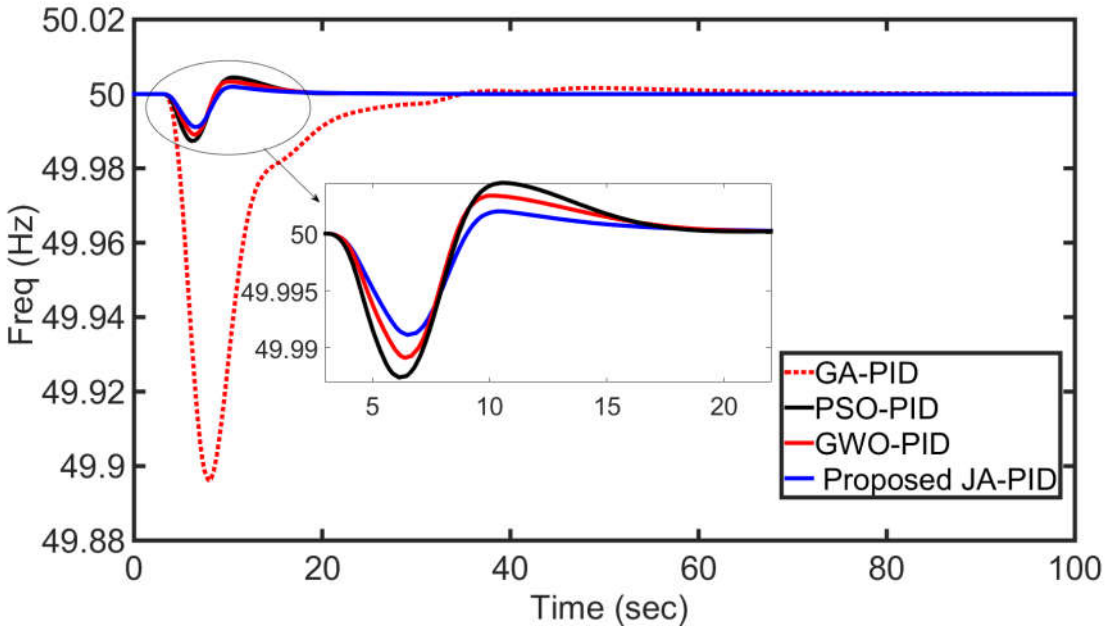

(b)

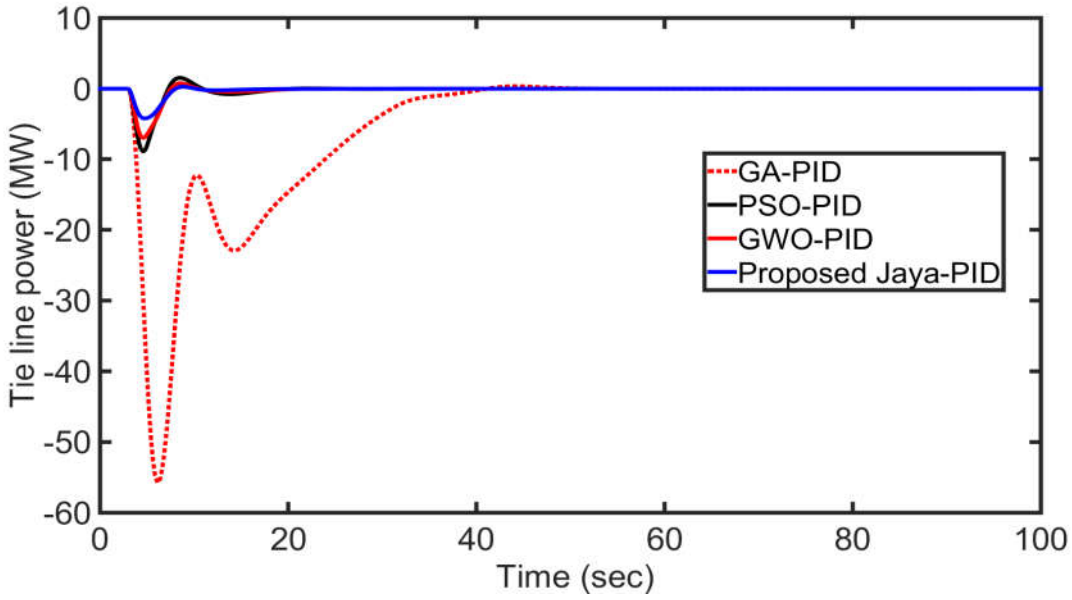

(c)

Fig 5.9 (a), (b) Frequency deviations of area-1 and area-2 for scenario 2 conditions

(c) Tie-line power deviations for scenario 2 conditions.

Table 5.2 Dynamic response of various controllers for scenario 2

Methods	Performance indices					
	Area 1		Area 2		Tie-line power deviation	
	Peak undershoot (Hz)	Settling time (sec)	Peak undershoot (Hz)	Settling time (sec)	Peak undershoot (MW)	Settling time (sec)
GA-PID[66]	49.941	44	49.895	52	55	45
PSO-PID[73]	49.969	24	49.987	21.5	9	19.5
GWO-PID[74]	49.976	21	49.989	18	7	17
JAYA-PID	49.98	18	49.9915	15	4	11

In scenarios 1 and 2, the LFC performance with classical and optimized PID controllers like Z-N, GA [66], PSO [73], and GWO [74] were compared with that of the proposed JA-PID controller. The frequency deviations and tie-line power fluctuations are minimized effectively with the proposed JA optimized LFC scheme. Moreover, the settling time with the proposed

controller was found to be the minimum in comparison to that of other methods used. Finally, it can be concluded that the proposed JA based PID controller gives the best results and hence, can be implemented in real-time LFC problems. The ITAE characteristics of various controllers for scenario 2 are given in Fig 5.10.

Table 5.3 Optimized PID parameters with different approaches

Methods	Area-1			Area-2		
	K_P	K_I	K_D	K_P	K_I	K_D
GA-PID[66]	0.06	1.13	0.1	0.0517	1.73	0.624
PSO-PID[73]	0.3064	2.3027	0.7361	2.2672	3.4816	3.1312
GWO-PID[74]	0.1639	1.9193	0.9317	0.12	2.965	4.15
JAYA-PID	0.0485	2.1321	0.2646	4.8334	2.8407	4.9085

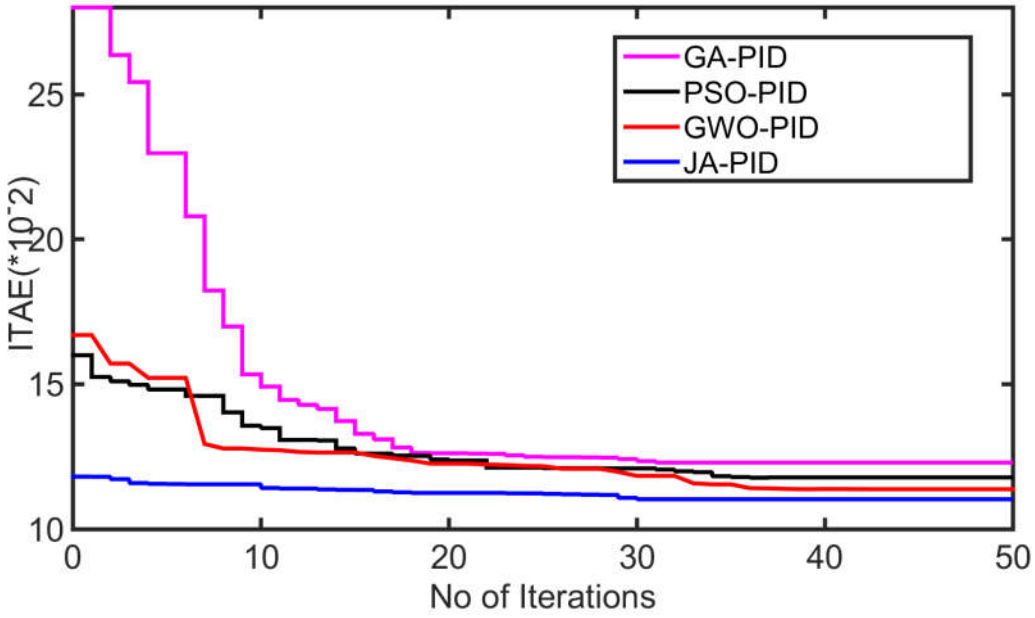

Fig. 5.10 ITAE characteristics of various controllers for scenario 2

Scenario 3 (In Fig. 5.2, the real-time load, solar and wind power fluctuations are considered simultaneously)

The objective of this scenario is to demonstrate the impact of PHEVs in minimizing the ACE of a renewable penetrated power system. For this, three control mechanisms are considered viz.:

1. Without any load frequency controller in the CPS side and no PHEVs involved in frequency control.
2. With JA optimized load frequency controller in the CPS side alone and no PHEVs involved in frequency control.
3. Proposed JA optimized coordinated control strategy between CPS and PHEV aggregator (PHEVs operating in LFC loop).

For this scenario, the following test conditions are considered; real-time wind farm, solar farm output power perturbations and random changes in the load of area-1 as shown in Fig. 5.11 (a)-(c) respectively.

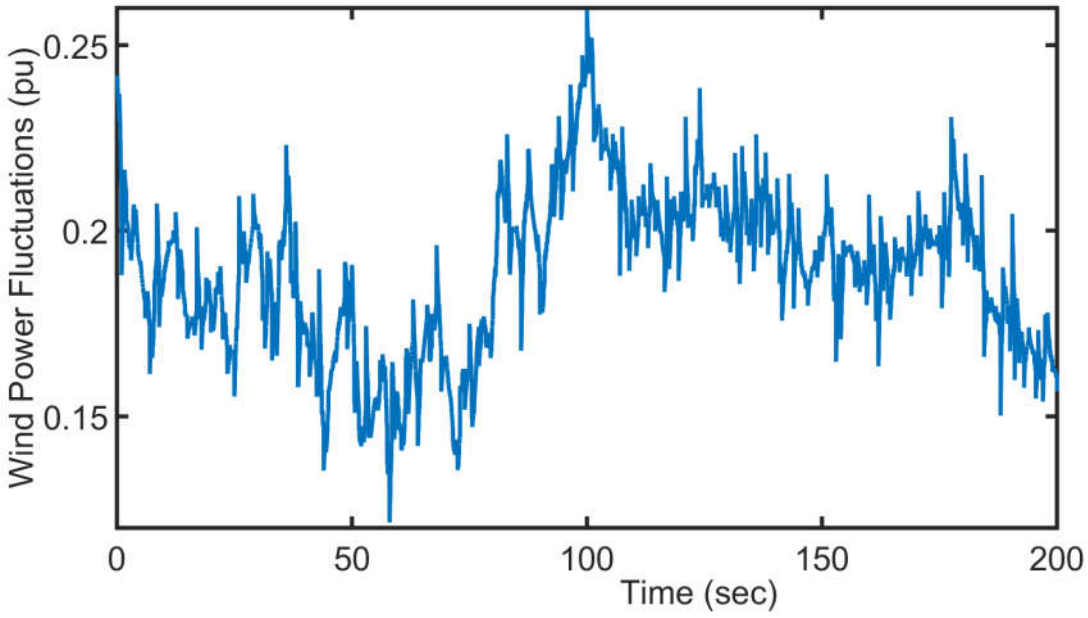

(a)

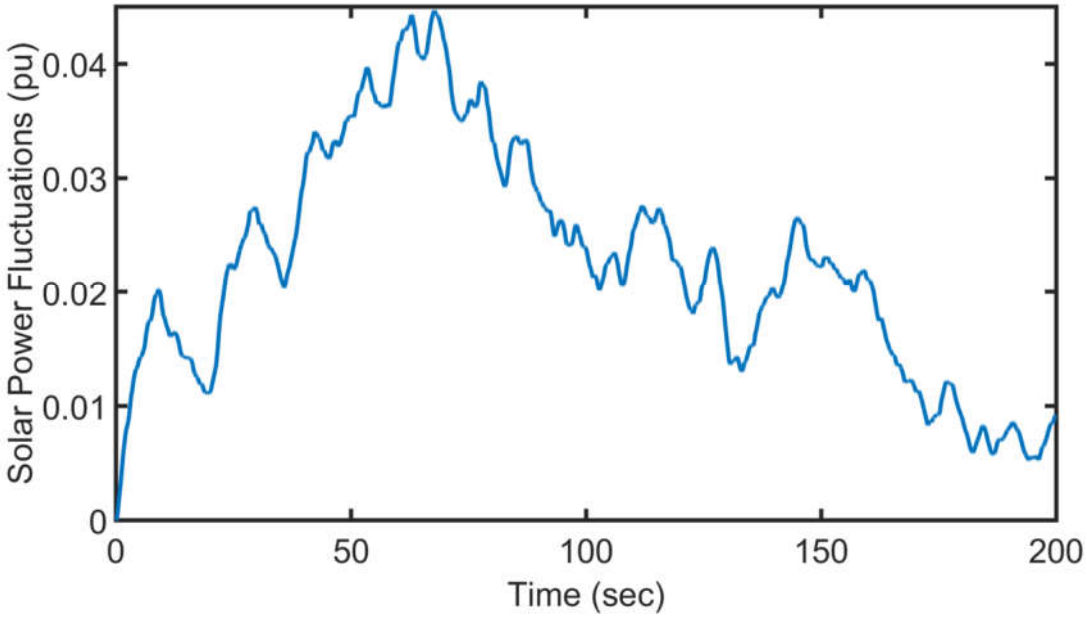

(b)

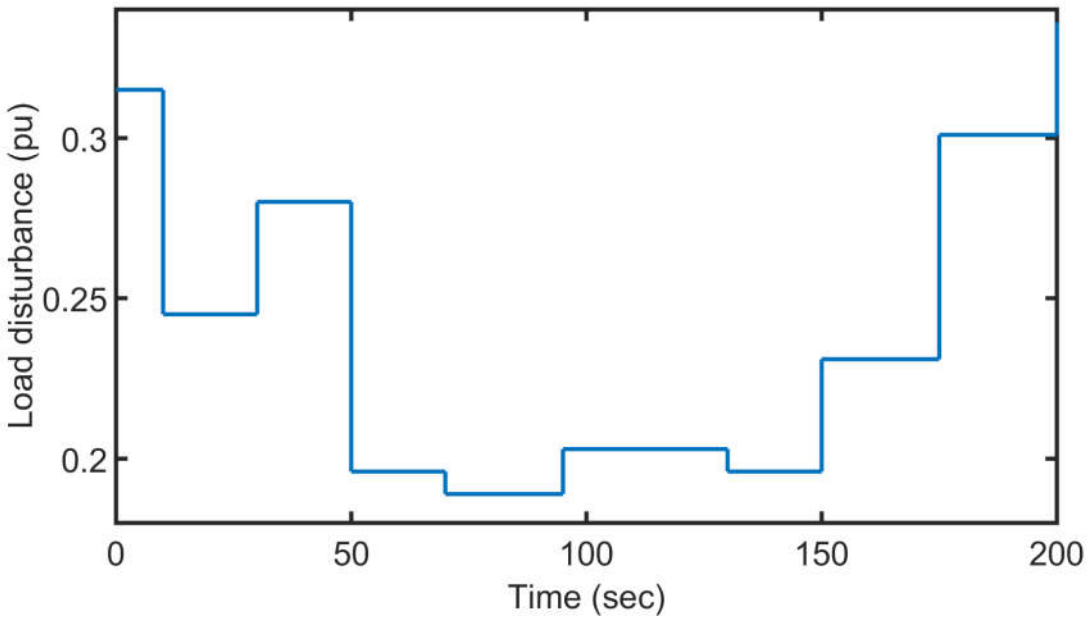

(c)

Fig. 5.11 Various disturbances in power system a) Wind farm power deviations, b) Solar power deviations and c) Load profile

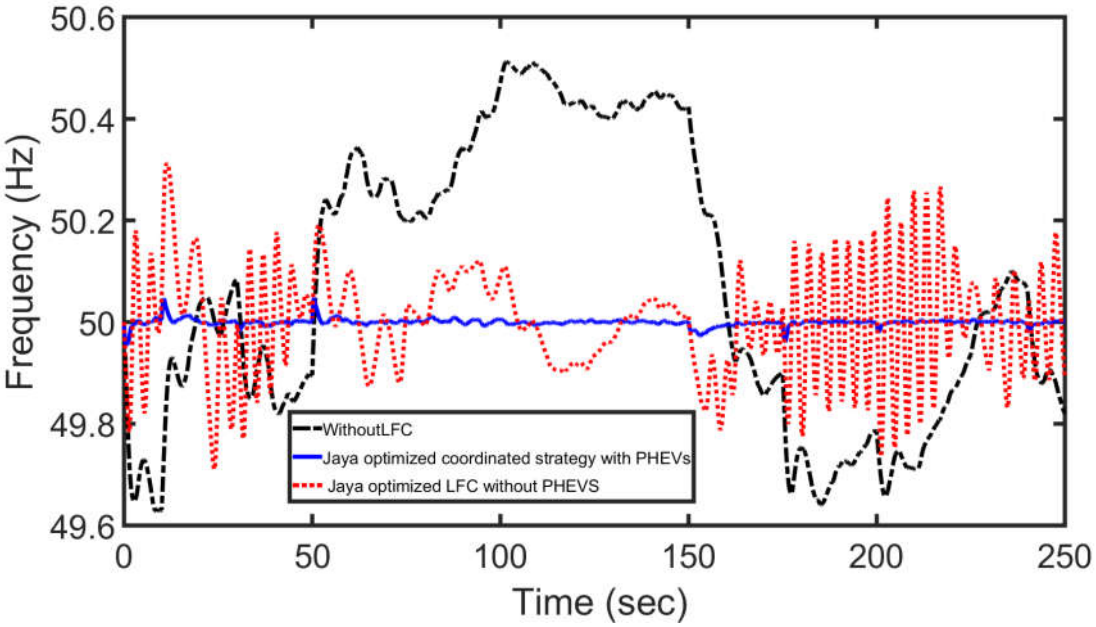
50.6
50.4
50.2
50
49.8
49.6
Frequency (Hz)
0
50
100
150
200
250
Time (sec)
WithoutLFC
Jaya optimized coordinated strategy with PHEVs
Jaya optimized LFC without PHEVS

(a)

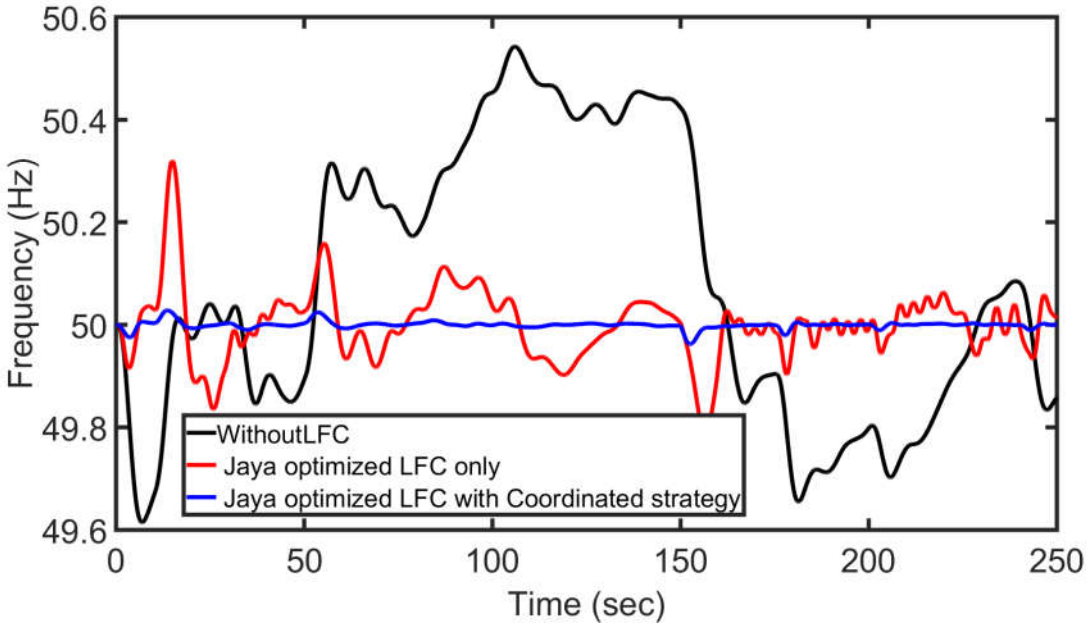
50.6
50.4
50.2
50
49.8
49.6
Frequency (Hz)
0
50
100
150
200
250
Time (sec)
WithoutLFC
Jaya optimized LFC only
Jaya optimized LFC with Coordinated strategy

(b)

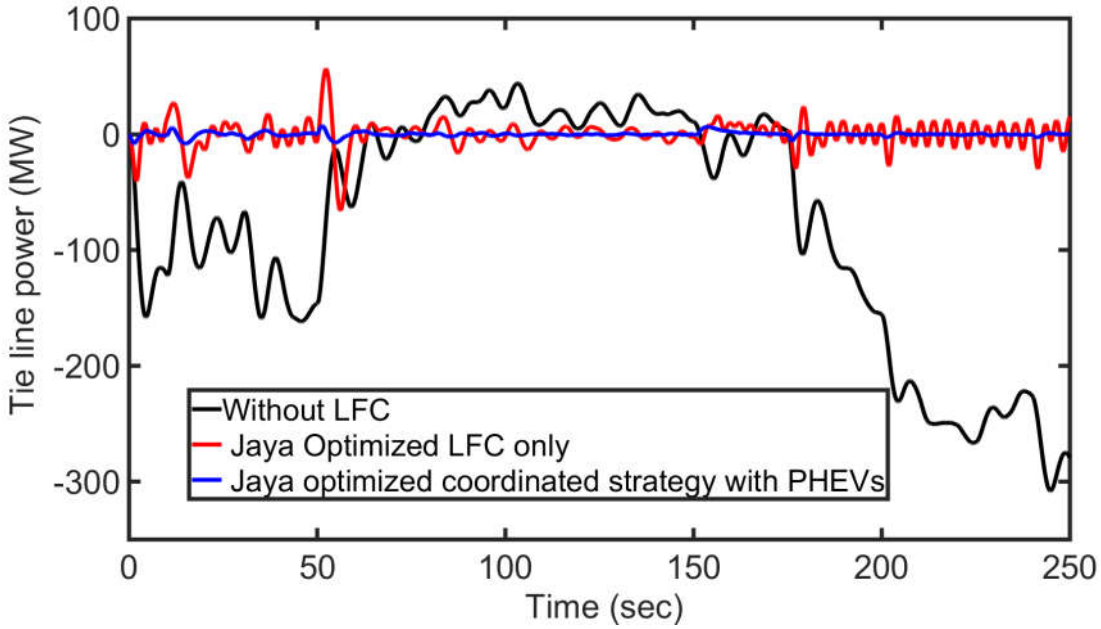

(c)

Fig 5.12 (a), (b) Frequency deviations of area-1 and area-2 for scenario 3 conditions

(c) Tie-line power deviations for scenario 3 conditions.

From the simulation results as shown in Fig. 5.12 (a)-(c), without any LFC control mechanism and also without any PHEVs, the power system experiences large frequency and tie-line power fluctuations (frequency deviations are shown with black lines). However, the system frequency and tie-line power deviations are reduced significantly, if in both the area's, CPS adopt LFC with the optimized PID controller (frequency deviations are shown with red lines). Furthermore, using the PHEV aggregator controlled by the optimal LFC signal and by coordinating with CPS, the frequency response of the power system enhanced significantly (frequency deviations are shown with blue lines). From Fig. 5.10 (d)-(f), it is also clear that the frequency and tie-line power oscillations due to RES uncertainties are quickly attenuated by the proposed JA optimized PID controller coordinated with PHEVs. The ITAE performance index as mentioned in Eq. (5.15) for scenario 3 is given in Table 5.4. It is also observed that the ITAE performance index has attained a minimum value with the proposed coordinated approach.

Table 5.4 ITAE performance (Eq.(5.15)) for scenario 3

Scenario	Without any LFC Scheme	With JAYA optimized LFC without any PHEV Aggregator	With JAYA optimized LFC coordinated with PHEV Aggregator
Scenario 3	0.28	0.092	0.0006

Scenario 4 (The same disturbance conditions as shown in Fig. 5.11 (a)-(c))

The objective of this scenario is to compare and to demonstrate the impact of coordinated control of CPS and PHEVs in minimizing the ACE of a renewable penetrated power system over non-coordinated control of CPS and PHEVs, when PHEVs are placed in the LFC and PFC loops respectively.

In this scenario, PHEVs are placed in primary frequency regulation loop, thus no coordination between CPS and PHEVs (i.e., PHEVs are included in PFC loop) is considered. These results are thus compared with that of the results obtained in scenario 3.

Fig. 5.13 (a) & (b) shows the frequency response of area-1 and area-2 and Fig. 5.13 (c) shows the tie-line power deviations between area-1 and area-2 respectively. From Fig. 5.13 (a)-(c), the dynamic response of various control mechanisms in terms of the ITAE performance index as mentioned in Eq.(5.15) is given in Table 5.5. It is also observed that the ITAE performance index has attained a minimum value with the proposed coordinated approach over non-coordinated control.

Table 5.5 ITAE performance (Eq.(5.15)) for scenario 4

Scenario	With JAYA optimized LFC, but PHEV aggregator in primary frequency control	With JAYA optimized LFC coordinated with PHEV Aggregator in secondary frequency control
Scenario 4	0.0018	0.0006

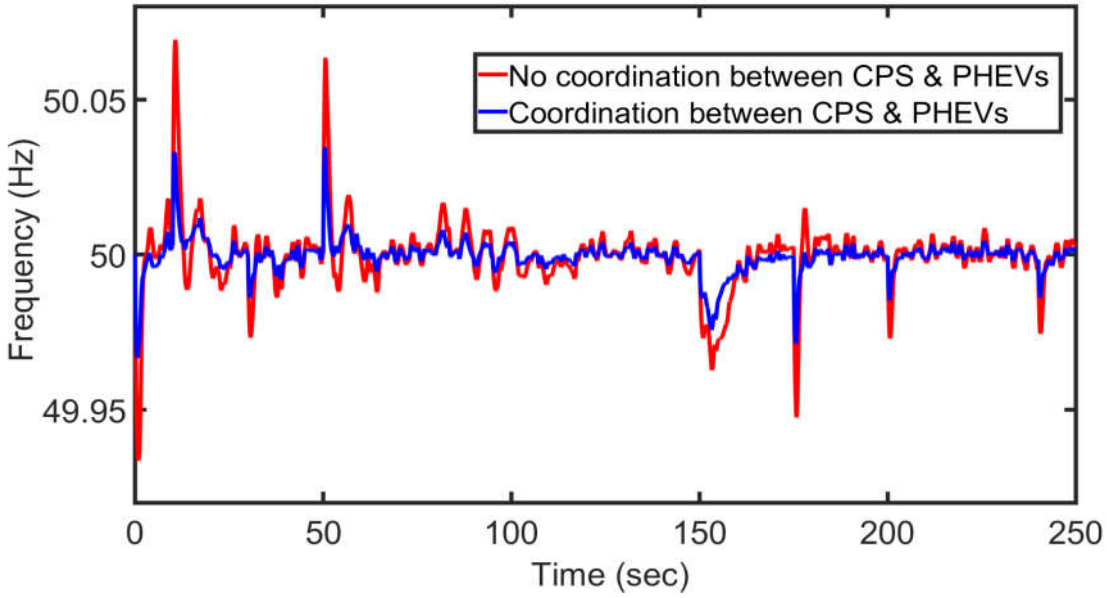
No coordination between CPS & PHEVs
Coordination between CPS & PHEVs
Frequency (Hz)
50.05
50
49.95
0
50
100
150
200
250
Time (sec)

(a)

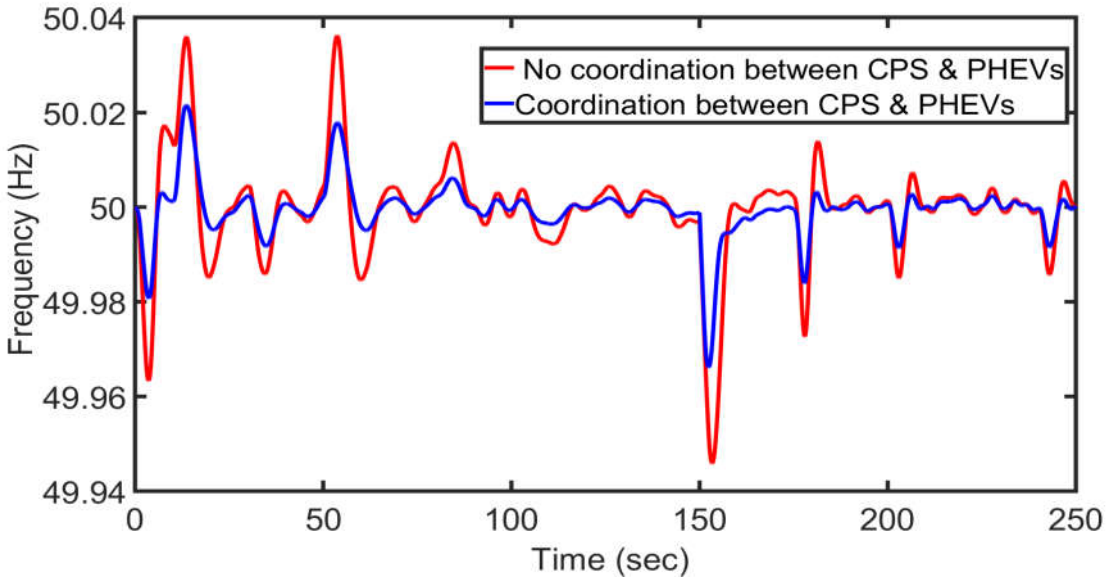
No coordination between CPS & PHEVs
Coordination between CPS & PHEVs
Frequency (Hz)
50.04
50.02
50
49.98
49.96
49.94
0
50
100
150
200
250
Time (sec)

(b)

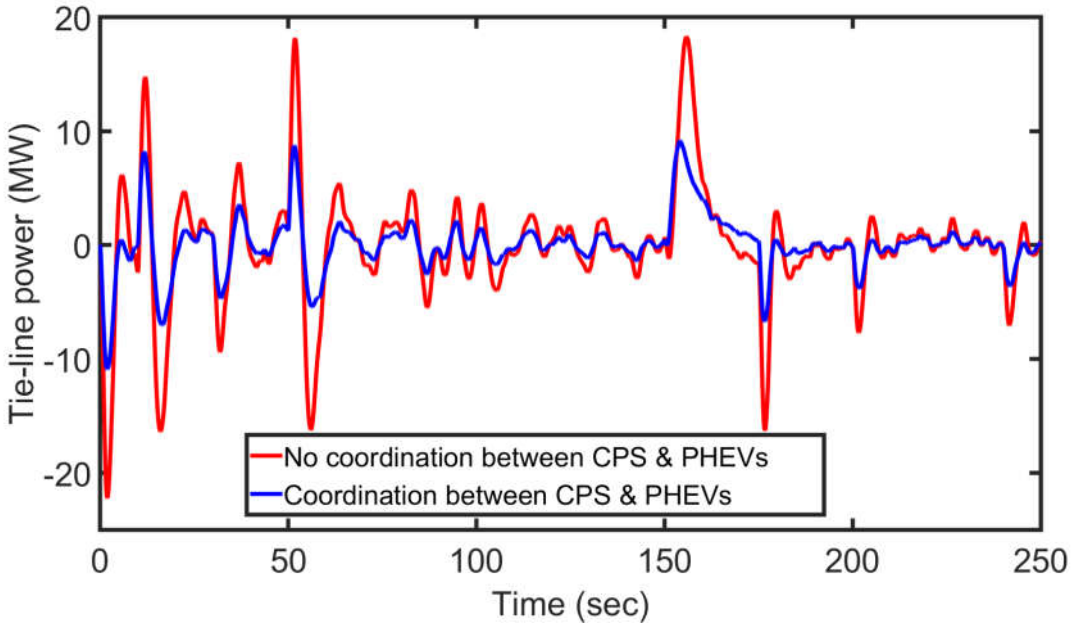

(c)

Fig. 5.13 a), b) Frequency deviation response of area-1 and area-2 for scenario 4 conditions

(c) Tie-line power deviations for scenario 4.

5.4.1 Summary of Simulation Results

1. From scenarios 1 & 2, the simulation results reveal that the proposed JA-PID controller is improving the dynamic response of the system for a step load disturbance over the recent and standard controllers published.
2. From scenario 3, it is clear that the interaction of PHEVs is reducing the system error (ACE) significantly. On the other hand, CPS alone is unable to maintain the system parameters within the tolerable limits of 0.4%. (i.e. 50±0.2 Hz).
3. From scenario 4, the simulation results reveal that the proposed coordinated approach is minimizing the system error (ACE) to a great extent over non-coordinated approach where PHEVs are placed in the primary frequency control loop.

5.5 Summary

This work presented a novel optimal LFC scheme coordinated with PHEVs to enhance the frequency response of a renewable penetrated power system. A recently developed swarm-intelligent technique named JAYA algorithm has been applied to design an optimized PID controller to achieve both the PHEVs output power control and frequency regulation of the power system. The PHEV aggregator was employed in the LFC and PFC loops in the presence of renewable energy sources. The impact of RES integration with PHEVs in an interconnected power system has been analyzed. To show the potential of the proposed control strategy, a comparative study of the performance of the proposed methodology with that of standard and recent optimization techniques were also performed.

From scenarios 1 and 2, with the JA-PID controller, improved dynamic responses in terms of undershoot/overshoots and settling times were achieved in the cases of step changes in load and RES perturbations. The simulation results obtained in the presence of real-time RES perturbations have been compared with and without consideration of the optimized PID controller and PHEVs in the LFC loop. Examination of the dynamic responses in scenarios 3 and 4 shows that the application of PHEVs in the LFC loop controlled by the designed coordinated LFC approach improves the frequency response of the power system significantly over other control mechanisms.

Chapter 6

Robust Frequency Control in a Renewable Penetrated Power System: An Adaptive Fractional Order Fuzzy PID Approach

6.1 Introduction

The proposed coordinated control strategy between the conventional power sources and PHEVs based on the Jaya algorithm optimized PID controller in chapter 4 gives a satisfactory performance under steady-state and dynamic conditions. However, the optimized PID controllers are widely used in early works for frequency control of power systems. They exhibit poor performance when the controlled systems contain high nonlinearities and rapid change in the operating points. To overcome this problem, optimized fractional order PID (FO-PID) controllers are proposed for frequency control of the power system. The FO-PID controllers can handle the known nonlinearities in the system efficiently over an optimized integer-order PID controller (IO-PID) due to its additional two degrees of freedom in tuning the two additional non-integer knobs (i.e., λ & μ). But for unknown nonlinearities (due to the intermittent nature of RES) and various power system constraints, this controller may not provide an optimal solution. For such conditions, as discussed in the literature survey and as proven in chapter 4, the fuzzy inference mechanism provides excellent assistance to the existed controller (either PID or FO-PID). But, the performance of the fuzzy logic approach highly depends on their optimal selection of membership functions (MFs) and rule base [115].

To overcome the specified problems in the optimized FO-PID controller and FLC, this chapter proposes a novel adaptive fractional order fuzzy PID controller for the LFC problem of a renewable penetrated power system. The proposed controller inherits the merits of both the FLC and FO-PID controller by overcoming their limitations. In this proposed controller, the parameters of FLC (MFs scaling factors and rule base weights) and FO-PID controller are tuned online using the Teaching Learning Based Optimization (TLBO) algorithm. This algorithm is selected because, unlike other algorithms, it is free from algorithm-specific parameters [116]. In this proposed work, a fuzzy supervisory correction term is applied as input to the FO-PID controller. The purpose of the fuzzy supervisory correction is to modify the command signal fed to the FO-PID controller to compensate for the overshoots and undershoots present in the output frequency response. Especially when the power system has unknown nonlinearities (from RES side) and ESS constraints. Such nonlinearities and constraints result in significant overshoots and undershoot if the FO-PID control scheme alone is used. This approach is, in essence, deploying the cooperation of fuzzy logic features and the FO-PID controller to improve the extensibility of

the control space investigated in the LFC problem. Besides, the robustness of the proposed adaptive fractional order fuzzy PID controller against concurrent changes in all possible disturbances, energy storage systems, inertia uncertainties and power system nonlinearities are tested in a single controller framework. Finally, a brief comparative assessment is formulated with other controllers (PID/FO-PID/Fuzzy-PID/FO-Fuzzy-PID) to show the merits of the proposed controller in this chapter.

6.2 Modelling of the Interconnected Power System

The detailed modelling of the test system and operating conditions of the test system are similar, as discussed in chapter 5. Finally, the corrective signal from the proposed controller to PHEV aggregator and governors of each area can be expressed as:

$$U_{ci} = (K_P + \frac{K_I}{s^{\lambda}} + K_D s^{\mu}) * ACE_i \text{ where i=1,2.} \quad (6.1)$$

where K_P, K_I, K_D denotes gains of the PID controller and λ, μ denotes the fractional parameters of the integrator and differentiator. The objective of the proposed controller is to minimize the frequency and tie-line power deviations to scheduled values by minimizing the ACE.

6.2.1 FO-PID Controller

Fractional analytics is a standout amongst the essential branches of the calculus in which the order of the integral and differential parameters can take a non-integer value. Since a recent couple of decades, the fractional calculus has been applied successfully in numerous fields of engineering. The detailed analysis regarding fractional calculus is available in [117]. The FO-PID controller can be expressed as:

$$G_c(s) = K_P + \frac{K_I}{s^{\lambda}} + K_D s^{\mu} \quad (6.2)$$

where K_P, K_I, and K_D denotes the gains of the proportional, integral, and derivative controllers. λ & μ denotes the order of integrator and differentiator. In this FO-PID controller, a total of five variables needs to be optimized, three parameters are K_P, K_I, and K_D (same as PID) and two fractional parameters λ and μ. These FOPID controllers can exhibit better dynamic performance over an IOPID controller due to its additional two degrees of freedom in tuning the two additional non-integer parameters (i.e., λ & μ) [118]. In Eq.(6.2), if (λ, μ) = (0,0) then it becomes the proportional controller; if (λ, μ) = (1,0) then it becomes PI controller; if (λ, μ) = (0,1) then it

becomes PD controller; if (λ, μ) = (1,1) then it becomes PID controller. Fig. 6.1 (a) illustrates the various IOPID controllers in the λ-μ plane. Fig. 6.1 (b) shows the realization of the FO-PID controller from the IOPID controller, which expands it from the entire λ-μ plane [119]. There exist a variety of definitions, such as Riemann–Liouville (RL), Cauchy integral formula and Grünwald–Letnikov (GL), which are applied to define the fractional-order control. Nonetheless, in the control frameworks, the Cauchy integral formula is often employed to realize the FO integrations and differentiation of the FO-PID controller [120].

$$DO_t^r f_x(t) = \frac{1}{\Gamma(m-r)} \int_0^t \frac{D^m f_x(t)}{(t-T)^{r+1-m}} dt, \text{ r} \in R^+, \text{m} \in Z^+ \ and \ \text{m-1} \leq r < \text{m} \tag{6.3}$$

where $D^m f_x(t)$ is the m^{th} derivative of function f(t). $'DO_t^r'$ denotes fractional-order differential operator (a combined differentiator/integrator). $'DO_t^r'$ for the function f(t) of order r ∈ R that generalizes the notation for derivatives (r > 0) and integrals (r < 0). It can be defined as:

$$DO_t^r f_x(t) = \begin{cases} \frac{d^r}{dt^r} f(t); & r > 0 \\ f(t); & r = 0 \\ \int_0^t f(T)\, dT^r; & r < 0 \end{cases} \tag{6.4}$$

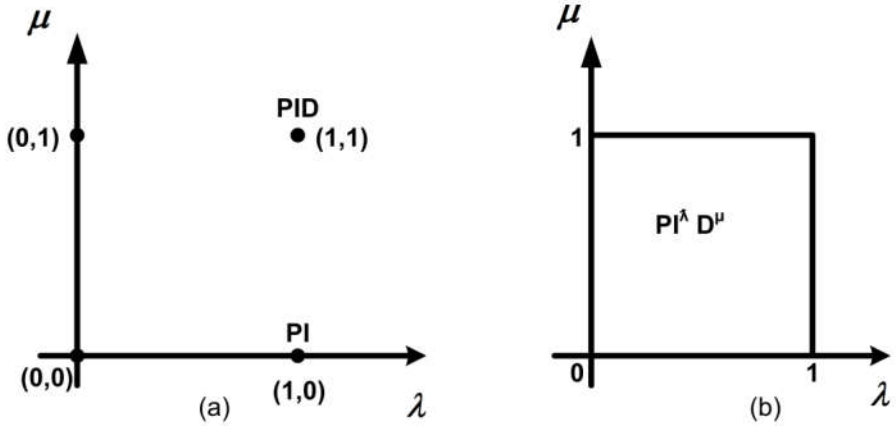

Fig. 6.1 Representation of PID and FO-PID controllers in the λ-μ plane: (a) IOPID Controller (b) FOPID controller

6.2.2 FO-Fuzzy-PID controller

Fig. 6.2 (a) illustrates the structure of the FO-Fuzzy-PID controller. The inputs of the controller are ACE, ACE* and the output is U_f. The fuzzy logic approach can be divided into three modules viz. fuzzifier, inference engine, and the defuzzifier. The fuzzifier assigns the MF ranges to the input and output variables. Fig 6.2 (b) depicts the MF ranges corresponding to the inputs

and output variables which are arranged as Negative Large (NL), Negative Medium(NM), Negative Small(NS), Zero(ZE), Positive Small(PS), Positive Medium(PM) and Positive Large(PL) having centroids at -1,-0.5,-0.25,0,0.25,0.5,1 respectively. The MFs map the crisp values into fuzzy variables. The triangular MFs are chosen for this work due to its simplicity and adaptability in the tuning process. The second module is the inference engine, which comprises the rule base and database. Decision making is an inference control action from the rule base, which is shown in Table 6.1.

The third module is the defuzzification, which converts the sum of fuzzy singleton output into an equivalent crisp value, which is the output of FLC. The defuzzified output of FLC based on centroid method can be expressed as:

$$U_f = \frac{\sum_{j=1}^{f} \mu_j U_j}{\sum_{j=1}^{f} \mu_j} \tag{6.5}$$

where μ_j represents the degree of MFs of fired rules, 'f ' represents the total number of partitions of the fired area, U_j represents the center of an area and U_f represents the crisp value of fuzzy output.

Table 6.1 FLC Rule base

ACE	**ACE***						
	NB	**NM**	**NS**	**ZE**	**PS**	**PM**	**PB**
NB	PB	PB	PB	PB	PM	PS	ZE
NM	PB	PB	PB	PM	PS	ZE	NS
NS	PB	PB	PM	PS	ZE	NS	NM
ZE	PB	PM	PS	ZE	NS	NM	NB
PS	PM	PS	ZE	NS	NM	NB	NB
PM	PS	ZE	NS	NM	NB	NB	NB
PB	ZE	NS	NB	NB	NB	NB	NB

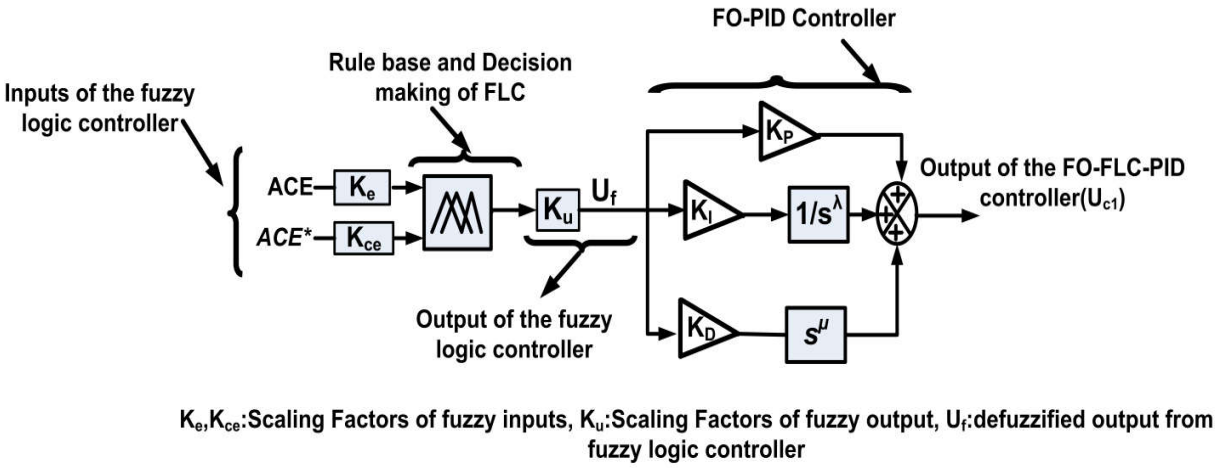

K_e,K_{ce}:Scaling Factors of fuzzy inputs, K_u:Scaling Factors of fuzzy output, U_f:defuzzified output from fuzzy logic controller

(a)

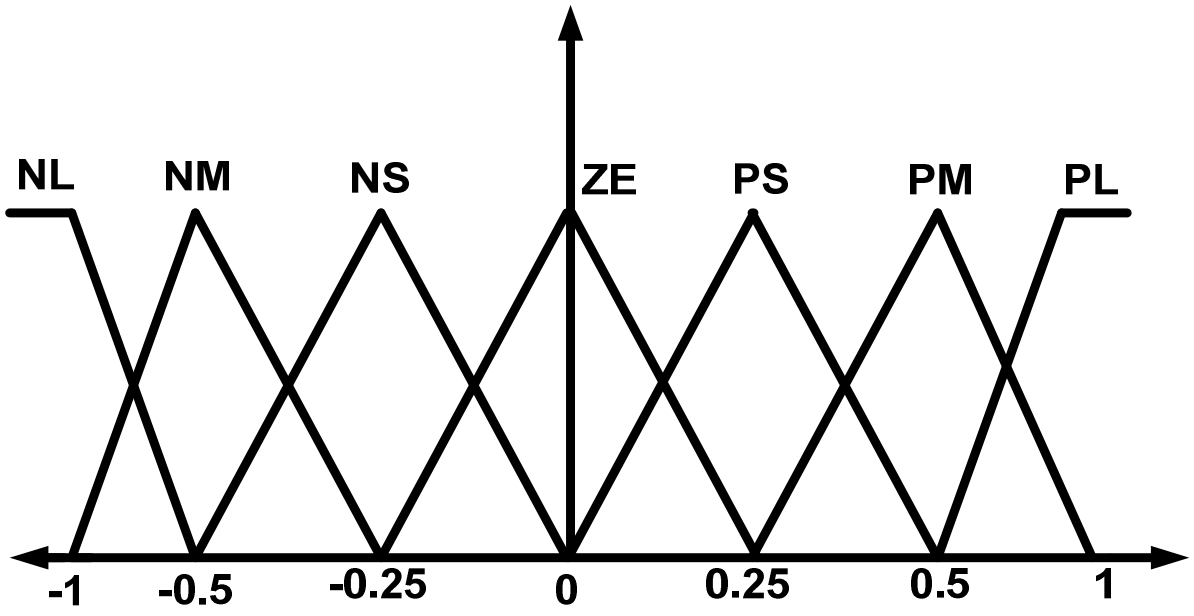

(b)

Fig. 6.2 (a) Structure of FOFPID controller, (b) MFs of inputs & output of FLC

As discussed in the literature, the FO-Fuzzy-PID controller has superior performance when compared to FO-PID and conventional PID controllers. The crucial factor about the FLC is, its performance highly depends on its parameters (i.e. MFs and rule base). Without precise information about the system, the optimal selection of fuzzy parameters may not be possible.

Hence, the designed FLC may not provide optimal performance over a wide range of operating conditions. To address the above problem, this research work proposes an adaptive FO-FLC-PID controller, in which MFs scaling factors and rule base weights are tuned online according to operating conditions of the system along with FO-PID parameters.

6.3 Proposed Method (Adaptive FO-FLC-PID Controller)

In the literature, there exist several approaches to tune the MFs scaling factors and the rule base of a fuzzy logic controller for various engineering problems. Several authors have proposed FO-PID controllers as a solution to some engineering problems including LFC [118-120]. However, no attempt has been made to combine both the techniques and inherit the merits of each technique by ignoring individual limitations in the process of resolving modern power system stability issues. Based on the requirements and complexities in the frequency control of renewable penetrated power systems, this work proposes a novel adaptive FO-FLC-PID controller for an interconnected power system. Fig. 6.3 depicts the block diagram of the online tuning mechanism of the proposed adaptive FO-FLC-PID controller. It can be observed that based on the ACE (which resembles the actual operating conditions of the system and feedback to the controller) and the desired set point; the parameters of the proposed controller are tuned online according to the operating conditions. The specific goal of ACE minimization through the proposed controller is attained by executing the following steps online:

1) Tuning of fuzzy parameters (MFs scaling factors and rule weights).
2) Tuning of FO-PID controller.

In order to perform this task, a TLBO algorithm has been employed. Most of the swarm intelligent techniques like GA, PSO, GWO, and BHO, etc. highly depended on their own algorithm-specific parameters unlike TLBO, hence TLBO is selected. Inappropriate choice of these parameters may lead the solution towards divergence. To overcome this problem, an algorithm-specific parameter-free optimization technique named the TLBO algorithm is used in this work. The TLBO algorithm is a teaching-learning process inspired algorithm and is based on the effect of the influence of a teacher on the output of learners in a class. The algorithm describes two basic modes of learning:

a) Through teacher is known as teacher phase
b) Through the interaction of learners with other learners is known as the learner phase.

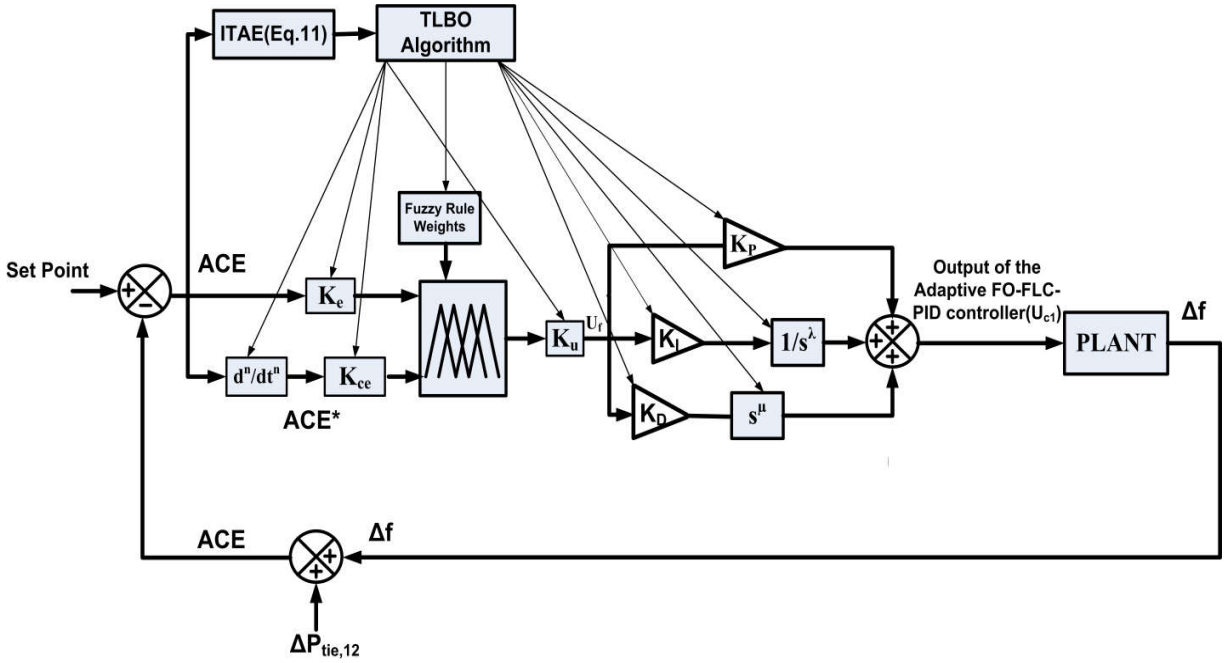

Fig. 6.3 Structure of proposed adaptive FO-Fuzzy-PID

6.3.1 Teacher Phase

It is the first part of the algorithm where learners learn through the teacher. During this phase a teacher tries to increase the mean result of the class in the subject taught by him or her depending on his or her capability. At any iteration 'i', assume that there is 'n' number of subjects (i.e. design variables), 'p' number of learners (i.e. population size, k=1,2,…,p). '$M_{n,j}$' represents the mean result of the learners in a particular subject 'j' (j=1,2,…,n). The best overall result $X_{n,kbest,i}$ considering all the subjects together obtained in the entire population of learners can be considered as the result of best learner 'kbest'. However, as the teacher is usually considered as a highly learned person who trains learners so that they can have better results, the best learner identified is considered by the algorithm as the teacher. The difference between the existing mean result of each subject and the corresponding result of the teacher for each subject is given by,

$$mean\_difference_{n,k,i} = rand() * [X_{n,kbest,i} - T_F M_{n,j}] \quad (6.6)$$

where $X_{n,kbest,i}$ is the best learner who is considered as the teacher; rand() = random number between [0-1]; T_F is a teaching factor which can be expressed as:

$$T_F = \text{Round}\,[1+\text{rand}\,()\,\{2-1\}] \quad (6.7)$$

T_F =1 indicates no increase in the knowledge level of learners in a particular subject 'n'. T_F=2 indicates the complete transfer of knowledge.

$$X'_{n,k,i} = X_{n,k,i} + mean\_difference_{n,k,i} \tag{6.8}$$

where $X'_{n,k,i}$ is the updated knowledge of each learner after the teaching phase.

6.3.2 Learners Phase

The second phase in this algorithm is the learner phase. In this phase, learners improve their knowledge by interacting among themselves. Select any two learners in the population A & B randomly such that $X'_{total_A,i} \neq X'_{total_B,i}$. Eq. (6.8) describes how the learners transfer their knowledge between each other, where $X'_{total_A,i}$ is the total fitness value of the learner in all subjects.

$$X''_{n,A,i} = X_{n,A,i} + rand*(X'_{n,A,i} - X'_{n,B,i}); \text{ if } X'_{n,B,i} < X'_{n,A,i}$$

$$X''_{n,B,i} = X_{n,B,i} + rand*(X'_{n,B,i} - X'_{n,A,i}); \text{ if } X'_{n,A,i} < X'_{n,B,i} \tag{6.9}$$

$X''_{n,A,i}$ denotes updated knowledge of A^{th} learner after learning phase.

The summarized steps for tuning the parameters of adaptive FO-FLC-PID controller with TLBO are given as follows:

Step 1: Initialize the population using $X_n = lb + rand * (ub - lb)$

where, lb = [**0 0 0 0 zeros (1,25)** 0 0 0 0 0]

ub = [**1 1 1 1 ones (1,25)** 5 5 1 5 1]

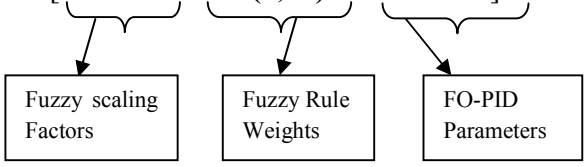

Step 2: Calculate the fitness of each learner (population) using the following fitness function

$$\text{ITAE} = \text{minimization of } \int_0^{t_{sim}} t * \left(K_P * (|ACE_1| + |ACE_2|) + \frac{K_I}{S^\lambda} * (|ACE_1| + |ACE_2|) + s^\mu * K_D * (|ACE_1| + |ACE_2|)\right) * dt \tag{6.10}$$

Where, t_{sim}= total simulation time ($t_{sim} = 200\ seconds$); t = time at which absolute sum of error samples are collected (t=1, 2, 3---200 seconds).

Step 3: The best fitness one in the population is considered as the teacher. Calculate the mean of learners (population) in each subject (variable). Calculate mean_difference & T_F using Eq. (6.5) & (6.6) respectively.

Step 4: Update each learner's knowledge with the help of the teacher's knowledge using the Eq. (6.7).

Step 5: Each learner improves his/her knowledge by interacting with other learners according to Eq. (6.8).

Step 6: If the termination criteria are met (terminate either the tolerance value of ITAE reaches below 0.001 or the iteration count reaches 50), then display the optimal parameters of FLC and FO-PID controller, else return to step 2.

Fig. 6.4 depicts the flow chart for the tuning process of the proposed controller with the TLBO algorithm.

6.4 Results and Discussions

The adequacy of the proposed controller in frequency control under various scenarios is tested on the IEE Japan East 107-bus-30- machine power system. The performance of the adaptive FO-FLC-PID controller is compared with other controllers proposed in literature i.e., FO-FLC-PID, Fuzzy-PID, FO-PID, and TLBO- PID under various test scenarios. It is well known that the system response relies upon the parameters of these controllers; all the parameters are optimized by using TLBO algorithm.

Scenario 1

The objective of this scenario is to show the superiority of the proposed controller in improving the settling time and overshoots when compared with the other techniques available in the literature. To perform this task, two cases are considered in area-1 alone as an isolated area.

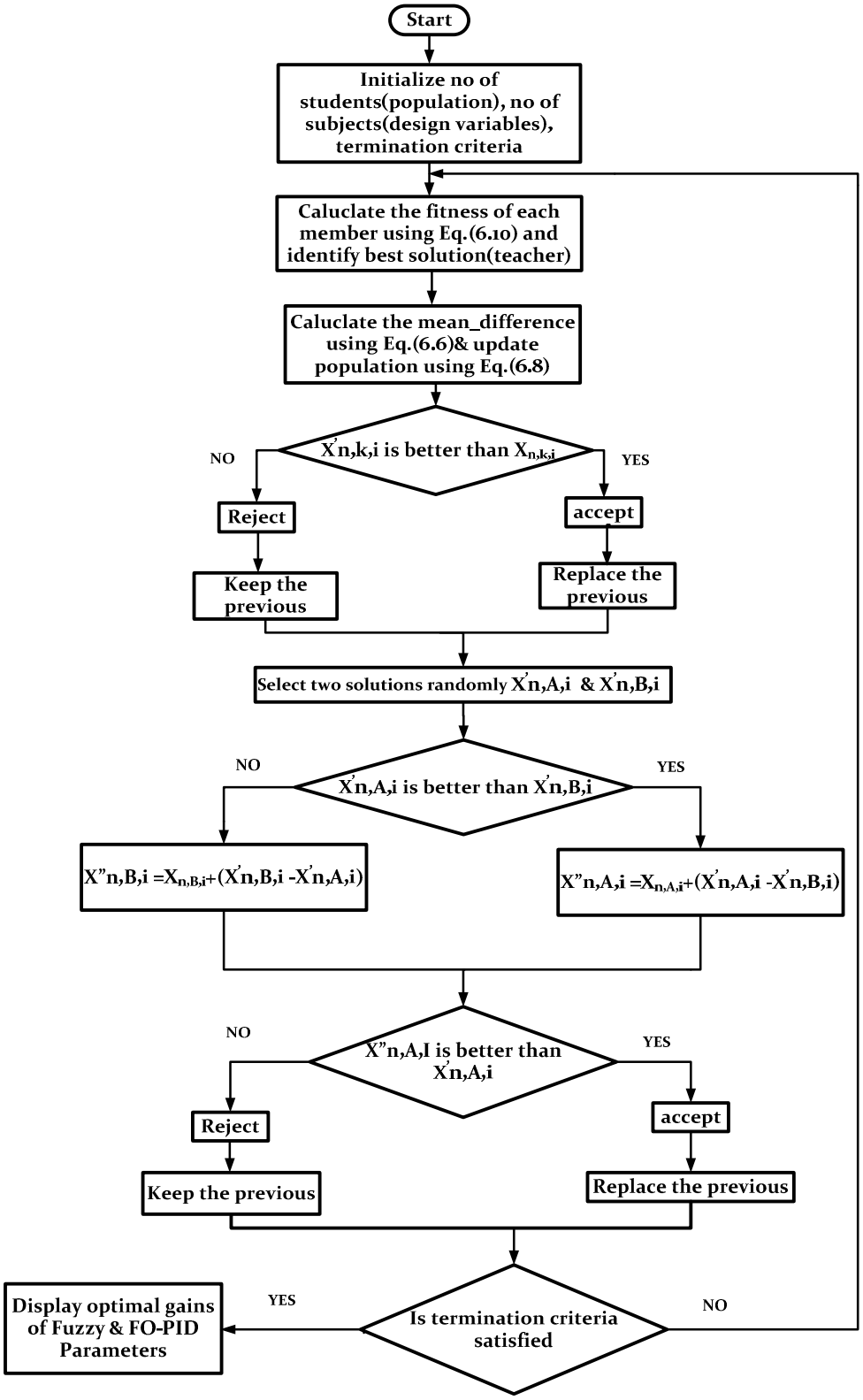

Fig. 6.4 Flowchart for tuning the proposed controller using TLBO algorithm

Case 1:

In the first case, a step change of 0.01 p.u. in load demand and RES output power are applied as a disturbance to the LFC in area-1 applied at the instants of t =10 & 100 seconds respectively. The frequency deviation response for this case is depicted in Fig. 6.5 (a).

Case 2:

In the second case, multi-step load deviations are applied as a disturbance to the LFC in area-1. Fig. 6.5 (b) shows the multi-step load deviations and Fig. 6.5 (c) depicts the frequency deviation response for this case.

From the Fig. 6.5 (a) and (c), it is observed that the dynamic performance is improved and the proposed LFC control scheme can eliminate the effect of load disturbance significantly when compared to other controllers. The dynamic performance of various controllers in cases 1 & 2 in terms of settling times and overshoots are listed in Table 6.2 and Table 6.3.

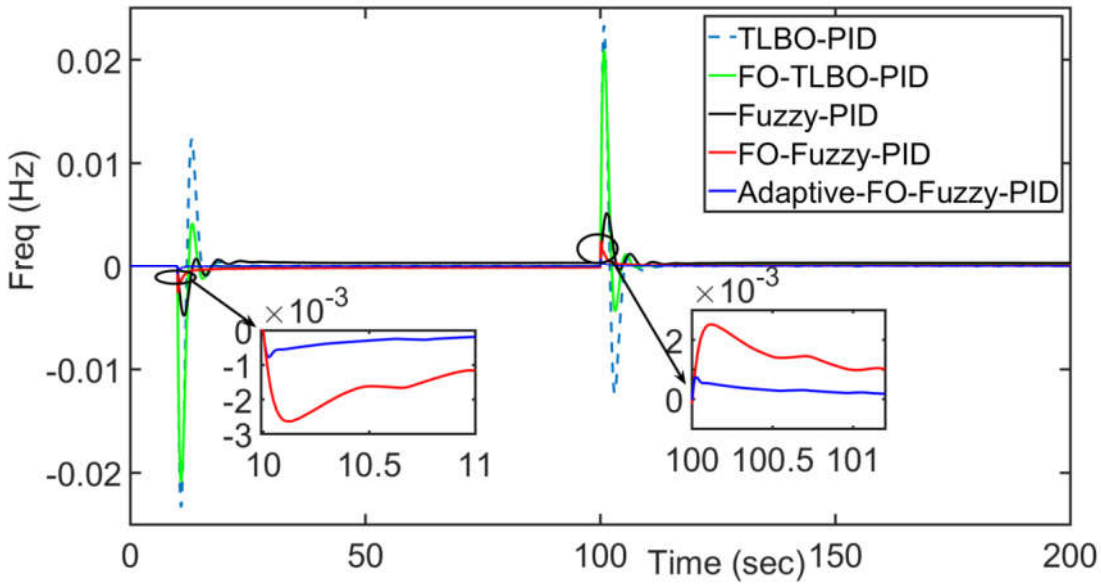

(a)

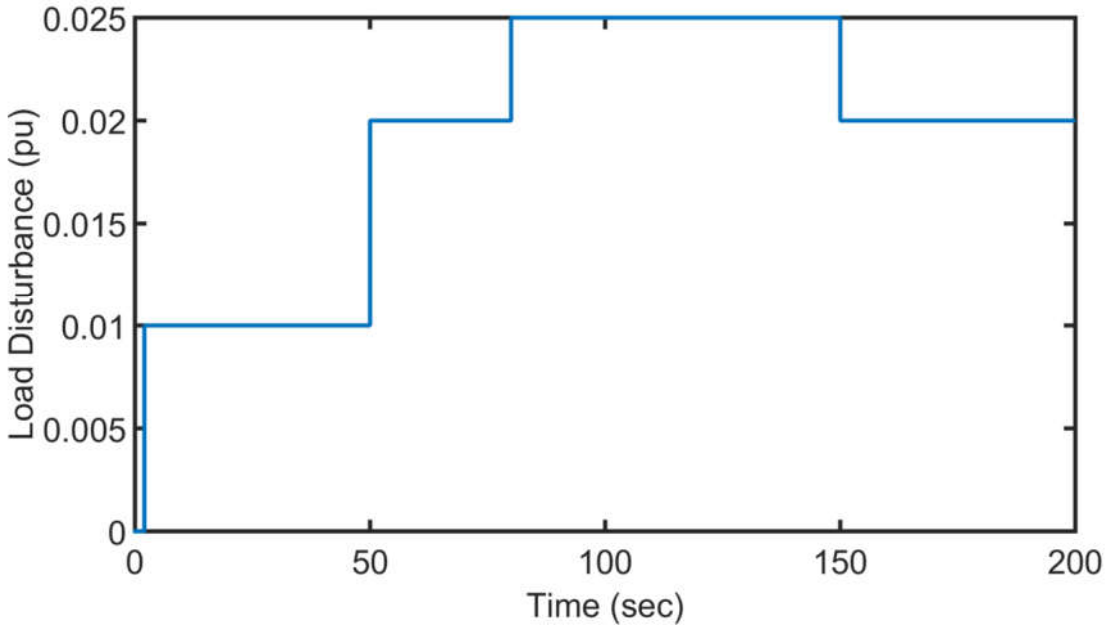

(b)

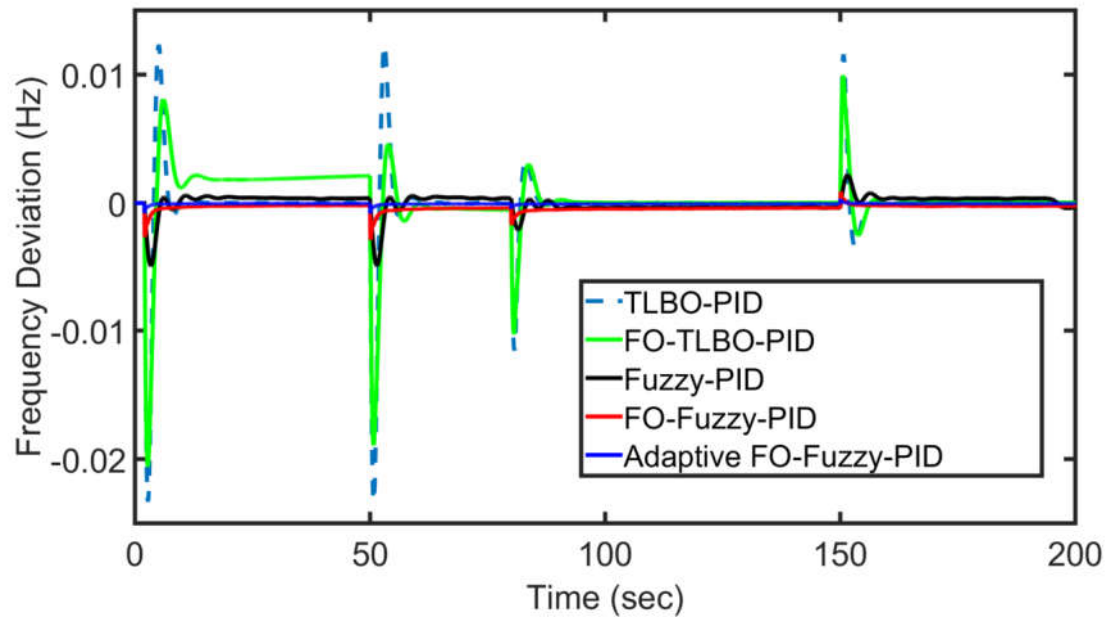

(c)

Fig. 6.5 Scenario 1 frequency response analysis; (a) Frequency deviation response of case 1, (b) Multistep load deviations, (c) Frequency deviation response of case 3

Table 6.2 Comparative study of various controllers for case 1

Controller	Dynamic response performance indices			
	For a load disturbance		RES power disturbance	
	Peak Under shoot(Hz)	Settling Time(sec)	Peak Over shoot(Hz)	Settling Time(sec)
TLBO-PID	-0.0235	20	0.024	21
FO-TLBO-PID	-0.021	16	0.021	16
Fuzzy-PID	-0.005	15	0.0045	15
FO-Fuzzy-PID	-0.0025	11	0.0025	11
Adaptive FO-Fuzzy-PID	-0.001	5	0.001	5

Table 6.3 Comparative study of various controllers for case 2

Controller	Dynamic response performance indices							
	At t=2 seconds		**At t=50 seconds**		**At t=80 seconds**		**At t=150 seconds**	
	Peak Under shoot(Hz)	Settling Time(sec)	Peak Over shoot(Hz)	Settling Time(sec)	Peak Over shoot(Hz)	Settling Time(sec)	Peak Overshoot(Hz)	Settling Time(sec)
TLBO-PID	-0.023	20	-0.024	71	-0.012	91	0.0115	168
FO-TLBO-PID	-0.0205	17	-0.019	66	-0.010	88	0.01	164
Fuzzy-PID	-0.005	15	0.0045	65	-0.002	87	0.0022	160
FO-Fuzzy-PID	-0.0025	10	0.003	61	-0.0017	86	0.001	155
Adaptive FO-Fuzzy-PID	-0.001	5	0.001	55	-0.0005	84	0.0005	153

Scenario 2

The objective of this scenario is to show the robustness of the proposed controller against parametric uncertainties in the system as well as the PHEV aggregator. The percentage changes in the parameters of the power system and PHEV aggregator are displayed in Table 6.4.

In this scenario, a step change of 0.05 p.u.in load is applied as a disturbance to the LFC in area-1 along with parametric uncertainties as mentioned in Table 6.4. The frequency deviation

response of area-1, area-2 and tie-line power deviations with various controllers are shown in Fig. 6.6 (a) - (c). The dynamic performance of various controllers for scenario 2 is listed in Table 6.5.

Table 6.4 Percentage uncertainty in the parameters of the test system and PHEV aggregator

Parameters	Variation Range (in %)
M	-20
D	-10
T_{GT},T_{GH}	+10
R	+15
T_w	+15
T_{EV}	+50
R_{AG}	-50
K_{EV}	-30

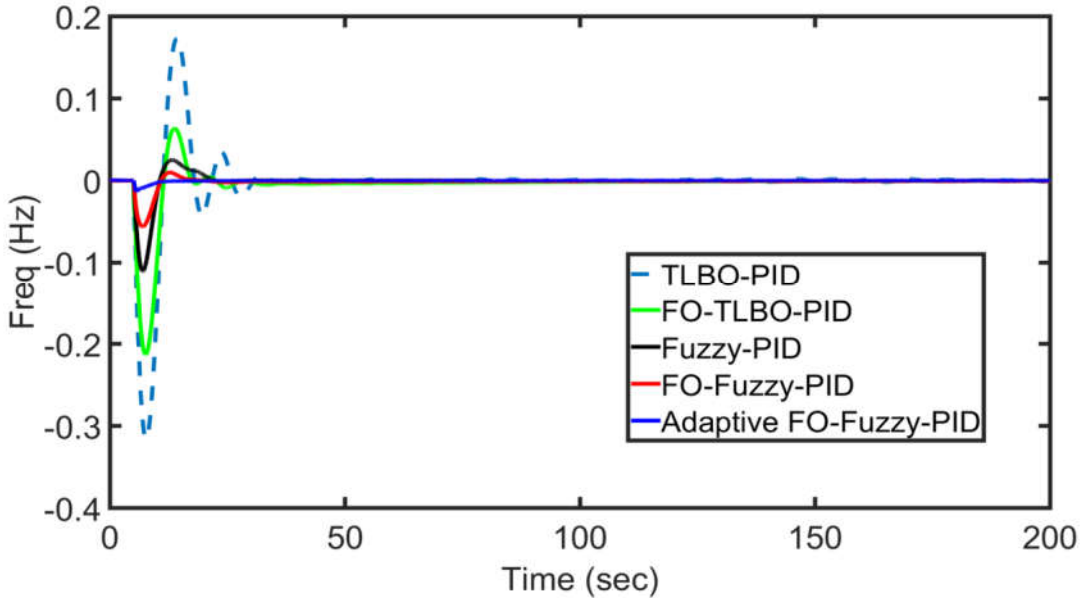

(a)

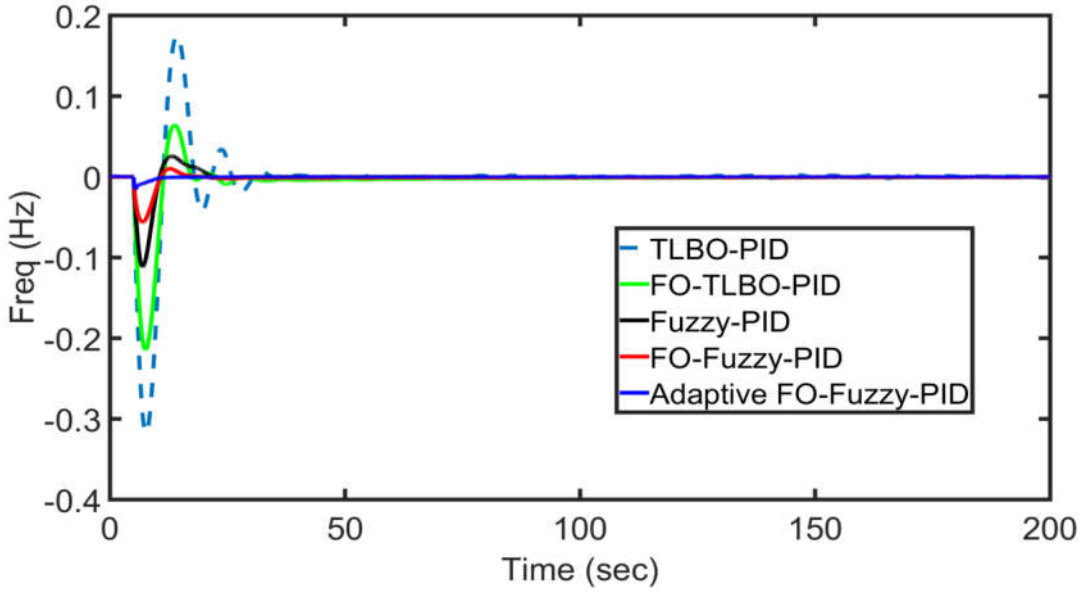

(b)

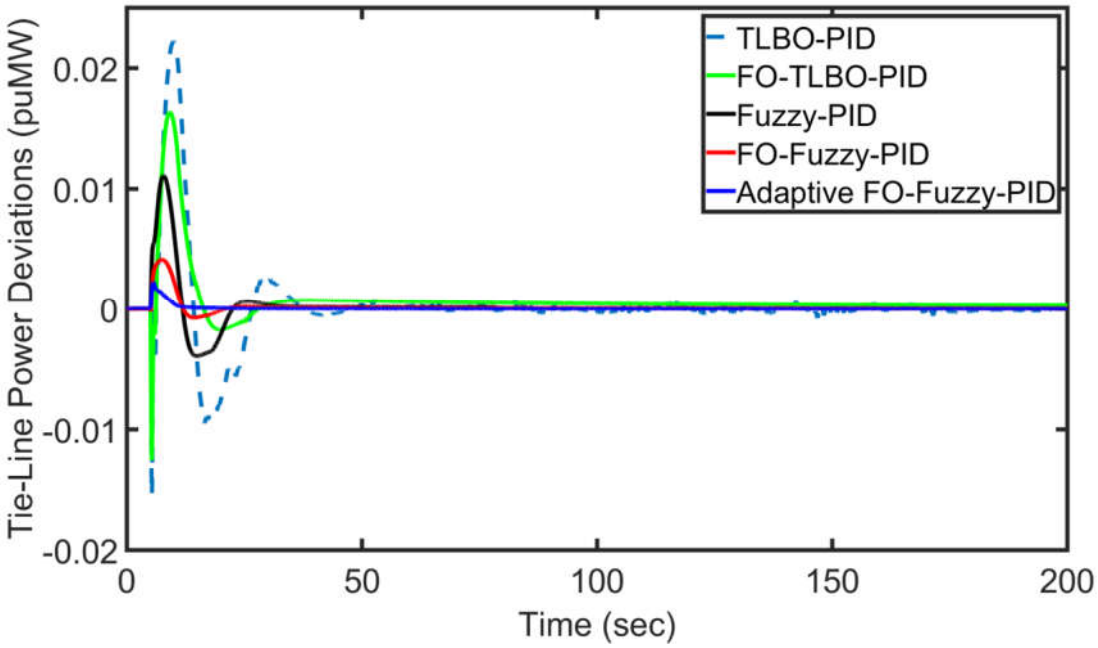

(c)

Fig. 6.6 a), b) Frequency response of area-1 and area-2 for scenario 2 conditions

(c) Tie-line power deviations for scenario 2 conditions.

Table 6.5 Comparative study of various controllers for scenario 2

Methods	Performance indices								
	Area-1			Area-2			Tie-line power deviation		
	PUS (Hz)	POS (Hz)	T_s (s)	PUS (Hz)	POS (Hz)	T_s(s)	PUS (puMW)	POS (puMW)	T_s(s)
TLBO-PID	-0.3	0.15	40	-0.31	0.17	42	-0.015	0.025	55
FO-TLBO-PID	-0.21	0.08	36	-0.22	0.09	38	-0.012	0.016	49
Fuzzy-PID	-0.11	0.03	21	-0.11	0.035	23	-0.005	0.011	36
FO-Fuzzy-PID	-0.061	0.01	15	-0.057	0.012	17	-0.002	0.004	20
Adaptive FO-Fuzzy-PID	-0.013	-	8	0.015	-	10	-	0.002	12

PUS: Peak Undershoot; POS: Peak Overshoot; T_s: Settling Time.

From Fig. 6.6 (a)-(c) and Table 6.5, it is clear that the proposed adaptive FO-Fuzzy-PID controller improves the dynamic response of the system significantly over the other methods. Moreover, the simulation results reveal that the proposed approach is more robust to parametric uncertainties over other controllers in the literature. On the other hand, the TLBO-PID, FO-TLBO-PID and fuzzy PID controllers have large overshoots and more settling time under the circumstances as mentioned in scenario 2.

Scenario 3

In this scenario, it is assumed that there are load changes and wind power changes in area-1 and solar power changes in area-2. The wind power data is extracted from GAMESA company WTG data sheet [99], solar power data from [69]. Fig. 6.7 (a) - (c) illustrates the load, wind power and solar power changes in area-1 and area-2 respectively. Fig. 6.8 (a) & (b) represents the frequency deviation response in area-1 and area-2. Fig. 6.8 (c) depicts the tie-line power flow deviations between area-1 and area-2.

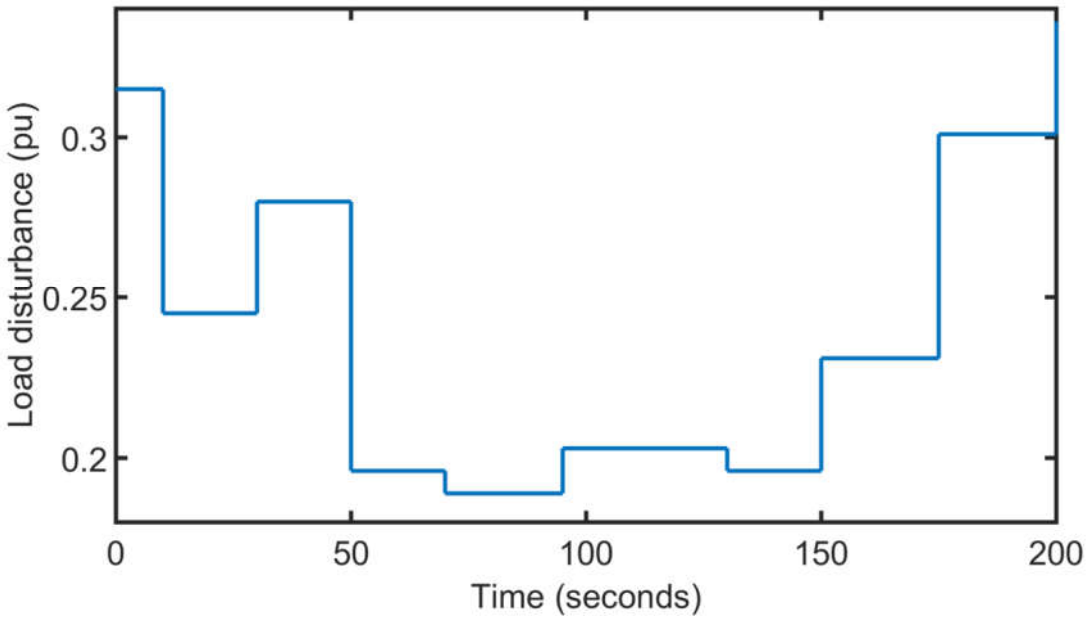
Load disturbance (pu)
0.3
0.25
0.2
0
50
100
150
200
Time (seconds)

(a)

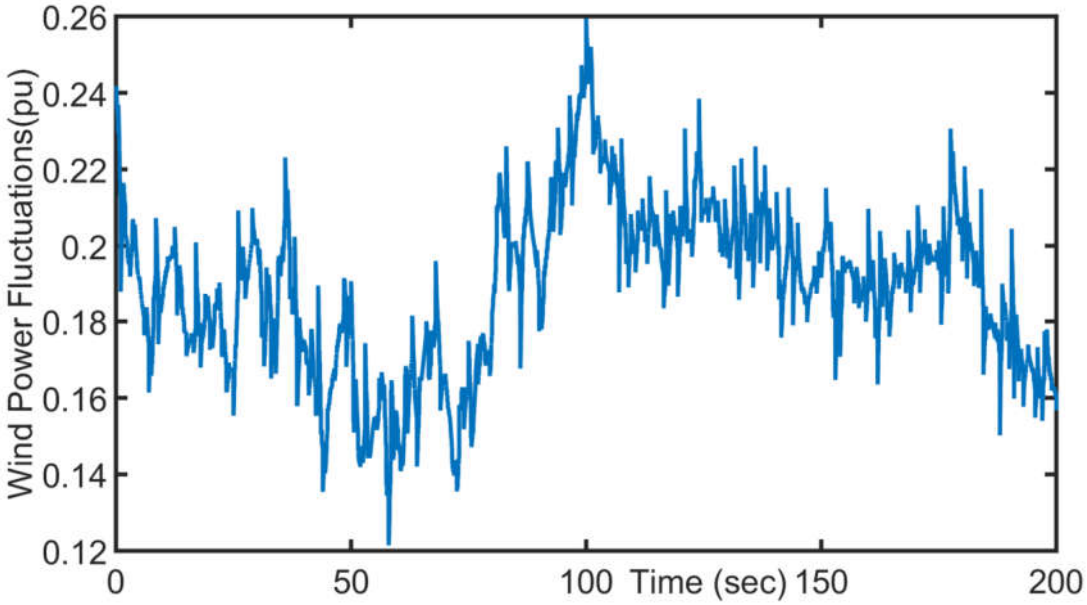
Wind Power Fluctuations(pu)
0.26
0.24
0.22
0.2
0.18
0.16
0.14
0.12
0
50
100
Time (sec)
150
200

(b)

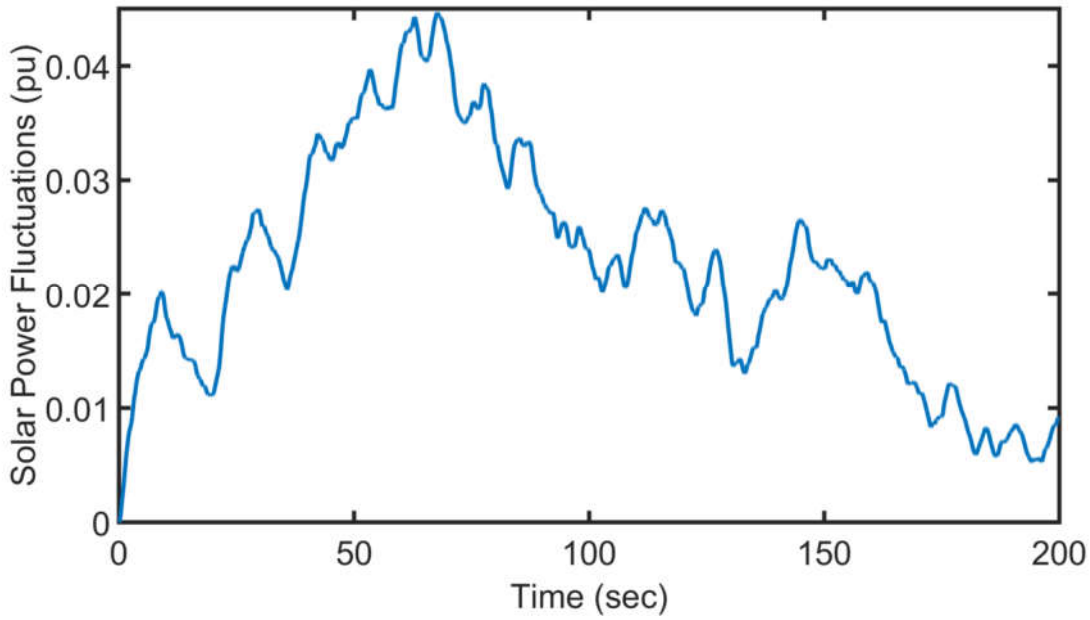

(c)

Fig. 6.7 Various disturbances in power system; a) Load profile b) Wind farm power deviations and c) Solar power deviations

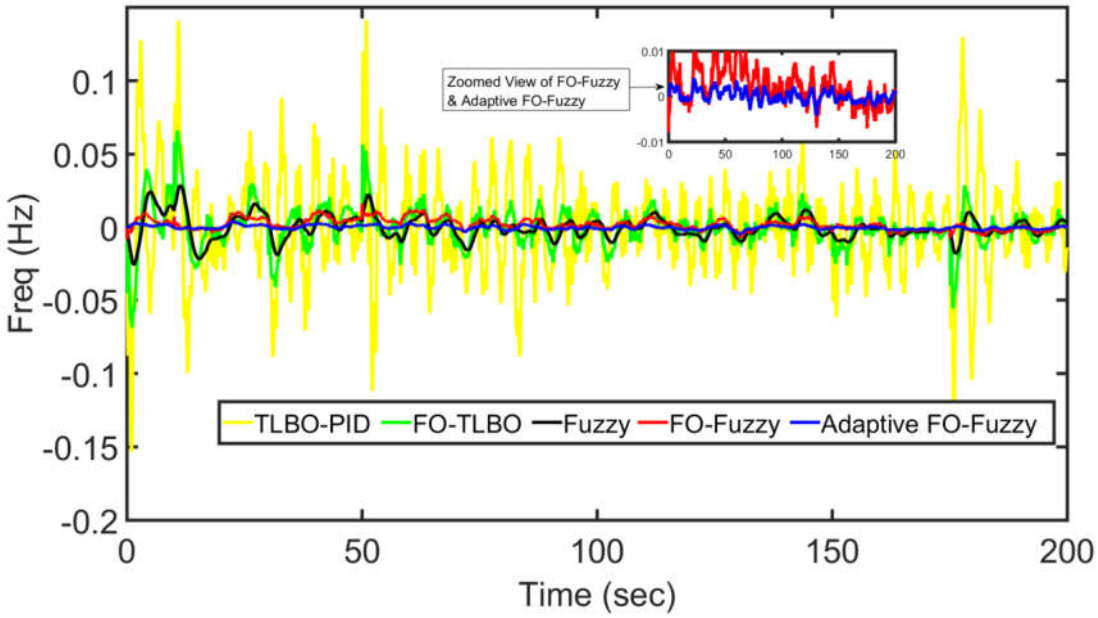

(a)

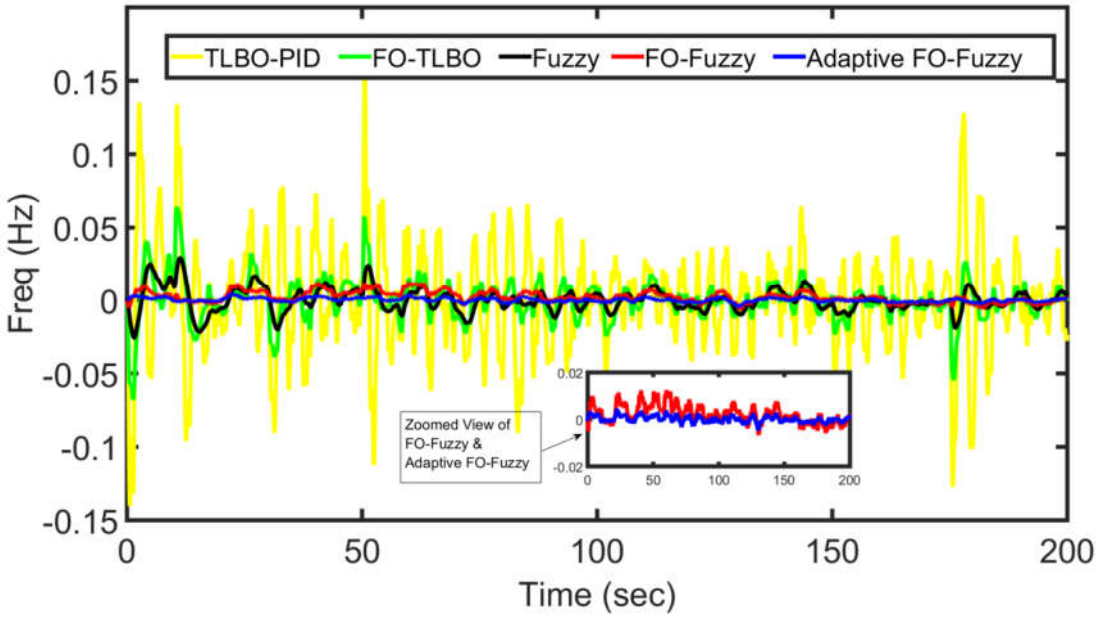

(b)

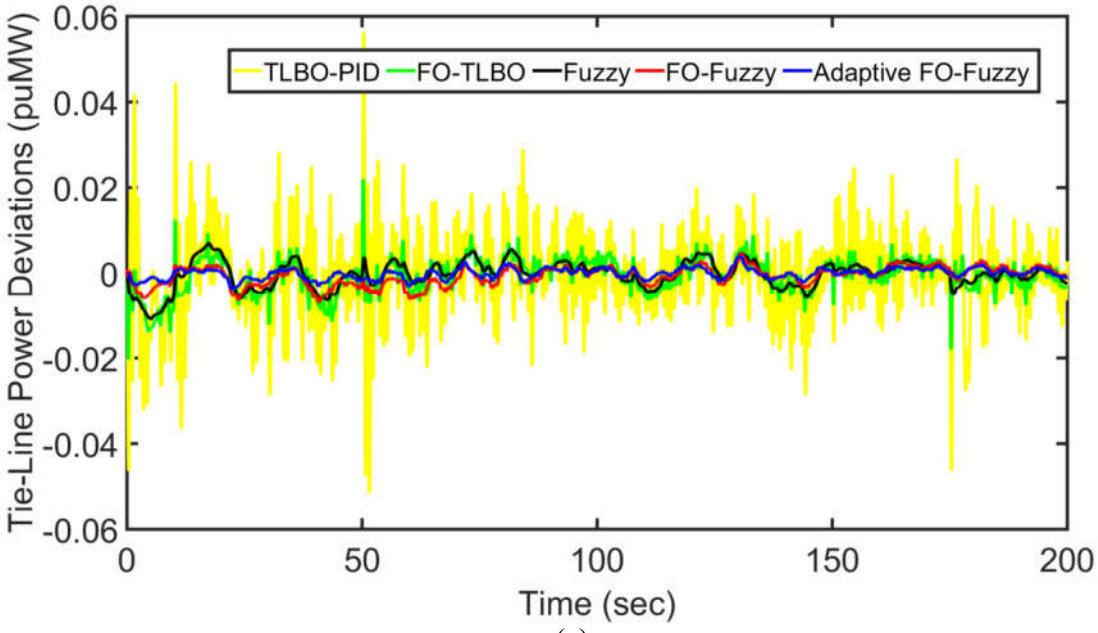

(c)

Fig. 6.8 a), b) Frequency response of area-1 and area-2 for scenario 2 conditions

(c) Tie-line power deviations for scenario 2 conditions.

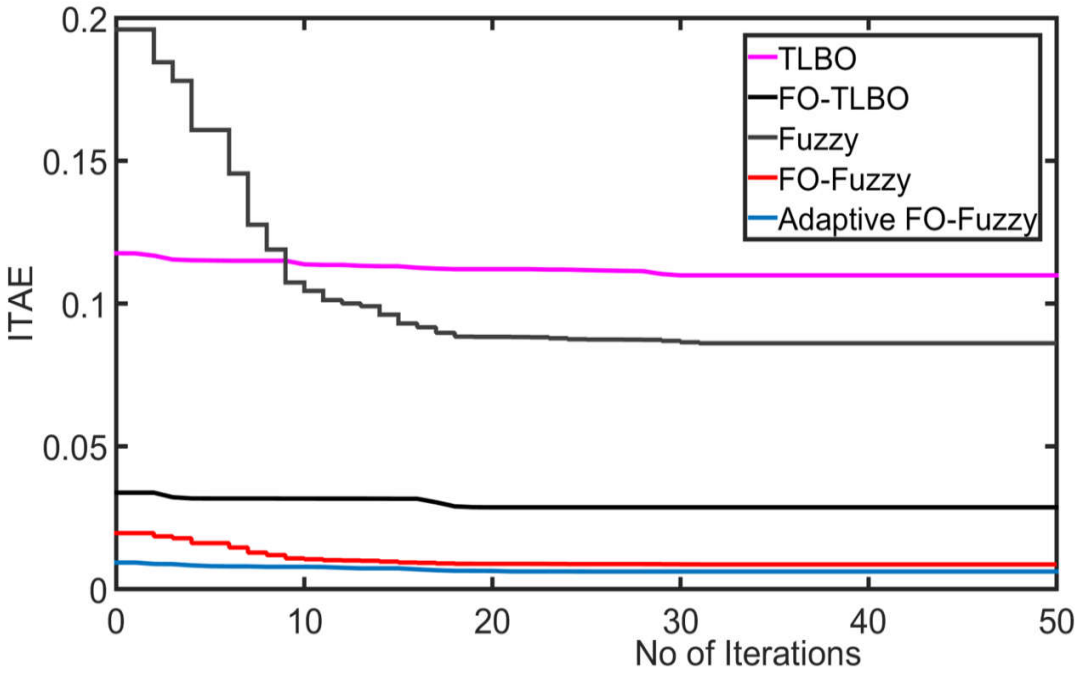

Fig. 6.9 ITAE performance index curve for scenario 3

Fig. 6.8 (a)-(c) reveal that the proposed controller has minimized the frequency and tie-line power deviations effectively with a lesser magnitude of the error and the overshoots with respect to other controllers. The ITAE performance index criteria of various controllers for scenario 3 are listed in Table 6.6 and the optimized gains of various controllers are given in Table 6.7. The rule weights of the proposed controller are listed in Table 6.8. Fig. 6.9 shows the convergence characteristics of the various controllers for scenario 3.

Table 6.6 Comparative study of various controllers for scenario 3

Controller	Area-1		Area-2		Tie-Line Power		ITAE
	PUS	POS	PUS	POS	PUS	POS	
TLBO-PID	-0.16	0.14	-0.14	0.1625	-0.052	0.056	0.11
FO-TLBO	-0.07	0.06	-0.063	0.0635	-0.021	0.022	0.086
Fuzzy	-0.029	0.028	-0.026	0.0292	-0.011	0.008	0.0281
FO-Fuzzy	-0.008	0.01	-0.005	0.012	-0.006	0.005	0.00985
Adaptive FO-Fuzzy	-0.004	0.005	-0.0001	0.0045	-0.002	0.0025	0.0061

Table 6.7 Optimized parameters of various controllers in area-1

Controller Parameters	TLBO-PID	FO-TLBO-PID	Fuzzy-PID	FO-Fuzzy-PID	Adaptive FO-Fuzzy-PID
K_e	-	-	1	0.1413	**0.1060**
K_{ce}	-	-	1	1	**0.2213**
K_u	-	-	1	0.672	**0.431**
K_P	4.4611	4.6969	2.4133	0.98247	**1.5099**
K_I	4.3982	2.4409	4.4003	3.0206	**3.0119**
K_D	3.3559	2.4587	3.3571	3.9201	**3.3571**
λ	-	0.773	-	0.7175	**0.4261**
μ	-	0.6078	-	0.6935	**0.0530**
$d^n/_{dt^n}$	-	-	1	0.5678	**0.1672**

In the proposed controller, in addition to scaling factors and controller parameters, the rule base weights also optimized as shown in Table 6.8

Table 6.8 Optimized rule weights of the proposed adaptive FO-Fuzzy-PID controller

Rule 1	**Rule 2**	**Rule 3**	**Rule 4**	**Rule 5**	**Rule 6**	**Rule 7**	**Rule 8**	**Rule 9**	**Rule 10**
0.6472	0.5551	0.5314	0.6093	0.9123	0.4630	0.8989	0.6900	0.4128	0.332
Rule 11	**Rule 12**	**Rule 13**	**Rule 14**	**Rule 15**	**Rule 16**	**Rule 17**	**Rule 18**	**Rule 19**	**Rule 20**
0.3977	0.7608	0.0622	0.4265	0.5241	0.5377	0.4644	0.6855	0.4749	0.5987
Rule 21	**Rule 22**	**Rule 23**	**Rule 24**	**Rule 25**					
0.7433	0.6897	0.2391	0.3964	0.3579					

Scenario 4

Finally, in order to explore the robustness of the proposed controller at the next level, the PHEV aggregator is disconnected from the grid at the instant of t=100 s. For analysis purposes, only a single area (i.e., area-1 as an isolated area) is considered. The same load, wind power and solar power disturbances as shown in Fig. 6.8 (a) - (c) are considered simultaneously in area-1.

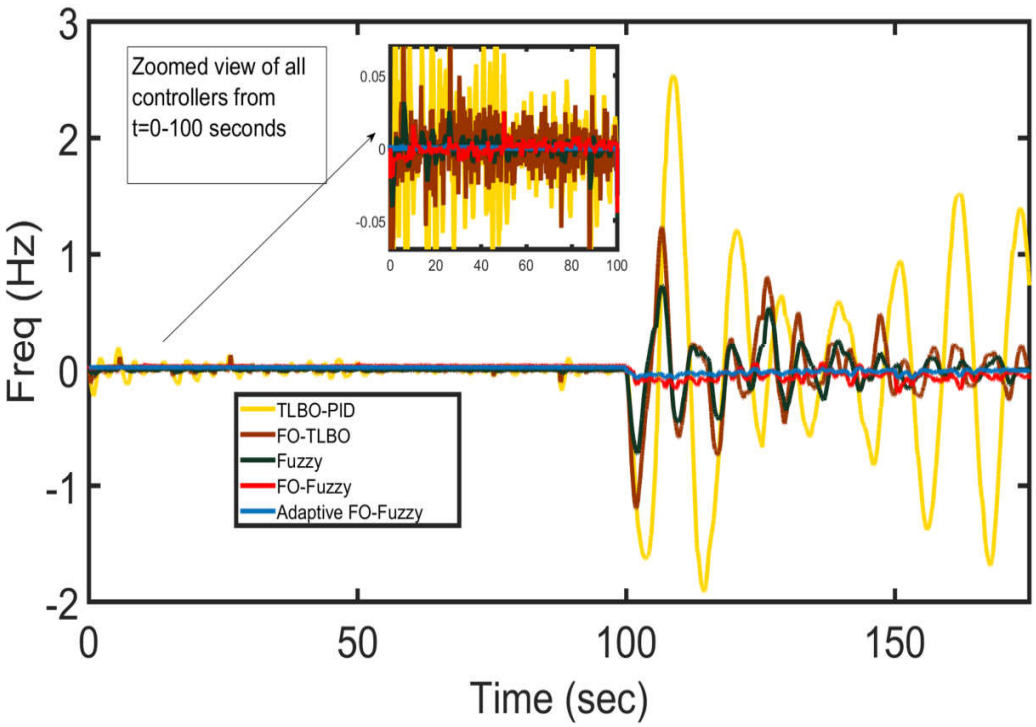

Fig. 6.10 Frequency deviation response of area-1 according to scenario 4

Fig. 6.10 illustrates the simulation results for this scenario. It also shows that the proposed controller improves the frequency response of the system in comparison to other controllers in the literature, especially where the overshoots are concerned. Certainly, from Fig. 6.10, despite parametric uncertainties and EV aggregator disconnection, the proposed controller shows its supremacy over the other four controllers. Furthermore, it can be noticed that the TLBO-PID, FO-TLBO-PID, and Fuzzy-PID controllers were unable to provide acceptable performance in scenario 4. But the FO-Fuzzy-PID controller and proposed adaptive FO-Fuzzy-PID controller have provided an agreeable performance in this scenario. In this duo, the proposed controller shows its superiority in error and overshoot reduction in comparison with the FO-Fuzzy-PID controller.

6.5 Summary

In this work, a novel adaptive FO-FLC-PID controller is proposed for the frequency control of an interconnected power system with RES penetration. In order to improve the robustness against RES intermittencies and load disturbances, the proposed controller is designed at two levels, i.e., Fuzzy and FO-PID control levels. Since the FLC's performance depends on its MFs

and rule base, both are tuned by using the TLBO algorithm along with FO-PID parameters. This proposed approach improves the performance of the LFC with low computational burden and complexity. Moreover, the proposed controller is found to be robust and adaptive enough to handle the uncertainty in the loads, RES power output and system parameters. The simulation results from the four scenarios validate that the proposed controller can minimize the frequency deviations significantly over the TLBO-PID, FO-TLBO-PID, fuzzy PID and FO-FLC-PID controllers.

Chapter 7

Conclusion and Future Scope

7.1 Concluding Remarks

Despite the various advantages, the integration of renewable energy sources to the grid poses a few challenges, in particular on frequency control of the microgrid and main grid. In this regard, this thesis had investigated and presented some AI techniques for the LFC problem in the modern power system with a pragmatic point of view. The key conclusions of this thesis are summarized as follows:

Conclusions on LFC of microgrid

In Chapter 3, the GOA optimized PID controller is proposed for the LFC of autonomous MG. Load perturbations, solar irradiance variations, and nature of wind speed variations are considered and its impact on frequency response has been demonstrated. The simulation and numerical results have proved that the proposed GOA-PID controller effectively eliminates the effects of load disturbances with a lower number of overshoots and fast settling time compared to other advanced controllers in the literature. Moreover, it is observed that the proposed controller is dynamic and effective with solar and wind power variations. Furthermore, the proposed controller is robust against concurrent changes in RES and load perturbations. To further evaluate the performance of the proposed controller, the effect of parametric and ESS uncertainties on MG frequency control have been analyzed. It has been noticed, that the proposed GOA optimized PID controller is very sensitive to these uncertainties and does not provide the desired performance. This is due to, the limited degree of freedom in controller tuning, and proper tuning also depends on the selection of its algorithmic specific parameters.

To overcome these problems, a novel two-stage adaptive fuzzy logic approach based PI controller has been proposed in Chapter 4. The performance of the proposed controller has been investigated on Bella-Coola MG, which has shown significant improvements in the frequency response of MG over all possible operating scenarios. The simulation results reveal that the proposed controller is robust and guarantees good performance against parametric and ESS uncertainties. In comparison with popular optimal, swarm intelligent, fuzzy and single-stage adaptive fuzzy controllers, the proposed controller satisfies the LFC requirements of MG with a much better dynamic response.

Conclusions on LFC of interconnected power systems

Later, in the second part of the thesis, an attempt has been made to study the dynamic performance of LFC of the interconnected power system with CPS, renewable sources and

PHEVs. In chapter 5, a modified LFC scheme is presented for the power system under a renewable environment. The proposed control strategy has been demonstrated on the IEEE Japan East 107-bus-30-machine power system. This model includes all possible nonlinearities in the power system and renewable intermittencies in the LFC study. A new coordinated control strategy between CPS and PHEVs have been proposed for frequency control of the power system. The coordinated control strategy is based on the PID controller which is optimally tuned by recently developed JAYA algorithm. The LFC performs well for the power system with PHEVs, giving better dynamic response compared to conventional power system LFC paradigms. Apart from this, the impact of PHEVs at various levels of frequency control has been analyzed. Significant improvement in LFC is observed when both conventional sources and PHEVs are coordinated with each other in contrast to LFC without PHEVs & with PHEVs with no coordination.

Later, it has been observed that for certain operating scenarios with some power system nonlinearities, swarm intelligent optimized PID controllers are associated with larger shoots and settling times. To overcome this, the fractional-order PID controller is incorporated for LFC studies. The FOPID controller provides better dynamic performance compared to PID controller due to an additional degree of freedom in tuning two non-integer parameters. However, for certain constraints imposed by ESS and renewable uncertainties, it has been observed that the FO-PID controller is too sensitive to these uncertainties and fails to provide acceptable performance. For such conditions, the fuzzy logic approach provides an efficient solution with proper tuning of its internal parameters.

To overcome the above-mentioned drawbacks and make the controller compatible under the renewable environment, integration of fuzzy logic controller with FO-PID is proposed as a feasible solution that inherits the benefits of both controllers. In this context, in Chapter 6, a novel adaptive fractional order fuzzy PID controller is proposed for LFC in a renewable penetrated power system. The LFC performs well for the power system with the proposed controller, provides a better dynamic response with fewer overshoots/undershoots and faster settling time compared to the recently advanced controllers in the literature. The proposed controller is stubborn to the internal system and PHEV constraints besides the step load variations, whereas the other controllers are associated with large overshoots, undershoots and more settling times. Besides, the robustness of the proposed controller is tested against the

sudden disconnection of EV aggregator. An extensive analysis is done for the LFC scheme considering various uncertainties in the system parameters, constraints, RES output power, and ESS output power. The dynamic responses obtained with the proposed controller with a wide range of variations in operating conditions have satisfied the LFC requirements efficiently and effectively. Hence for all practical applications, the proposed controller will be suitable for its robust nature and efficiency.

Attains the specifications and objectives of LFC with proposed controllers

A comprehensive review of LFC literature was carried out, where the pros and cons of various control techniques that are accounted for good LFC, based on minimum specifications were compared (Table 2.9). The literature review revealed that no particular control technique meets all specifications of LFC simultaneously. The comparative analysis in Table 2.9 reveals that AI techniques can bring some added advantages but its strengths are under-exploited in certain specifications under renewable environment. Concerning this, four AI methods are introduced for the LFC in a renewable penetrated microgrid and interconnected power systems. All these methods have met the specific objectives of LFC quite effectively with faster settling times, reduced overshoots and a low ITAE error value. Moreover, the proposed two-stage adaptive fuzzy PI in microgrid and adaptive fractional order fuzzy PID in interconnected power systems have also met all the specifications for good LFC simultaneously under various critical operating scenarios. Hence, these controllers are quite robust, efficient and can perform well under the modern power system environment. The significant features of the proposed intelligent techniques found in this research work are:

a. Proposed adaptive fuzzy controllers are free from the mathematical model of the system.
b. Independent from system size and nonlinearities.
c. Significantly fast, efficient and reliable.
d. A multi-agent parallel stochastic search of solutions.
e. Less sensitive to load and renewable disturbances and robust to system and ESS uncertainties.
f. Adaptable and flexible in tuning based on the system operating conditions

7.2 Future Scope

This thesis can be carried forward in the following area:

- The integration of intermittent natured energy sources like wind and solar power with energy storage systems enhances the quality of power and reliability of the system. The frequency regulation in a renewable penetrated power system is a major concern and a lot of control strategies have been developed over the last decade to enhance the frequency response of the power system. Further efforts are therefore required to design novel frequency control strategies that can take microgrid dynamics into account if they are con nected to the main grid.
- The level of RES penetration has been increasing day by day in modern interconnected power systems. However, not much work is reported with respect to the integration of wind and solar energy sources in secondary frequency control. Nevertheless, with rapid growth in the penetration of such sources, their dynamic participation in the design of frequency control of the power system needs to be investigated.
- It is also possible to integrate proposed control techniques with aforementioned control schemes to further improve them in terms of their better reliability.
- Some advanced AI techniques like deep learning and machine learning techniques with the proposed method can be used and for different power system models.

REFERENCES

[1] P. Kundur, "Power system stability and control," 2nd ed. McGraw-Hill, 2001.

[2] D. P. Kothari and I. J. Nagrath, "Modern power system analysis," 4th ed. Mcgraw-Hill, 2011.

[3] O. I. Elgerd and C. E. Fosha, "Optimum megawatt-frequency control of multi area electric energy systems," in *IEEE Transactions on Power Apparatus and Systems*, vol. 89, no. 4, pp. 556-563, April 1970.

[4] Gary D. Price " Power systems and renewable energy: Design, Operation, and Systems Analysis," Momentum Press, 2014.

[5] H. H. Alhelou, M. E. Hamedani-Golshan, R. Zamani, E. Heydarian-Forushani, and P. Siano, "Challenges and opportunities of load frequency control in conventional, modern and future smart power systems: a comprehensive review," *Energies*, vol. 11, no. 10, 2018.

[6] H. Bevrani, A. Ghosh and G. Ledwich, "Renewable energy sources and frequency regulation: survey and new perspectives," in *IET Renewable Power Generation*, vol. 4, no. 5, pp. 438-457, September 2010.

[7] T. Liu, D. J. Hill and C. Zhang, "Non-disruptive load-side control for frequency regulation in power systems," in *IEEE Transactions on Smart Grid*, vol. 7, no. 4, pp. 2142-2153, July 2016.

[8] T. Mai, R. Wiser, D. Sandor, G. Brinkman, G. Heath, P. Denholm, D. J.Hostick, N. Darghouth, A. Schlosser, and K. Strzepek, "Exploration of high-penetration renewable electricity futures. vol. 1 of renewable electricity futures study," National Renewable Energy Laboratory, Golden, CO, NREL/TP-6A20-52409-1, 2012.

[9] G. Strbac, A. Shakoor, M. Black, D. Pudjianto, and T. Bopp, "Impact of wind generation on the operation and development of the UK electricity systems," *Electric Power Systems Research*, vol. 77, no. 9, pp. 1214–1227, 2007.

[10] Z. A. Obaid, L. M. Cipcigan, L. Abrahim, and M. T. Muhssin, "Frequency control of future power systems: reviewing and evaluating challenges and new control methods," *Journal of Modern Power Systems and Clean Energy*, vol. 7, no. 1, pp. 9–25, 2019.

[11] N. Hatziargyriou, H. Asano, R. Iravani, and C. Marnay, "Microgrids," *IEEE Power and Energy Magazine*, vol. 5, no. 3, pp. 78–94, 2007.

[12] IEEE Guide for Design, Operation, and Integration of Distributed Resource Island Systems with Electric Power Systems," in *IEEE Std 1547.4-2011* , pp.1-54, 20 July 2011.

[13] P. K. Ray, S. R. Mohanty, and N. Kishor, "Proportional–integral controller based small-signal analysis of hybrid distributed generation systems," *Energy Conversion and Management*, vol. 52, no. 4, pp. 1943–1954, 2011.

[14] I. Şerban and C. Marinescu, "Aggregate load-frequency control of a wind-hydro autonomous microgrid," *Renewable Energy*, vol. 36, no. 12, pp. 3345–3354, 2011.

[15] G. Mallesham, S. Mishra, and A. N. Jha, "Ziegler-Nichols based controller parameters tuning for load frequency control in a microgrid," *Proceedings in International Conference on Energy, Automation and Signal*, 2011, pp. 1–8.

[16] M. Datta, T. Senjyu, A. Yona, T. Funabashi and C. Kim, "A frequency control approach by photovoltaic generator in a PV-diesel hybrid power system," *IEEE Trans. On Energy Conversion*, vol. 26, no. 2, pp. 559-571, 2011.

[17] T. Senjyu T. Kaneko A. Yona A. Uhera H. Sekine Ch. Kim "Output power control for large wind power penetration in small power system," *Renewable Energy*, vol. 34, pp. 2334-2343, 2009.

[18] M. N. Anwar and S. Pan, "A new PID load frequency controller design method in frequency domain through direct synthesis approach," *International Journal of Electrical Power & Energy Systems*, vol. 67, pp. 560–569, 2015.

[19] Milan Calovic, "Linear Regulator Design for a Load and Frequency Control," *IEEE Trans. Power Appar. Syst.*, vol. PAS-91, no. 6, pp. 2271–2285, 1972.

[20] Y. Ota, H. Taniguchi, T. Nakajima, K. M. Liyanage, J. Baba and A. Yokoyama, "Autonomous distributed V2G (Vehicle-to-Grid) satisfying scheduled charging," in *IEEE Transactions on Smart Grid*, vol. 3, no. 1, pp. 559-564, March 2012.

[21] A. Khodabakhshian and R. Hooshmand, "A new PID controller design for automatic generation control of hydro power systems," *Electr. Power Energy Syst.*, vol. 32, no. 5, pp. 375–382, 2010.

[22] H. Liu, Z. Hu, Y. Song, J. Wang, and X. Xie, “Vehicle-to-Grid control for supplementary frequency regulation considering charging demands,” *IEEE Transactions on Power Systems*, vol. 30, no. 6, pp. 3110–3119, Nov. 2015.

[23] C. Yang *et al.*., “Dynamic event-triggered robust secondary frequency control for islanded AC microgrid,” *Applied Energy*, vol. 242, pp. 821–836, 2019.

[24] C. Mu, W. Liu, W. Xu, and M. Rabiul Islam, “Observer-based load frequency control for island microgrid with photovoltaic power,” *International Journal of Photoenergy*, vol. 7, pp. 2851436, 2017.

[25] C. Wang, J. Li and Y. Hu, "Frequency control of isolated wind-diesel microgrid power system by double equivalent-input-disturbance controllers," in *IEEE Access*, vol. 7, pp. 105617-105626, 2019.

[26] A. Mehrizi-Sani and R. Iravani, “Potential-function based control of a microgrid in islanded and grid-connected modes,” *IEEE Transactions on Power Systems*, vol. 25, no. 4, pp. 1883–1891, Nov. 2010.

[27] D. H. Tungadio, R. C. Bansal, and M. W. Siti, “Optimal control of active power of two micro-grids interconnected with two AC tie-lines,” *Electric Power Components and Systems*, vol. 45, no. 19, pp. 2188–2199, 2017.

[28] R. Mandal, K. Chatterjee, and B. K. Patil, “Load frequency control of a single area hybrid power system by using integral and LQR based integral controllers,” in *2018 20th National Power Systems Conference (NPSC)*, 2018, pp. 1–6.

[29] S. D. Hanwate and Y. V Hote, “Optimal PID design for load frequency control using QRAWCP approach,” *IFAC-Papers Online*, vol. 51, no. 4, pp. 651–656, 2018.

[30] S. Saxena and Y. V Hote, “Decentralized PID load frequency control for perturbed multi-area power systems,” *International Journal of Electrical Power & Energy Systems*, vol. 81, pp. 405–415, 2016.

[31] G. Ray, A. N. Prasad, and G. D. Prasad, “A new approach to the design of robust load-frequency controller for large scale power systems,” *Electric Power Systems Research*, vol. 51, no. 1, pp. 13–22, 1999.

[32] E. Rakhshani and J. Sadeh, “Practical viewpoints on load frequency control problem in a deregulated power system,” *Energy Conversion and Management*, vol. 51, no. 6, pp.1148–1156, 2010.

[33] K.P. Parmar, S. Majhi, and D.P. Kothari, “LFC of an interconnected power system with multi-source power generation in deregulated power environment,” *Int. J. of Elect. Power & Energy Sys.*, vol. 57, pp.277–286, 2014.

[34] A. Jeya Veronica, N.Senthil Kumar, "Internal model-based load frequency controller design for hybrid microgrid system," *Energy Procedia*, Volume 117, pp.1032-1039, 2017.

[35] A. Jeya Veronica, N.Senthil Kumar, "Load frequency controller design for microgrid using internal model approach," *International Journal of Renewable Energy Research*, Vol.7, Issue 2, pp.778-786, 2017.

[36] J. Yang, Z. Zeng, Y. Tang, J. Yan, H. He, and Y. Wu, “Load frequency control in isolated micro-Grids with electrical vehicles based on multivariable generalized predictive theory,” *Energies*, vol. 8, no. 3, pp. 2145–2164, 2015.

[37] J. Pahasa and I. Ngamroo, "Coordinated control of wind turbine blade pitch angle and PHEVs using MPCs for load frequency control of microgrid," in *IEEE Systems Journal*, vol. 10, no. 1, pp. 97-105, March 2016.

[38] S. Kayalvizhi and D. M. Vinod Kumar, "Load frequency control of an Isolated microgrid using fuzzy adaptive model predictive control," in *IEEE Access*, vol. 5, pp. 16241-16251, 2017.

[39] M.-R. Chen, G.-Q. Zeng, Y.-X. Dai, K.-D. Lu, and D.-Q. Bi, “Fractional-Order model predictive frequency control of an Islanded microgrid,” *Energies*, vol. 12, no. 1, 2018.

[40] W. Tan, "Unified tuning of PID load frequency controller for power systems via IMC," *IEEE Transactions on Power Systems*, vol. 25, no. 1, pp.341–350, 2010.

[41] M. Elsisi, M. Soliman, M. A. S. Aboelela and W. Mansour, "Model predictive control of plug-in hybrid electric vehicles for frequency regulation in a smart grid," in *IET Generation, Transmission & Distribution*, vol. 11, no. 16, pp. 3974-3983, 2017.

[42] A. S. Mir and N. Senroy, "Adaptive model predictive control scheme for application of SMES for load frequency control," in *IEEE Transactions on Power Systems*., pp.1-6, 2017.

[43] M. A. Mohamed, A. A. Z. Diab, H. Rezk, and T. Jin, “A novel adaptive model predictive controller for load frequency control of power systems integrated with DFIG wind turbines,” *Neural Computing and Applications*, vol. 31, pp.1-11, 2019.

[44] M. M. Mahdi, E. Mhawi Thajeel and A. Z. Ahmad, "Load frequency control for hybrid microgrid using MRAC with ANN under sudden load changes," *Proceedings in Third Scientific Conference of Electrical Engineering (SCEE)*, Baghdad, Iraq, pp. 220-225, 2018.

[45] M. R. Khalghani, M. H. Khooban, E. Mahboubi-Moghaddam, N. Vafamand, and M. Goodarzi, "A self-tuning load frequency control strategy for microgrids: Human brain emotional learning," *International Journal of Electrical Power & Energy Systems*, vol. 75, pp. 311–319, 2016.

[46] Y. Qudaih, I. Moukhtar, T. H. Mohamed, "Parallel PI/CDM frequency controller to support V2G plan for microgrid," *Energy Procedia,* Vol.100, pp. 342–351, 2016.

[47] J. Hu, Y. Shan, Y. Xu, and J. M. Guerrero, "A coordinated control of hybrid ac/dc microgrids with PV-wind-battery under variable generation and load conditions," *International Journal of Electrical Power & Energy Systems*, vol. 104, pp. 583–592, 2019.

[48] K. Liu, J. He, Z. Luo, X. Shen, X. Liu and T. Lu, "Secondary frequency control of isolated microgrid based on LADRC," in *IEEE Access*, vol. 7, pp. 53454-53462, 2017.

[49] A. Rubaai and V. Udo, "Self-tuning load frequency control: multilevel adaptive approach," *IEE Proceedings-Generation, Transmission and Distribution*, vol. 141, no. 4, pp.285–290, 1994.

[50] D. G. Padhan and S. Majhi, "A new control scheme for PID load frequency controller of single-area and multi-area power systems," *ISA Transactions*, vol. 52, no. 2, pp. 242–251, 2013.

[51] S. Hanwate, Y. V. Hote and S. Saxena, "Adaptive policy for load frequency control," in *IEEE Transactions on Power Systems*, vol. 33, no. 1, pp. 1142-1144, Jan. 2018.

[52] H. Grover, J. Ojha, A. Verma and T. S. Bhatti, "Adaptive load frequency control of a grid connected solar PV system," *Proceedings in IEEE International Conference on Environment and Electrical Engineering (EEEIC / I&CPS Europe)*, Genova, Italy, pp. 1-4, 2019.

[53] V. P. Singh, S. R. Mohanty, N. Kishor, and P. K. Ray, "Robust H-infinity load frequency control in hybrid distributed generation system," *International Journal of Electrical Power & Energy Systems*, vol. 46, pp. 294–305, 2013.

[54] B. E. Sedhom, M. M. El-Saadawi, M. A. Elhosseini, M. A. Saeed, and E. E. Abd-Raboh, "A harmony search-based H-infinity control method for islanded microgrid," *ISA Transactions*, vol. 99, pp.252-269, 2019.

[55] K. P. Shashi, and R. Soumya, "Frequency regulation in hybrid power systems particle swarm optimization and linear matrix inequalities based robust controller design," *International Journal of Electrical Power & Energy Systems*, vol. 63, pp. 887–900, 2014.

[56] S. K. Pandey, N. Kishor, and S. R. Mohanty, "Frequency regulation in hybrid power system using iterative proportional-integral-derivative H-∞ Controller," *Electric Power Components and Systems*, vol. 42, no. 2, pp. 132–148, 2014.

[57] H. Bevrani, M. R. Feizi and S. Ataee, "Robust frequency control in an islanded microgrid: H-∞ and μ-synthesis approaches," in *IEEE Transactions on Smart Grid*, vol. 7, no. 2, pp. 706-717, March 2016.

[58] D. Qian, S. Tong, H. Liu, and X. Liu, "Load frequency control by neural-network-based integral sliding mode for nonlinear power systems with wind turbines," *Neuro computing*, vol. 173, no. 3, pp.875–885, 2016.

[59] T. N. Pham, H. Trinh, L. V. Hien and K. P. Wong, "Integration of electric vehicles for load frequency output feedback H-∞ control of smart grids," in *IET Generation, Transmission & Distribution*, vol. 10, no. 13, pp. 3341-3352, 2016.

[60] P. D. Shendge, B. M. Patre, and S. B. Phadke, "Robust load frequency sliding mode control based on uncertainty and disturbance estimator," in *Advances in Industrial Engineering and Operations Research*, A. H. S. Chan and S.-I. Ao, Eds. Boston, MA: Springer US, 2008, pp. 361–374.

[61] S. Trip, M. Cucuzzella, C. De Persis, A. Ferrara, and J. M. A. Scherpen, "Robust load frequency control of nonlinear power networks," *International Journal of Control*, vol. 93, no. 2,pp. 1–14, 2018.

[62] K. W. Kow, Y. W. Wong, R. K. Rajkumar, and R. K. Rajkumar, "A review on performance of artificial intelligence and conventional method in mitigating PV grid-tied related power quality events," *Renewable and Sustainable Energy Reviews*, vol. 56, no. C, pp. 334–346, 2016.

[63] J. Kubacki, “Artificial intelligence,” in *Technology Guide: Principles - Applications - Trends*, 2009.

[64] W. R. Anis Ibrahim and M. M. Morcos, "Artificial intelligence and advanced mathematical tools for power quality applications: a survey," in *IEEE Transactions on Power Delivery*, vol. 17, no. 2, pp. 668-673, April 2002.

[65] A. Ray, K. Jana, M. Assadi, and S. De, “Distributed polygeneration using local resources for an Indian village: multi objective optimization using meta-heuristic algorithm,” *Clean Technologies and Environmental Policy*, vol. 20, no. 6, pp. 1323–1341, 2018.

[66] D. C. Das, A. K. Roy, and N. Sinha, “GA based frequency controller for solar thermal–diesel–wind hybrid energy generation/energy storage system,” *Int J. Electr. Power Energy Syst.*, vol. 43, no. 1, pp. 262–279, 2012.

[67] G. Shankar, and V. Mukherjee, “Load frequency control of an autonomous hybrid power system by quasioppositional harmony search algorithm,” *Int J. Electr. Power Energy Syst.*, vol. 78, pp. 715–734, 2016.

[68] A. M. Abdel-hamed, A. E.-E. K. M. Ellissy, A. S. El-Wakeel, and A. Y. Abdelaziz, “Optimized control scheme for frequency/power regulation of microgrid for fault tolerant operation,” *IEEE Transaction on Smart Grid*, vol. 7, no. 3, pp. 1429–1440, 2016.

[69] A. A. El-Fergany and M. A. El-Hameed, “Efficient frequency controllers for autonomous two-area hybrid microgrid system using social-spider optimiser,” *IET Gener. Transm. Distrib.,* vol. 11, no. 3, pp. 637–648,2017.

[70] P. K. Ray and A. Mohanty, “A robust firefly–swarm hybrid optimization for frequency control in wind/PV/FC based microgrid,” *Applied Soft Computing*, vol. 85, pp.105823, 2018.

[71] C. Sreenivasaratnam, C. Yammani, and S. Maheswarapu, “Load frequency control of multi-microgrid System considering renewable energy sources using grey wolf optimization,” *Smart Science*, vol. 7, no. 3, pp. 198–217, 2019.

[72] F. Daneshfar and H. Bevrani, "Load-frequency control: a GA-based multi-agent reinforcement learning," in *IET Generation, Transmission & Distribution*, vol. 4, no. 1, pp. 13-26, 2010.

[73] G. Magdy, G. Shabib, A. A. Elbaset, and Y. Mitani, “Optimized coordinated control of LFC and SMES to enhance frequency stability of a real multi-source power system

considering high renewable energy penetration," *Protection and Control of Modern Power Systems*, vol. 3, no. 1, p. 39, 2018.

[74] N. E. Y. Kouba, M. Menaa, M. Hasni and M. Boudour, "LFC enhancement concerning large wind power integration using new optimised PID controller and RFBs," in *IET Generation, Transmission & Distribution*, vol. 10, no. 16, pp. 4065-4077, 2016.

[75] S. Debbarma and A. Dutta, "Utilizing electric vehicles for LFC in restructured power systems using fractional order controller," in *IEEE Transactions on Smart Grid*, vol. 8, no. 6, pp. 2554-2564, 2017.

[76] R. Khezri, A. Oshnoei, M. Tarafdar Hagh, and S. M. Muyeen, "Coordination of heat pumps, electric vehicles and AGC for efficient LFC in a smart hybrid power system via SCA-Based optimized FOPID controllers," *Energies*, vol. 11, no. 2, pp.1-21, 2018.

[77] A. Saha and L. C. Saikia, "Performance analysis of combination of ultra-capacitor and superconducting magnetic energy storage in a thermal-gas AGC system with utilization of whale optimization algorithm optimized cascade controller," *Journal of Renewable and Sustainable Energy*, vol. 10, no. 1, pp. 14103, 2018.

[78] H. Shayeghi, A. Molaee, K. Valipour and A. Ghasemi, "Multi-source power system FOPID based load frequency control with high-penetration of distributed generations," *Proceedings in 21st Conference on Electrical Power Distribution Networks Conference (EPDC)*, Karaj, pp. 131-136,2016.

[79] T. Mahto, H. Malik and M. Saad Bin Arif, "Load frequency control of a solar-diesel based isolated hybrid power system by fractional order control using partial swarm optimization," *Journal of Intelligent & Fuzzy Systems (JIFS)*, vol. 35, pp. 5055-5061, 2018.

[80] F. Ornelas-Tellez, J. J. Rico-Melgoza, A. E. Villafuerte, and F. J. Zavala-Mendoza, "Chapter 3 - Neural Networks: A methodology for modelling and control design of dynamical systems," in *Artificial Neural Networks for Engineering Applications*, , Eds. Academic Press, 2019, pp. 21–38.

[81] P. C. Sekhar and S. Mishra, "Storage free smart energy management for frequency control in a Diesel-PV-Fuel Cell-based hybrid AC microgrid," in *IEEE Transactions on Neural Networks and Learning Systems*, vol. 27, no. 8, pp. 1657-1671, Aug. 2016.

[82] A. Safari, F. Babaei, and M. Farrokhifar, “A load frequency control using a PSO-based ANN for microgrids in the presence of electric vehicles,” *International Journal of Ambient Energy*, vol.40, no. 2, pp. 1–13, 2018.

[83] H. Bevrani, F. Habibi, S. Shokoohi, “ANN-based self-tuning frequency control design for an isolated microgrid,” *Meta-Heuristics Optimization Algorithms in Engineering, Business, Economics, and Finance. P. Vasant (Ed)*, *IGI Global*, Chapter 12, pp. 357-385, 2013.

[84] K. Kumari, G. Shankar, S. Kumari and S. Gupta, "Load frequency control using ANN-PID controller," *Proceedings in IEEE 1st International Conference on Power Electronics, Intelligent Control and Energy Systems (ICPEICES)*, Delhi, 2016, pp. 1-6.

[85] D. Qian and G. Fan, "Neural-network-based terminal sliding mode control for frequency stabilization of renewable power systems," in *IEEE/CAA Journal of Automatica Sinica*, vol. 5, no. 3, pp. 706-717, 2018.

[86] A. Ghafouri, J. Milimonfared and G. B. Gharehpetian, "Coordinated control of distributed energy resources and conventional power plants for frequency control of power systems," in *IEEE Transactions on Smart Grid*, vol. 6, no. 1, pp. 104-114, 2015.

[87] Y. Bai and D. Wang, “Fundamentals of fuzzy logic control --- Fuzzy sets, Fuzzy rules and Defuzzifications,” in *Advanced Fuzzy Logic Technologies in Industrial Applications*, Y. Bai, H. Zhuang, and D. Wang, Eds. London: Springer London, pp. 17–36, 2006.

[88] N. Siddique and H. Adeli "Computational intelligence-synergies of fuzzy logic, neural networks and evolutionary computing": John Wiley & Sons, 2013.

[89] M. Marzband, A. Sumper, O. Gomis-Bellmunt, P. Pezzini and M. Chindris, "Frequency control of isolated wind and diesel hybrid microgrid power system by using fuzzy logic controllers and PID controllers," *Proceedings in 11th International Conference on Electrical Power Quality and Utilisation*, Lisbon, 2011, pp. 1-6.

[90] H. Bevrani, F. Habibi, P. Babahajyani, M. Watanabe and Y. Mitani, "Intelligent frequency control in an AC Microgrid: Online PSO-based fuzzy tuning approach," in *IEEE Transactions on Smart Grid*, vol. 3, no. 4, pp. 1935-1944, 2012.

[91] M.-H. Khooban, T. Niknam, F. Blaabjerg, P. Davari, and T. Dragicevic, “A robust adaptive load frequency control for microgrids,” *ISA Transactions*, vol. 65, pp. 220–229, 2016.

[92] H. Bevrani and P. R. Daneshmand, “Fuzzy logic based load frequency control concerning high penetration of wind turbines,” *IEEE Systems Journal*, vol. 6, no. 1, pp. 173–180, 2012.

[93] M. H. Khooban and T. Niknam, “A new intelligent online fuzzy tuning approach for multi-area load frequency control: Self adaptive modified bat algorithm,” *International Journal of Electrical Power & Energy Systems*, vol. 71, no. 4, pp. 254–261, 2015.

[94] A. Abazari, M. Ghazavi, and H. Monsef, “An optimal fuzzy-logic based frequency control strategy in a high wind penetrated power system,” *Journal of the Franklin Institute*, vol. 71, no. 14, 2018.

[95] Y. Arya, “AGC of restructured multi-area multi-source hydrothermal power systems incorporating energy storage units via optimal fractional-order fuzzy PID controller,” *Neural Computing and Applications*, vol. 31, no. 3, pp. 851–872, 2017.

[96] S. Saremi, S. Mirjalili, and A. Lewis, “Grasshopper optimisation algorithm: Theory and application,” *Adv. Eng. Softw.*, vol. 105, no. 1, pp. 30–47, 2017.

[97] S. A. Papathanassiou and M. P. Papadopoulos, “Dynamic characteristics of autonomous wind–diesel systems,” *Renewable Energy*, vol. 23, no. 2, pp. 293–311, 2001.

[98] D. Lee and L. Wang, "Small-signal stability analysis of an autonomous hybrid renewable energy power generation/energy storage system part I: Time-domain simulations," in *IEEE Transactions on Energy Conversion*, vol. 23, no. 1, pp. 311-320, 2008.

[99] WINDPOWER.Available at https://www.thewindpower.net/turbine_en_42_gamesa_g52-850.php. Accessed 12 Nov 2017.

[100] El-Fergany, “Electrical characterisation of proton exchange membrane fuel cells stack using grasshopper optimiser,” *IET Renew.Power Gener.*, vol. 12, no. 1, pp. 9–17, 2018.

[101] M. Mafarja *et al.*., “Evolutionary population dynamics and grasshopper optimization approaches for feature selection problems,” *Knowledge-Based Syst.*, vol. 145, pp. 25–45, 2018.

[102] B. K. Sahu, S. Pati and S. Panda, "Hybrid differential evolution particle swarm optimisation optimised fuzzy proportional–integral derivative controller for automatic generation control of interconnected power system," in *IET Generation, Transmission & Distribution*, vol. 8, no. 11, pp. 1789-1800, 2014.

[103] R. Khezri, S. Golshannavaz, S. Shokoohi, and H. Bevrani, “Fuzzy logic based fine-tuning approach for robust load frequency control in a multi-area power system,” *Electric Power Components and Systems*, vol. 44, no. 18, pp. 2073–2083, 2016.

[104] R. K. Mudi and N. R. Pal, "A robust self-tuning scheme for PI- and PD-type fuzzy controllers," in *IEEE Transactions on Fuzzy Systems*, vol. 7, no. 1, pp. 2-16,1999.

[105] K. A. El-Metwally, "An adaptive fuzzy logic controller for a two area load frequency control problem," *Proceedings in 12th International Middle-East Power System Conference*, Aswan, 2008, pp. 300-306.

[106] J. Kennedy and R. Eberhart, "Particle swarm optimization," *Proceedings in International Conference on Neural Networks*, Perth, WA, Australia, 1995, pp. 1942-1948.

[107] H. Jia, X. Li, Y. Mu, C.cXu, Y. Jiang, X. Y. Wu and C. Dong, " Coordinated control for EV aggregators and power plants in frequency regulation considering time-varying delays, " *Applied Energy*, vol.210, pp. 1363-1376, 2018.

[108] W. Tan, S. Chang and R. Zhou, "Load frequency control of power systems with non-linearities," in *IET Generation, Transmission & Distribution*, vol. 11, no. 17, pp. 4307-4313, Nov. 2017.

[109] S. Izadkhast, P. Garcia-Gonzalez, P. Frías, L. Ramírez-Elizondo and P. Bauer, "An aggregate model of plug-in electric vehicles including distribution network characteristics for primary frequency control," *Proceedings in IEEE Power and Energy Society General Meeting (PESGM)*, Boston, MA, 2016, pp. 1-6.

[110] S. Izadkhast, P. Garcia-Gonzalez, P. Frìas, L. Ramìrez-Elizondo and P. Bauer, "An aggregate model of plug-in electric vehicles including distribution network characteristics for primary frequency control," in *IEEE Transactions on Power Systems*, vol. 31, no. 4, pp. 2987-2998, 2016.

[111] R. V. Rao and D. P. Rai, “Optimization of selected casting processes using jaya algorithm,” *Materials Today: Proceedings*, vol. 4, no. 10, pp. 11056–11067, 2017.

[112] K. Abhishek, V. R. Kumar, S. Datta, and S. S. Mahapatra, “Application of JAYA algorithm for the optimization of machining performance characteristics during the turning of CFRP (epoxy) composites: comparison with TLBO, GA, and ICA,” *Engineering with Computers*, vol. 33, no. 3, pp. 457–475, 2017.

[113] N. Kumar, I. Hussain, B. Singh and B. K. Panigrahi, "Rapid MPPT for uniformly and partial shaded PV system by using Jaya-DE algorithm in highly fluctuating atmospheric conditions," in *IEEE Transactions on Industrial Informatics*, vol. 13, no. 5, pp. 2406-2416, 2017.

[114] S. Mishra and P. K. Ray, "Power quality improvement using photovoltaic fed DSTATCOM based on JAYA optimization," in *IEEE Transactions on Sustainable Energy*, vol. 7, no. 4, pp. 1672-1680, 2016.

[115] Y. K. Bhateshvar, H. D. Mathur, and R. C. Bansal, "Power-frequency balance in multi-generation System Using optimized fuzzy logic controller," *Electric Power Components and Systems*, vol. 45, no. 12, pp. 1275–1286, 2017.

[116] R. V Rao, V. J. Savsani, and J. Balic, "Teaching–learning-based optimization algorithm for unconstrained and constrained real-parameter optimization problems," *Engineering Optimization*, vol. 44, no. 12, pp. 1447–1462, 2012.

[117] "Numerical issues and MATLAB implementations for fractional-order control systems," *in Fractional-order Systems and Controls: Fundamentals and Applications*, London: Springer London, 2010, pp. 213–256.

[118] S. Sondhi and Y. V Hote, "Fractional order PID controller for load frequency control," *Energy Conversion and Management*, vol. 85, no. 4, pp. 343–353, 2014.

[119] M. Dulău, A. Gligor, and T.-M. Dulău, "Fractional order controllers versus Integer order controllers," *Procedia Engineering*, vol. 181, pp. 538–545, 2017.

[120] M. Khooban, T. Niknam, M. Shasadeghi, T. Dragicevic and F. Blaabjerg, "Load frequency control in microgrids based on a stochastic noninteger controller," in *IEEE Transactions on Sustainable Energy*, vol. 9, no. 2, pp. 853-861, 2018.

[121] A. H. Hajimiragha and M. R. D. Zadeh, "Research and development of a microgrid control and monitoring system for the remote community of Bella Coola: Challenges, solutions, achievements and lessons learned," *Proceedings in IEEE International Conference on Smart Energy Grid Engineering (SEGE)*, 2013, pp. 1–6.

LIST OF PUBLICATIONS

International Journals

1. A. Annamraju and S. Nandiraju, “Robust Frequency Control in an Autonomous Microgrid: A Two-Stage Adaptive Fuzzy Approach,” ***Electric Power Components and Systems*****, Taylor and Francis Inc.,** vol 46, issue 1, pp. 83–94, Mar.2018. (**SCIE Journal**)
   (DOI: 10.1080/15325008.2018.1432723)
2. A. Annamraju and S. Nandiraju, “Robust frequency control in a renewable penetrated power system: an adaptive fractional order-fuzzy approach,” ***Protection and Control of Modern Power Systems*****, Springer.,** vol. 4, no. 1:16, pp. 1-16, Dec. 2019. (**ESCI & Scopus Journal**)
   (DOI: 10.1186/s41601-019-0130-8)
3. A. Annamraju and S. Nandiraju, “Coordinated control of conventional power sources and PHEVs using JAYA algorithm optimized PID controller for frequency control of a renewable penetrated power system,” ***Protection and Control of Modern Power Systems*****, Springer.,** vol. 4, no. 1:28, pp. 1-13, Dec. 2019. (**ESCI & Scopus Journal**)
   (DOI: 10.1186/s41601-019-0144-2)

International Conferences

1. A. Annamraju and S. Nandiraju, "Frequency Control in an Autonomous Two-area Hybrid Microgrid using Grasshopper Optimization based Robust PID Controller," ***2018 8th IEEE India International Conference on Power Electronics (IICPE)***, MNIT JAIPUR, India, 2018, pp. 1-6.
   (DOI: 10.1109/IICPE.2018.8709428)
2. A. Annamraju and S. Nandiraju, " Load Frequency Control in an Autonomous Microgrid using Robust Fuzzy PI Controller," ***2019 8th IEEE India International Conference on Power Systems (ICPS)*****,** MNIT JAIPUR, India, 2019, pp. 1-6.
   (DOI:10.1109/ICPS48983.2019.9067613)

APPENDIX A

A.1 Two-Area MG Simulation model operating conditions

Table A.1 Operating Conditions of Two-Area Microgrid [121]

Area-1	Area-2
Total rated power: 8 MW Total load: 4.9 MW Wind power: 3.4 MW RFB storage: 3 MW	Total rated power: 7 MW Total load: 4.9 MW Wind power: 1.2 MW RFB storage: 3 MW

Table A.2 Parameter values of GA, SSO and GOA algorithm

GA [66]	SSO [69]	GOA [96]
Population size=20	Population size=20	Population size=20
Crossover rate (P_c)=0.8	Attenuation Rate (γ_A)=[0-1] Chaotic parameter (γ_t)=[0.75-1]	Attractive length scale (l)=1.5, Intensity of attraction (f)=0.5
Mutation rate (M_c)=0.02	Memory factor(Δ)= [0-1]	Adaptation factor c=[0.0001-4]
No. of generations=50	No. of generations=50	No. of generations=50

APPENDIX A

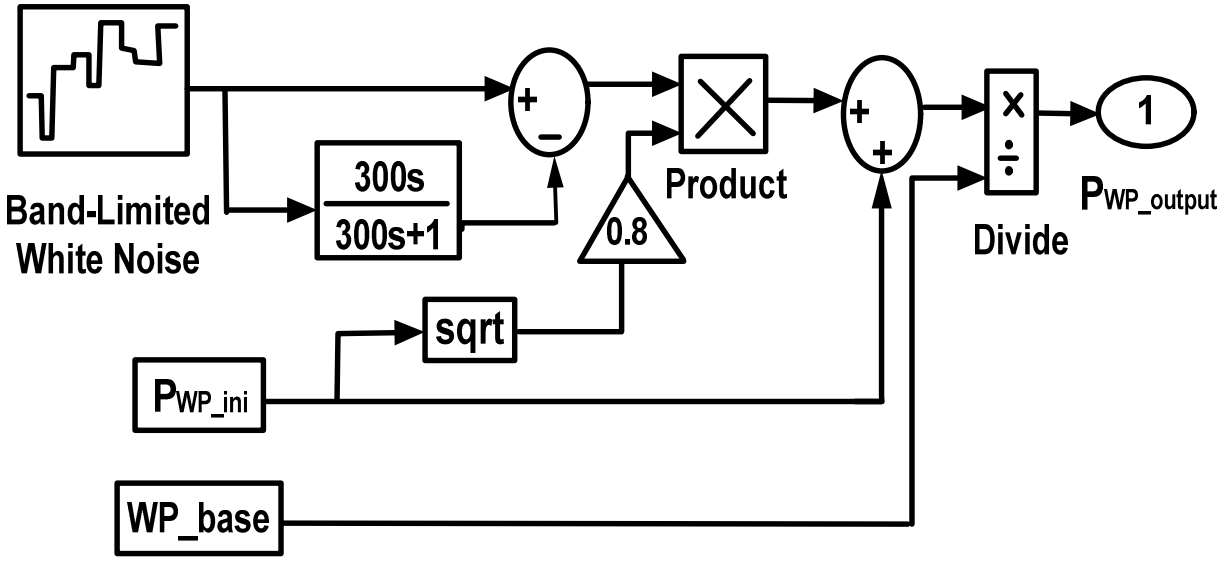

Fig. A1 Simulink model to generate wind speed and solar radiation patterns

Table A.3 Operating Conditions of BELLACOOLA Microgrid [121]

Test system	Installed Capacity	Peak Load	RES Penetration	Fuel cell overall rated power output
BELLACOOLA MG (Canada) (Isolated Area)	8 MW	4.7 MW	2.1 MW	3 MW

APPENDIX A

Table A.4 Parameter values of PSO and GWO algorithm

PSO[73]	GWO[74]
Population size=20	Population size=20
Cognitive factors (C_1, C_2)= 1	Coefficient vectors $\vec{A}$ *and* $\vec{C}$ (These values vary randomly from iteration to iteration)
Inertia Weight (w) = 0.65 Inertia Damping Ratio (W_{damp}) = 0.5	Controlling parameter $\vec{a}$, decreases from [2-0] as the number of iterations progress.
No. of generations=50	No. of generations=50

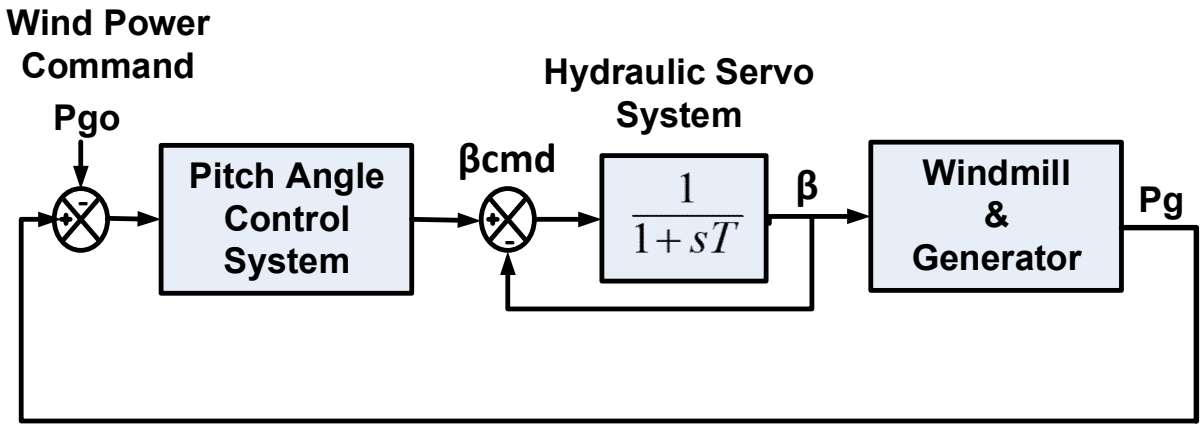

Fig.A2 WTG system

APPENDIX A

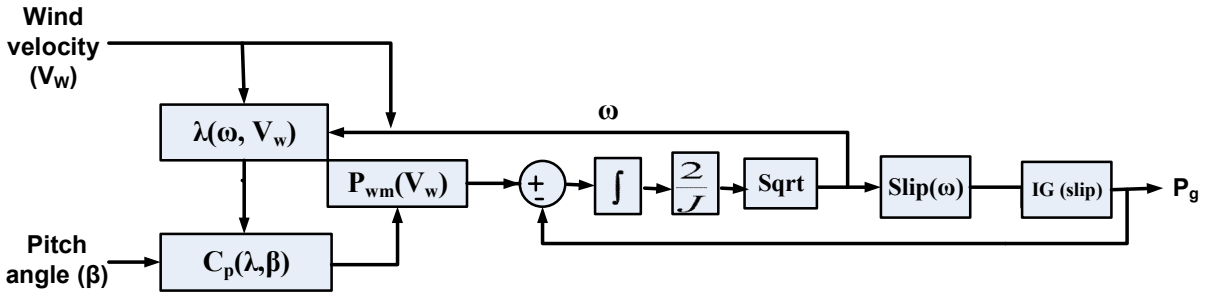

Fig. A3 Windmill and generator model

Table A.5 Gamesa Company WTG Data

Various Specifications of WTG		
Power Specifications	**Rotor Specifications**	**Generator Specifications**
Rate output power: 850 kW	Rotor diameter: 22.0 m	Type: Squirrel Cage Induction Generator
Cut-in wind speed: 4.0 m/s	Swept area: 2124.0 m^2	Voltage: 690 v
Cut-out wind speed: 25.0 m/s	Number of Blades: 2	Frequency: 50/60 Hz
Rated wind speed: 16.0 m/s	Tip speed : 90 m/s	Maximum generator output speed:1900 rpm
J=62,999 Kg-m^2 ρ =1.225 Kg/m^2	Rotor Resistance (R_r): 0.00443 Ω Rotor Reactance (X_r): 0.0536 Ω	Stator Resistance (R_s): 0.00397 Ω Stator Reactance (X_s): 0.0376 Ω

The output power from induction generator can be expressed as:

$$P_g = \frac{-3V^2 s(1+s)R_r}{(R_r - sR_s)^2 + s^2(X_s + X_r)^2} \quad \text{(A.1)}$$

Where 's' is the slip of SQIG which is defined as:

$$s = \frac{\omega_0 - \omega}{w_0} \quad \text{(A.2)}$$

APPENDIX A

The angular speed (ω) can be expressed as:

$$\omega = \sqrt{\frac{2}{J}}(P_{wm} - P_g) \quad \text{(A.3)}$$

Where 'J' is the moment of inertia of induction generator.

Table A.6 Kyocera Company PV Module Data (KC200GT Model)

Electrical Performance at Standard Test Conditions STC: 1000 w/m^2 at Temperature 25^{o}C	
Rate output power: 200 kW	Open circuit voltage (V_{oc}): 38.6 v
Maximum power voltage: 26.3 V	Short circuit current (I_{sc}): 8.21 A
Maximum power current: 7.61 A	Number of cells per module: 54
Maximum System Voltage: 600 V	

APPENDIX B

B.1 IEE Japan East 107-bus-30-machine power system (Main grid data)

Table B.1 IEEE-Japan East-107-bus-30-Machine Power System Rated Operating Conditions

Area-1	Area-2	Maximum Allowable tie-line Power
Total MVA: 9388 MVA Total rated power: 8000 MW Total load: 7260 MW RES: 800 MW PHEV aggregator power: 400 MW	Total MVA: 9388 MVA Total rated power: 8000 MW Total load: 7260 MW	500 MW

B.2 IEE-Japan-East-107-Bus Data:

M_1=8.85 s; M_2=9.2 s; D_1, D2=0.04puMW/Hz; β_1, β_2=0.4566puMW/Hz; R_1-R_4=2.4Hz/puMW; T_{12}=5.

B.3 Thermal and Hydro Generator Data:

T_{TT}=0.3 s, T_{r1}=10 s, T_{GT}=0.2 s, K_{r1}=0.333, T_{GH}=0.1 s, T_1=0.513 s, T_2= 10 s and T_w=1 s, governor dead-band effect of both units= 0.0125 puMW, GRC for thermal unit = 0.0017 puMW/s, GRC for hydro unit for rising = 0.035 puMW/s and for lowering = 0.06 puMW/s.

B.4 Boiler Dynamics Data:

K_1, = 0.85, K_2 = 0.095, K_3 = 0.92, C_b=200, T_f=10 s, K_{rb} = 0.03, K_{ib} = 0.06, T_{rb} =26 s.

APPENDIX B

B.5 PHEV Aggregator Data:

Δf_l, Δf_u = Lower and upper frequency dead bands (-100 mHz & 100 mHz); R_{av}=2.4 Hz/ puMW; $K_{EV,i}$(average)=0.55, $T_{EV,i}$=0.1, SOC_1= 0.2 and SOC_2= 0.5 (in case of idle mode), SOC_1= 0.1, SOC_2= 0.2, SOC_3= 0.8 and SOC_3= 0.9 (in case of charging mode).

Table B.2 Parameter values of GA, SSO and GOA algorithm

PSO [73]	GA [66]	GWO [74]	TLBO [116]	JA [112]
Population size=20	Population size=20	Population size=20	Population size=20	Population size=20
C_1 , C_2 = 2	Crossover rate (P_c)=0.8	Coefficient vectors $\vec{A}$ and $\vec{C}$	- **(No algorithm specific parameters)**	- **(No algorithm specific parameters)**
Inertia Weight (w) = 0.65, Inertia Damping Ratio (W_{damp}) = 0.5	Mutation rate (M_c)=0.02	Controlling parameter $\vec{a}$, decreases from [2-0] as the number of iterations progress.		
No. of generations=50	No. of generations=50	No. of generations=50	No. of generations=50	No. of generations=50